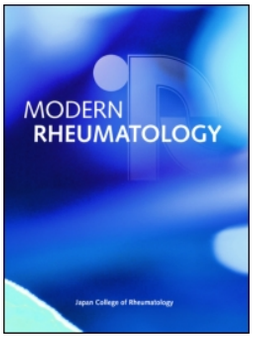

Taylor & Francis
Taylor & Francis Group

Modern Rheumatology

ISSN: 1439-7595 (Print) 1439-7609 (Online) Journal homepage: https://www.tandfonline.com/loi/imor20

Rheumatic diseases associated with immune checkpoint inhibitors in cancer immunotherapy

Kei Ohnuma, Ryo Hatano, Nam H. Dang & Chikao Morimoto

To cite this article: Kei Ohnuma, Ryo Hatano, Nam H. Dang & Chikao Morimoto (2018): Rheumatic diseases associated with immune checkpoint inhibitors in cancer immunotherapy, Modern Rheumatology, DOI: 10.1080/14397595.2018.1532559

To link to this article: https://doi.org/10.1080/14397595.2018.1532559

Accepted author version posted online: 04 Oct 2018.
Published online: 20 Dec 2018.

MODERN RHEUMATOLOGY
https://doi.org/10.1080/14397595.2018.1532559

Japan College of Rheumatology
MODERN RHEUMATOLOGY
Taylor & Francis
Taylor & Francis Group

REVIEW ARTICLE

Rheumatic diseases associated with immune checkpoint inhibitors in cancer immunotherapy

Kei Ohnuma[a], Ryo Hatano[a], Nam H. Dang[b] and Chikao Morimoto[a]

[a]Department of Therapy Development and Innovation for Immune Disorders and Cancers, Graduate School of Medicine, Juntendo University, Tokyo, Japan; [b]Division of Hematology/Oncology, University of Florida, Gainesville, FL, USA

ABSTRACT

Immune checkpoint inhibitors (ICIs) have drastically altered cancer treatment paradigms, with increasing numbers of novel ICIs being currently evaluated in numerous clinical trials for various cancers. ICIs release 'brakes' against tumor immunity to control cancer growth through T cell-dependent anti-tumor activity. Meanwhile, side effects associated with ICIs are directly related to their mechanism of action, as nonspecific immune activation targeting non-tumor organs results in undesirable off-target inflammation and autoimmunity. Accumulating data reveal that immune-related adverse events (irAEs) of ICIs in cancer patients can resemble various rheumatic diseases. Moreover, while patients with preexisting rheumatic diseases can theoretically experience irAEs and disease flares, observational studies have shown that ICIs can be used successfully in these patients. As ICIs continue to provide long-lasting disease control in cancer patients and their usage correspondingly increases, the rheumatologist will be managing new ICI-associated clinical entities mimicking common autoimmune diseases and will need to be prepared to rapidly diagnose and treat these irAEs. Early recognition and treatment of these rheumatic adverse events will allow for improved outcomes and quality of life for cancer patients faced with previously rapidly fatal disease.

ARTICLE HISTORY
Received 19 July 2018
Accepted 1 October 2018

KEYWORDS
Immune checkpoint inhibitor; immune-related adverse events; inflammatory arthritis; rheumatic disease

Introduction

Monoclonal antibodies (mAbs) against coinhibitory immune checkpoint molecules have demonstrated clinical activities in various malignancies [1]. Targets include cytotoxic T-lymphocyte-associated antigen 4 (CTLA-4 or CD152), programmed cell-death protein 1 (PD-1 or CD279) and its ligand (PD-L1; B7-H1 or CD274), which negatively regulate T cell activation and T cell receptor (TCR) signaling, respectively. By disinhibiting these regulatory pathways, immune checkpoint inhibitors (ICIs) overcome self-tolerance and promote T cell-mediated expansion, leading to robust anti-tumor immunity [1]. Originally approved by the US Food and Drug Administration (FDA) for the treatment of advanced melanoma [2], ICIs have led to a paradigm shift in the field of cancer therapy, with the list of indications for ICI use in advanced cancers being now ever-expanding, to include non-small cell lung carcinoma, bladder cancer, head and neck squamous carcinoma, breast cancer, gastric cancer, colorectal carcinoma or solid tumors with high microsatellite instability or mismatch-repair deficiency, hepatocellular carcinoma, Merkel cell carcinoma, urothelial carcinoma, Hodgkin's lymphoma and leukemia [1].

As a consequence of their mechanism of action, ICI therapy can induce nonspecific immune activation, which can target non-tumor tissues. These side effects are collectively referred to as immune-related adverse events (irAEs) [3]. irAEs can resemble various rheumatic diseases, such as inflammatory arthritis (IA) [4], but also exhibit diverse manifestations throughout the body [5,6] (Figure 1). As indications for ICIs use expand and as these novel agents are combined with each other, it becomes increasingly important for rheumatologists to recognize irAEs and appropriate management. In this paper, we summarize the underlying immune mechanisms and the latest findings regarding the rheumatic manifestations and the general approach to management of ICI-associated irAEs in cancer patients treated with these novel agents. Reviewing many recently published work on rheumatic irAEs, this review will provide rheumatologists an updated understanding of these emerging cancer therapies, with particularly a focus on their associated immunopathologic mechanisms and rheumatic complications, and their management.

Normal immune response and immune homeostasis

The classical definition of immunity is protection from infectious pathogens, and the mechanisms of host defense fall into two broad categories, innate immunity and adaptive immunity [7]. During the innate response process, activation of antigen-presenting cells (APCs) leads to enhanced expression of costimulatory molecules. The principal T cell costimulatory molecule CD28 is recognized by the B7

CONTACT Kei Ohnuma kohnuma@juntendo.ac.jp Department of Therapy Development and Innovation for Immune Disorders and Cancers, Graduate School of Medicine, Juntendo University, 2-1-1, Hongo, Bunkyo-ku, Tokyo 113-8421, Japan.

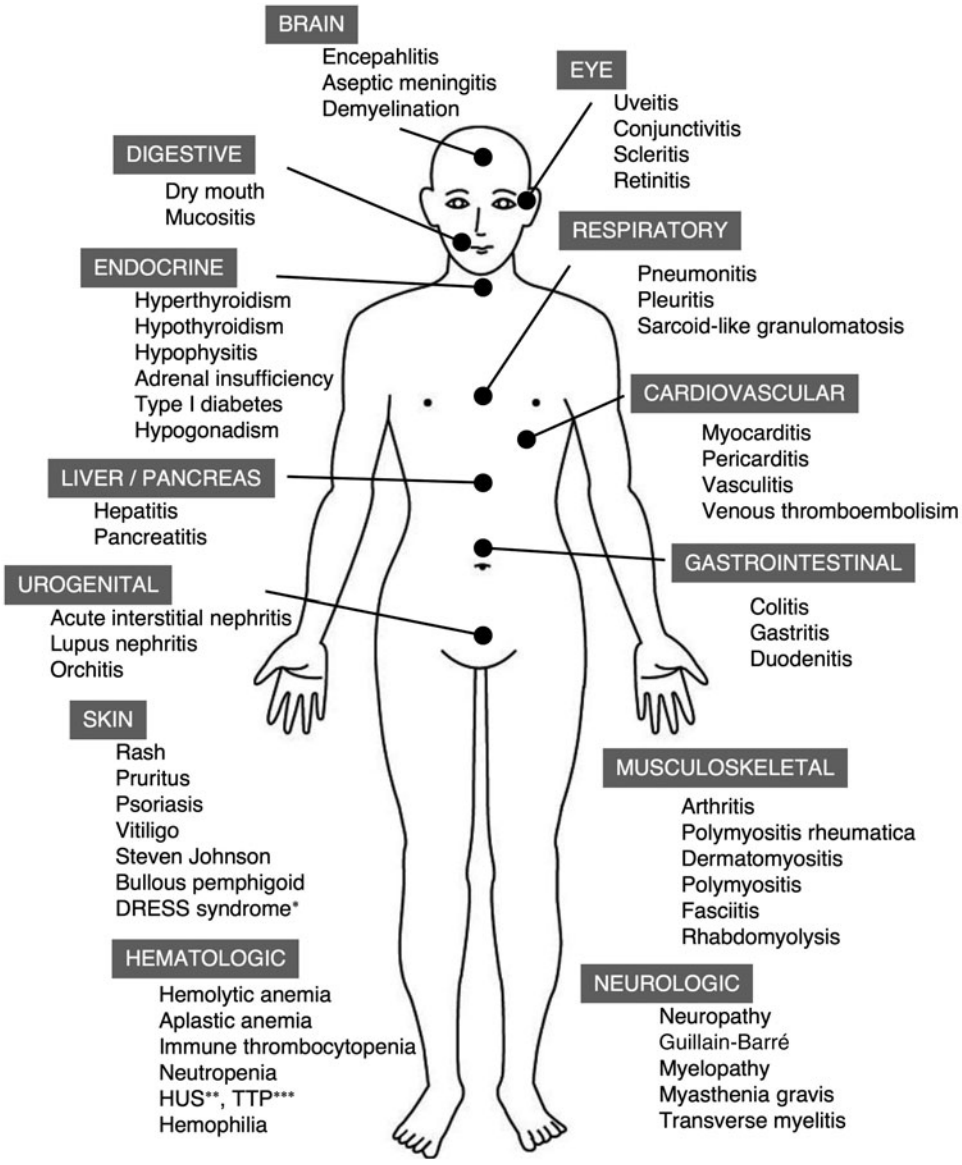

Figure 1. Spectrum of immune-related adverse events induced by immune checkpoint inhibitors. Details are described in the text. *DRESS: drug reaction with eosinophilia and systemic symptoms; **HUS: hemolytic uremic syndrome; ***TTP: thrombotic thrombocytopenic purpura.

molecules CD80 (B7-1) and CD86 (B7-2) that are expressed on APCs [8,9]. Antigen-specific T cells are activated by specific antigens ('signal 1') and the costimulatory molecules ('signal 2') [8,10] (Figure 2(A)). Once activated, proliferated and expanded clonally, antigen-specific T cells exhibit enhanced cell surface expression of immune inhibitory molecules (immune checkpoints) to prevent uncontrolled immune responses and inflammatory tissue damages and to maintain self-tolerance [8,9,11].

CTLA-4 is a transmembrane glycoprotein that is a homolog of the immune costimulatory protein CD28 [9,12] and plays a key role in the development of peripheral tolerance to self-proteins by neutralizing the function of CD28 [9,13]. CTLA-4 is a receptor that inhibits T cell activation by blocking CD28-CD80/CD86 engagement through its approximately 20 times greater affinity to CD80/CD86 on APCs [9,14–16] (Figure 2(B)). In addition, regulatory T cells (Treg), a CD4 subset involved in global regulation of the innate and adaptive immunity, constitutively express CTLA-4, which binds to CD80/CD86 on APCs to reduce their ability to activate T cells through CD28 [17] (Figure 2(C)). The significant role of CTLA-4 in immunity is clearly demonstrated in the CTLA-$4^{-/-}$ mouse model, with the animals being moribund at 3–4-week-old and exhibiting severe pancreatitis, myocarditis and T cell infiltration in the liver, heart, lung and pancreas [18,19].

PD-1 molecules are expressed on the T cell surface within 24 h of activation, and subsequently, disappear once the antigen is eradicated [8]. While CTLA-4 mainly affects naïve T cells, PD-1 is primarily expressed on mature T cells in peripheral tissues and the tumor microenvironment (TME) through downmodulation of TCR signaling [20], hence altering effector T cell survival, proliferation and biological function [21,22] (Figure 2(D)). There are two known ligands to PD-1: PD-L1 and PD-L2 (B7-DC or CD273) [21,22]. PD-L1 is widely expressed on hematopoietic and non-hematopoietic cells, including heart, endothelium, pancreatic islets, small bowel and placenta, while PD-L2 is

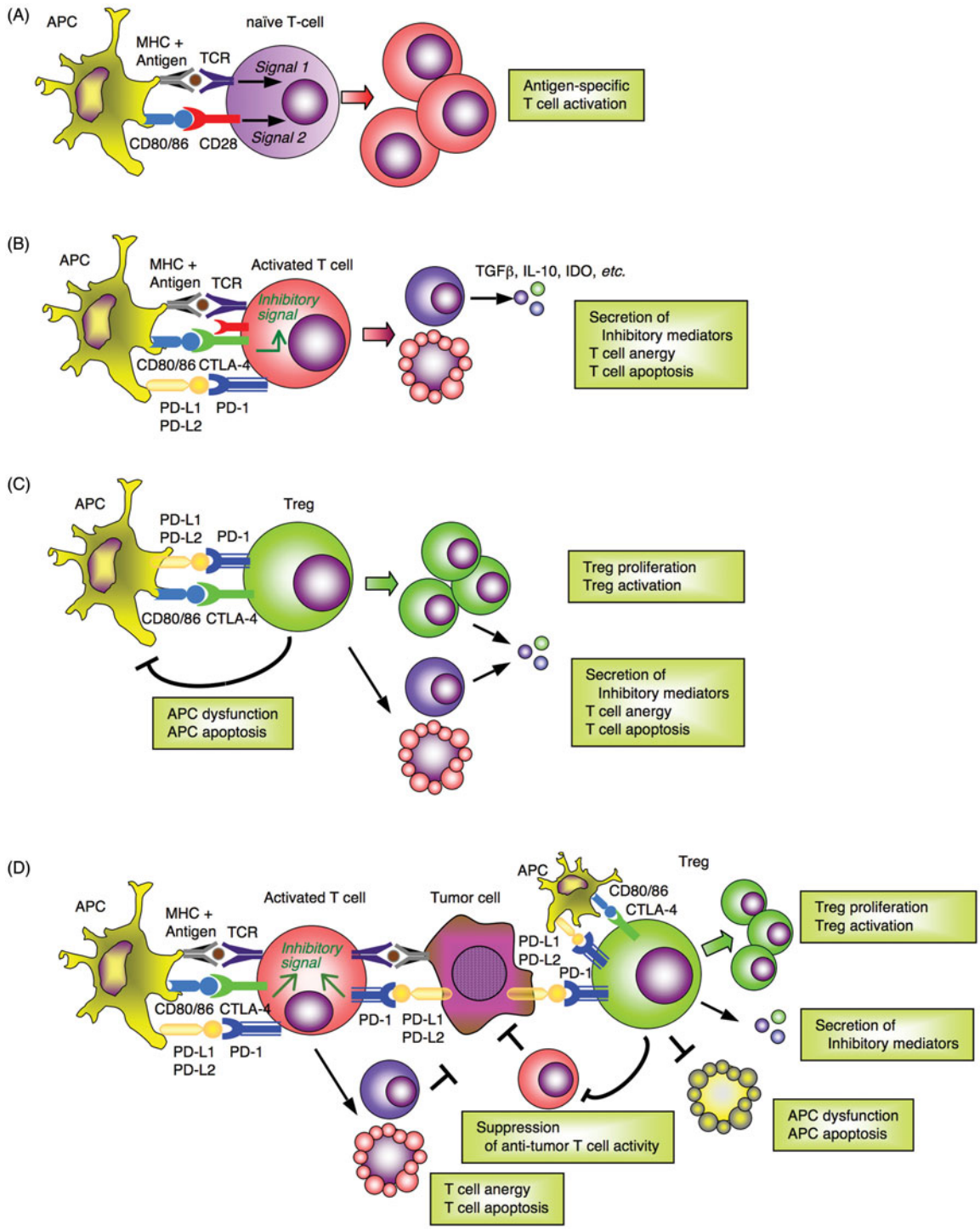

Figure 2. Mechanisms of T cell costimulation, coinhibition, and T cell dependent anti-tumor immunity. (**A**) Adaptive immune response develops in a stepwise fashion, consisting of initial antigen recognition, followed by activation of specific lymphocyte subsets that results in proliferation and differentiation into effector and memory cells, then elimination of the antigen, and decline of the response, with memory cells being the long-lived survivors of the process. In an activation step, T cells are primed by antigen-presenting cells (APCs) with antigen peptides loaded by major histocompatibility complex (MHC) molecule. TCR complex recognizes peptide antigens that are presented by MHC molecules (class I MHC for CD8+ and class II for CD4+ T cell) on the surface of APC, followed by engagement of CD28 on the surface of T cells by CD80 or CD86 expressed on APCs which provides a costimulatory second signal, cooperatively activating antigen-specific T cells. (**B**) After activation, T cells express PD-1 and CTLA-4 coinhibitory molecules that bind to PD-L1/PD-L2 and CD80/86 (with significantly higher affinity than CD28), respectively, leading to suppression of antigen-specific T cell activity through anergy and apoptosis, and secretion of inhibitory mediators including TGF-β, IL-10 and indoleamine 2,3-dioxygenase (IDO). If the antigen is presented to T cells without adequate levels of costimulatory signals, the cells become anergic to the antigen, a process which is mediated by coinhibitory molecules including CTLA-4 and PD-1. (**C**) Regulatory T cells (Treg) also constitutively express CTLA-4 and PD-1 as an inhibitory extrinsic mechanism leading to proliferation and activation of Treg, induction of T cell anergy and apoptosis, and secretion of inhibitory mediators. Meanwhile, a key role of Treg is to prevent immune reactions against self-antigens, a function mediated in part by the secretion of immunosuppressive cytokines such as IL-10 and TGF-β, which inhibit lymphocyte activation and effector function. (**D**) Mechanisms described in panels of B and C on PD-1 and CTLA-4 immune checkpoint molecules lead to tumor escape in the tumor microenvironment. PD-L1 and PD-L2 are expressed on various tumor cells, which could partly explain the ability of tumor cells to evade the process of immune surveillance. Following continuous exposure of effector T cells to antigens, such as in the setting of the tumor microenvironment, T cells lose the ability to respond to the antigen, a process termed T cell exhaustion, with PD-1 signaling playing a critical role. PD-1 is also highly expressed on Treg, and enhances their proliferation and suppressive activity upon ligand binding, likely further helping tumor escape by suppressing effective immune response.

expressed mainly on dendritic cells and macrophages [22]. Induction of PD-L1 expression on tissue cells in the inflammatory regions may be a protective mechanism to downregulate effector T cell activity and reduce immune-mediated injury [23] (Figure 2(B)). PD-1$^{-/-}$ mice demonstrate evidence of autoimmunity, specifically, mild lupus-like autoimmunity and dilated cardiomyopathy [23,24]. The PD-1 knockout autoimmune effects appear to be less severe and display a later onset than those observed in CTLA-4$^{-/-}$ mice [22,25]. As is the case with CTLA-4, PD-1 is also highly expressed on Treg, and enhances their proliferation and suppressive activity upon ligand binding [26] (Figure 2(C)).

An important group of diseases which reflects the failure of the normal control mechanisms described above is autoimmune diseases, which result from the lack of tolerance to self-antigens. The mechanisms of self-tolerance can be broadly classified into two groups: central tolerance and peripheral tolerance [11]. In central tolerance, immature self-reactive T and B lymphocyte clones that recognize self-antigens during their maturation in the central lymphoid organs are eliminated or rendered harmless by negative selection [11]. Autoreactive lymphocytes which manage to escape from the central tolerance mechanisms are subsequently silenced in peripheral tolerance by anergy, Treg and apoptotic deletion [11] (Figure 2(B,C)).

Taken together, immune checkpoints such as CTLA-4 and PD-1 systems are regulatory inhibitory pathways that contribute to immune homeostasis, being essential in preventing autoimmunity, maintaining self-tolerance and avoiding tissue damage that could result from persistent immune activation.

Mechanism of action of immune checkpoint inhibitors

Multiple studies have demonstrated that many tumors use the same pathways involved in immune regulation to evade immune attack [1]. This realization has led to the development of mAbs that block CTLA-4 and PD-1 for tumor immunotherapy, by removing the brakes on the immune response and promoting responses against tumors [1]. The first approved ICI by FDA was ipilimumab, a fully human IgG_1 anti-CTLA-4 mAb, and subsequently, several agents including anti-PD-1 mAb and anti-PD-L1 mAb have been developed for clinical use as shown in Figure 3(A).

Anti-cytotoxic T-lymphocyte-associated antigen 4 inhibitors

Following the discovery of the CTLA-4 receptor in 1986, work involving a murine preclinical model revealed the anti-tumor activity of anti-CTLA-4 Ab [13]. Clinical studies subsequently demonstrated that ipilimumab extended survival time by nearly four months in patients with advanced melanoma [27,28]. Tremelimumab, a fully-human IgG_2 that also targets CTLA-4, is currently under development as monotherapy or combined therapy [29]. Treatment with CTLA-4 mAb results in persistent T cell activation by blocking the inhibitory pathway in the antigen priming phase (Figure 3(A,B)). Moreover, anti-CTLA-4 mAb-mediated inhibition increases the ratio of effector T cells to Treg in the TME, due to depletion of intratumoral Treg through complement-dependent cytotoxicity (CDC) and antibody-dependent cell-mediated cytotoxicity (ADCC) [30] (Figure 3(A)). Of note is that the therapeutic agent for rheumatoid arthritis (RA) abatacept, a fusion protein consisting of the extracellular domain of CTLA-4 and the Fc region of IgG_1, acts in an opposite manner as ICIs, by facilitating coinhibitory signaling of T cells through its binding affinity for CD80/CD86 [31,32].

Anti-programmed cell-death protein-1 inhibitors

Generation of tumor-reactive CD8+ T cells requires the successful processing and presentation of tumor-derived peptide antigens with class I major histocombatibility complex (MHC) molecules by APCs [10,33]. Once developed, tumor-specific CD8+ T cells subsequently differentiate into effector T cells, undergo clonal expansion, migrate to the TME, and ultimately eliminate tumor cells expressing tumor-specific antigens bound to class I MHC molecules through the release of cytotoxic granules [10]. The presence of enhanced PD-1 expression on CD8+ tumor infiltrating lymphocytes (TILs) may either reflect an anergic or exhausted state, consistent with the findings that cytokine production by PD-1+ TILs is decreased [34]. Initial studies showed that PD-1/PD-L1 blockade reversed the exhausted state of effector T cells in the TME, leading to the clinical development of anti-PD-1 inhibitors for cancer immunotherapy [20]. In addition, a large proportion of intratumoral CD4+ T cells are Treg with increased level of PD-1 expression. These findings thus provide an important scientific rationale for a therapeutic approach involving anti-tumor immunity through PD-1/PD-L1 blockade [35]. Currently, pembrolizumab, a humanized IgG_4 mAb, and nivolumab, a fully human IgG_4 mAb, are approved as anti-PD-1 mAbs for clinical use. Treatment with anti-PD-1 mAbs leads to persistent T cell activation by blocking the inhibitory pathway both in the antigen priming phase as well as the effector phase (Figure 3(A,B)).

Anti-programmed cell-death protein-ligand 1 inhibitors

Atezolizumab is a humanized IgG_1 anti-PD-L1 mAb, engineered to delete binding to the Fc receptor [36]. It upregulates T cell activation by blocking the interaction between PD-1 and PD-L1 or CD80 and PD-L1, with a safety profile similar to that of anti-PD-1 mAbs [37]. Other novel anti-PD-L1 mAbs being evaluated currently in various clinical trials are the fully human IgG_1 mAbs durvalumab and avelumab.

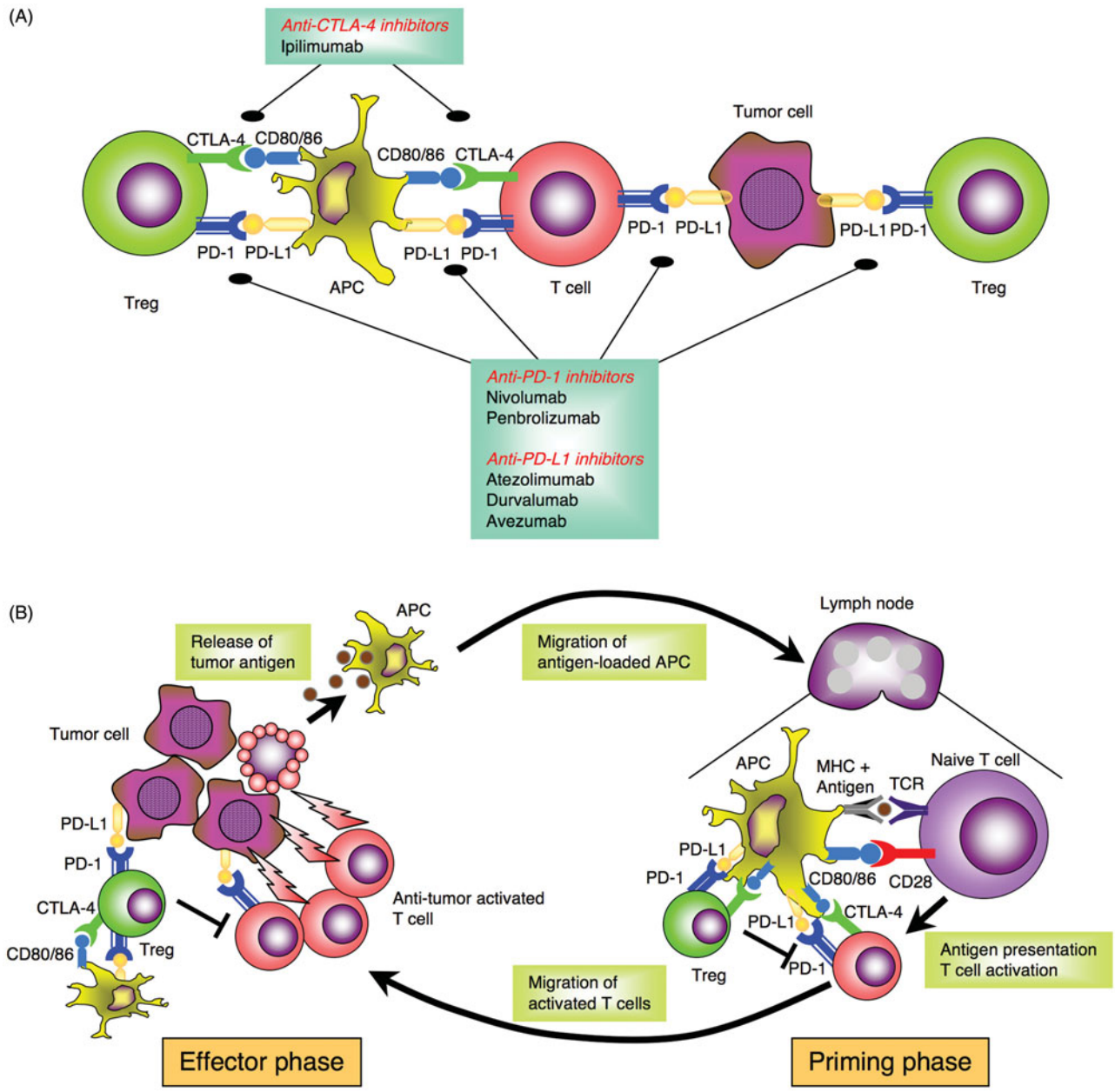

Figure 3. Points of action of anti-PD-1, anti-PD-L1 and anti-CTLA-4 inhibitors. **(A)** Anti-CTLA-4 inhibitor prevents CTLA-4 from binding to CD80/86, reinvigorating the inhibited T cell. Anti-PD-1/PD-L1 inhibitors restore down-modulated TCR signaling and reinvigorate the exhausted T cell. Anti-CTLA-4 and anti-PD-1/PD-L1 inhibitors also deplete regulatory T cells (Treg). **(B)** Cycle of tumor antigen loading to antigen-presenting cells (APCs), migration to lymph node of APC, tumor-specific T cell activation by antigen-loaded APC, accumulation of activated tumor-specific T cells in the tumor microenvironment and targeting of tumor cells. Activation of Treg concomitantly leads to tumor escape. Anti-CTLA-4 inhibitor results in persistent T cell activation by blockade of inhibitory pathway in antigen priming phase. Anti-PD-1/PD-L1 inhibitors result in persistent T cell activation by blockade of inhibitory pathway both in antigen priming phase and in effector phase. They also exert anti-tumor activity through depletion and suppression of Treg.

Combined therapy

The combination of ipilimumab and nivolumab has been approved for the treatment of metastatic melanoma by the US-FDA [38]. Other combined ICI therapy such as tremelimumab and durvalumab is under clinical trials for various cancers. Although these combinations may improve efficacy, they can result in significantly increased toxicity [3,6,39–43].

Immune-related adverse events

As discussed earlier, human immune system normally exists in a state of equilibrium in which lymphocyte activation for protection against pathogens is delicately balanced by the mechanisms of tolerance to prevent deleterious reactions against self-antigens, and the failure of tolerance allows for responses against self-antigens, leading to autoimmune diseases [8,11,44]. Consequently, ICI-mediated blocking of the inhibitory checkpoints can enhance immune activation to result in unwanted off-target effects, including immune-related and inflammatory events [3–6]. Involving any organ system (Figure 1), irAEs from ICIs are increasingly recognized as unique entities mimicking classical rheumatic diseases [4]. The accurate diagnosis and management of these side effects are of the utmost importance, given the fact that the use of ICIs in cancer patients with preexisting autoimmune disease

TABLE 1. Summary of relevant literature regarding arthro-musculoskeletal manifestations of rheumatic irAEs.

	No. of patients (N)	ICI drugs PD/CTLA/Combi[a] (N)	Treatment N/S/M/B[b] (N)	ICI therapy (N)	Outcome of irAEs (N)	Ref.
Inflammatory arthritis	20 (3.8%) 7, RA-pattern 2, PsA-pattern 11, PMR	 6/1/0 2/0/0 11/0/0	 0/7/1/0 2/0/1/0 2/9/0/0	19, Continued 1, Withheld	20, Remission	[48]
–	30	16/0/14	–/24/3/7	Cessation	3, Remission 18, Persistence	[46]
–	14 (3.5%)	12/1/1	11/14/8/0	3, Continued 3, Withheld 8, Cessation	3, Remission 10, Persistence 1, Unknown	[49]
Myositis	5 (0.8%)	5/0/0	0/5/0/0	Discontinued	3, Remission 2, Fatal	[55]
Myositis-fasciitis	2 (0.9%)	2/0/0	N/A	Discontinued	Remission after ICI cessation	[59]
Non-inflammatory musculoskeletal conditions	15 (2.8%)	14/0/1	2/3/0/0	Continued	Remission	[48]

irAEs: immune related adverse events; ICI: immune checkpoint inhibitor; N/A: not applicable; Ref: reference.
[a]PD, anti-PD-1 or anti-PD-L1 therapy; CLTA, anti-CTLA-4 therapy, Combi, anti-PD plus anti-CTLA-4 therapy.
[b]N, NSAIDS; S, Corticosteroids; M, Methotrexate; B, TNF inhibitor.

is expected to increase in the future as ICI therapy becomes more prevalent in a variety of human neoplasms [3].

Arthritis

While arthralgia and myalgia were by far the most commonly reported rheumatic irAEs in clinical trials [45,46], their exact prevalence may have been underestimated since only high-grade irAEs were noticed in some trials. On the other hand, case series and case reports have provided details on patients with IA including seropositive RA [47]. Large cohort studies on ICIs and rheumatic irAEs have been recently reported (Table 1). A single-center prospective study in France revealed that 35 patients (6.6%) among 524 patients receiving ICIs developed musculoskeletal symptoms [48]. All but two patients had no prior history of autoimmune disease – one with axial spondyloarthritis (AxSpA) and one with psoriasis (PSO). Among 20 patients (3.8%) who developed IA, 11 patients (1.9%) were diagnosed with polymyalgia rheumatica (PMR), exhibiting clinical findings that fulfilled the 2012 EULAR (European League Against Rheumatism)/ACR (American College of Rheumatology) criteria for PMR, and 1 patient was diagnosed with PMR based on the typical clinical presentation and complete disease resolution following treatment with 12.5 mg of prednisone. One patient with preexisting stable condition of AxSpA developed a PMR-like condition 20 days after commencement of ICI therapy. Seven patients (1.3%) developed bilateral and symmetric hand pain and stiffness, mimicking RA. One patient had a positive result for anti-cyclic citrullinated peptide (CCP) antibodies while testing negative for rheumatoid factor (RF). Two patients (0.4%) developed psoriatic arthritis (PsA), including one with pre-existing PSO. All of nine patients with clinical findings mimicking RA or PsA required prednisone treatment, which resulted in clinical improvement or remission. Two patients required methotrexate (MTX) to achieve remission of IA. All patients but one continued on ICI therapy. For the one exception, ICI therapy was temporally withheld as per the requirements of the study protocol in which this patient participated.

More recently, investigators at Johns Hopkins University reported a retrospective longitudinal cohort study on IA patients receiving ICI therapy with no prior history of autoimmune disease [45]. Thirty patients with ICI-induced IA were identified in longitudinal visits to Rheumatology from January 1, 2013 to July 1, 2017 (The incidence of IA in this study was not ascertained since the overall size of the patient population was not stated). Fourteen patients treated with combined CTLA-4/PD-1 therapy were more likely to present with knee arthritis, to have higher levels of C-reactive protein (CRP) and to have negative results for anti-CCP antibodies, RF and anti-nuclear antibodies (ANA). Sixteen patients treated with PD-1 or PD-L1 monotherapy were more likely to have initial small joint involvement and to have IA as their only irAEs. One patient had low levels of anti-CCP antibodies, one had a high titer of RF and one had low titer of ANA. Twenty four among 30 IA patients required systemic steroids for the management of IA. Ten patients had additional immunosuppressant including tumor necrosis factor-inhibitors (TNFi) and/or MTX with clinical improvement of their arthritis. Those receiving combined ICI therapy were more likely to require additional immunosuppressant. Tumor progression while on TNFi and/or MTX was not observed in those with initial tumor response to ICIs. Outcome regarding IA symptoms was evaluated in 21 patients with clinic visits at least 3 months following cessation of their ICI treatment. Eighteen patients still exhibited IA symptoms after ICI discontinuation.

A group from Israel has also reported 14 patients (3.5%) with rheumatic manifestations among 400 patients receiving ICI therapy between January 1, 2013 and April 30, 2017 [49]. Twelve patients were treated with anti-PD-1 mAb, one with anti-CTLA-4 mAb, and one with a combination of anti-PD-1 and anti-CTLA-4 mAbs. IA was identified in 12 patients (3.0%), including 4 patients with predisposing factors such as a personal or family history of PSO, a prior episode of uveitis or anti-CCP antibodies positivity. Other rheumatic diseases such as pulmonary sarcoidosis and biopsy-proven eosinophilic fasciitis were diagnosed in two patients (0.5%). Treatment of IA with non-steroidal anti-

inflammatory drugs (NSAIDs) was mostly unsuccessful while steroid therapy was beneficial in dose ≥20 mg/day. The addition of MTX allowed steroid tapering without an excess of adverse events or tumor progression in the short follow-up time available. There was no patient treated with TNFi in this cohort study. Among 14 patients with rheumatic manifestations, ICI therapy was discontinued in 8 patients, temporarily withheld in 3 patients and continued in 3 patients. Among the 8 patients who stopped ICI treatment, 3 patients experienced remission and had their anti-rheumatic medicine withdrawn, while 5 patients continued on anti-rheumatic medication with low disease activity. In the 6 patients with continued or temporarily withheld ICI therapy, all patients but one continued on anti-rheumatic medication with low or moderate disease activity (one patient with ICI therapy withheld was classified as 'unknown' for anti-rheumatic medication and rheumatic disease status).

Findings from recent large cohort studies indicated that IA appears to be the most common type of rheumatic irAEs, mimicking seronegative RA and PMR [50,51]. Most patients with IA have been reported to be seronegative for anti-CCP antibodies or RF. Meanwhile, in general, imaging studies including magnetic resonance imaging and ultrasonography have shown joint erosion, tenosynovitis, Doppler-positive synovitis and joint effusion [52–54]. It is therefore important for the rheumatologist to recognize IA as an irAEs related to ICI therapy and to understand the diagnosis and management of IA with atypical signs/symptoms of arthralgia and myalgia, given the expected increase use of ICIs in cancer patients in the future.

Inflammatory and non-inflammatory muscle disease

Myositis is less common than IA (Table 1). One retrospective study which included 654 patients receiving anti-PD-1 therapy showed that biopsy-proven myositis was diagnosed in five patients (0.8%) [55]. A severe case of dermatomyositis related to anti-CTLA-4 mAb administration for metastatic melanoma has been reported [56]. The signs/symptoms were initially resolved by treatment with steroids and discontinuation of ICI therapy. The patient was again treated with anti-CTLA-4 mAb on recurrence, followed by prompt flaring of dermatomyositis. Recently, three cases of ICI-related muscle disorder were reported in patients with pulmonary adenocarcinoma by French investigators [57]. These patients had initially moderate bilateral proximal weakness with elevated levels of serum creatine kinase. Two patients subsequently developed myastheniform symptoms while one patient's case was complicated by severe myocarditis. One case of ICI-related myo-fasciitis has also been reported [58]. The muscle symptoms were resolved by treatment with steroids and discontinuation of ICI therapy, while myocarditis was irreversible. A recent retrospective study of 220 patients with anti-PD-1 therapy showed that 2 patients (0.9%) developed symptomatic inflammatory myositis with fasciitis in lower extremities [59]. The French group above also reported that non-inflammatory musculoskeletal conditions developed in 15 patients of 35 rheumatic irAEs among 524 patients receiving ICIs (2.8%) [48]. The symptoms were characterized by arthralgia of proximal or distal joints, which worsened with physical activity and improved with rest, and the absence of joint stiffness. Elevated levels of CRP were observed in 4 patients, likely associated with their malignancies since increased CRP values had been present prior to the development of rheumatic symptoms. The patients were managed successfully with NSAIDs, analgesics and/or physiotherapy, and no modification of ICI therapy was necessary.

Other rheumatic immune-related adverse events

Sicca syndrome including dry mouth with or without dry eyes has been reported in patients receiving ICI therapy [46,54,60]. Johns Hopkins investigators described four patients who developed sicca syndrome associated with ICI therapy [54]. Three patients had positive results for ANA while one patient was positive for anti-La/SSB antibodies with low titer. Dry mouth tended to be more severe than dry eyes. Most patients with ICI-related siccas syndrome have reported not to have concomitant parotitis, in contrast to the typical form of sicca syndrome including Sjögren's syndrome.

irAEs involving blood vessels such as vasculitides are quite rare and appear to be at a reported rate of less than 1% [61]. Recent work elucidated the molecular mechanisms involved in immune checkpoint-mediated medium and large vessel vasculitis such as giant cell arteritis (GCA) [62], which may be the most commonly described vascular IRAE in patients undergoing ICI therapy. Two cases of GCA with PMR following anti-CTLA-4 mAb administration were reported, with high responsiveness to steroids [63]. One case of isolated lymphocytic uterine vasculitis and digital vasculitis was also reported [64]. More recently, a case of small vessel vasculitis during anti-CTLA-4 mAb therapy was reported [65]. After receiving anti-CTLA-4 mAb therapy for melanoma, this patient developed digital vasculitis with negative results for ANA, cytoplasmic and perinuclear anti-neutrophil cytoplasmic antibody (C- and P-ANCA), and cryoglobulin. Despite intensive treatment with high dose steroids, epoprostenol, botulinum toxin and rituximab, the patient had to undergo multiple distal digital amputations.

One patient with melanoma developed nephrotic syndrome after two doses of anti-CTLA-4 mAb [66], with results from a kidney biopsy suggestive of lupus nephritis. Glomerulonephritis resolved following treatment with anti-coagulation and steroids. Circulating anti-double-stranded deoxyribonucleic acid (dsDNA) antibodies appeared concomitantly and subsided following withdrawal of ipilimumab.

Cases of sarcoidosis or sarcoid-like reactions related to ICI therapy have also been reported [60,67,68]. Biopsy is the gold standard for evaluation of new lesions to guide management and to minimize the risk of premature discontinuation of ICI therapy with the potential to provide durable tumor response. Management of patients should be tailored

for each individual situation. In general, asymptomatic patients benefiting from ICI therapy with sufficient tumor response can be continued on therapy with appropriate monitoring, while symptomatic patients may need long courses of steroids or secondary immunosuppressants to control the inflammatory process and avoid organ dysfunction and fibrosis caused by sarcoidosis or sarcoid-like reactions.

Non-rheumatic immune-related adverse events

Skin manifestations are the most common irAEs in all ICIs [6,69], including rash, vitiligo, pruritus and bullous pemphigoid. A recent meta-analysis showed that development of a rash with ipilimumab is fairly common, with mild cases occurring in about 24% of patients and high-grade rashes occurring in 2% [70]. In patients with anti-PD-1, skin toxicities have been reported to occur in 30–40% [71–74]. On the other hand, severe cutaneous irAEs such as toxic epidermal necrolysis rarely developed [6,69].

Enterocolitis as gastrointestinal irAEs are manifested by diarrhea, obstruction, perforation and toxic megacolon [75]. Onset is usually 10–12 weeks following the commencement of treatment [75–77]. Diarrhea occurs in up to 30% of patients receiving anti-CTLA-4 mAb therapy and less frequently in patients undergoing anti-PD-1 therapy [6]. Enterocolitis is most pronounced in patients treated with combination therapy [6,78]. Colonoscopic and histologic findings resemble those observed in inflammatory bowel disease [79].

Several endocrinopathies have been reported in patients receiving ICI therapy, with thyroiditis being the most common, often presenting as hypothyroidism but occasionally as hyperthyroidism, occurring in 6–20% of patients with ICI therapy [80–82]. The pituitary gland can also be affected by ICI therapy, manifesting as hypophysitis, which can occur up to 1–16% of patients [2,39,40,83,84]. Other endocrinopathies include autoimmune diabetes mellitus (DM) or type 1 DM, pancreatitis, hypogonadism and primary adrenal insufficiency [80,81]. Although the acute inflammatory process can be treated, most patients with ICI-induced endocrinopathies develop long-term sequelae and require long-term hormone replacement therapy [81].

Neurologic irAEs are less frequently reported and include paresthesia, altered sensation, aseptic meningitis, encephalopathy, seizures, transverse myelitis, acute and chronic inflammatory demyelinating polyneuropathy, metabolic myopathy, Guillain-Barré syndrome and myasthenia gravis-like syndrome [85].

Pneumonitis is found in less than 5% of patients, ranging from dyspnea to hypoxic respiratory failure [86,87]. The median time to onset is 2.8 months [87]. High dose steroids therapy is required for moderate to severe pneumonitis. ICI-induced pneumonitis is reported with both anti-PD-1 and anti-CTLA-4 therapy and occurs more often with combination therapy [86].

Autoimmune hepatitis is manifested as elevated levels of hepatic enzymes and occurs in up to 5% of patients [2,39,40,72,84,88]. Liver biopsy reveals a pan lobular active hepatitis picture with a predominant CD8-positive inflammatory infiltrate [89]. More rarely, predominant injury to bile ducts can be seen with mild portal mononuclear infiltrate around proliferated bile ductules.

Myocarditis related to ICI therapy has been rarely reported to cause severe irAEs [90]. With the increased application of ICI therapy, incidence of ICI-induced myocarditis is seen to rise over time. A recent report indicated that there were 46 deaths among the 101 patients with severe myocarditis following ICI therapy [91]. Fatality rate was higher with combination therapy than with monotherapy. Myocarditis induced by ICIs tends to occur early after treatment initiation, has a generally fulminant course and responds to higher steroids doses [92].

Other reported ICI-mediated irAEs include uveitis, conjunctivitis, scleritis, retinitis, pericarditis, acute kidney injury, acute interstitial nephritis, rhabdomyolysis, hemolytic anemia, thrombocytopenia, neutropenia and hemophilia [5,60,93–96].

Immune-related adverse events with preexisting rheumatic diseases

While the underlying mechanisms involved in the development of irAEs are not completely understood, the nonspecific upregulation of T cell activation and the suppression of Treg activity resulting from ICI treatment could conceivably exacerbate inflammation and autoimmunity in patients with preexisting autoimmune diseases. It is important to understand whether irAE development in patients with preexisting rheumatic diseases represents flares of their disease or new autoimmune events following ICI therapy. Of note is the fact that patients with preexisting autoimmune or rheumatic disease were typically excluded from the original trials, resulting in a relative paucity of data to fully address this issue. Retrospective analyses have demonstrated that a flare of preexisting autoimmune disease was induced by ICI therapy in 6–43% of patients with preexisting autoimmune disease and that new irAEs developed in 16–33% of the cohorts [97–100]. In general, flares were mild, occurred more often in those with active autoimmune disease, did not lead to discontinuation of ICI therapy, and were readily manageable with standard therapies when intervened in a timely fashion [5]. While preexisting autoimmune diseases should not be an absolute contraindication to ICIs, a careful assessment of disease activity is important prior to starting ICI therapy because of the risk of potential flares.

Management of immune related adverse events in cancer treatment

No definitive prospective trial for the treatment of irAEs has been conducted, and therefore the best approaches and recommendations are based on expert consensus opinion [3]. Several recent publications proposed useful clinical recommendations for the management of irAEs [5,93,101]. The diagnosis of irAEs is primarily clinical, and most patients do

not express the more generic autoantibodies. Many of the initial symptoms, such as arthralgia and fatigue, are relatively nonspecific and can potentially arise from comorbidities or concomitant use of other medications. Approach to the diagnosis and management of irAEs always includes a thorough evaluation for infection. Most patients with irAEs are initially treated with steroids and supportive therapy. The initial steroid dose depends on the relative disease severity, the relative degree of end-organ damages and the presence of potentially life-threatening signs/symptoms [5,93,101].

irAEs are graded according to the National Cancer Institute Common Terminology Criteria for Adverse Events (CTCAE) [102], which were developed primarily to standardize reporting of adverse events for clinical trials, although they are included in toxicity management algorithms in recent irAEs guidelines [5,93,101]. As general recommendation guidelines, for grade 1 toxicities, ICI therapy may be continued with close monitoring, with the exception of some neurologic (such as aseptic meningitis, encephalitis and transverse myelitis), hematologic (such as aplastic anemia, hemolytic uremic syndrome, thrombotic thrombocytopenic purpura and hemophilia), and cardiac toxicities (such as myocarditis, pericarditis and arrhythmia). For grade 2 toxicities, ICI therapy should be withheld, and generally lower doses of steroids may be administered. For grade 3 toxicities, ICI therapy should be withheld, and high doses of steroids may be administered with a gradual tapering course with resolution of signs/symptoms. Grade 4 toxicities warrant permanent discontinuation of ICIs, with the possible exception of endocrinopathies controlled by hormone or insulin replacement. Of note is that for the relative rate situations where steroids are not effective, other immunosuppressive agents would need to be used, taken into consideration the patients' overall performance status and end-organ functions. For non-life-threatening rheumatic events such as IA, while there are no clear guidelines, published reports suggest that most patients respond well to moderate doses of steroids [5,93,101]. Occasionally, MTX or TNFi might be necessary to allow for quicker tapering of steroids. Meanwhile, severe colitis will require discontinuation of ICIs and treatment with high dose steroids and possibly other immunosuppressive drugs such as TNFi. Recent large observational studies have demonstrated that treatment with TNFi is not associated with increased risks of tumor development, cancer progression, recurrence or survival when used to treat IA such as RA [103,104]. However, it should be noted that the risk for tumor progression or impaired cancer response is theoretically possible with TNFi [105].

The decision to recommence ICI therapy following resolution of high-grade irAEs represents a challenge for rheumatologists as well as oncologists. The safety of temporarily withholding ICI therapy in patients who developed high-grade irAEs with the combination of ipilimumab/nivolumab has been studied [106]. This retrospective analysis was to evaluate the safety and efficacy of re-challenging 80 patients with anti-PD-1 monotherapy who discontinued anti-CTLA-4/anti-PD-1 combination therapy for metastatic melanoma due to clinically significant irAEs (including colitis, hepatitis and pneumonitis). Fourteen patients (18%) had recurrent irAEs at a median of 14 days following resumption of prior ICI therapy (including 1 patient with grade 5 Steven-Johnson syndrome). Moreover, distinct toxicities occurred in an additional 17 (21%) patients. Of the 14 patients with recurrence of the same irAEs, 7 had grade 3–4 toxicities, and 10 discontinued treatment due to the recurrent irAEs. Colitis was less likely to recur than other irAEs, with only 2 of 33 (6%) patients experiencing recurrent colitis or diarrhea with anti-PD-1 resumption. With the exception of endocrine toxicities which can be treated with hormone replacement therapy, recent guidelines recommend permanent discontinuation of ICIs following a CTCAE grade 4 toxicity [5,93,101]. Due to the potential for morbidity and mortality, permanent discontinuation for grade 1 cardiac toxicities and grade 3 hepatitis, pneumonitis, neurologic, hematologic and ophthalmologic toxicities are recommended [5,93,101]. Prospective studies are needed to determine whether resumption of anti-PD-1 maintenance is beneficial for patients who cease combination ICI therapy due to toxicity.

Conclusions

Despite their proven efficacies in the treatment of various human neoplasms, ICIs can cause severe irAEs that limit their full therapeutic benefits and result in considerable morbidity and mortality. The role of the rheumatologist will be of increasing importance as ICI therapy becomes more established in cancer treatment, given its demonstrated benefits in many cancer patients, including those with advanced diseases refractory to other treatment modalities. As shown in recent large cohort studies, increased awareness of IA, as well as other rheumatic manifestations, as an adverse association with ICI therapy is required to make the correct diagnosis and determine the correct course of action. The CTCAE grading system has recently been noted to be insufficiently suitable for grading the severity of many rheumatic complications, and while rheumatology-specific modifications of the CTCAE have been proposed [107], these changes have not been applied to ICI trials to date. Rheumatic irAEs can be late adverse events occurring up to 2 years following initiation of ICI therapy [60,105], and occasionally even after the patient has stopped the therapy. Until larger, well-powered studies are available to help determine in a more precise way the potential risks of ICI therapy, careful evaluation of the risks and benefits and individual preferences need to be considered when making decisions regarding ICI therapy for patients with cancer and autoimmune disease.

Conflict of interest

None.

Funding

This study was supported in part by a grant of the Ministry of Health, Labour, and Welfare, Japan [Grant Number 150401-01 (C.M.) and 180101-01 (C.M.)], JSPS KAKENHI Grant Numbers JP16H05345 (C.M.), JP18H02782 (K.O.), and JP17K10008 (R.H.).

References

1. Ribas A, Wolchok JD. Cancer immunotherapy using checkpoint blockade. Science. 2018;359(6382):1350–5.
2. Hodi FS, O'Day SJ, McDermott DF, Weber RW, Sosman JA, Haanen JB, et al. Improved survival with ipilimumab in patients with metastatic melanoma. N Engl J Med. 2010;363(8): 711–23.
3. Postow MA, Sidlow R, Hellmann MD. Immune-related adverse events associated with immune checkpoint blockade. N Engl J Med. 2018;378(2):158–68.
4. Suarez-Almazor ME, Kim ST, Abdel-Wahab N, Diab A. Immune-related adverse events with use of checkpoint inhibitors for immunotherapy of cancer. Arthritis Rheumatol. 2017; 69(4):687–99.
5. Brahmer JR, Lacchetti C, Schneider BJ, Atkins MB, Brassil KJ, Caterino JM, et al. Management of immune-related adverse events in patients treated with immune checkpoint inhibitor therapy: American Society of Clinical Oncology Clinical Practice Guideline. J Clin Oncol. 2018;36(17):1714–68.
6. Michot JM, Bigenwald C, Champiat S, Collins M, Carbonnel F, Postel-Vinay S, et al. Immune-related adverse events with immune checkpoint blockade: a comprehensive review. Eur J Cancer. 2016; 54:139–48.
7. Iwasaki A, Medzhitov R. Control of adaptive immunity by the innate immune system. Nat Immunol. 2015;16(4):343–53.
8. Chen L, Flies DB. Molecular mechanisms of T cell co-stimulation and co-inhibition. Nat Rev Immunol. 2013;13(4):227–42.
9. Rudd CE, Taylor A, Schneider H. CD28 and CTLA-4 coreceptor expression and signal transduction. Immunol Rev. 2009; 229(1):12–26.
10. Martinez-Lostao L, Anel A, Pardo J. How do cytotoxic lymphocytes kill cancer cells? Clin Cancer Res. 2015;21(22):5047–56.
11. Luo X, Miller SD, Shea LD. Immune tolerance for autoimmune disease and cell transplantation. Annu Rev Biomed Eng. 2016; 18:181–205.
12. Walunas TL, Lenschow DJ, Bakker CY, Linsley PS, Freeman GJ, Green JM, et al. CTLA-4 can function as a negative regulator of T-cell activation. Immunity 1994;1(5):405–13.
13. Leach DR, Krummel MF, Allison JP. Enhancement of antitumor immunity by CTLA-4 blockade. Science. 1996;271(5256): 1734–6.
14. Linsley PS, Greene JL, Brady W, Bajorath J, Ledbetter JA, Peach R. Human B7-1 (CD80) and B7-2 (CD86) bind with similar avidities but distinct kinetics to CD28 and CTLA-4 receptors. Immunity. 1994;1(9):793–801.
15. Zou W, Chen L. Inhibitory B7-family molecules in the tumour microenvironment. Nat Rev Immunol. 2008;8(6):467–77.
16. Qureshi OS, Zheng Y, Nakamura K, Attridge K, Manzotti C, Schmidt EM, et al. Trans-endocytosis of CD80 and CD86: a molecular basis for the cell-extrinsic function of CTLA-4. Science. 2011;332(6029):600–3.
17. Wing K, Onishi Y, Prieto-Martin P, Yamaguchi T, Miyara M, Fehervari Z, et al. CTLA-4 control over Foxp3^{+} regulatory T cell function. Science. 2008;322(5899):271–5.
18. Tivol EA, Borriello F, Schweitzer AN, Lynch WP, Bluestone JA, Sharpe AH. Loss of CTLA-4 leads to massive lymphoproliferation and fatal multiorgan tissue destruction, revealing a critical negative regulatory role of CTLA-4. Immunity. 1995;3(5): 541–7.
19. Waterhouse P, Penninger JM, Timms E, Wakeham A, Shahinian A, Lee KP, et al. Lymphoproliferative disorders with early lethality in mice deficient in Ctla-4. Science. 1995; 270(5238):985–8.
20. Dong H, Strome SE, Salomao DR, Tamura H, Hirano F, Flies DB, et al. Tumor-associated B7-H1 promotes T-cell apoptosis: a potential mechanism of immune evasion. Nat Med. 2002;8(8): 793–800.
21. Boussiotis VA. Molecular and biochemical aspects of the PD-1 checkpoint pathway. N Engl J Med. 2016;375(18):1767–78.
22. Keir ME, Butte MJ, Freeman GJ, Sharpe AH. PD-1 and its ligands in tolerance and immunity. Annu Rev Immunol. 2008; 26:677–704.
23. Nishimura H, Nose M, Hiai H, Minato N, Honjo T. Development of lupus-like autoimmune diseases by disruption of the PD-1 gene encoding an ITIM motif-carrying immunoreceptor. Immunity. 1999;11(2):141–51.
24. Nishimura H, Okazaki T, Tanaka Y, Nakatani K, Hara M, Matsumori A, et al. Autoimmune dilated cardiomyopathy in PD-1 receptor-deficient mice. Science. 2001;291(5502):319–22.
25. Baumeister SH, Freeman GJ, Dranoff G, Sharpe AH. Coinhibitory pathways in immunotherapy for cancer. Annu Rev Immunol. 2016;34:539–73.
26. Ribas A. Adaptive immune resistance: how cancer protects from immune attack. Cancer Discov. 2015;5(9):915.
27. Hodi FS, Mihm MC, Soiffer RJ, Haluska FG, Butler M, Seiden MV, et al. Biologic activity of cytotoxic T lymphocyte-associated antigen 4 antibody blockade in previously vaccinated metastatic melanoma and ovarian carcinoma patients. Proc Natl Acad Sci U S A. 2003;100(8):4712–7.
28. Phan GQ, Yang JC, Sherry RM, Hwu P, Topalian SL, Schwartzentruber DJ, et al. Cancer regression and autoimmunity induced by cytotoxic T lymphocyte-associated antigen 4 blockade in patients with metastatic melanoma. Proc Natl Acad Sci USA. 2003;100(14):8372–7.
29. Ribas A. Clinical development of the anti-CTLA-4 antibody tremelimumab. Semin Oncol. 2010;37(5):450–4.
30. Peggs KS, Quezada SA, Chambers CA, Korman AJ, Allison JP. Blockade of CTLA-4 on both effector and regulatory T cell compartments contributes to the antitumor activity of anti-CTLA-4 antibodies. J Exp Med. 2009;206(8):1717–25.
31. Kremer JM, Westhovens R, Leon M, Di Giorgio E, Alten R, Steinfeld S, et al. Treatment of rheumatoid arthritis by selective inhibition of T-cell activation with fusion protein CTLA4Ig. N Engl J Med. 2003;349(20):1907–15.
32. Harigai M, Ishiguro N, Inokuma S, Mimori T, Ryu J, Takei S, et al. Postmarketing surveillance of the safety and effectiveness of abatacept in Japanese patients with rheumatoid arthritis. Mod Rheumatol. 2016;26(4):491–8.
33. Golstein P, Griffiths GM. An early history of T cell-mediated cytotoxicity. Nat Rev Immunol. 2018;18(8):527–35.
34. Ahmadzadeh M, Johnson LA, Heemskerk B, Wunderlich JR, Dudley ME, White DE, et al. Tumor antigen-specific CD8 T cells infiltrating the tumor express high levels of PD-1 and are functionally impaired. Blood. 2009;114(8):1537–44.
35. Zou W. Regulatory T cells, tumour immunity and immunotherapy. Nat Rev Immunol. 2006;6(4):295–307.
36. Shah NJ, Kelly WJ, Liu SV, Choquette K, Spira A. Product review on the Anti-PD-L1 antibody atezolizumab. Hum Vaccin Immunother. 2018;14(2):269–76.
37. Sun C, Mezzadra R, Schumacher TN. Regulation and function of the PD-L1 checkpoint. Immunity. 2018;48(3):434–52.
38. Postow MA, Callahan MK, Wolchok JD. Immune checkpoint blockade in cancer therapy. J Clin Oncol. 2015;33(17):1974–82.
39. Wolchok JD, Kluger H, Callahan MK, Postow MA, Rizvi NA, Lesokhin AM, et al. Nivolumab plus ipilimumab in advanced melanoma. N Engl J Med. 2013;369(2):122–33.
40. Larkin J, Chiarion-Sileni V, Gonzalez R, Grob JJ, Cowey CL, Lao CD, et al. Combined nivolumab and ipilimumab or monotherapy in untreated melanoma. N Engl J Med. 2015;373(1): 23–34.

41. Friedman CF, Proverbs-Singh TA, Postow MA. Treatment of the immune-related adverse effects of immune checkpoint inhibitors: a review. JAMA Oncol. 2016;2(10):1346–53.
42. Wu Y, Shi H, Jiang M, Qiu M, Jia K, Cao T, et al. The clinical value of combination of immune checkpoint inhibitors in cancer patients: a meta-analysis of efficacy and safety. Int J Cancer. 2017;141(12):2562–70.
43. Zhang B, Wu Q, Zhou YL, Guo X, Ge J, Fu J. Immune-related adverse events from combination immunotherapy in cancer patients: a comprehensive meta-analysis of randomized controlled trials. Int Immunopharmacol. 2018; 63:292–8.
44. Ohnuma K, Dang NH, Morimoto C. Revisiting an old acquaintance: CD26 and its molecular mechanisms in T cell function. Trends Immunol. 2008;29(6):295–301.
45. Cappelli LC, Brahmer JR, Forde PM, Le DT, Lipson EJ, Naidoo J, et al. Clinical presentation of immune checkpoint inhibitor-induced inflammatory arthritis differs by immunotherapy regimen. Semin Arthritis Rheum. 2018. [Epub ahead of print] DOI: 10.1016/j.semarthrit.2018.02.011.
46. Cappelli LC, Gutierrez AK, Bingham CO, 3rd, Shah AA. Rheumatic and musculoskeletal immune-related adverse events due to immune checkpoint inhibitors: a systematic review of the literature. Arthritis Care Res. 2017;69(11):1751–63.
47. Naidoo J, Cappelli LC, Forde PM, Marrone KA, Lipson EJ, Hammers HJ, et al. Inflammatory arthritis: a newly recognized adverse event of immune checkpoint blockade. Oncologist. 2017;22(6):627–30.
48. Kostine M, Rouxel L, Barnetche T, Veillon R, Martin F, Dutriaux C, et al. Rheumatic disorders associated with immune checkpoint inhibitors in patients with cancer-clinical aspects and relationship with tumour response: a single-centre prospective cohort study. Ann Rheum Dis. 2018;77(3):393–8.
49. Lidar M, Giat E, Garelick D, Horowitz Y, Amital H, Steinberg-Silman Y, et al. Rheumatic manifestations among cancer patients treated with immune checkpoint inhibitors. Autoimmun Rev. 2018;17(3):284–9.
50. Cappelli LC, Naidoo J, Bingham CO, 3rd, Shah AA. Inflammatory arthritis due to immune checkpoint inhibitors: challenges in diagnosis and treatment. Immunotherapy. 2017; 9(1):5–8.
51. Abdel-Rahman O, ElHalawani H, Fouad M. Risk of endocrine complications in cancer patients treated with immune check point inhibitors: a meta-analysis. Future Oncol. 2016;12(3): 413–25.
52. Chan MM, Kefford RF, Carlino M, Clements A, Manolios N. Arthritis and tenosynovitis associated with the anti-PD1 antibody pembrolizumab in metastatic melanoma. J Immunother. 2015;38(1):37–9.
53. Albayda J, Bingham CO, 3rd, Shah AA, Kelly RJ, Cappelli L. Metastatic joint involvement or inflammatory arthritis? A conundrum with immune checkpoint inhibitor-related adverse events. Rheumatology (Oxford). 2018;57(4):760–2.
54. Cappelli LC, Gutierrez AK, Baer AN, Albayda J, Manno RL, Haque U, et al. Inflammatory arthritis and sicca syndrome induced by nivolumab and ipilimumab. Ann Rheum Dis. 2017; 76(1):43–50.
55. Liewluck T, Kao JC, Mauermann ML. PD-1 inhibitor-associated myopathies: emerging immune-mediated myopathies. J Immunother. 2018;41(4):208–11.
56. Sheik Ali S, Goddard AL, Luke JJ, Donahue H, Todd DJ, Werchniak A, et al. Drug-associated dermatomyositis following ipilimumab therapy: a novel immune-mediated adverse event associated with cytotoxic T-lymphocyte antigen 4 blockade. JAMA Dermatol. 2015;151(2):195.
57. Gallay L, Bourgeois-Vionnet J, Joubert B, Streichenberger N, Hot A. Muscular disorder related to immune checkpoint inhibitors: forewarned is forearmed. Neuro Oncol. 2018;20(6):861–2.
58. Daoussis D, Kraniotis P, Liossis SN, Solomou A. Immune checkpoint inhibitor-induced myo-fasciitis. Rheumatology (Oxford). 2017;56(12):2161.
59. Narváez J, Juarez-Lopez P, Lluch J, Narváez JA, Palmero R, Garcia Del Muro X, et al. Rheumatic immune-related adverse events in patients on anti-PD-1 inhibitors: fasciitis with myositis syndrome as a new complication of immunotherapy. Autoimmun Rev. 2018;17(10):1040–5.
60. Le Burel S, Champiat S, Mateus C, Marabelle A, Michot JM, Robert C, et al. Prevalence of immune-related systemic adverse events in patients treated with anti-Programmed cell Death 1/anti-Programmed cell Death-Ligand 1 agents: A single-centre pharmacovigilance database analysis. Eur J Cancer. 2017; 82: 34–44.
61. Ipilimumab FDA, label. 2015. https://www.accessdata.fda.gov/drugsatfda_docs/label/2015/125377s073lbl.pdf.
62. Watanabe R, Zhang H, Berry G, Goronzy JJ, Weyand CM. Immune checkpoint dysfunction in large and medium vessel vasculitis. Am J Physiol Heart Circ Physiol. 2017;312(5): H1052–H9.
63. Goldstein BL, Gedmintas L, Todd DJ. Drug-associated polymyalgia rheumatica/giant cell arteritis occurring in two patients after treatment with ipilimumab, an antagonist of CTLA-4. Arthritis Rheumatol. 2014;66(3):768–9.
64. Minor DR, Bunker SR, Doyle J. Lymphocytic vasculitis of the uterus in a patient with melanoma receiving ipilimumab. J Clin Oncol. 2013;31(20):e356
65. Padda A, Schiopu E, Sovich J, Ma V, Alva A, Fecher L. Ipilimumab induced digital vasculitis. J Immunother Cancer. 2018;6(1):12
66. Fadel F, El Karoui K, Knebelmann B. Anti-CTLA4 antibody-induced lupus nephritis. N Engl J Med. 2009;361(2):211
67. Gaughan EM. Sarcoidosis, malignancy and immune checkpoint blockade. Immunotherapy. 2017;9(13):1051–3.
68. Cornejo CM, Haun P, English J, 3rd, Rosenbach M. Immune checkpoint inhibitors and the development of granulomatous reactions. J Am Acad Dermatol. 2018. [Epub ahead of print] DOI: 10.1016/j.jaad.2018.07.051.
69. Sibaud V. Dermatologic reactions to immune checkpoint inhibitors: skin toxicities and immunotherapy. Am J Clin Dermatol. 2018;19(3):345–61.
70. Minkis K, Garden BC, Wu S, Pulitzer MP, Lacouture ME. The risk of rash associated with ipilimumab in patients with cancer: a systematic review of the literature and meta-analysis. J Am Acad Dermatol. 2013;69(3):e121–8.
71. Robert C, Long GV, Brady B, Dutriaux C, Maio M, Mortier L, et al. Nivolumab in previously untreated melanoma without BRAF mutation. N Engl J Med. 2015;372(4):320–30.
72. Robert C, Schachter J, Long GV, Arance A, Grob JJ, Mortier L, et al. Pembrolizumab versus ipilimumab in advanced melanoma. N Engl J Med. 2015;372(26):2521–32.
73. Naidoo J, Page DB, Li BT, Connell LC, Schindler K, Lacouture ME, et al. Toxicities of the anti-PD-1 and anti-PD-L1 immune checkpoint antibodies. Ann Oncol. 2016;27(7):1362.
74. Belum VR, Benhuri B, Postow MA, Hellmann MD, Lesokhin AM, Segal NH, et al. Characterisation and management of dermatologic adverse events to agents targeting the PD-1 receptor. Eur J Cancer. 2016; 60:12–25.
75. Wang DY, Ye F, Zhao S, Johnson DB. Incidence of immune checkpoint inhibitor-related colitis in solid tumor patients: A systematic review and meta-analysis. Oncoimmunology. 2017; 6(10):e1344805.
76. Palmieri DJ, Carlino MS. Immune checkpoint inhibitor toxicity. Curr Oncol Rep. 2018;20(9):72
77. Bertrand A, Kostine M, Barnetche T, Truchetet ME, Schaeverbeke T. Immune related adverse events associated with anti-CTLA-4 antibodies: systematic review and meta-analysis. BMC Med. 2015;13:211.
78. Tandon P, Bourassa-Blanchette S, Bishay K, Parlow S, Laurie SA, McCurdy JD. The risk of diarrhea and colitis in patients with advanced melanoma undergoing immune checkpoint inhibitor therapy: a systematic review and meta-analysis. J Immunother. 2018;41(3):101–8.

79. Adler BL, Pezhouh MK, Kim A, Luan L, Zhu Q, Gani F, et al. Histopathological and immunophenotypic features of ipilimumab-associated colitis compared to ulcerative colitis. J Intern Med. 2018;283(6):568–77.
80. Konda B, Nabhan F, Shah MH. Endocrine dysfunction following immune checkpoint inhibitor therapy. Curr Opin Endocrinol Diabetes Obes. 2017;24(5):337–47.
81. Barroso-Sousa R, Ott PA, Hodi FS, Kaiser UB, Tolaney SM, Min L. Endocrine dysfunction induced by immune checkpoint inhibitors: practical recommendations for diagnosis and clinical management. Cancer. 2018;124(6):1111–21.
82. Morganstein DL, Lai Z, Spain L, Diem S, Levine D, Mace C, et al. Thyroid abnormalities following the use of cytotoxic T-lymphocyte antigen-4 and programmed death receptor protein-1 inhibitors in the treatment of melanoma. Clin Endocrinol (Oxf). 2017;86(4):614–20.
83. Joshi MN, Whitelaw BC, Palomar MT, Wu Y, Carroll PV. Immune checkpoint inhibitor-related hypophysitis and endocrine dysfunction: clinical review. Clin Endocrinol (Oxf). 2016; 85(3):331–9.
84. Eggermont AM, Chiarion-Sileni V, Grob JJ, Dummer R, Wolchok JD, Schmidt H, et al. Prolonged survival in stage III melanoma with ipilimumab adjuvant therapy. N Engl J Med. 2016;375(19):1845–55.
85. Fellner A, Makranz C, Lotem M, Bokstein F, Taliansky A, Rosenberg S, et al. Neurologic complications of immune checkpoint inhibitors. J Neurooncol. 2018;137(3):601–9.
86. Tabchi S, Messier C, Blais N. Immune-mediated respiratory adverse events of checkpoint inhibitors. Curr Opin Oncol. 2016;28(4):269–77.
87. Naidoo J, Wang X, Woo KM, Iyriboz T, Halpenny D, Cunningham J, et al. Pneumonitis in patients treated with anti-programmed death-1/programmed death ligand 1 therapy. J Clin Oncol. 2017;35(7):709–17.
88. Sanjeevaiah A, Kerr T, Beg MS. Approach and management of checkpoint inhibitor-related immune hepatitis. J Gastrointest Oncol. 2018;9(1):220–4.
89. Karamchandani DM, Chetty R. Immune checkpoint inhibitor-induced gastrointestinal and hepatic injury: pathologists' perspective. J Clin Pathol. 2018;71(8):665–71.
90. Ganatra S, Neilan TG. Immune checkpoint inhibitor-associated myocarditis. The Oncologist. 2018;23(8):879–86.
91. Moslehi JJ, Salem JE, Sosman JA, Lebrun-Vignes B, Johnson DB. Increased reporting of fatal immune checkpoint inhibitor-associated myocarditis. Lancet. 2018;391(10124):933.
92. Johnson DB, Balko JM, Compton ML, Chalkias S, Gorham J, Xu Y, et al. Fulminant myocarditis with combination immune checkpoint blockade. N Engl J Med. 2016;375(18):1749–55.
93. Puzanov I, Diab A, Abdallah K, Bingham CO, 3rd, Brogdon C, Dadu R, et al. Managing toxicities associated with immune checkpoint inhibitors: consensus recommendations from the Society for Immunotherapy of Cancer (SITC) Toxicity Management Working Group. J Immunother Cancer. 2017;5: 95.
94. Wanchoo R, Karam S, Uppal NN, Barta VS, Deray G, Devoe C, et al. Adverse renal effects of immune checkpoint inhibitors: a narrative review. Am J Nephrol. 2017;45(2):160–9.
95. Antoun J, Titah C, Cochereau I. Ocular and orbital side-effects of checkpoint inhibitors: a review article. Curr Opin Oncol. 2016;28(4):288–94.
96. Cortazar FB, Marrone KA, Troxell ML, Ralto KM, Hoenig MP, Brahmer JR, et al. Clinicopathological features of acute kidney injury associated with immune checkpoint inhibitors. Kidney Int. 2016;90(3):638–47.
97. Johnson DB, Sullivan RJ, Ott PA, Carlino MS, Khushalani NI, Ye F, et al. Ipilimumab therapy in patients with advanced melanoma and preexisting autoimmune disorders. JAMA Oncol. 2016;2(2):234–40.
98. Gutzmer R, Koop A, Meier F, Hassel JC, Terheyden P, Zimmer L, et al. Programmed cell death protein-1 (PD-1) inhibitor therapy in patients with advanced melanoma and preexisting autoimmunity or ipilimumab-triggered autoimmunity. Eur J Cancer. 2017;75:24–32.
99. Menzies AM, Johnson DB, Ramanujam S, Atkinson VG, Wong ANM, Park JJ, et al. Anti-PD-1 therapy in patients with advanced melanoma and preexisting autoimmune disorders or major toxicity with ipilimumab. Ann Oncol. 2017;28(2):368–76.
100. Richter MD, Pinkston O, Kottschade LA, Finnes HD, Markovic SN, Thanarajasingam U. Brief report: cancer immunotherapy in patients with preexisting rheumatic disease: the Mayo Clinic experience. Arthritis Rheumatol. 2018;70(3):356–60.
101. Haanen J, Carbonnel F, Robert C, Kerr KM, Peters S, Larkin J, et al. Management of toxicities from immunotherapy: ESMO Clinical Practice Guidelines for diagnosis, treatment and follow-up. Ann Oncol. 2017;28(suppl_4):iv119–iv42.
102. U.S. Departments of Health and Human Services. National Institutes of Health. National Cancer Institutes. Common Terminology Criteria for Adverse Events (CTCAE), 4.03. Bethesda, MD: National Institutes of Health; 2010. [Available from: https://evs.nci.nih.gov/ftp1/CTCAE/CTCAE_4.03].
103. Mercer LK, Askling J, Raaschou P, Dixon WG, Dreyer L, Hetland ML, et al. Risk of invasive melanoma in patients with rheumatoid arthritis treated with biologics: results from a collaborative project of 11 European biologic registers. Ann Rheum Dis. 2017;76(2):386–91.
104. Mercer LK, Galloway JB, Lunt M, Davies R, Low AL, Dixon WG, et al. Risk of lymphoma in patients exposed to antitumour necrosis factor therapy: results from the British Society for Rheumatology Biologics Register for Rheumatoid Arthritis. Ann Rheum Dis. 2017;76(3):497–503.
105. Cappelli LC, Shah AA, Bingham CO, 3rd. Immune-related adverse effects of cancer immunotherapy- implications for rheumatology. Rheum. Dis Clin North Am. 2017;43(1):65–78.
106. Pollack MH, Betof A, Dearden H, Rapazzo K, Valentine I, Brohl AS, et al. Safety of resuming anti-PD-1 in patients with immune-related adverse events (irAEs) during combined anti-CTLA-4 and anti-PD1 in metastatic melanoma. Ann Oncol. 2018;29(1):250–5.
107. Woodworth T, Furst DE, Alten R, Bingham CO, 3rd, Yocum D, Sloan V, et al. Standardizing assessment and reporting of adverse effects in rheumatology clinical trials II: the Rheumatology Common Toxicity Criteria v.2.0. J Rheumatol. 2007;34:1401–14.

Biochemical and Biophysical Research Communications 504 (2018) 491–498

Contents lists available at ScienceDirect

Biochemical and Biophysical Research Communications

journal homepage: www.elsevier.com/locate/ybbrc

Targeting CD26 suppresses proliferation of malignant mesothelioma cell via downmodulation of ubiquitin-specific protease 22

Toshihiro Okamoto [a], Hiroto Yamazaki [a], Ryo Hatano [a], Taketo Yamada [b], Yutaro Kaneko [c], C. Wilson Xu [d], Nam H. Dang [e], Kei Ohnuma [a, *], Chikao Morimoto [a]

[a] Department of Therapy Development and Innovation for Immune Disorders and Cancers, Graduate School of Medicine, Juntendo University, Tokyo, Japan
[b] Department of Pathology, Saitama Medical University, Saitama, Japan
[c] Y's AC Company, Tokyo, Japan
[d] Biological Research Institute, CA, USA
[e] Division of Hematology/Oncology, University of Florida Shands Cancer Center, Gainesville, FL, USA

ARTICLE INFO

Article history:
Received 20 August 2018
Accepted 29 August 2018
Available online 6 September 2018

Keywords:
CD26
Ubiquitin-specific protease 22
Malignant pleural mesothelioma
Humanized anti-CD26 monoclonal antibody

ABSTRACT

Malignant pleural mesothelioma (MPM) is an aggressive malignancy arising from mesothelial lining of pleura. It is associated with a poor prognosis, partly due to the lack of a precise understanding of the molecular mechanisms associated with its malignant behavior. In the present study, we expanded on our previous studies on cell cycle control of MPM cells by targeting CD26 molecule with humanized anti-CD26 monoclonal antibody (HuCD26mAb), focusing particularly on ubiquitin-specific protease 22 (USP22). We showed that USP22 protein expression is detected in clinical specimens of MPM and that USP22 knockdown, as well as CD26 knockdown, significantly inhibits the growth and proliferation of MPM cells *in vitro* and *in vivo*. Moreover, depletion of both USP22 and CD26 suppresses MPM cell proliferation even more profoundly. Furthermore, expression levels of USP22 correlate with those of CD26. HuCD26mAb treatment induces a decrease in USP22 level through its interaction with the CD26 molecule, leading to increased levels of ubiquitinated histone H2A and p21. By demonstrating a CD26-related linkage with USP22 in MPM cell inhibition induced by HuCD26mAb, our present study hence characterizes USP22 as a novel target molecule while concurrently suggesting a new therapeutic strategy for MPM.

1. Introduction

Malignant pleural mesothelioma (MPM) is an aggressive malignancy arising from mesothelial lining of pleura [1]. It is generally associated with a history of asbestos exposure and has a very poor prognosis. Once rare, the incidence of MPM has increased in industrialized nations as a result of past wide spread exposure to asbestos [1]. Its incidence is predicted to increase further in the next decades, especially in developing countries where asbestos has not yet been prohibited [1]. Due to the lack of efficacy of conventional treatments, novel therapeutic strategies are urgently needed to improve outcomes [2].

We recently showed that mesothelioma cells expressing high level of CD26 displayed high proliferative activity and invasiveness, and microarray analysis of CD26 knockdown and CD26-transfected mesothelioma cells showed that CD26 expression was closely linked to the expression of genes contributing to cell proliferation and cell cycle regulation [3–5]. We have reported that treatment with anti-CD26 antibody induced G1 cell cycle arrest and enhanced cyclin-dependent kinase inhibitor (CDKI) p21 (CIP1/WAF1) expression [6–8]. More recently, we demonstrated that humanized anti-CD26 monoclonal antibody (HuCD26mAb) exhibited a favorable safety profile and substantial clinical activity in heavily pretreated CD26-positive MPM patients who had previously progressed on conventional standard chemotherapies [9]. However, the precise cellular mechanisms involved in the regulation of

Abbreviations: CD26si, siRNA against CD26; CSC, cancer stem cell; Csh, control shRNA; Csi, control siRNA; CDKI, cyclin-dependent kinase inhibitor; HuCD26mAb, humanized anti-CD26 monoclonal antibody; MPM, malignant pleural mesothelioma; s.c., subcutaneous; USP22, Ubiquitin-specific protease 22; USP22-shRNA, shRNA against USP22.

* Corresponding author. Department of Therapy Development and Innovation for Immune Disorders and Cancers, Graduate School of Medicine, Juntendo University, 2-1-1, Hongo, Bunkyo-ku, Tokyo, 113-8421, Japan
E-mail address: kohnuma@juntendo.ac.jp (K. Ohnuma).

https://doi.org/10.1016/j.bbrc.2018.08.193
0006-291X/

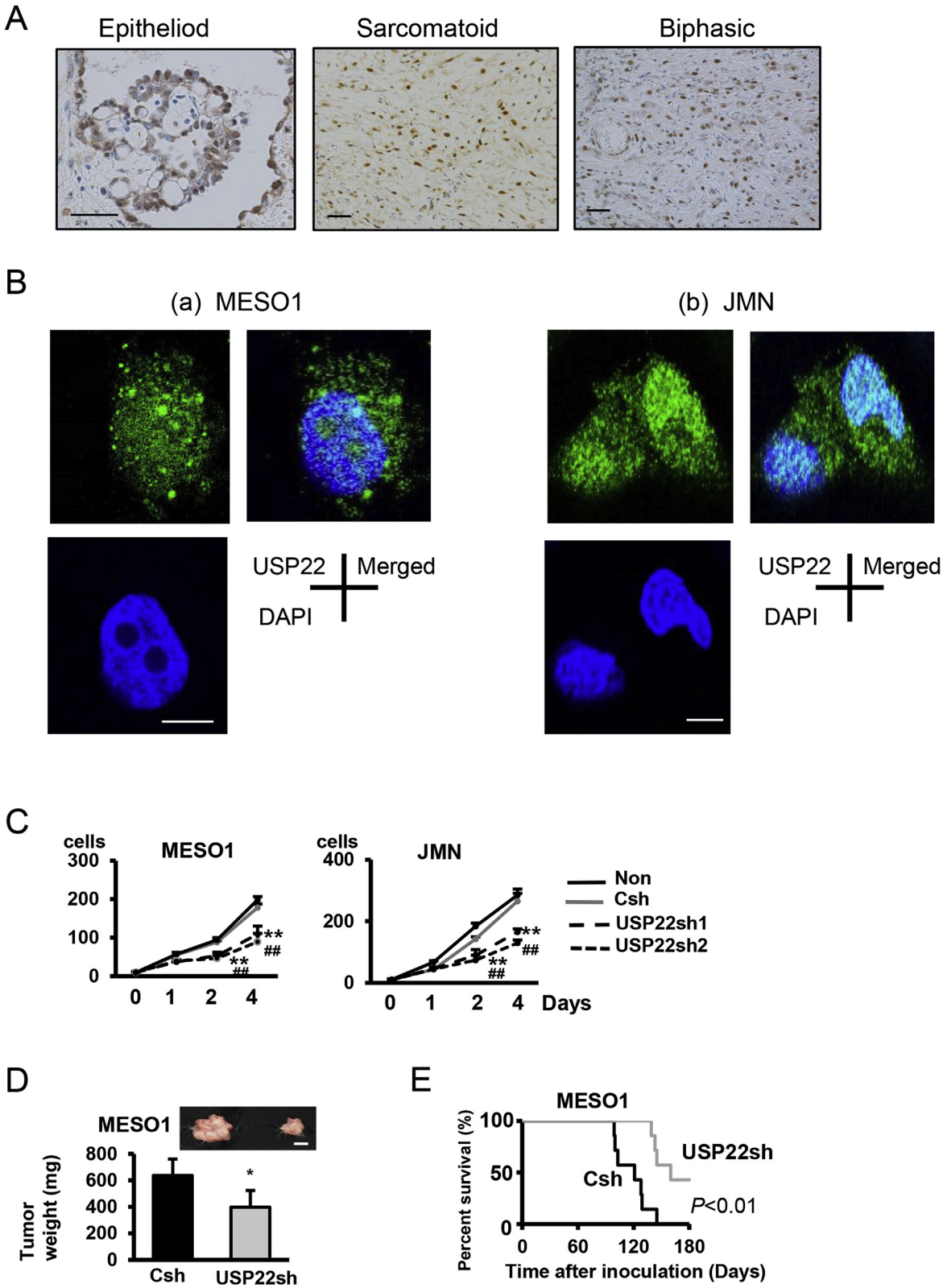

Fig. 1. Suppression of USP22 decreases tumor growth and proliferation in MPM cells.
(A) Representative immunohistochemistry images of USP22 in MPM clinical specimens, including epithelioid, sarcomatoid, and biphasic type. USP22 (brown staining in nuceli) was highly expressed in each MPM type. Scale bars, 50 μm
(B) Confocal microscopy images of USP22 (green) in MPM cell lines, (a) MESO1 and (b) JMN. Nuclei (blue) were stained with DAPI. USP22 was expressed in both the cytosol and the nuclei, and was barely detectable on the cell surface. Scale bars, 10 μm
(C) MESO1 or JMN cells were stably transfected with USP22-shRNA-1, USP22-shRNA-2 or control shRNA (Csh). Cell proliferation was directly examined at the indicated days. Proliferation was significantly decreased following transfection of USP22-shRNA-1 or -shRNA-2. $^{**}p < 0.01$, USP22-shRNA-1 *vs* Csh; $^{\#\#}p < 0.01$, USP22-shRNA-2 vs Csh.
(D) MESO1 cells were stably transfected with USP22-shRNA-1 or control shRNA (Csh), and were inoculated s.c. into the dorsal region of SCID mice (3×10^5 cells/mouse, n = 8). Tumors were resected at day 10 to be weighed. Tumor weight was significantly decreased in the group transplanted with USP22-shRNA-1-transfected cells ($^{*}p < 0.01$).

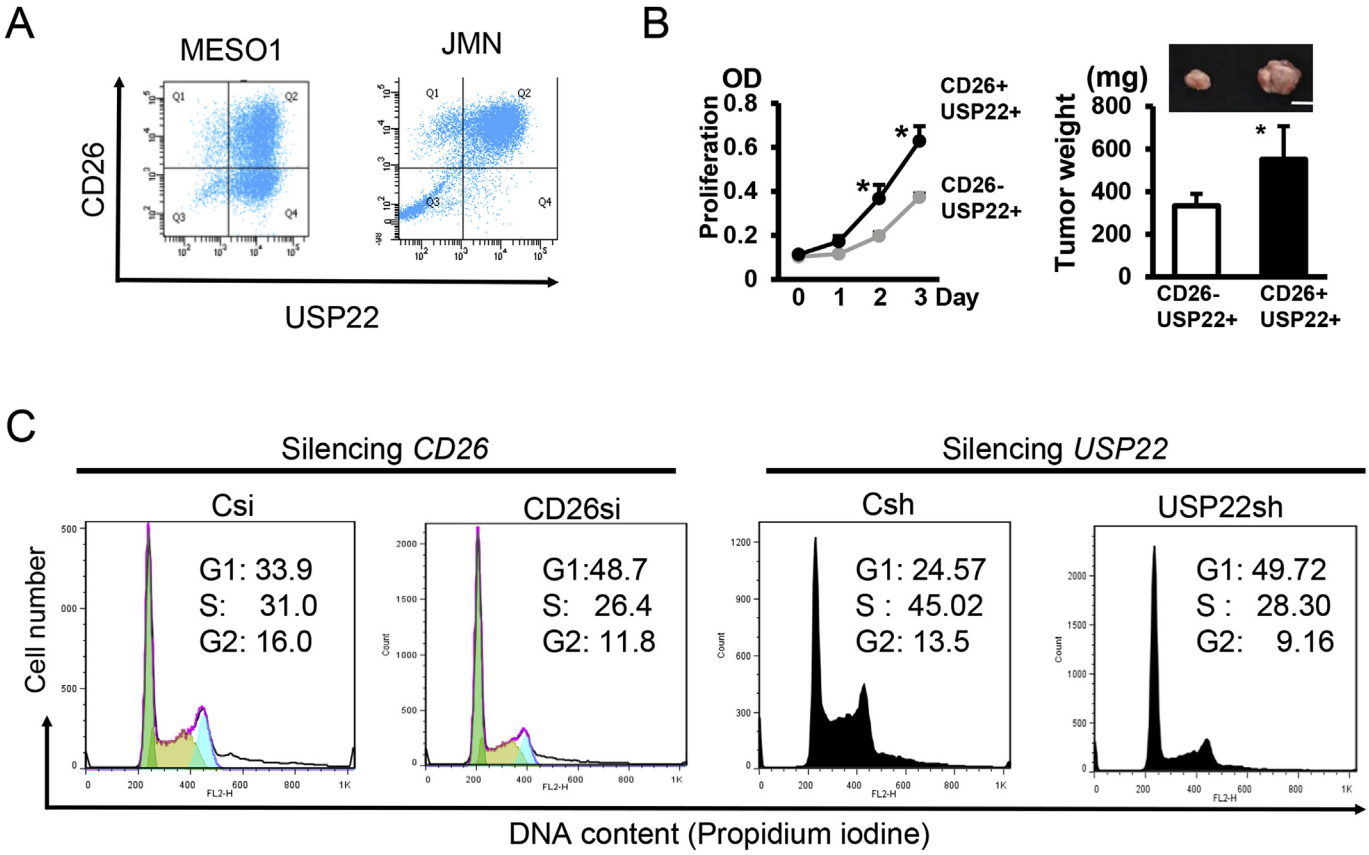

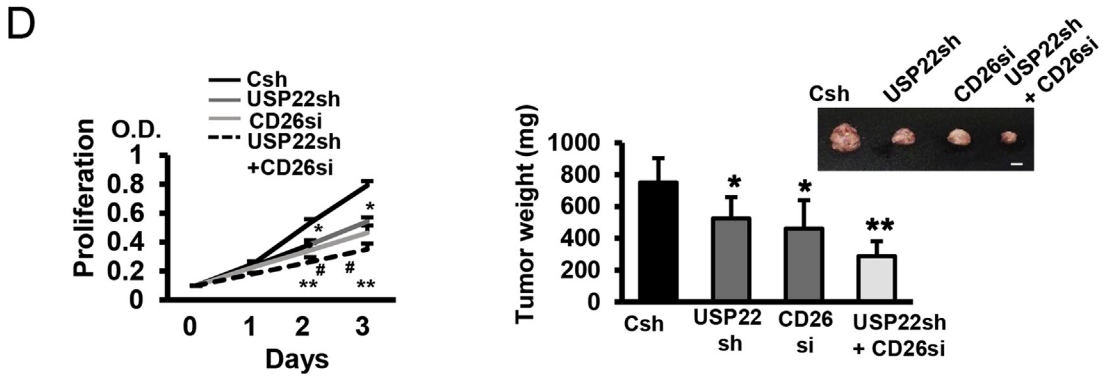

Fig. 2. Silencing of both USP22 and CD26 contributes to a more profound suppression of MPM cell growth than either alone.
(A) Representative 2-D dot plots of CD26 (PE) and USP22 (FITC) in MESO1 and JMN cell lines. MESO1 cells contained CD26 $^{+}$ USP22^{+} and CD26^{-} USP22^{+} populations. JMN cells contained mainly CD26^{+} USP22^{+} with faint amount of CD26^{+} USP22^{-} cells.
(B) CD26 $^{+}$ or CD26^{-} MESO1 cells were sorted by a flow cytometric cell sorter. As shown in **(A)**, both CD26^{+} and CD26^{-} MESO1 cells expressed USP22 (CD26^{+} USP22^{+} and CD26^{-} USP22^{+} populations, respectively). *In vitro* proliferation of CD26^{+} USP22^{+} or CD26^{-} USP22^{+} cells was evaluated by MTT assay at the indicated time points (*left panel*). CD26^{+} USP22^{+} cells exhibited significantly higher proliferative activity than CD26^{-} USP22^{+} cells (*$p < 0.05$). For *in vivo* proliferation assay, each CD26^{+} USP22^{+} and CD26^{-} USP22^{+} cell population was inoculated s.c. into the dorsal region of SCID mice (3×10^5 cells/mouse, each n = 6). Tumors were resected at day 10 to be weighed. Tumor weight was significantly increased in the group transplanted with CD26^{+} USP22^{+} cells (*$p < 0.01$). Representative macroscopic plot is indicated in the upper panel. Scale bar, 1 cm
(C) Cell cycle analysis of the MESO1 cells transfected with CD26-siRNA (CD26si) or control siRNA (Csi) (*left two panels*) and USP22-shRNA-1 (USP22sh) or control shRNA (Csh) (*right two panels*). Representative histograms are shown. Accumulation in G1 phase (green area) with decreased S (greenish brown area) and G2/M (light blue area) phase was observed in CD26si and USP22sh cells compared with each control cell population (similar results were obtained in five independent experiments) ($p < 0.01$).
(D) *In vitro* proliferation of MESO1 cells stably transfected with USP22-shRNA-1 (USP22sh), CD26-siNRA (CD26si), both USP22sh and CD26si, or control shRNA and siRNA (Csh) was evaluated by MTT assay at the indicated time points (*left panel*). The combined knockdown of USP22 and CD26 resulted in a more profound inhibition of MPM cell proliferation, compared with knockdown of USP22 or CD26 alone or Csh (*$p < 0.05$, USP22sh *vs* Csh; #$p < 0.05$, CD26si *vs* Csh; **$p < 0.01$, USP22sh plus CD26si *vs* Csh. For *in vivo* tumor growth assay, (*right panel*) MESO1 cells stably transfected with USP22sh, CD26si, both USP22sh and CD26si, or control shRNA and siRNA (Csh) were inoculated s.c. into the dorsal region of SCID mice (3×10^5 cells/mouse, n = 8). Tumors were resected at day 10 to be weighed. Tumor weight was significantly decreased in the group transplanted with the combined knockdown of USP22 and CD26 (*$p < 0.05$, **$p < 0.01$ *vs* Csh). Representative macroscopic plot is indicated in the upper panel. Scale bar, 1 cm. (For interpretation of the references to color in this figure legend, the reader is referred to the Web version of this article.)

Representative macroscopic plot is indicated in the upper panel. Scale bar, 1 cm
(E) USP22-shRNA-1 or control shRNA (Csh) stably transfected MESO1 cells were injected into SCID mice intravenously (3×10^5 cells/mouse, n = 8). Survival was evaluated by Kaplan-Meier analysis. Survival of mice transplanted with USP22sh MESO1 cells was prolonged significantly. *P* value was calculated by log-rank test. (For interpretation of the references to color in this figure legend, the reader is referred to the Web version of this article.)

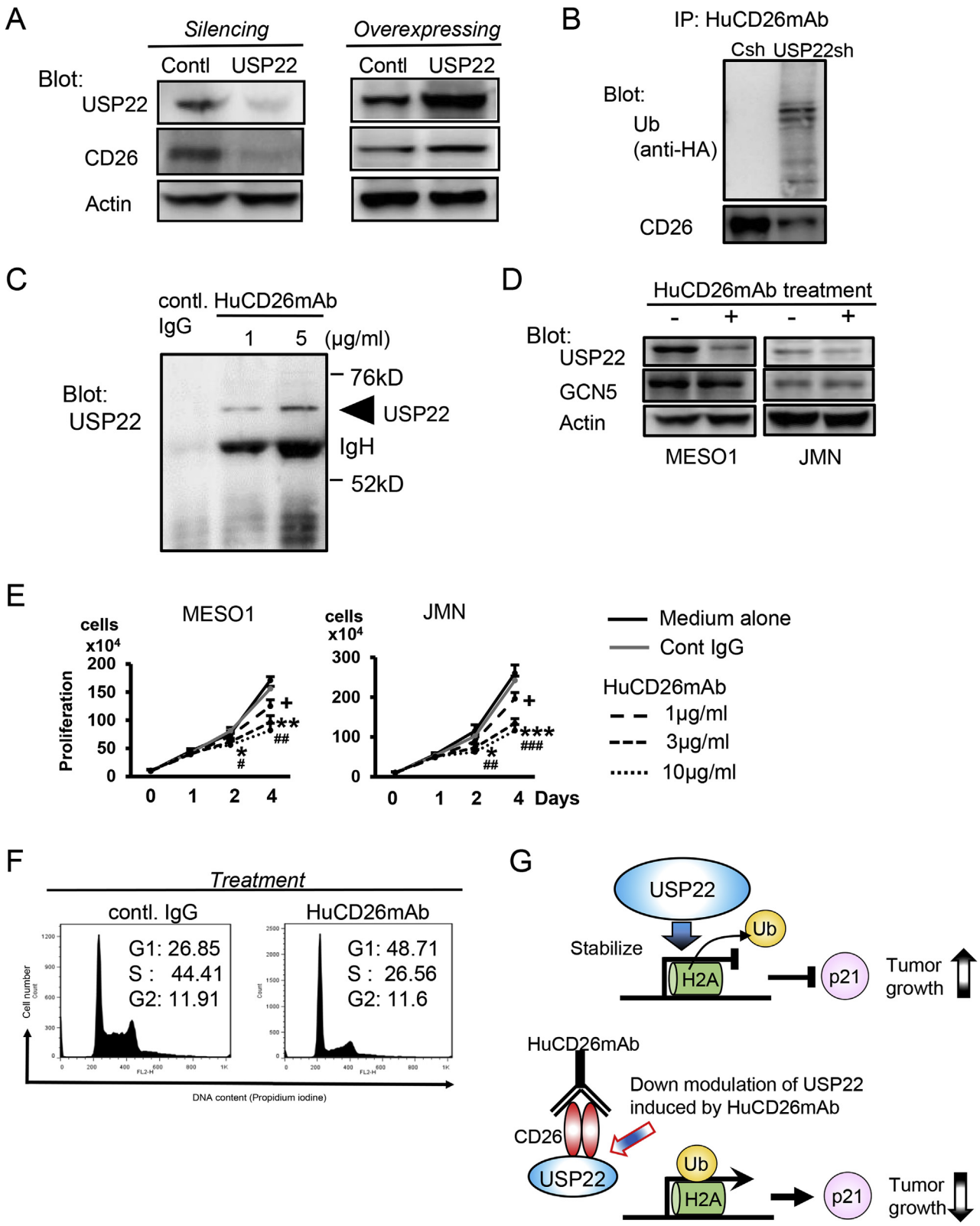

Fig. 3. HuCD26mAb treatment suppresses MPM cell growth, associated with USP22-CD26 complex formation and decreased USP22 expression.
(A) Western blot analysis of expression of USP22 and CD26 in MESO1 cells stably transfected with USP22-shRNA-1 or control shRNA (Csh) (*left panels*) and USP22 expression vector or control vector (Contl) (*right panels*). Decreased expression of CD26 was associated with USP22 knockdown, while increased expression of CD26 was associated with USP22 overexpression. Representative result is shown in the panels, with similar results being obtained in five independent experiments.
(B) MESO1 cells stably transfected with USP22-shRNA-1 (USP22sh) or control shRNA (Csh) were incubated with HA-tagged ubiquitin (5 μM) for 1 h. Cell lysates were immunoprecipitated (IP) with HuCD26mAb and the samples were probed with anti-HA, or anti-CD26, antibodies. Amount of CD26 protein was decreased and immunoprecipitants of HuCD26mAb was significantly ubiquitinated in USP22sh cells (right lane).
(C) Following treatment of MESO1 cells with HuCD26mAb (1 or 5 μg/ml) or control human IgG for 1 h at 37 °C, cell lysates were prepared and immunoprecipitation by protein G-

MPM cell cycle checkpoint by HuCD26mAb have not yet been elucidated.

Ubiquitin-specific protease 22 (USP22) is a novel deubiquitinating enzyme and is also known to be a component of the SAGA (Spt-Ada-Gcn5-Acetyltransferase) transcriptional cofactor complex [10]. It was first identified as one of the cohort of genes that predict the recurrence of metastasis and therapeutic responses of various types of cancers, known as the "death-from-cancer" signature. In cancer cells, USP22 deubiquitylates histone H2A and H2B, and is necessary to counteract heterochromatin silencing and thereby transactivate specific target genes including CDKI p21, contributing to aberrant cell cycle control [10–13]. Overexpression of USP22 is detected in many human cancers and elevated USP22 protein levels are associated with advanced tumor stage and poor prognosis in several cancer types [14]. However, the expression and function of USP22 in MPM remain to be clearly characterized.

In this study, we investigate the role of USP22 in the growth and progression of MPM in association with CD26-mediated cell cycle regulation through p21 expression. We showed that USP22 protein expression is detected in clinical specimens of MPM and that USP22 knockdown, as well as CD26 knockdown, significantly inhibits the growth and proliferation of MPM cells *in vitro* and *in vivo*. Moreover, depletion of both USP22 and CD26 suppresses MPM cell proliferation even more profoundly. Furthermore, expression levels of USP22 correlate with those of CD26. HuCD26mAb treatment induces a decrease in USP22 level through its interaction with the CD26 molecule, leading to increased levels of ubiquitinated histone H2A and p21. By demonstrating a CD26-related linkage with USP22 in MPM cell inhibition induced by HuCD26mAb, our present study hence characterizes USP22 as a novel target molecule while concurrently suggesting a new therapeutic strategy for MPM.

2. Materials and methods

2.1. Cells and antibodies

MPM cell line ACC-MESO1 (MESO1) was obtained from RIKEN Bioresource Center. JMN was a kind gift from Dr. Brenda Gerwin (Laboratory of Human Carcinogenesis, NIH, Bethesda, MD). HuCD26mAb was manufactured and provided by Y's AC Co., Ltd (Tokyo, Japan) [9,15]. Other antibodies used in this study were described in the Supplementary material.

2.2. Histology and immunohistochemistry

MPM specimens from autopsies were generously permitted for research use by the bereaved families. The purpose of the study was explained to all patients and their written, informed consent was obtained. Methods of histology and immunohistochemistry were described in the Supplementary material. Histological studies were conducted in the Department of Pathology of Keio University School of Medicine, after official approval of the Keio University School of Medicine Review Board was obtained (ID number 2012-100-1).

2.3. Flow cytometry and immunofluorescence analysis

Cells were collected, fixed and permeabilized using cytofix and cytoperm solution (BD Biosciences), and washed and stained with appropriate antibodies. For detection of only cell surface molecules, cells were stained without fixation and permeabilization. The samples were analyzed using BD FACSCalibur (BD Biosciences). For cell sorting, BD FACSAria (BD Biosciences) was utilized. Data were analyzed by FACSDiva version 6.1.2. and FlowJo software (Tree Star Inc). Flow cytometric cell cycle analysis by DNA staining with propidium iodide was conducted by the same methods described previously [7]. Immunocytochemistry was conducted by the same methods described previously [16].

2.4. Transfection of shRNA and cDNAs

For transfection of shRNAs, lentiviral plasmids containing USP22 shRNA-1, or -2, or plasmids containing non-targeting control were co-transfected with ViraPower Lentiviral packaging mix to 293FT cells using Lipofectamine 2000 (Invitrogen), generating lentiviral particles. The MPM cell lines were infected with these shRNA-expressing lentiviral particles, and stable cell lines were generated by selection with puromycin (Sigma-Aldrich). For transfection of USP22 expressing vector, MESO1 cells were cultured for 2 days and transfected with full-length cDNA of USP22 subcloned into pDON5 vector (TAKARA BIO Inc) with Lipofectamine reagent. As controls, cells were transfected with pDON5 vector. For siRNA transfection, 3×10^4 cells were cultured for 24 h and CD26 siRNA dissolved in Opti-MEM1 was transfected using Lipofectamine RNAiMAX (Invitrogen). The sequences of oligonucleotides used in this study were described in the Supplementary material.

2.5. Immunoprecipitation and western blotting

Immunoprecipitation was performed as previously described [4,16–18]. Briefly, after cells were treated as indicated, cell lysates were prepared and incubated with HuCD26mAb. The immune complexes were precipitated by protein G-agarose beads to the lysate (GE Healthcare). The incubated beads were centrifuged and washed with ice-cold lysis buffer. The samples were suspended and denatured in SDS sample buffer. Cell lysate and nuclear extract samples for western blotting were prepared and submitted to western blotting analysis as the same method described previously [4,16–18]. Quantification of protein expression was measured by using C-DiGit Blot Scanner (M&S TechnoSystems, Inc).

2.6. In vitro cell proliferation assay and murine xenograft model of tumor progression and survival

Cells were grown to exponential phase and their proliferations were determined by MTT assay or direct counting by the same methods described earlier [4,5].

Female SCID mice (5–6 weeks age) (Charles River) were used for *in vivo* tumor growth experiments by the same method as

agarose was performed. USP22 (bands at an arrow head) was co-precipitated in the presence of HuCD26mAb (right two lanes). Representative result is shown in the panels, with similar results being obtained in five independent experiments. IgH denotes immunoglobulin heavy chain.

(D) Western blot analysis of nuclear extracts of the HuCD26mAb-treated (incubated with 10 μg/ml of HuCD26mAb for 12 h at 37 °C) MESO1 (*left panels*) and JMN (*right panels*) cells. Suppression of USP22 expression with following HuCD26mAb treatment was observed, while expression of GCN5 was not changed. Representative result is shown in the panels, with similar results being obtained in five independent experiments.

(E) Proliferation of MESO1 (*left panel*) and JMN (*right panel*) cells treated with HuCD26mAb was evaluated by MTT assay. Proliferation of each cell line was significantly decreased following HuCD26mAb treatment in a dose-dependent manner (HuCD26mAb *vs* control IgG, $^{+}p < 0.05$, $^{*}p < 0.05$, $^{**}p < 0.01$, $^{***}p < 0.001$, $^{\#}p < 0.05$, $^{\#\#}p < 0.01$, $^{\#\#\#}P < 0.001$, each $n = 6$).

(F) Cell cycle analysis of MESO1 cells treated with HuCD26mAb or control IgG (10 μg/ml) for 12 h. Representative histograms are shown. Accumulation in G1 phase with decreased S and G2/M phase was observed following HuCD26mAb treatment compared with control IgG treatment ($p < 0.01$). Similar results were obtained in five independent experiments.

(G) Hypothetical schema of the effect of HuCD26mAb treatment on USP22-mediated cell cycle control and tumor growth in MPM cells. See text for more details.

described previously [4,5]. Briefly, for *in vivo* tumor progression, mice were anesthetized with isoflurane and subjected to subcutaneous (s.c.) inoculation of MPM cells into the dorsal region. For murine xenograft survival study, mice were intravenously implanted with MESO1 cells transfected with USP22 shRNA-1 or control vector shRNA.

2.7. Statistics

Data are represented as mean±standard deviations (SD) for murine xenograft study and mean±standard errors (SE) for other assays. Data were analyzed by two-tailed Student's *t*-test for two group comparison or by ANOVA test for multiple comparison testing followed by the Tukey-Kramer *post-hoc* test. P values ≤ 0.05 were considered statistically significant. In murine xenograft survival study, prolonged survival was evaluated by Kaplan-Meier analysis.

3. Results and discussion

3.1. Expression of USP22 in MPM clinical specimens and inhibitory effect of USP22 depletion on MPM cell proliferation

USP22 overexpression is detected in many human tumors, including non-small cell lung cancer, salivary duct carcinoma, bladder cancer, colorectal cancer, oral squamous cell carcinoma, and esophageal squamous cell carcinoma [14,19]. However, a role for USP22 in MPM has not yet been clearly elucidated. To address this issue, we first evaluated USP22 expression in clinical specimens of all three histopathologic subtypes (epithelioid, sarcomatoid, and biphasic). Among 26 patients with epithelioid type, 21 patients (81%) had USP22$^+$ MPM histopathology. Moreover, 3 (60%) among 5 patients with sarcomatoid type and 7 (58%) among 12 with biphasic type had USP22$^+$ MPM histopathology. Fig. 1A shows a representative immunohistochemistry study demonstrating that USP22 protein expression was clearly detected in all three histopathologic subtypes. We next examined USP22 expression in the MPM cell lines used in our experimental studies. As shown in Fig. 1B, USP22 was found to be localized both in the nucleus and the cytosol of the MPM cell lines MESO1 and JMN (Fig. 1B). We therefore used these cell lines for our present study. Since depletion of USP22 expression has been reported to suppress tumor growth in various cancers other than MPM [14,19], we next examined the potential regulatory effect of USP22 on MPM cell proliferation. For this purpose, we conducted knockdown experiments in MPM cells utilizing shRNA transfection. As shown in Fig. 1C, knockdown of USP22 by shRNA (USP22-shRNA-1 or -2) significantly inhibited *in vitro* proliferation of MESO1 (left panel) and JMN (right panel). Moreover, knockdown of USP22 in MESO1 cells suppressed *in vivo* proliferation in transplantation assay (Fig. 1D), which was associated with prolonged survival of mice receiving USP22-abrogated cells (Fig. 1E). Similar results were obtained in transplantation assay utilizing JMN cells with knockdown of USP22 (data not shown). Collectively, these results suggest that USP22 depletion attenuates tumor growth and proliferation of MPM.

3.2. Silencing of both USP22 and CD26 contributes to more profound suppression of MPM cell growth than either alone

We previously demonstrated that abrogation of CD26 expression in MPM suppressed cell growth, invasion and proliferation *in vitro* and *in vivo* [4,5]. Moreover, we have found that cell surface expression of CD26 is one of the cancer stem cell (CSC) markers that correlated with CSC properties in MPM cells [20,21]. On the other hand, we previously found that USP22 played a role in the CSC property in human B-acute lymphocytic leukemia [22], as well as in various other cancers [23]. We therefore explored the potential cooperative effect of USP22 and CD26 on cell proliferation in MPM. Flow cytometric analysis revealed that the MESO1 cell line contained both CD26$^+$ USP22$^+$ and CD26$^-$ USP22$^+$ cell populations and that the JMN cell line contained CD26$^+$ USP22$^+$ cells almost exclusively (Fig. 2A). We then characterized the biological functions of USP22$^+$ MPM cells that differed in the expression of CD26. For this purpose, CD26$^+$ (and USP22$^+$) and CD26$^-$ (and USP22$^+$) cells were isolated from the MESO1 cell line through cell sorting analysis, and then subjected to various biological assays. As shown in Fig. 2B, USP22$^+$ cells exhibited greater increase in *in vitro* proliferation and *in vivo* growth in the CD26$^+$population than the CD26$^-$population (left and right panels, respectively). These data suggest that CD26 and USP22 have a cooperative effect on tumor growth in MPM. We previously demonstrated that decreased expression of CD26 played a role in cell cycle control of tumor cells via enhanced expression of CDKI p21 [6–8]. Moreover, USP22 expression counteracted heterochromatin silencing and thereby transactivated specific target genes including CDKI p21, contributing to aberrant cell cycle control [10–13]. We therefore performed cell cycle analysis of CD26 or USP22-depleted MPM cells. As shown in Fig. 2C, G1/S arrest was provoked by the abrogation of CD26 or USP22 expression, suggesting that the inhibitory effect of CD26 and USP22 depletion on MPM cell growth was exerted via cell cycle arrest at the G1/S checkpoint. Further analysis showed that the combined knockdown of USP22 and CD26 resulted in a greater level of inhibition of MPM cell proliferation *in vitro* (left panel of Fig. 2D) as well as *in vivo* (right panel of Fig. 2D), compared to knockdown of USP22 or CD26 alone. In the above clinical specimens of USP22$^+$ MPM histology, co-expression of CD26 was revealed in 15 patients (71%) with epithelioid type, 1 (33%) with sarcomatoid type, and 5 (71%) with biphasic type. The clinical outcome was relatively worsened in these 21 patients with USP22$^+$ CD26$^+$ MPM histology than other groups, although small number of each groups made it hard to have statistical significance. Taken together, our data indicate that USP22 and CD26 cooperatively contribute to a more profound regulation of MPM cell growth.

3.3. HuCD26mAb induces suppression of MPM cell growth via a decrease in CD26-associated USP22

The results described above suggested a molecular association between USP22 and CD26 in MPM cells. To further investigate the mechanisms involved in this interaction, we analyzed the effect of changes in the expression level of USP22 on CD26 expression. As shown in Fig. 3A, silencing or overexpression of USP22 led to decreased (left panel) or increased (right panel) CD26 expression, respectively. These data hence suggest that expression level of USP22 regulates CD26 expression in MPM. Since USP22 contains a deubiquitinating enzyme activity [10], we next examined a ubiquitination state of CD26 molecules in association with USP22 expression. As shown in Fig. 3B, decreased USP22 expression led to increased ubiquitination of CD26 clearly. These data suggest that USP22 expression regulates CD26 expression through its physical interaction of a deubiquitinating enzyme activity in USP22$^+$ CD26$^+$ MPM cells.

We have previously shown that CD26 is expressed mainly on the cell surface of MPM cells [3,15,24], while USP22 is a nuclear protein, a component of the SAGA transcriptional cofactor complex [12], and is mainly localized in the nucleus (as shown Fig. 1A and 1B). In view of their cellular localization, the mechanisms involved in CD26-USP22 interaction in MPM cells would need to be elucidated. We recently demonstrated that treatment of MPM cells with

HuCD26mAb led to internalization of cell surface CD26 molecule into the nucleus and inhibition of tumor cell growth [25]. We therefore hypothesize that nuclear localization of CD26 molecule by HuCD26mAb potentiates an association of USP22 with CD26, leading to the abrogation of USP22 protein and p21 upregulation in MPM cells. As shown in Fig. 3C, treatment with HuCD26mAb induced the formation of a CD26-USP22 complex in CD26$^+$ MPM cells in a dose dependent manner of exogenous HuCD26mAb. Moreover, while HuCD26mAb treatment led to decreased expression of USP22 in the nucleus, there was no noticeable alteration in the expression level of GCN5, another component of the SAGA transcriptional cofactor complex (Fig. 3D). These results suggest that HuCD26mAb mediates the formation of a CD26-USP22 complex and the removal of USP22 from the nucleus.

We further examined a functional analysis on HuCD26mAb-mediated removal of USP22 in the nucleus. A key function of USP22 is to deubiquitinate histone H2A, which regulates p21 expression [10,12,13]. As shown in Fig. 2C, knockdown of USP22 induced G1/S arrest in MPM cells, similar to the effect seen with CD26 depletion. We further investigate that HuCD26mAb treatment increases expression of p21 via ubiquitination of histone H2A in MPM cells. Furthermore, we showed that HuCD26mAb treatment led to enhanced ubiquitination of histone H2A and expression level of p21 in MPM cells (Table 1), similar to findings observed following knockdown of USP22. In addition, HuCD26mAb treatment suppressed cell proliferation in a dose-dependent manner (Fig. 3E), and induced G1/S arrest in MPM cells (Fig. 3F). These results strongly suggest that HuCD26mAb-mediated targeting of CD26 suppresses proliferation of MPM cells via downmodulation of USP22 in the nucleus.

Based on our experimental findings, Fig. 3G depicts a schematics of the effect of HuCD26mAb on USP22-mediated cell cycle control and tumor growth in MPM cells; constitutive expression of USP22 stabilizes de-ubiquitination of histone H2A (also probably H2B), leads to heterochromatin silencing and suppresses expression of p21, resulting in enhanced tumor growth (upper panel). On the other hand, HuCD26mAb-mediated internalization of cell surface CD26 leads to the formation of a CD26-USP22 complex and the removal of USP22 from the nucleus to counteract heterochromatin silencing, thereby transactivating specific target genes including CDKI p21 to suppress tumor growth (lower panel).

In summary, we have demonstrated that suppression of USP22 results in decreased growth and proliferation of MPM cells, and that HuCD26mAb treatment of MPM cells internalizes cell surface CD26 molecules, leading to a physical association with USP22 and suppressing tumor growth via increased expression of CDKI p21. While USP22 is a potential therapeutic target for various cancers, the direct targeting of USP22 by its specific antibody is technically challenging due to the lack of target accessibility, given its subcellular localization. Meanwhile, our present study showing that HuCD26mAb-mediated targeting of CD26 can induce downmodulation of USP22 suggests a potentially promising approach to suppress growth of MPM cells as well as other CD26$^+$ cancers, including colorectal cancer, lung adenocarcinoma, hepatocellular carcinoma and selected hematologic malignancies.

Table 1
Increased level of ubiquitinated histone H2A and p21 expression in USP22-depleted cells or cells treated with humanized anti-CD26 monoclonal antibody.

	Ubiquitinated histone H2A (%)	p21 (%)
Control-shRNA	95.6	32.5
USP22-shRNA	98.4*	40.8*
Control IgG	93.3	64.0
HuCD26mAb	98.8**	68.2**

MESO1 cells stably transfected with control shRNA, or USP22-shRNA-1 (USP22-shRNA), or cells treated with HuCD26mAb (5 μg/ml, for 24 h at 37 °C) or control IgG (5 μg/ml) were stained with anti-ubiquitinated histone H2A or anti-p21 antibodies, followed by staining with FICT-secondary antibody and analyzed utilizing flow cytometry. USP22-shRNA cells or HuCD26mAb treated cells demonstrated significantly increased expression of ubiquitinated histone H2A and p21 (*$p < 0.01$ *vs* Control shRNA or **$p < 0.01$ *vs* Control IgG treated cell, respectively). Representative data are shown in the Table, and similar results were obtained in five independent experiments.

Conflicts of interest

Chikao Morimoto is an inventor of the humanized CD26 monoclonal antibody (HuCD26mAb), YS110 (US Patent #7402698). Y's AC. owns this patent, and Taketo Yamada, Nam H. Dang, Kei Ohnuma and Chikao Morimoto are founding members of this company. Yutarao Kaneko is the CEO of Y's AC.

Author contributions

T.O., and H.Y. contributed to the conception and design of the study, or acquisition of data, R.H., and Y.K. contributed to analysis and interpretation of data, T.Y. conduced histopathology, K.O. and C.M. designed the research, interpreted the data and wrote the paper, C.W.X. and N.H.D. interpreted the data, assisted with the paper, and proofread the manuscript. All authors showed final approval of the version to be submitted.

Acknowledgements

The authors thank Kazunori Kajino (Department of Pathology and Oncology, Graduate School of Medicine, Juntendo University, Tokyo, Japan.) for excellent assistance in immunocytochemistry.

This study was supported in part by a grant of the Ministry of Health, Labour and Welfare, Japan (Grant Number 150401-01 (C.M.) and 180101-01 (C.M.)), JSPS KAKENHI Grant Numbers JP16H05345 (C.M.), JP18H02782 (K.O.), and JP17K10008 (R.H.).

Appendix A. Supplementary data

Supplementary data related to this article can be found at https://doi.org/10.1016/j.bbrc.2018.08.193.

Transparency document

Transparency document related to this article can be found online at https://doi.org/10.1016/j.bbrc.2018.08.193.

References

[1] B.W. Robinson, R.A. Lake, Advances in malignant mesothelioma, N. Engl. J. Med. 353 (2005) 1591–1603, https://doi.org/10.1056/NEJMra050152.
[2] A.R. Haas, D.H. Sterman, Malignant pleural mesothelioma: update on treatment options with a focus on novel therapies, Clin. Chest Med. 34 (2013) 99–111, https://doi.org/10.1016/j.ccm.2012.12.005.
[3] K. Aoe, V.J. Amatya, N. Fujimoto, K. Ohnuma, O. Hosono, A. Hiraki, M. Fujii, T. Yamada, N.H. Dang, Y. Takeshima, K. Inai, T. Kishimoto, C. Morimoto, CD26 overexpression is associated with prolonged survival and enhanced chemosensitivity in malignant pleural mesothelioma, Clin. Canc. Res. 18 (2012) 1447–1456, https://doi.org/10.1158/1078-0432.CCR-11-1990.
[4] J. Yamamoto, K. Ohnuma, R. Hatano, T. Okamoto, E. Komiya, H. Yamazaki, S. Iwata, N.H. Dang, K. Aoe, T. Kishimoto, T. Yamada, C. Morimoto, Regulation of somatostatin receptor 4-mediated cytostatic effects by CD26 in malignant pleural mesothelioma, Br. J. Canc. 110 (2014) 2232–2245, https://doi.org/10.1038/bjc.2014.151.
[5] T. Okamoto, S. Iwata, H. Yamazaki, R. Hatano, E. Komiya, N.H. Dang, K. Ohnuma, C. Morimoto, CD9 negatively regulates CD26 expression and inhibits CD26-mediated enhancement of invasive potential of malignant mesothelioma cells, PLoS One 9 (2014), e86671, https://doi.org/10.1371/journal.pone.0086671.
[6] L. Ho, U. Aytac, L.C. Stephens, K. Ohnuma, G.B. Mills, K.S. McKee, C. Neumann,

R. LaPushin, F. Cabanillas, J.L. Abbruzzese, C. Morimoto, N.H. Dang, In vitro and in vivo antitumor effect of the anti-CD26 monoclonal antibody 1F7 on human CD30+ anaplastic large cell T-cell lymphoma Karpas 299, Clin. Canc. Res. 7 (2001) 2031–2040.

[7] K. Ohnuma, T. Ishii, S. Iwata, O. Hosono, H. Kawasaki, M. Uchiyama, H. Tanaka, T. Yamochi, N.H. Dang, C. Morimoto, G1/S cell cycle arrest provoked in human T cells by antibody to CD26, Immunology 107 (2002) 325–333.

[8] M. Hayashi, H. Madokoro, K. Yamada, H. Nishida, C. Morimoto, M. Sakamoto, T. Yamada, A humanized anti-CD26 monoclonal antibody inhibits cell growth of malignant mesothelioma via retarded G2/M cell cycle transition, Canc. Cell Int. 16 (2016) 35, https://doi.org/10.1186/s12935-016-0310-9.

[9] E. Angevin, N. Isambert, V. Trillet-Lenoir, B. You, J. Alexandre, G. Zalcman, P. Vielh, F. Farace, F. Valleix, T. Podoll, Y. Kuramochi, I. Miyashita, O. Hosono, N.H. Dang, K. Ohnuma, T. Yamada, Y. Kaneko, C. Morimoto, First-in-human phase 1 of YS110, a monoclonal antibody directed against CD26 in advanced CD26-expressing cancers, Br. J. Canc. 116 (2017) 1126–1134, https://doi.org/10.3892/or.2011.1449.

[10] X.Y. Zhang, M. Varthi, S.M. Sykes, C. Phillips, C. Warzecha, W. Zhu, A. Wyce, A.W. Thorne, S.L. Berger, S.B. McMahon, The putative cancer stem cell marker USP22 is a subunit of the human SAGA complex required for activated transcription and cell-cycle progression, Mol. Cell 29 (2008) 102–111, https://doi.org/10.1016/j.molcel.2007.12.015.

[11] W.W. Pijnappel, H.T. Timmers, Dubbing SAGA unveils new epigenetic cross-talk, Mol. Cell 29 (2008) 152–154, https://doi.org/10.1016/j.molcel.2008.01.007.

[12] X.Y. Zhang, H.K. Pfeiffer, A.W. Thorne, S.B. McMahon, USP22, an hSAGA subunit and potential cancer stem cell marker, reverses the polycomb-catalyzed ubiquitylation of histone H2A, Cell Cycle 7 (2008) 1522–1524, https://doi.org/10.4161/cc.7.11.5962.

[13] S.B. Ling, D.G. Sun, B. Tang, C. Guo, Y. Zhang, R. Liang, L.M. Wang, Knock-down of USP22 by small interfering RNA interference inhibits HepG2 cell proliferation and induces cell cycle arrest, Cell. Mol. Biol. 58 (Suppl) (2012) OL1803–OL1808.

[14] R.S. Schrecengost, J.L. Dean, J.F. Goodwin, M.J. Schiewer, M.W. Urban, T.J. Stanek, R.T. Sussman, J.L. Hicks, R.C. Birbe, R.A. Draganova-Tacheva, T. Visakorpi, A.M. DeMarzo, S.B. McMahon, K.E. Knudsen, USP22 regulates oncogenic signaling pathways to drive lethal cancer progression, Canc. Res. 74 (2014) 272–286, https://doi.org/10.1158/0008-5472.CAN-13-1954.

[15] T. Inamoto, T. Yamada, K. Ohnuma, S. Kina, N. Takahashi, T. Yamochi, S. Inamoto, Y. Katsuoka, O. Hosono, H. Tanaka, N.H. Dang, C. Morimoto, Humanized anti-CD26 monoclonal antibody as a treatment for malignant mesothelioma tumors, Clin. Canc. Res. 13 (2007) 4191–4200, https://doi.org/10.1158/1078-0432.CCR-07-0110.

[16] K. Ohnuma-Ishikawa, T. Morio, T. Yamada, Y. Sugawara, M. Ono, M. Nagasawa, A. Yasuda, C. Morimoto, K. Ohnuma, N.H. Dang, H. Hosoi, E. Verdin, S. Mizutani, Knockdown of XAB2 enhances all-trans retinoic acid-induced cellular differentiation in all-trans retinoic acid-sensitive and -resistant cancer cells, Canc. Res. 67 (2007) 1019–1029, https://doi.org/10.1158/0008-5472.CAN-06-1638.

[17] K. Ohnuma, Y. Munakata, T. Ishii, S. Iwata, S. Kobayashi, O. Hosono, H. Kawasaki, N.H. Dang, C. Morimoto, Soluble CD26/dipeptidyl peptidase IV induces T cell proliferation through CD86 up-regulation on APCs, J. Immunol. 167 (2001) 6745–6755.

[18] K. Ohnuma, T. Yamochi, M. Uchiyama, K. Nishibashi, N. Yoshikawa, N. Shimizu, S. Iwata, H. Tanaka, N.H. Dang, C. Morimoto, CD26 up-regulates expression of CD86 on antigen-presenting cells by means of caveolin-1, Proc. Natl. Acad. Sci. U. S. A. 101 (2004) 14186–14191, https://doi.org/10.1073/pnas.0405266101.

[19] H.D. Zhao, H.L. Tang, N.N. Liu, Y.L. Zhao, Q.Q. Liu, X.S. Zhu, L.T. Jia, C.F. Gao, A.G. Yang, J.T. Li, Targeting ubiquitin-specific protease 22 suppresses growth and metastasis of anaplastic thyroid carcinoma, Oncotarget 7 (2016) 31191–31203, https://doi.org/10.18632/oncotarget.9098.

[20] H. Yamazaki, M. Naito, F.I. Ghani, N.H. Dang, S. Iwata, C. Morimoto, Characterization of cancer stem cell properties of CD24 and CD26-positive human malignant mesothelioma cells, Biochem. Biophys. Res. Commun. 419 (2012) 529–536, https://doi.org/10.1016/j.bbrc.2012.02.054.

[21] F.I. Ghani, H. Yamazaki, S. Iwata, T. Okamoto, K. Aoe, K. Okabe, Y. Mimura, N. Fujimoto, T. Kishimoto, T. Yamada, C.W. Xu, C. Morimoto, Identification of cancer stem cell markers in human malignant mesothelioma cells, Biochem. Biophys. Res. Commun. 404 (2011) 735–742, https://doi.org/10.1016/j.bbrc.2010.12.054.

[22] H. Yamazaki, C.W. Xu, M. Naito, H. Nishida, T. Okamoto, F.I. Ghani, S. Iwata, T. Inukai, K. Sugita, C. Morimoto, Regulation of cancer stem cell properties by CD9 in human B-acute lymphoblastic leukemia, Biochem. Biophys. Res. Commun. 409 (2011) 14–21, https://doi.org/10.1016/j.bbrc. 2011.04.098.

[23] G.V. Glinsky, O. Berezovska, A.B. Glinskii, Microarray analysis identifies a death-from-cancer signature predicting therapy failure in patients with multiple types of cancer, J. Clin. Invest. 115 (2005) 1503–1521, https://doi.org/10.1172/JCI23412.

[24] V.J. Amatya, Y. Takeshima, K. Kushitani, T. Yamada, C. Morimoto, K. Inai, Overexpression of CD26/DPPIV in mesothelioma tissue and mesothelioma cell lines, Oncol. Rep. 26 (2011) 1369–1375, https://doi.org/10.3892/or.2011.1449.

[25] K. Yamada, M. Hayashi, H. Madokoro, H. Nishida, W. Du, K. Ohnuma, M. Sakamoto, C. Morimoto, T. Yamada, Nuclear localization of CD26 induced by a humanized monoclonal antibody inhibits tumor cell growth by modulating of POLR2A transcription, PLoS One 8 (2013), e62304, https://doi.org/10.1371/journal.pone.0062304.

Data in Brief 17 (2018) 1078–1081

Contents lists available at ScienceDirect

Data in Brief

journal homepage: www.elsevier.com/locate/dib

Data Article

Gene expression microarray data from mouse CBS treated with rTMS for 30 days, mouse cerebrum and CBS treated with rTMS for 40 days

Tetsurou Ikeda [a,b,*], Satoru Kobayashi [c], Chikao Morimoto [b]

[a] Laboratory for Structural Neuropathology, RIKEN Brain Science Institute, 2-1 Hirosawa, Wako City, Saitama 351-0198, Japan
[b] Clinical Immunology, Institute of Medical Science, The University of Tokyo, 4-6-1 Shirokanedai, Minato-ku, Tokyo 108-8639, Japan
[c] Technical Support, Thermo Fisher Scientific K.K., 3-9 Moriya, Kanagawa-ku, Yokohama 221-0022, Japan

ARTICLE INFO

Article history:
Received 14 September 2017
Received in revised form
17 January 2018
Accepted 29 January 2018
Available online 8 February 2018

Keywords:
rTMS
Microarray data

ABSTRACT

This data article contains complementary tables related to the research article study entitled, 'Effects of repetitive transcranial magnetic stimulation on ER stress–related genes and glutamate, γ–aminobutyric acid, and glycine transporter genes in mouse brain' (Ikeda et al. (2017) [1]), which showed that rTMS modulates glutamate, GABA and glycine transporters and regulates ER stress–related genes. Here, we provide accompanying data collected using Affymetrix GeneChip microarrays to identify changes in gene expression in mouse CBS treated with rTMS for 30 days (Tables 1–21) and mouse cerebrum (Tables 22–57) and CBS (Tables 58–94) treated with rTMS for 40 days.

Specifications Table

Subject area	*Neuroscience*
More specific subject area	*Gene expression*

Abbreviations: CBS, cerebellum with brain stem

* Correspondence to: Kochi Medical School, Kochi University, Kohasu, Oko, Nankoku-city, Kochi, Japan.
E-mail address: ikedatetsurou@kochi-u.ac.jp (T. Ikeda).

http://dx.doi.org/10.1016/j.dib.2018.01.079

Type of data	*Tables*
How data was acquired	*Affymetrix GeneChip RNA microarray*
Data format	*Filtered, analysed*
Experimental factors	*Mouse brain treated with rTMS for 30 and 40 days*
Experimental features	*RNA isolation, global gene expression analyses*
Data source location	*Wako, Saitama, Japan*
Data accessibility	*Data are contained within this article*

Value of the data

- Global gene expression analysis of mouse cerebellum with brain stem (CBS) treated with repetitive transcranial magnetic stimulation (rTMS) for 30 and 40 days
- These data may be useful for comparison with microarray data obtained from rTMS of different durations.
- Genes identified as differentially expressed in this data set could be useful in further studies investigating the effects of rTMS on mouse brain.
- In contrast to the advantage of using microelectrodes, inflammation never occurs while using TMS because it is non–invasive. Immune system may recognise the microelectrode and cause inflammation.

1. Data

Affymetrix GeneChip microarray analyses of mRNA isolated from mouse CBS after 30days rTMS showed altered expression of several genes (Tables 1–21), including glutamatergic, GABAergic and glycinergic (e.g. glycine transporter) neurotransmission systems and ER stress–related genes. Affymetrix GeneChip microarray analyses of mRNA isolated from mouse cerebrum after 40 days rTMS also showed altered expression of several genes (Tables 22–57), including glutamatergic (e.g. glutamate transporters), GABAergic and glycinergic neurotransmission systems. Furthermore, Affymetrix GeneChip microarray analyses of mRNA isolated from mouse CBS after 40days rTMS showed altered expressions of several genes (Tables 58–94), including glutamatergic (e.g. glutamate transporters), GABAergic and glycinergic neurotransmission systems. Mice CBS and cerebrum stimulated by rTMS for 30 or 40days were denoted as M1 and M2, and sham control were denoted as C1 and C2 (n=2). All the expression ratios were converted into the $\log_2$ (expression ratio) values. L1: Signal Log Ratio (M1/C1), L2: Signal Log Ratio (M2/C1), L3: Signal Log Ratio (M1/C2), L4: Signal Log Ratio (M1/C2). C1 and C2 were used as control, and M1 and M2 were normalized with regard to C1 and C2 to obtain expression ratios. Expression Console (EC) Ver.1.4 and Transcriptome Analysis Console (TAC) Ver.3 were used for comparison analysis as a manufacturer procedure. C means data analysis output for a comparison analysis showing change p–values with the associated Increase (I) or Decrease (D) call. Increase calls have change p–values closer to zero and Decrease calls have Change p–values closer to one. Finally, the change algorithm assesses probe pair saturation, calculates a change p–values, and assigns an (I), marginal increase (MI), no change (NC), marginal decrease (MD), or (D) call for C. Genes with more than two significant difference calls were chosen. Abbreviations; TC ID: Transcript Cluster ID, GS: gene symbol, *: Total number of increase, #: Total number of decrease. TC ID is available for pathway analysis.

2. Experimental design, materials and methods

We performed a comprehensive analysis of altered gene expression in CBS after chronic rTMS by using a high–density oligonucleotide array (GeneChip; Affymetrix, Santa Clara, CA, USA. MG_U74Av2 probe array), as described elsewhere [2]. Using the Affymetrix algorithm [3] and multiple analysis comparison software for assessing gene expression differences, mRNAs that

increased or decreased in the mouse brain after chronic rTMS relative to levels in the control mouse brain were identified. Pathway analysis was used to identify the significant pathway of the differential genes based on KEGG. Furthermore, gene ontology (GO) analysis was performed to analyse the main function of the differentially expressed genes based on GO, which is the key functional classification of NCBI that can organise genes into hierarchical categories and uncover the gene regulatory network based on biological process and molecular function [4]. Stimulation was performed using a round–coil (7.5 cm outer diameter) and a Nihon Kohden Rapid Rate Stimulator (Nihon Kohden, Japan). Stimulation conditions were as follows: 20 Hz, 2 s; 20 times/day; inter–stimulus 1–min interval (30% machine output, representing approximately 0.75 T). The coil was placed over the head without touching the skull. Sham control mice were 'stimulated' $>$ 10 cm from the head. rTMS did not produce either notable seizures or changes in behaviour, such as excessive struggling. The animals were killed 24 h after the last stimulation, and their brains were processed for further analysis [6,7]. Whole mouse brain was divided at the midbrain into the cerebrum and CBS. This method of stimulation is applied to the whole brain but not to specific regions of brain. Hence, the feedback effect of the afferent pathway should be considered. Total RNA was isolated from the cerebrum and CBS by acid–phenol extraction [5]. Poly(A)+ RNA was isolated from the samples using an mRNA purification kit (TaKaRa Bio, Japan).

Acknowledgements

The authors would like to thank Enago for the English language review. The authors would like to thank Mr. Masaru Kurosawa and Dr. Nobuyuki Nukina for the support for the experiment.

Funding sources

This work was partly supported by a grant from the Japanese Society for the Promotion of Science (No. 17109011). Furthermore, this work was supported by the Global COE Program 'Center of Education and Research for the Advanced Genome–Based Medicine–For personalized medicine and the control of worldwide infectious disease' and MEXT Japan.

Transparency document. Supporting information

Supplementary data associated with this article can be found in the online version at http://dx.doi.org/10.1016/j.dib.2018.01.079.

Appendix A. Supporting information

Supplementary data associated with this article can be found in the online version at http://dx.doi.org/10.1016/j.dib.2018.01.079.

References

[1] T. Ikeda, W. Kobayashi and C. Morimoto, Effects of repetitive transcranial magnetic stimulation on ER stress–related genes and glutamate, γ–aminobutyric acid, and glycine transporter genes in mouse brain. Submitted for publication.
[2] S. Kotliarova, N.R. Jana, N. Sakamoto, et al., Decreased expression of hypothalamic neuropeptides in Huntington disease transgenic mice with expanded polyglutamine–EGFP fluorescent aggregates, J. Neurochem. 93 (2005) 641–653.
[3] R.J. Lipshutz, S.P. Fodor, T.R. Gingeras, et al., High density synthetic oligonucleotide arrays, Nat. Genet. 21 (1999) 20–24.
[4] C. Gene Ontology, The Gene Ontology (GO) project in 2006, Nucleic. Acids. Res. 34 (2006) D322–D326.

[5] P. Chomczynski, N. Sacchi, Single–step method of RNA isolation by acid guanidinium thiocyanate–phenol–chloroform extraction, Anal. Biochem. 162 (1987) 156–159.
[6] T. Ikeda, M. Kurosawa, C. Uchikawa, et al., Modulation of monoamine transporter expression and function by repetitive transcranial magnetic stimulation, Biochem. Biophys. Res. Commun. 327 (2005) 218–224.
[7] T. Ikeda, M. Kurosawa, C. Morimoto, et al., Multiple effects of repetitive transcranial magnetic stimulation on neuropsychiatric disorders, Biochem. Biophys. Res. Commun. 436 (2013) 121–127.

[Frontiers In Bioscience, Landmark, 23, 1754-1779, June 1, 2018]

A novel role for CD26/dipeptidyl peptidase IV as a therapeutic target

Kei Ohnuma[1], Ryo Hatano[1], Eriko Komiya[1], Haruna Otsuka[1], Takumi Itoh[1], Noriaki Iwao[2], Yutaro Kaneko[3], Taketo Yamada[4,5], Nam H. Dang[6], Chikao Morimoto[1]

[1]Department of Therapy Development and Innovation for Immune Disorders and Cancers, Graduate School of Medicine, Juntendo University, 2-1-1, Hongo, Bunkyo-ku, Tokyo 113-8421, Japan, [2]Department of Hematology, Juntendo University Shizuoka Hospital, Nagaoka 1129, Izunokuni-city, Shizuoka 410-2295, Japan, [3]Y's AC Co., Ltd., 5-3-14, Toranomon, Minato-ku, Tokyo 105-0001, Japan, [4]Department of Pathology, Keio University school of Medicine, 35 Shinanomachi, Shinjuku-ku, Tokyo 160-8582, Japan, [5]Department of Pathology, Saitama Medical University, 38 Morohongo, Moroyama-cho, Iruma-gun, Saitama 350-0459, Japan, [6]Division of Hematology/Oncology, University of Florida, 1600 SW Archer Road-Box 100278, Room MSB M410A, Gainesville, FL 32610, U.S.A.

TABLE OF CONTENTS

1. ABSTRACT

CD26 is a 110 kDa surface glycoprotein with intrinsic dipeptidyl peptidase IV activity that is expressed on numerous cell types and has a multitude of biological functions. The role of CD26 in immune regulation has been extensively characterized, with recent findings elucidating its linkage with signaling pathways and structures involved in T-lymphocyte activation as well as antigen presenting cell-T-cell interaction. In this paper, we will review emerging data on CD26-mediated immune regulation suggesting that CD26 may be an appropriate therapeutic target for the treatment of selected immune disorders as well as Middle East respiratory syndrome coronavirus. Moreover, we have had a long-standing interest in the role of CD26 in cancer biology and its suitability as a novel therapeutic target in selected neoplasms. We reported robust *in vivo* data on the anti-tumor activity of anti-CD26 monoclonal antibody in mouse xenograft models. We herein review significant novel findings and the early clinical development of a CD26-targeted therapy in selected immune disorders and cancers, advances that can lead to a more hopeful future for patients with these intractable diseases.

2. INTRODUCTION

CD26 is a 110-kDa cell surface glycoprotein with known dipeptidyl peptidase IV (DPPIV, EC3.4.1.4.5) activity in its extracellular domain (1-3), capable of cleaving amino-terminal dipeptides with either L-proline or L-alanine at the penultimate position (3). CD26 activity is dependent on the expressing cell type and the microenvironment which influence its multiple biological roles (4-7). CD26 plays an important role in immunology, autoimmunity, diabetes and cancer (8-12). Interacting directly with various other cell surface and intracellular molecules, CD26 can regulate receptor specificity and the function of various interleukins (ILs), cytokines and chemokines via its DPPIV activity (13).

In this review, we summarize our recent work on CD26/DPPIV that elucidated its suitability as a potential therapeutic target in selected immune diseases and cancers. We also discuss our current knowledge of the molecular mechanisms of CD26/DPPIV-mediated T-cell regulation, focusing particularly on CD26/DPPIV role in immune checkpoint pathways and programs associated with human immune regulation. In addition, we describe CD26/DPPIV involvement in cancer immunology.

3. IMMUNE MEDIATED DISORDERS

3.1. Chronic graft-versus-host disease

3.1.1. T cell costimulation in chronic graft-versus-host disease

Graft-versus-host disease (GVHD) is a severe complication and major cause of morbidity and mortality following allogeneic hematopoietic stem cell transplantation (alloHSCT) (14). Based on differences in clinical manifestations and histopathology, GVHD can be divided into acute and chronic forms (14). Acute GVHD (aGVHD) and chronic GVHD (cGVHD) are traditionally diagnosed primarily by time of onset, with cGVHD occurring after day 100 of transplantation (15). However, cGVHD has distinct clinicopathologic features and is often diagnosed based on these features regardless of time of onset, being characterized by cutaneous fibrosis, involvement of exocrine glands, hepatic disease, and obliterative bronchiolitis (OB) (16, 17). OB, characterized by airway blockade, peribronchiolar and perivascular lymphofibroproliferation and obliteration of bronchioles, is a late-stage complication of cGVHD (18). Patients diagnosed with OB have a 5-year survival rate of only 10 to 40%, compared to more than 80% of patients without OB (19, 20). Furthermore, while multiple strategies to control cGVHD involving T cell depletion from the graft or global immunosuppression have been developed, cGVHD is still a common clinical outcome in many alloHSCT patients (17, 21). In addition, immunosuppression potentially abrogates the graft-versus-leukemia (GVL) effect, associated with increased relapses following alloHSCT (22). Novel therapeutic approaches are thus needed to prevent cGVHD without eliminating the GVL effect.

GVHD is initiated when donor-derived T cells are primed by professional antigen presenting cells (APCs) to undergo clonal expansion and maturation (14). Costimulatory pathways are required to induce T cell proliferation, cytokine secretion and effector function following antigen-mediated T cell receptor activation (23), and the important role of costimulatory pathways in transplant biology has been established (24). CD26 is associated with T cell signal transduction processes as a costimulatory molecule, as well as being a marker of T cell activation (1, 25, 26). We previously showed that CD26-mediated costimulation in human CD4 T cells exerts an effect on production of T_H1 type proinflammatory cytokines such as interferon (IFN)-γ (6). Moreover, $CD26^{high}$CD4 T cells respond maximally to recall antigens with a high competence for trafficking to inflammatory tissues and for antibody synthesis by B cells (6, 26). We also showed that CD26-caveolin-1 interaction leads to activation of both CD4 T cells and APCs (27-29). More recently, we demonstrated in *in vitro* experiments that blockade of CD26-mediated T cell costimulation by soluble Fc fusion proteins containing the N-terminal domain of caveolin-1 (Cav-Ig) diminished primary and secondary proliferative responses not only to recall antigen, but also to unrelated allogeneic APC (30). Other investigators recently reported that $CD26^{high}$ T cells contain T_H17 cells, and that $CD26^{high}$ T_H17 cells are enriched in inflamed tissues including rheumatoid arthritis (RA) and inflammatory bowel diseases (IBD) (31). These accumulating data strongly suggest that CD26-mediated costimulation plays an important role in memory response to recall antigens, and that blockade of CD26 costimulation may be an effective therapeutic strategy for immune disorders including GVHD or autoimmune diseases.

3.1.2. Newly established humanized murine model of cGVHD

We previously analyzed a humanized murine aGVHD model involving mice transplanted with human adult peripheral blood lymphocytes (PBL), and showed that liver and skin were predominantly involved as target organs in this model of aGVHD, which was clearly impeded by the administration of humanized anti-CD26 monoclonal antibody (mAb) (32). Our data suggest that $CD26^+$ T cells play an effector role in this aGVHD model. However, since the mice studied in our previous work succumbed to aGVHD around 4 weeks after transplantation of human adult PBL, this early-onset model of aGVHD does not permit the assessment of longer term consequences of interventional therapies, such as their effect on the development of OB, a form of cGVHD of the lung.

In contrast to adult PBL, human umbilical cord blood (HuCB) lymphocytes have been reported to be immature, predominantly consisting of $CD45RA^+$ naïve cells (33, 34). We previously showed that, while all HuCB CD4 T cells constitutively express CD26, CD26-mediated costimulation was considerably attenuated in HuCB CD4 T cells, compared to the robust activation via CD26 costimulation of adult PBL (34). These findings provided further insights into the cellular mechanisms of immature immune response in HuCB. Based on these findings, we hypothesized that HuCB naïve CD4 T cells gradually acquire a xenogeneic response via attenuated stimulatory

signaling with indolent inflammation in the target organs, leading eventually to chronic inflammatory changes. We therefore sought to develop a humanized murine pulmonary cGVHD model utilizing HuCB donor cells, and to overcome the limitations seen in the humanized murine aGVHD model such as vigorous activation of all engrafted T cells and extensive loss of B cell maturation and activation (35, 36).

We first attempted to establish a humanized murine model utilizing NOD/Shi-*scid*IL2rγ^{null} (NOG) mice as recipients and HuCB as donor cells (37). Whole CB transplant mice exhibited clinical signs/ symptoms of GVHD as early as 4 weeks post-transplant, and demonstrated significantly decreased survival rate. The lung of whole CB transplant mice showed perivascular and subepithelial inflammation and fibrotic narrowing of the bronchiole. Skin of whole CB transplant mice manifested fat loss, follicular drop-out and sclerosis of the reticular dermis in the presence of apoptosis of the basilar keratinocytes while the liver exhibited portal fibrosis and cholestasis. These findings indicate that whole CB transplant mice develop pulmonary cGVDH as well as concomitant active GVHD in skin and liver. Taken together, our data demonstrate that the lung of whole CB transplant mice exhibits OB as manifestation of pulmonary cGVHD.

3.1.3. IL-26 contributes to the pathophysiology of pulmonary cGVHD

To determine the potential cellular mechanisms involved in the pathogenesis of pulmonary cGVHD, we next analyzed the composition of donor-derived human lymphocytes in the GVHD lung. Utilizing flow cytometric analysis for cell suspension isolated from the lung specimens, donor-derived human CD3$^+$ cells were found to be the predominant cell type observed in the lung of whole CB transplant mice, comprising more than 99% of the lymphocyte population. Moreover, the human CD4 T cell subset was observed to be the predominant cell type compared to CD8 T cells in the lung of whole CB transplant mice. We next analyzed the expression profile of mRNAs of various inflammatory cytokines in human CD4 T cells isolated from the lung of whole CB transplant mice. We found that *IFNG*, *IL17A, IL21* and *IL26* were significantly increased over the course of GVHD development following whole CB transplantation, while *IL2*, *TNF* (TNF-α), *IL4*, *IL6* and *IL10* were decreased. In addition, substantial increases were seen in levels of *IFNG* and *IL26*, with *IL17A* and *IL21* remained at a low level. It has been reported that IFN-γ is produced by T_H1 cells (6), while IL-17A and IL-26 are produced by T_H17 cells (38, 39). Since both T_H1 and T_H17 cells strongly express CD26 (6, 31), we next analyzed the expression level of CD26/ DPP4, finding that *DPP4* mRNA expression in human CD4 T cells infiltrating in the lung of mice with OB was significantly increased. These findings regarding mRNA expression levels were further supported by enzyme-linked immunosorbent assay (ELISA) studies examining protein levels in sera of recipient mice. To determine whether these cytokines were produced by the infiltrating human CD26$^+$CD4 T cells, we next conducted flow cytometric analyses of lymphocytes isolated from the lung of the recipient mice. Levels of human IFN-γ$^+$ or IL-26$^+$CD26$^+$CD4 T cells were significantly increased in whole CB transplant mice. Multicolor-staining flow cytometric studies showed that CD26$^+$CD4 T cells in the lung of whole CB transplant mice predominantly produced IL-26 rather than IFN-γ. In addition, while CD26$^+$IFN-γ$^+$CD4 cells exclusively expressed IL-26, CD26$^+$IL-26$^+$CD4 cells were predominantly IFN-γ-negative cells, and IL-17A$^+$ cells were exclusively IL-26-negative. These data suggest that CD26$^+$CD4 T cells in the lung of mice with OB express IL-26 as well as IFN-γ but do not belong to the T_H17 cell population.

To further extend the above *in vitro* results to an *in vivo* system, we analyzed the lung of murine alloreactive GVHD using human *IL26* transgenic (Tg) mice. For this purpose, we used mice carrying human *IFNG* and *IL26* transgene (190-*IFNG* Tg mice) or mice carrying human *IFNG* transgene with deleting *IL26* transcription (ΔCNS-77 Tg mice). 190-*IFNG* Tg mice exhibited production of IL-26 by CD4 T cells under T_H1- or T_H17-polarizing conditions, while expression of IL-26 was completely abrogated in ΔCNS-77 Tg mice (38). In addition, production of IFN-γ by T or NK cells was equivalent in both 190-*IFNG* Tg and ΔCNS-77 Tg mice (40). Histologic examinations of the lung of recipient NOG mice deriving from parental C57BL/6 (B6 WT) mice or ΔCNS-77 Tg mice showed peribronchial infiltration and cuffing denoting GVHD, while collagen deposits were not detected by Mallory staining, and IL-26$^+$ cells were not detected. On the other hand, the lung of recipient NOG mice deriving from 190-*IFNG* Tg mice showed peribronchial infiltration and cuffing denoting GVHD with collagen deposition and IL-26$^+$ cell infiltration. These results suggest that human IL-26, but not human IFN-γ, plays a critical role in pulmonary fibrosis associated with lung cGVHD.

3.1.4. IL-26 production via CD26-mediated T cell costimulation

To test whether human CD4 T cells produce IL-26 following CD26 costimulation, we conducted *in vitro* costimulation experiments using HuCB CD4 T cells and analyzed expression of various inflammatory cytokines. We found that levels of *IL26* and *DPP4* were significantly increased following CD26 costimulation compared with CD28 costimulation. We next conducted costimulation experiments evaluating dose and time kinetics using the CD26 costimulatory ligand Cav-Ig as well as anti-CD26 or anti-CD28 mAbs. We showed that production of IL-26 was increased

following CD26 costimulation with Cav-Ig or anti-CD26 mAb in dose- and time-dependent manners, while a slight increase in IL-26 level was observed following CD28 costimulation only at higher doses of mAb and longer stimulation periods. Blocking experiments were then performed for further confirmation, showing that IL-26 production induced by Cav-Ig or anti-CD26 mAb was clearly inhibited by treatment with soluble Cav-Ig in a dose-dependent manner, while no change was observed with CD28 costimulation. These findings strongly suggest that production of IL-26 by HuCB CD4 T cells is regulated via CD26-mediated costimulation. Moreover, since the functional sequences of the N-terminal of caveolin-1 are highly conserved between human and mouse (41) allowing for the capability to bind human CD26 as a costimulatory ligand, it is conceivable that donor HuCB T cells transferred into mice were activated via CD26 costimulation triggered by murine caveolin-1. In fact, using polyclonal antibody recognizing the N-terminal of both human and murine caveolin-1, expression of caveolin-1 was detected in endothelial cells and macrophage-like cells of OB-like lesions in cGVHD lung. Taken together, CD26-mediated IL-26 production triggered by caveolin-1 is identified as a possible therapeutic target in cGVHD using HuCB NOG mice.

3.1.5. Prevention of lung cGVHD development by Cav-Ig administration

Given the role of CD26 costimulation in IL-26 production and IL-26 regulation of collagen production, we therefore sought to determine whether disruption of CD26 costimulation by a blocking reagent, Cav-Ig, prolonged survival of the recipient mice associated with a reduction in the incidence of OB. Recipients treated with Cav-Ig survived for 7 months without any clinical findings of cGVHD. Meanwhile, the survival rate of recipient mice treated with control Ig was significantly reduced, with clinical signs/symptoms of cGVHD. Human cells were engrafted similarly in both groups. Histologic examinations of the lung showed the development of OB in the control Ig cohort, while the lung of Cav-Ig recipient mice displayed normal appearances with none having positive pathology scores. These effects of Cav-Ig were also observed in other GVHD-target organs such as the skin and liver. Moreover, collagen contents in the lung were reduced in Cav-Ig administered-recipients. Taken together, the above results support the notion that Cav-Ig administration prevents the development of pulmonary cGVHD in whole CB transplant mice by decreasing the number of IL-26$^+$CD26$^+$CD4 T cells.

3.1.6. Treatment with Cav-Ig preserves GVL capability

Since GVHD and GVL effect are highly linked immune reactions (42), we evaluated the potential influence of Cav-Ig treatment on GVL effect. For this purpose, cohorts of Cav-Ig or control Ig treated recipient mice of whole CB transplant were irradiated at sublethal doses and then injected intravenously with luciferase-transfected A20 (A20-luc) cells 1 day prior to whole CB transplantation to allow for dissemination of tumor cells. The next day following transplantation, treatment with Cav-Ig or control Ig thrice a week began on day +1 until day +28. Mice inoculated with A20 cells alone all died of tumor progression within 6 weeks. Recipients treated with control Ig exhibited clinical evidence of GVHD such as weight loss and ruffled fur and died of GVHD without tumor progression in 13 weeks. In contrast, recipient mice treated with Cav-Ig displayed significantly prolonged survival without involvement of A20-luc cells. To better characterize the potency of the GVL effect, we repeated these studies with injection of A20-luc cells on day +28 after whole CB transplantation to allow for acquisition of immunosuppression by Cav-Ig treatment. Mice inoculated with A20 cells alone all died of tumor progression within 2 weeks after tumor inoculation. Recipient mice treated with control Ig demonstrated clinical evidence of GVHD such as weight loss and ruffled fur and died of GVHD without tumor progression within 13 weeks after transplantation. In contrast, recipients treated with Cav-Ig exhibited significantly prolonged survival without involvement of A20-luc cells. Collectively, these results demonstrate that Cav-Ig treatment of recipient mice of whole CB transplant was effective in reducing the symptoms of cGVHD without a concomitant loss of the GVL effect.

3.1.7. Role of CD26 in cGVHD

While the human CD26 amino acid (AA) sequence has 85% AA identity with the mouse CD26 (43), the mouse CD26 has different biologic properties from the human CD26, including the fact that the mouse CD26 is not a T cell activation marker, and does not bind to adenosine deaminase (ADA) (43, 44). Therefore, humanized murine models need to be developed to explore the role of CD26-mediated costimulation in cGVHD. With relevance as a costimulatory ligand for human CD26, human caveolin-1 has 95% AA identity with the mouse caveolin-1 (41), and the binding regions of the mouse caveolin-1 for human CD26 are well conserved. Therefore, costimulatory activation of human T cells in NOG mice can occur via CD26-caveolin-1 interaction. Moreover, the N-terminal domain is present in the outer cell surface during the antigen presenting process (27), and caveolin-1 forms homo-dimer or homo-oligomer via its N-terminal domain (41). These collective data suggest that the administered Cav-Ig binds to the N-terminal of caveolin-1 on the cell surface of APCs as well as to CD26 in T cells, leading to suppression of cGVHD in HuCB-NOG mice via blockade of CD26-caveolin-1 interaction. Conclusively, our work

demonstrates that caveolin-1 blockade controls cGVHD by suppressing the immune functions of donor-derived T cells and decreasing IL-26 production. Moreover, IL-26$^+$CD26$^+$CD4 T cell infiltration appears to play a significant role in cGVHD of the lung and skin. While complete suppression of cGVHD with current interventional strategies represents a difficult challenge at the present time, our data demonstrate that control of cGVHD clinical findings can be achieved in a murine experimental system by regulating IL-26$^+$CD26$^+$CD4 T cells with Cav-Ig. Our work also suggests that Cav-Ig treatment may be a novel therapeutic approach for chronic inflammatory diseases, including RA and IBD, in which IL-26 plays an important role.

3.2. Middle East respiratory syndrome coronavirus

3.2.1. Current efforts against Middle East respiratory syndrome coronavirus

Middle East respiratory syndrome coronavirus (MERS-CoV) was first identified in a 60-year-old patient in June 2012 who presented with acute pneumonia, followed by acute respiratory distress syndrome and renal failure with a fatal outcome (45). Between 2012 and August 28, 2017, 2067 laboratory-confirmed cases of MERS-CoV infection were reported to the World Health Organization (WHO), which has notified of at least 720 deaths (around 35% fatality rate) related to MERS-CoV since September 2012 (46). Efforts to develop effective preventive and therapeutic intervention strategies are currently ongoing. Several treatment modalities have been investigated to develop effective therapies against MERS-CoV, including interferon, ribavirin, cyclosporin A, protease inhibitors, convalescent plasma and immunoglobulins. Several promising anti-MERS-CoV therapeutic agents have recently been reviewed extensively (47), while broad spectrum antiviral agents might not be sufficient to treat severe MERS-CoV patients because of its limited effective therapeutic window of opportunity (48).

An alternative approach using prophylactic regimens would be theoretically suitable to limit the spread of MERS-CoV. This scenario includes MERS-CoV vaccine and neutralizing MERS-CoV-specific mAb (48). The MERS-CoV genome encodes for 16 non-structural proteins (nsp1-16) and 4 structural proteins, the spike (S), envelope (E), membrane (M), and nucleocapsid (N) (49). The viral structural proteins, S and N, show the highest immunogenicity (50). While both S and N proteins induce T-cell responses, neutralizing antibodies are almost solely directed against the S protein, with the receptor binding domain (RBD) being the major immunodominant region (51). These great challenges have been extensively reviewed in previously published papers (48, 52).

Recent reports indicated that the spike protein S1 of MERS-CoV is required for viral entry into human host cells (53-55), using CD26/DPPIV as a functional receptor (56). Inhibiting virus entry into host cells could also be achieved by targeting the host receptor CD26/DPPIV. While inhibitors of the CD26/DPPIV enzymatic activity are used clinically to treat type 2 diabetes patients, commercially available DPPIV inhibitors would not serve this purpose since these agents have been shown not to inhibit binding of the RBD of MERS-CoV to CD26/DPPIV (57). We previously showed that human CD26 is a binding protein for ADA (58). Currently, it is known that there are two isoforms of ADA, ADA1 and ADA2 (59). ADA1 is particularly present in lymphocytes and macrophages, while ADA2 is found predominantly in the serum and other body fluids including pleural effusion (59). CD26/DPPIV binds to ADA1, but not ADA2 (58, 60, 61). The crystal structure of CD26/DPPIV and the S protein of MERS-CoV allowed for visualization of the interacting AA in both proteins. However, our *in vitro* experiments showed that blockade of MERS-CoV binding to CD26/DPPIV by ADA1 is incomplete (62). Therefore, mAbs blocking CD26/DPPIV binding to the RBD of MERS-CoV needs to be developed.

3.2.2. CD26/DPPIV is a functional receptor for MERS-CoV entry into host cells

CD26/DPPIV, a host receptor for MERS-CoV, is conserved among different species such as bats and humans, partially explaining the large host range of MERS-CoV (63). In addition to being widely expressed in most cell types including T lymphocytes, bronchial mucosa or the brush border of proximal tubules, CD26/DPPIV exists in systemic circulation as soluble form (13). This distribution of CD26 may play a role in the systemic dissemination of MERS-CoV infection in human (64-66). Therefore, an effective therapy for MERS-CoV is needed not only to block the entry of MERS-CoV into CD26-expressing organs such as the respiratory system, kidney, liver or intestine, but also to eliminate circulating MERS-CoV. In this regard, manipulation of CD26/DPPIV levels or the development of inhibitors that target the interaction between the MERS-CoV S1 domain and its receptor may provide therapeutic opportunities to combat MERS-CoV infection. More recently, the RBD in the S protein was mapped to a 231-AA fragment of MERS-CoV S proteins (residues 358-588) (51).

3.2.3. Identification of specific anti-CD26 mAb clone for blocking MERS-CoV

We have recently mapped MERS-CoV S protein-binding regions in human CD26 molecule and demonstrated that anti-CD26 mAbs, which had been developed in our laboratory, effectively blocked the interaction between the spike protein and

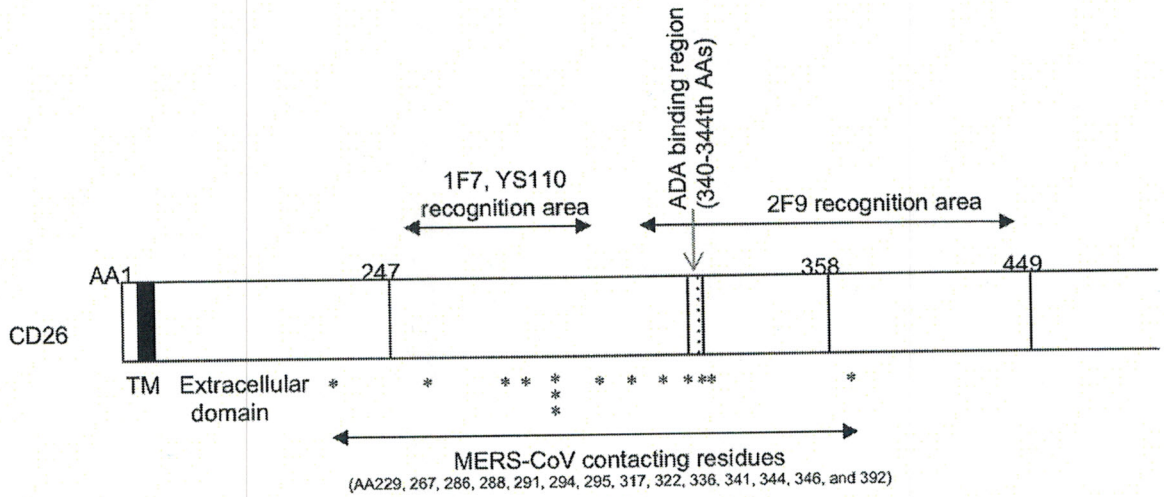

Figure 1. Schematic diagram of human CD26 profiling the predicted contacting areas of anti-CD26 mAbs 2F9, 1F7, YS110 and MERS-CoV S1. 2F9 recognizes between 248-449th AAs including the ADA binding regions, and 1F7 or YS110 recognize between 248-358th AAs excluding the ADA binding regions. MERS-CoV contacting residues of human CD26 are indicated in stars, with available information obtained from recently published data (55, 69). TM indicates the transmembrane region of human CD26 (black box), and the extracellular domain of CD26 is located at the C-terminal residues of TM. This Figure is reprinted with permission from K Ohnuma *et al.*, *J Virol* 87: 13892-13899, 2013 (62).

CD26, thereby neutralizing MERS-CoV infectivity. To determine the specific CD26 domain involved in MERS-CoV infection, we chose six different clones of anti-CD26 mAbs (4G8, 1F7, 2F9, 16D4B, 9C11, 14D10), and the humanized anti-CD26 mAb YS110, which recognize 6 distinct epitopes of the CD26 molecule (67, 68), to conduct MERS-CoV S1-Fc (S1 domain of MERS-CoV fused to the Fc region of human IgG) binding inhibition assays (62). 2F9 inhibited fully binding of MERS-CoV S1-Fc to JKT-hCD26WT (Jurkat cells transfected with full-length human CD26/DPPIV), while other anti-CD26 mAbs demonstrated certain levels of inhibition (1F7, or YS110) or no significant inhibition (4G8, 16D4B, 9C11 or 14D10). These results strongly suggest that the anti-CD26 mAb 2F9 has better therapeutic potential than recombinant MERS-CoV S1-Fc in preventing viral entry into susceptible cells, and that 1F7 or YS110 also block MERS-CoV infection.

Moreover, we have characterized the CD26 epitope involved in MERS-CoV S1-Fc binding to CD26 through the use of various CD26 mutants with deletion in the C-terminal extracellular region, since CD26 is a type II transmembrane protein (9, 29). Our biological experiments on binding regions of CD26 to MERS-CoV using mAbs showed results comparable to those obtained from crystal structure analysis (55, 69), which are summarized in a schematic diagram of human CD26 at 1-449th AAs (Figure 1). Our observations strongly suggest that the main binding regions of CD26 to MERS-CoV appear to be close to the 358th AAs recognized by 2F9, and the regions of CD26 defined by 1F7 and YS110 (248-358th AAs) are also partially involved in MERS-CoV binding.

To determine whether treatment with anti-CD26 mAbs 2F9 as well as 1F7 and YS110 could inhibit MERS-CoV infection, susceptible cells, Huh-7, were pre-incubated with various anti-CD26 mAbs prior to inoculation with the virus (62). In this experimental system, infection was almost completely blocked by 2F9 but not by control IgG or several other anti-CD26 mAbs recognizing other epitopes (4G8, 16D4B, 14D10 or 9C11). Moreover, the anti-CD26 mAbs 1F7 and YS110 considerably inhibited MERS-CoV infection of Huh-7 cells. These results demonstrate that 2F9 inhibits MERS-CoV entry, and therefore can potentially be developed as a preventive or therapeutic agent for MERS-CoV infection in the clinical setting. More importantly, the humanized anti-CD26 mAb YS110 has been evaluated in patients with CD26-expressing cancers in our recent first-in-human (FIH) phase I clinical trial (70). Since no apparent adverse effects of YS110 have been reported besides transient and tolerable injection reactions, YS110 may be an immediate therapeutic candidate for clinical use as potential treatment for MERS-CoV infection.

3.3. Psoriatic pruritus

3.3.1. CD26/DPPIV and psoriasis

Psoriasis (PSO) is one of the most common inflammatory skin diseases, found in about 1-3% of the world general population (71). For a long time, PSO had been considered as a non-pruritic dermatitis. However, within the past 30 years, a number of studies have demonstrated that approximately 60-90% of patients with PSO suffer from pruritus (71-76). Pruritus is an important symptom of PSO. Despite

the fact that several studies have been undertaken to investigate the pathogenesis of pruritus in PSO, many aspects have not yet been studied (71, 77). Therefore, the pathogenesis of this symptom is far from being well-understood and, as a consequence, the therapy of pruritic psoriatic patients still remains a significant challenge for clinicians (78). It has been demonstrated that DPPIV is expressed at high levels on keratinocytes and that DPPIV inhibition suppresses keratinocyte proliferation *in vitro*, and restores partially keratinocyte differentiation *in vivo* (79). Moreover, it has been reported that DPPIV is expressed on keratinocytes and its activity is upregulated in PSO (80, 81), findings which support a potential role for DPPIV enzyme activity in the pathogenesis of PSO. While other investigators have reported a significant improvement in disease severity in PSO patients treated with a DPPIV inhibitor (82, 83), the precise mechanisms involved in DPPIV-mediated regulation of PSO have not been elucidated (84). Recent report showed that T-cell bound expression of CD26/DPPIV in psoriatic skin was explicitly present, albeit in small quantities (81). One hypothesis of potential effect of DPPIV in PSO is that T cell activation mediated by DPPIV is associated with the pathogenesis of PSO (85). Cytokines and chemokines represent the third key player in the psoriatic chronic immune response (86). They are considered as mediators responsible for activation and recruitment of infiltrating leukocytes and therefore play a crucial role in the development and persistence of psoriatic skin lesions (87). DPPIV likely plays a pivotal role in the processing of these molecules (84). The extracellular protease domain of DPPIV (both on keratinocytes and T cells) can cleave dipeptides from the amino terminus of proteins, such as cytokines and chemokines, which are abundantly present in a chronic immune response in PSO, resulting in alterations in receptor specificity and subsequent modifications of biological activity. Taken together, it is conceivable that PSO is a disease involving the complex interplay among activated T cells, keratinocytes and cytokines, and that DPPIV has a key regulatory role in the interactions of these three disease components.

3.3.2. Elevation of sCD26 and DPPIV enzyme in sera of PSO patients

To determine whether serum soluble CD26 (sCD26) and soluble DPPIV (sDPPIV) enzyme play a role in PSO, we evaluated levels of sCD26 and sDPPIV enzyme activity in sera of patients with PSO (88). For this purpose, we performed our in-house capture assay method using anti-human CD26 mAb as a capture antibody for detecting DPPIV enzyme activity specific to sCD26 (89). Since commercially available DPPIV enzyme assay kits measure DPPIV activity in whole serum, but not in captured sCD26 molecules from the samples, it is possible that DPPIV-like peptidase activity other than that possessed by the captured sCD26 molecules was measured, leading to an overestimate of the DPPIV activity in the samples (90). Analyses of serum samples obtained from 18 healthy adult volunteers and 48 PSO patients demonstrated that serum sCD26 concentration of PSO patients was significantly higher than that of healthy adults. Moreover, serum levels of sDPPIV enzyme activity were also significantly higher in patients with PSO compared with healthy adult controls. These data suggest that DPPIV enzyme activity is increased in sera of patients with PSO, which is linked to a concomitant increase in sCD26 in the same patient population. These observations also suggest that DPPIV enzyme plays a role in the pathogenesis of PSO.

3.3.3. Increased pruritus by truncation of substance P, a ligand for CD26/DPPIV

Among various mediators of pruritus investigated in inflammatory skin diseases, substance P (SP) is a key molecule in an itch sensory nerve (91-93), consisting of 11 AA residues with dual DPPIV cleavage sites at its N-terminal position. In fact, DPPIV enzyme digests full-length SP(1-11) resulting in a truncated form of SP(5-11), an activity inhibited by the presence of the DPPIV enzyme inhibitor sitagliptin (88). Moreover, we observed that levels of SP degraded by DPPIV were increased in sera of patients with PSO. Taken together with the above data regarding an increase of sCD26/DPPIV levels in PSO patients, these results also suggest that the increase in DPPIV activity appears to play an important role in PSO by truncating SP.

We next utilized an itchy mouse model by intradermal injection (i.d.) of recombinant SP and quantified scratching behavior in mice to determine an itchy symptom. Mice treated with SP(5-11) i.d. demonstrated a significant increase in scratching behavior, compared with mice receiving control solvent or mice receiving full-length SP(1-11). On the other hand, scratching behavior in SP(1-11) i.d. mice was significantly decreased in mice treated with the DPPIV inhibitor sitagliptin. Furthermore, SP-induced scratching behavior was significantly attenuated in CD26/DPPIV knockout (CD26KO) mice compared with that observed in B6 WT mice. Our data suggest that truncated form of SP cleaved by DPPIV enzyme increases an itch sensation and that SP-induced itch sensation is attenuated by inhibition of the DPPIV activity.

To further determine that DPPIV inhibition affects pruritus, we evaluated scratching behavior utilizing an imiquimod (IMQ)-induced psoriatic itch model (94, 95). Serum levels of truncated form of SP were significantly increased in IMQ-treated mice compared with control cream-treated mice. Moreover, scratching behavior was significantly increased in IMQ-treated mice than control cream-treated mice. These data indicate that IMQ induces psoriatic itchy

skin lesions in mice associated with an increase in the truncation of SP. We next analyzed the frequencies of itch scratching behavior following DPPIV inhibitor administration. IMQ-treated mice receiving sitagliptin showed significant decrease of scratching behavior compared with IMQ-treated mice receiving control solvent. Meanwhile, there was no change in scratching behavior between control cream-treated mice receiving sitagliptin or control saline, with baseline levels of scratching behavior in both cohorts. Taken together, our data suggest that treatment with the DPPIV inhibitor sitagliptin attenuates psoriatic itch sensation via a decrease in the truncated form of SP.

Previous studies have reported that serum levels of SP were decreased in patients with PSO (96-98). Meanwhile, since SP is cleaved by DPPIV enzyme and DPPIV enzyme activity is increased in PSO (88), it is important for a detailed understanding of the role of SP in PSO to precisely measure the truncated form of SP separately from full-length SP. In our recent study, we evaluated full-length SP(1-11) and truncated forms of SP and demonstrated that there was no change in the serum levels of full-length SP(1-11), SP(2-11) and SP(3-11) between PSO and healthy adult controls (88). However, we found that DPPIV enzyme activity and the truncated form of SP were significantly increased in PSO, and that the truncated form of SP(5-11) resulting from DPPIV enzyme activity is associated with an increase in itch sensation. In the IMQ-induced PSO model, the truncated form of SP was significantly increased in sera compared with control mice, and scratching behavior was decreased by administration of sitagliptin. On the other hand, there were no differences in serum levels of DPPIV enzyme activity between IMQ and control cream-treated mice. It is conceivable that the persistent existence of psoriatic skin lesions may be required for the increased serum levels of DPPIV enzyme activity seen in PSO patients, and that SP truncation may result from the increased levels of DPPIV enzyme activity in skin lesions rather than in the circulation (80, 99, 100). Our recent study has conclusively demonstrated that increase in DPPIV enzyme activity exacerbates pruritus in PSO, and that inhibition of DPPIV enzyme reduces severity of itch scratching behavior. Moreover, our results suggest that DPPIV inhibitors are useful as therapeutic agents for pruritus including PSO.

4. CANCERS

4.1. Novel mechanism of CD26/DPPIV in cancer immunology

4.1.1. Anti-tumor effect of CXCL10-mediated CXCR3$^+$ lymphocyte via DPPIV inhibition

CD26/DPPIV regulates the activities of a number of cytokines and chemokines. However, direct *in vivo* evidence for a role for CD26 in tumor biology and its interaction with the tumor microenvironment (TME) has not yet been reported. Recent work has demonstrated clearly the interaction between DPPIV and substrate CXCL10, as well as the functional role of DPPIV-mediated post-translational modification of chemokines in regulating tumor immunity (101). Preservation of the full length, bioactive CXCL10 by DPPIV inhibition results in increased level of CXCR3$^+$ effector T cells in the TME and subsequent tumor growth reduction. CXCR3 has been shown to be a functional receptor for CXCL10 (102). Importantly, the combination of DPPIV inhibition and checkpoint blockade therapy remarkably augments the efficacy of naturally occurring and immunotherapy-based tumor immunity. These investigators therefore provide the direct evidence of DPPIV as an *in vivo* regulator of CXCL10-mediated T cell trafficking with relevance for tumor immunity and immunotherapy (Figure 2). The TME consists of numerous cell types along with the neoplastic cells. Among them are the effector lymphocytes capable of infiltrating into the tumor sites that are specifically required for anti-cancer immune response (103). CXCL10 is a chemoattractant for immune cells such as monocytes, T cells and NK cells and is secreted from a variety of cells in response to IFN-γ, including monocytes, neutrophils, eosinophils, epithelial cells, endothelial cells, fibroblasts and keratinocytes (104). CXCL10 appears to have a dual role on tumor growth, with its proliferative or anti-proliferative activity being cell-type-dependent as a result of differences in the subtype of its receptor CXCR3 (104). CXCR3 is rapidly induced on naïve T cells following activation and preferentially remains highly expressed on T_H1-type CD4$^+$ cells and CD8$^+$ cytotoxic T lymphocytes (CTL), resulting in enhancement of T cell migration to facilitate tumor immune responses (105). Although strong T_H1 and CTL responses in the TME are beneficial for tumor suppression, these responses are counterbalanced to prevent unwanted tissue damage and immunopathology by disrupting the proinflammatory loop. CXCR3$^+$ T_{reg} has been recently identified (106) , as IFN-γ signaling activates the T_H1 transcription factor *T-bet*, which in turn promotes CXCR3 expression to induce T_H1-specific T_{reg} in the inflammatory sites. Moreover, CXCR3 is a marker of CD8$^+$ IL-10-producing cells with suppressive activity in both mice and human (107). The exact factors determining whether CXCR3$^+$ effector T cells and CXCR3$^+$ regulatory lymphocytes will oppose or cooperate with each other during the tumor growth process *in vivo* remain to be elucidated.

4.1.2. Immune checkpoint mechanism via CD26/DPPIV

Although the cellular and molecular mechanisms involved in CD26-mediated T cell activation have been extensively evaluated by our

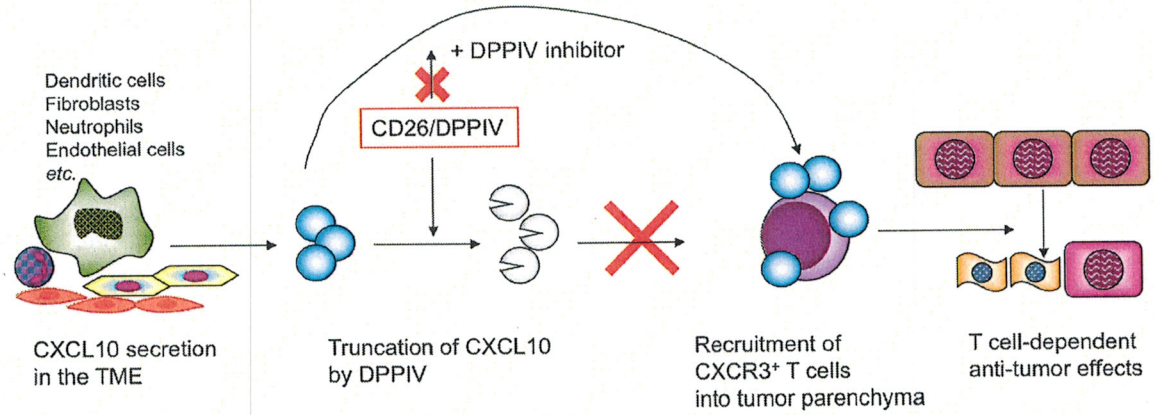

Figure 2. DPP4 inhibition suppresses truncation of its ligand CXCL10, leading to recruitment of CXCR3+ T cells into tumor parenchyma. Through an *in vivo* xenotransplant models, DPPIV inhibitor is found to reduce tumor growth through the preservation of bioactive CXCL10 in the tumor microenvironment (TME). In the normal physiological state, CXCL10 is rapidly degraded by CD26/DPPIV, resulting in decreased recruitment and migration of CXCR3+ T cells into the tumor parenchyma. In contrast, DPPIV inhibition enhances tumor rejection by preserving the full-length biologically active form of CXCL10, leading to increased trafficking of CXCR3+ T cells into the tumor parenchyma. This anti-tumor response is potentiated in combination with other anti-tumor immunotherapeutic approaches including CpG adjuvant therapy, adoptive T cell transfer therapy and checkpoint blockade therapy. This Figure is reprinted with permission from K Ohnuma *et al.*, *Nat Immunol* 16: 791-792, 2015 (156).

group and others (4-6, 9, 13, 90), potential negative feedback mechanisms to regulate CD26-mediated activation still remain to be elucidated. Utilizing human PBL, we found that production of IL-10 by CD4+ T cells is preferentially increased following CD26-mediated costimulation compared with CD28-mediated costimulation (108). IL-21 production was also greatly enhanced in the late phase of CD26 costimulation. On the other hand, production of IL-2, IL-5 or TNF-α was much lower following CD26 costimulation than CD28 costimulation. In contrast, no difference in the production of IL-17A, IFN-γ, or IL-4 was observed following CD26 or CD28-mediated costimulation. These data indicate that CD26 and CD28 costimulation of CD4+ T cells results in different cytokine production profiles, with IL-10 production being preferentially enhanced following CD26 costimulation. Furthermore, we found that both the cell surface and intracellular expression of LAG3 (lymphocyte activation gene-3) was clearly enhanced with increasing doses of anti-CD26 mAb, and that CD26-induced enhancement of LAG3 was more pronounced than the effect of CD28-mediated costimulation. On the other hand, both CD26 and CD28-mediated costimulation enhanced the expression of CTLA-4 (cytotoxic T-lymphocyte-associated antigen 4) and FOXP3 (forkhead box protein P3), with no significant difference being detected between these two costimulatory pathways. In contrast with CD28 costimulation, LAP (latency associated protein) complexed with TGF-β1 was hardly induced following CD26 costimulation. We showed that all the CD4+ T cells expressed LAG3 following CD26 or CD28 costimulation, and that no difference was observed in the percentage of LAG3 expressing cells, while the expression intensity of LAG3 after CD26-mediated costimulation was significantly higher than after CD28-mediated costimulation. LAG3 serves as a marker of IL-10 producing T_{reg} (109), and binds to major histocompatibility complex (MHC) class II molecules with higher affinity than CD4, leading to transduction of inhibitory signals for both T cells and APCs (110, 111). Therefore, our data strongly suggest that signaling events via CD26 may induce the development of CD4+ T cells to a Type 1 regulatory T cells (Tr1)-like phenotype. By expression analysis with Western blotting and quantitative real-time polymerase chain reaction (RT-PCR) experiments and by cell functional analysis utilizing chemical inhibitors and small interfering RNA (siRNA) experiments, we showed that co-engagement of CD3 and CD26 induces preferential production of IL-10 in human CD4+ T cells, mediated through NFAT (nuclear factor of activated T cells) and Raf (rapidly accelerated fibrosarcoma)-MEK (mitogen-activated protein kinase (MAPK)/extracellular signal-regulated kinase (ERK) kinase)-ERK pathways (108). High level of early growth response 2 (EGR2) is also induced following CD26 costimulation, possibly via NFAT and AP-1 (activator protein-1)-mediated signaling, and knock down of EGR2 leads to decreased IL-10 production. Taken together, these observations strongly suggest that CD26-mediated costimulation of CD4+ T cells results in enhanced NFAT/AP-1-dependent EGR2 expression, which is associated with the preferential production of IL-10. Finally, we demonstrated that CD3/CD26-stimulated CD4+ T cells clearly suppress proliferative activity and effector cytokine production of bystander T cells in an IL-10-dependent manner (108). Collectively, our results above suggest that CD3/CD26 costimulation induces the development of

human Tr1-like cells from $CD4^+$ T cells with high level of IL-10 production and LAG3 expression. Preclinical models showed that antibody-mediated blocking of LAG3 as potential anti-cancer therapy led to enhanced activation of antigen-specific T cells at the tumor sites and disruption of tumor growth (112). Moreover, anti-LAG3/anti-PD-1 (programmed cell death 1) antibody treatment cured most mice of established tumors that were largely resistant to single antibody treatment (112). Taken together, it is conceivable that CD26 itself may function as an inhibitory molecule of an immune checkpoint system in certain disease conditions, similar to LAG3 or PD-1.

4.2. Malignant pleural mesothelioma

4.2.1. FIH phase I clinical trial of humanized anti-CD26 mAb

Our previous work analyzing extracellular matrix (ECM) interactions and intracellular signaling events demonstrated that the malignant mesothelial cell line JMN expresses CD26 (113). Our recent in-depth studies of CD26 expression in malignant pleural mesothelioma (MPM) revealed that CD26 is preferentially expressed in MPM cells but not in normal mesothelial cells (114, 115). These intriguing findings propelled our development of CD26-targeted therapy for MPM. For this purpose, we had developed a novel humanized anti-CD26 mAb, namely YS110. YS110 is a recombinant DNA-derived humanized mAb that selectively binds with high affinity to the extracellular domain of CD26. The antibody is an $IgG_1\kappa$ with a molecular weight of 144 kDa and was humanized via an *in silico* design based on the AA sequence of anti-human CD26 murine mAb (14D10), which inhibited tumor cell growth, migration and invasion, and enhanced survival of mouse xenograft models (116). YS110 is produced by fermentation in CHO (Chinese hamster ovary) mammalian cell suspension culture with the Glutamine Synthetase Expression System. *In vitro* pharmacologic evaluation of YS110 demonstrated its selective binding to human CD26 on a number of human cancer cell lines and tissues, with no apparent effect on immune activation and no inhibition of DPPIV activity, while exhibiting direct cytotoxic effect on certain human CD26-positive cancer cell lines. Moreover, our *in vitro* data indicated that YS110 induces cell lysis of MPM cells via antibody-dependent cellular cytotoxicity (ADCC) in addition to its direct anti-tumor effect via cyclin-dependent kinase inhibitor (CDKI) $p27^{kip1}$ and $p21^{cip1}$ accumulation (68, 117). *In vivo* experiments with mouse xenograft models involving human MPM cells demonstrated that YS110 treatment drastically inhibits tumor growth in tumor-bearing mice and reduces formation of metastases, resulting in enhanced survival (68). Our data strongly suggest that YS110 may have potential clinical use as a novel cancer therapeutic agent for CD26-positive malignant mesothelioma.

In addition to our robust *in vitro* and *in vivo* data on antibody-mediated dose-dependent tumor growth inhibition, YS110 exhibited excellent safety and pharmacological profiles in non-human primate models using single and repeated increasing intravenous doses. Considering the lack of T cell proliferation and cytokine production *in vitro*, YS110 was therefore considered not to have an agonistic nor activating effect on human CD26-positive lymphocytes. Other key safety findings were obtained from studies involving cynomolgus monkeys which express YS110-reactive CD26 molecules, with similar tissue distribution profiles and expression levels to human CD26. We therefore conducted the FIH clinical trial of YS110 for patients with MPM and other CD26-positive solid tumors (70). Thirty-three heavily pre-treated patients with CD26-positive cancers including 22 malignant mesothelioma, 10 renal cell carcinoma (RCC) and 1 urothelial carcinoma underwent YS110 administration. A total of 232 infusions (median 3 (range 1-30)) of YS110 were administered across 6 dose levels ranging from 0.1 to 6.0 mg/kg. Maximum tolerated dose (MTD) was not reached and 2 dose limiting toxicities (DLTs) (1 patient with grade 3 anaphylactic reaction at 1.0 mg/kg and 1 patient with grade 3 allergic reaction at 2.0 mg/kg) were reported with complete resolution following dose omission. Subsequent use of systemic steroid prophylaxis and exclusion of patients with significant allergy histories improved safety profile. No dose-dependent adverse events were observed. Blood exposure pharmacokinetics parameters (AUC and C_{max}) increased in proportion with the dose. Cytokines and immunophenotyping assays indicated CD26 target modulation with no occurrence of infectious nor autoimmune disease complications. These results demonstrated that YS110 is tolerable in human subjects. A secondary objective of this FIH study was to evaluate the potential antitumor activity of YS110 according to RECIST 1.0 (response evaluation criteria in solid tumors) criteria (or modified RECIST criteria for mesothelioma). No objective response was achieved in any of the treated patients. However, stable disease as the best overall response was observed in 13 out of the 26 valuable patients on Day 43 of the first cycle (1 at 0.1 mg/kg, 2 at 0.4 mg/kg, 7 at 2.0 mg/kg, 1 at 4.0 mg/kg and 2 at 6.0 mg/kg). Prolonged stabilization with 26 weeks or more was observed in 7 out of 13 stable disease patients who have received a total of 143 (5 to 30 infusions/patients) infusions with a median PFS (progression-free survival) of 33 weeks (26 to 57 weeks). This FIH study conclusively demonstrated that YS110 exhibits a favorable safety profile and substantial clinical activity in heavily pretreated CD26-positive MPM patients

who had previously progressed on conventional standard chemotherapies. Further clinical trial of YS110 for MPM is in progress worldwide (118).

4.2.2. DPPIV enzyme activity and efficacy of YS110

The FIH clinical study of YS110 revealed that an increase in YS110 infusion dose was associated with decreased serum sCD26 level, particularly in cohorts 4-6 (2.0 to 6.0 mg/kg), with an approximately 80% decrease in sCD26 level (70). Moreover, since sCD26 level reflects DPPIV enzyme activity in sera (119), similar reduction in DPPIV enzyme activity was observed, again particularly in patients in cohorts 4-6. Although DPPIV inhibitors are clinically used as oral hypoglycemic agents (120), hypoglycemia was not observed during YS110 administration. Of note is the fact that greater than 80% inhibition of serum DPPIV activity was obtained 24 hours after oral administration of clinically available DPPIV inhibitors (drug information published by manufacturers of sitagliptin, vildagliptin, saxagliptin and *etc.*), a level of inhibition comparable to that seen in patients treated with YS110. Our current data would therefore indicate that YS110 therapy is tolerable in the clinical setting. As described in the previous section, recent work has demonstrated the functional role of DPPIV-mediated post-translational modification of chemokines in regulating tumor immunity through its interaction with its substrate CXCL10 (101). This anti-tumor response is potentiated in combination with other anti-tumor immunotherapeutic approaches including CpG adjuvant therapy, adoptive T cell transfer therapy and checkpoint blockade therapy (anti-CTLA-4 and anti-PD-1) (101). In view of these recent findings, data from our current trial showing that serum DPPIV activity was decreased following treatment with YS110 in a dose-dependent manner would suggest that anti-tumor activity via DPPIV inhibition may constitute yet another mechanism of action for the anti-tumor activity of YS110.

4.2.3. Mechanisms of action of YS110 for cancer treatment

We previously showed that depletion of CD26 by RNAi results in the loss of adhesive property, suggesting that CD26 is a binding protein to the ECM (68). Moreover, our observations regarding the CD26-CD9-α5β1 integrin complex suggest that CD26 regulates the interaction of MPM cells with the ECM via yet-to-be-determined integrin adhesion molecules (121). Recently, we found that expression of CD26 upregulates periostin secretion by MPM cells, leading to enhanced MPM cell migratory and invasive activity (122). Periostin is a secreted cell adhesion protein of approximately 90 kDa, which shares a homology with the insect cell adhesion molecule fasciclin 1 (FAS1) (123). We also demonstrated that the cytoplasmic region of CD26 plays a crucial role in MPM tumor biology through its linkage to somatostatin receptor 4 (SSTR4) and SHP-2 protein tyrosine phosphatase in cell membrane lipid rafts, leading to cytostatic effects in MPM cells without direct association of the ECM to CD26 by anti-CD26 mAb treatment (Figure 3) (124). In view of the findings above, we propose that CD26 forms macromolecular complexes in the cell surface of MPM by connecting periostin and ECM to intracellular signaling events (125); (i) In CD26-negative MPM cells, SSTR4 mediated inhibitory signaling to suppress cell proliferation and motility. In contrast, by locking the signaling domain of SSTR4 with CD26 association, SSTR4-mediated anti-tumor effects were abrogated, leading to increased cell proliferation and motility in CD26-positive MPM cells. (ii) In addition, CD26 regulated ECM-associated tumor cell behavior in association with integrins and periostin-ECM complex. CD9 suppressed cell invasion and migration by inhibiting the formation of CD26-α5β1 integrin complex. Moreover, expression of CD26 upregulated periostin secretion by MPM cells, leading to enhanced MPM cell migratory and invasive activity. (iii) Furthermore, periostin is a secreted cell adhesion protein. The N-terminal region regulates cellular functions by binding to integrins at the plasma membrane of the cells through cell adhesion domain. The C-terminal region of the protein regulates cell–matrix organization and interaction by binding such ECM proteins, leading to increased MPM cell motility. As a result, CD26 molecule in MPM also plays a pivotal role in connecting ECM to intracellular signaling events associated with cell proliferation and motility. It is therefore conceivable that targeting CD26 may be a novel and effective therapeutic approach for MPM.

In addition to the ECM association, our *in vitro* data indicate that YS110 induces cell lysis of MPM cells via ADCC in addition to its direct anti-tumor effect via CDKI $p27^{kip1}$ accumulation (68). More recently, we evaluated the direct anti-tumor effect of YS110 against the MPM cell lines H2452 and JMN, and investigated its effects on cell cycle and on the cell cycle regulator molecules (117). YS110 suppressed the proliferation of H2452 cells by approximately 20% in 48 hours of incubation. Cell cycle analysis demonstrated that the percentage of cells in G2/M phase increased by 8.0.% on average following YS110 treatment. In addition, level of the cell cycle regulator $p21^{cip1}$ was increased and cyclin B1 was decreased after YS110 treatment. Inhibitory phosphorylation of both cdc2 (Tyr15) and cdc25C (Ser216) was elevated. Furthermore, activating phosphorylation of p38 MAPK (Thr180/Tyr182) and ERK1/2 (Thr202/Tyr204) was augmented following 24 hours of YS110 treatment. In addition, we investigated the synergistic effects of YS110 and the anti-tumor agent pemetrexed on selected MPM cell

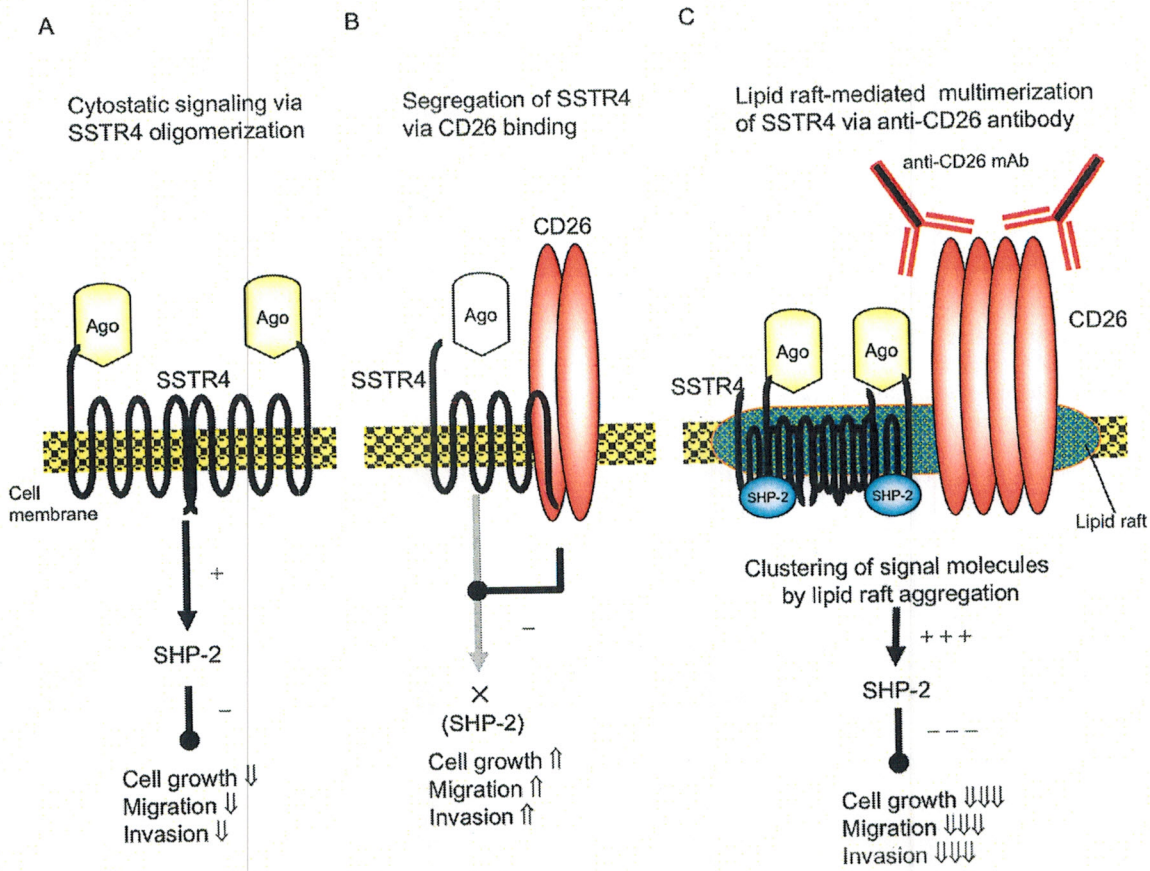

Figure 3. A model for cytostatic signaling mediated by SSTR4 and CD26 coassociation in MPM cells. SSTR4 molecules form homo- or oligo-dimers when stimulated by its agonists (Ago), followed by manifestation of their cytostatic effects via SHP-2 signaling **(A)**. When coassociation of SSTR4 with CD26 occurs, CD26 binds to the C-terminal region of SSTR4, which is necessary to transduce SSTR4 signaling, hence blocking the SSTR4-mediated cytostatic effects **(B)**. Meanwhile, anti-CD26 mAb ligates CD26, leading to dissociation of SSTR4 from CD26 and to recruiting lipid rafts with clustering of SSTR4 molecules **(C)**. As a result, downstream signaling of SSTR4 occurs with activation of SHP-2, leading to the observed cytostatic effects.

lines in both *in vitro* and *in vivo* studies. Pemetrexed rapidly induced CD26 expression on cell surface, and treatment with both YS110 and pemetrexed inhibited *in vivo* tumor growth accompanied by a synergistic reduction in the MIB-1 index (117).

We also demonstrated that treatment with YS110, which inhibited cancer cell growth, induced nuclear translocation of both cell-surface CD26 and YS110 (126, 127). In response to YS110 treatment, CD26 was translocated into the nucleus via caveolin-dependent endocytosis, and interacted with a genomic flanking region of the *POLR2A* gene, a component of RNA polymerase II. This interaction consequently led to transcriptional repression of the *POLR2A* gene, resulting in retarded cancer cell proliferation. Furthermore, impaired nuclear transport of CD26 reversed the *POLR2A* repression induced by YS110 treatment. These findings reveal that nuclear CD26 functions in the regulation of gene expression and tumor growth, and yet another novel mechanism of action of anti-CD26 mAb therapy may involve the regulation of inducible traffic of surface CD26 molecules into the cell nucleus.

4.3. Other cancers

In contrast to our robust findings regarding the role of CD26/DPPIV on MPM, the exact role of CD26/DPPIV in other cancers remains to be elucidated, partly due to its variable expression on these tumors. In general, it is strongly expressed on some cancers, while being absent or present at low levels in others (8). Furthermore, given its multiple biological functions, including its ability to associate with several key proteins and its cleavage of a number of soluble factors to regulate their function, it is likely that the CD26/DPPIV effect on tumor biology is at least partly mediated by the effect of these biological functions on specific tumor types (128).

CD26 has also been shown to be expressed on RCC (129, 130), including the cell lines Caki-1, Caki-2, ACHN, and VMRC-RCW (116). We previously showed that anti-CD26 mAb inhibition of the Caki-2 cell line was associated with G1/S cell cycle arrest, enhanced $p27^{kip1}$ expression, down regulation of cyclin-dependent kinase 2 (CDK2) and dephosphorylation of retinoblastoma substrate (Rb) (116). We also found that anti-CD26 mAb therapy attenuated Akt activity and internalized cell surface CD26 leading to decreased CD26 binding to collagen and fibronectin. Finally, we showed that anti-CD26 mAb inhibited human RCC in a mouse xenograft model (116).

Immunofluorescence analysis revealed expression of CD26/DPPIV on peripheral blood lymphocytes of patients with B chronic lymphocytic leukemia (B-CLL), but not on peripheral B cells from normal donors (131). CD26/DPPIV could also be induced in normal B cells following treatment with IL-4, indicating that expression was regulated at the level of transcription (131). CD26/DPPIV has also been shown to be a marker for aggressive T-large granular lymphocyte (T-LGL) lymphoproliferative disorder. Our work indicated that patients with CD26-positive disease were more likely to require therapies for cytopenia and infections associated with the disease than those with CD26-negative T-LGL (132). Furthermore, CD26-related signaling may be aberrant in T-LGL as compared to T-lymphocytes from normal donors (132). Disease aggressiveness is also correlated with CD26/DPPIV expression in other subsets of T-cell malignancies including T-lymphoblastic lymphoma/ acute lymphoblastic leukemia (LBL/ALL), as those with CD26-positive T-LBL/ALL had a worse clinical outcome compared to patients with CD26-negative tumors (133, 134).

JKT-hCD26WT cells resulted in a greater sensitivity to doxorubicin and etoposide compared to mock transfected cells (135-138). Jurkat cells transfected with a nonfunctional DPPIV catalytic site mutant (Ser630Ala) did not show increased doxorubicin and etoposide sensitivity, suggesting that DPPIV activity is required for chemo-sensitization. A CD26 transfectant with a mutation at the ADA binding site retains DPPIV activity and had a higher level of doxorubicin sensitivity. Surface CD26 expression and DPPIV activity are associated with increased doxorubicin sensitivity and cell cycle arrest in Jurkat cells. Also, there are differences in hyperphosphorylation and inhibition of $p34^{cdc2}$ kinase activity, phosphorylation of cdc25C, and alteration in cyclin B1 expression associated with doxorubicin sensitivity in Jurkat cell lines (136). Therefore, inhibition of CD26 increases cell survival, while increased CD26 expression is associated with decreased drug resistance. The mechanism of this decreased resistance appears to be attributed to enhanced expression of topoisomerase IIα mediated by CD26 – the target for both doxorubicin and etoposide. The increased sensitivity to doxorubicin and etoposide in CD26 expressing tumors may be important in T-cell hematologic malignancies as well as other cancers. Surface expression of CD26 increases topoisomerase IIα level in the B-cell line Jiyoye and increases doxorubicin sensitivity (139). This was demonstrated by using CD26 transfection constructs in the Jiyoye B-cell lymphoma cell line as well as by target specific siRNA inhibition of CD26 in the Karpas-299 T-cell leukemia cell line. Therefore, CD26 has effects on topoisomerase IIα and doxorubicin sensitivity in both B-cell and T-cell lines. Increased CD26/DPPIV levels are associated with increased phosphorylation of p38 and its upstream regulators – MAPK kinase (MAPKK) 3/6 and apoptosis signal-regulating kinase 1 (ASK1). Therefore, the p38 signaling pathway may be involved in the regulation of topoisomerase IIα expression. Doxorubicin treated SCID mice had increased survival in those injected with wild type CD26 compared to vector or DPPIV catalytic site mutant (Ser630Ala) injected mice. CD26/DPPIV levels may be useful predictive markers for doxorubicin treatment of cancer. CD26 level is also associated with etoposide resistance. CD26 mediated changes include hyperphosphorylation of $p34^{cdc2}$, variation in cdc25C level and phosphorylation, and changes in cyclin B1 level. Since CD26/DPPIV cleaves substrates resulting in altered function (140, 141), it is possible that CD26-associated drug sensitivity may therefore be mediated by serum-derived factors. However, our work showed that the increased doxorubicin and etoposide sensitivity of JKT-hCD26WT was independent of serum, data which suggest an effect of CD26 on cell-mediated processes, such as signal transduction, rather than serum-derived factors (137).

Pang *et al.* identified a subpopulation of $CD26^+$ cells uniformly presenting in both primary and metastatic tumors in colorectal cancer (CRC), and showed that $CD26^+$ cancer cells were associated with enhanced invasiveness and chemoresistance (142). These investigators showed that in $CD26^+$ CRC cells, mediators of epithelial to mesenchymal transition (EMT) contribute to the invasive phenotype and metastatic capacity. These results suggest that $CD26^+$ cells are cancer stem cells in CRC, and that CD26/DPPIV can be targeted for metastatic CRC therapy. Recently, other investigators demonstrated in a murine model that lung metastasis of CRC was suppressed by treatment with a DPPIV inhibitor (143). They showed a reduction of EMT markers, suggesting that the EMT status of the murine colon cancer cell line MC38 was at least in part affected by DPPIV inhibition, with a diminution in the growth of metastases. They also showed that DPPIV inhibition decreased the growth of lung metastases of colon cancer by downregulating autophagy, increasing apoptosis and arresting the cell cycle. These data

therefore suggest that DPPIV inhibition may be an effective therapeutic strategy for the treatment of cancers with pulmonary metastases (143).

Yamada *et al.* comprehensively investigated gene expression profiles in surgical samples of untreated gastrointestinal stromal tumors (GIST) of the stomach and small intestine. They found that the disease-free survival of patients with CD26-positive GIST of the stomach was worse than that of patients with CD26-negative GIST (144). Moreover, the postoperative recurrence rate of CD26-negative gastric GIST cases was as low as 2.0.%. They concluded that CD26 is a significant prognostic factor of gastric GIST and may also serve as a therapeutic target (144). Meanwhile, CD26 expression was not associated with clinical outcome of small intestinal GIST.

5. SUMMARY AND PERSPECTIVES

Initially described in 1966 as an enzyme with intrinsic DPPIV activity (145), this activity was subsequently found to be identical to CD26, a 110 kDa extracellular membrane-bound glycoprotein expressed on many tissues including brain, endothelium, heart, intestine, kidney, liver, lung, skeletal muscle, pancreas, placenta, and lymphocytes (26, 146, 147). Originally characterized as a T cell differentiation antigen, CD26 is preferentially expressed on a specific population of T lymphocytes, the subset of $CD4^+CD45RO^+$ memory T cells, and is upregulated following T cell activation (15, 26). Besides being a marker of T cell activation, CD26 is also associated with T cell signal transduction processes as a costimulatory molecule (5-7). CD26 therefore has an important role in T cell biology and overall immune function, and represents a novel therapeutic target for various immune disorders (13, 52, 148-150). CD26 is also expressed on various tumors such as MPM, CRC, RCC, hepatocellular carcinoma, lung cancer, prostate cancer, GIST, thyroid cancer, and hematologic malignancies such as T-anaplastic large cell lymphoma and T-LBL/ALL (10). Moreover, in several human malignancies including CRC, chronic myeloid leukemia, gastric adenocarcinoma and MPM, CD26/DPPIV expression is reported to be a marker of cancer stem cells (142, 151-155). Given the potential role of CD26 surface expression in cancer biology, YS110 therapy may also influence tumor growth through its potential effect on the cancer stem cells of selected tumors. We recently developed novel anti-human CD26 mAbs that can be used as companion diagnostic reagents suitable for immunohistochemical staining of CD26 in formalin-fixed tissue sections with reliable clarity and intensity (155). Since these mAbs display no cross-reactivity with the therapeutic humanized anti-CD26 mAb YS110, they may be suitable for assays analyzing CD26 expression during or following treatment with YS110, with important implications in the clinical setting.

Since CD26/DPPIV has a multitude of biological functions in immune system and human tumor cells, further detailed understanding of the role of this molecule in various clinical settings may lead potentially to novel therapeutic approaches.

6. ACKNOWLEDGEMENT

This work was supported by a Grant-in-Aid (S1311011) from the Foundation of Strategic Research Projects in Private Universities from the Ministry of Education, Culture, Sports, Science, and Technology, Japan; JSPS KAKENHI Grant Number 15H04879; JSPS KAKENHI Grant Number 16H05345; JSPS KAKENHI Grant Number 26830114; a grant of the Ministry of Health, Labour, and Welfare, Japan (Grant Number 150401-01). KO, TY, NHD and CM are founding members of Y's AC Co., Ltd. YK is the CEO of of Y's AC Co., Ltd. Parts of Figures shown in Figures 1 and 2 are reproduced with permission from K Ohnuma *et al.*, *J Virol* 87: 13892-13899, 2013 (*Copyright 2013. American Society for Microbiology*), and K Ohnuma *et al.*, *Nat Immunol* 16: 791-792, 2015 (*Copyright 2015. Nature Publishing Group*).

7. REFERENCES

1. D. A. Fox, R. E. Hussey, K. A. Fitzgerald, O. Acuto, C. Poole, L. Palley, J. F. Daley, S. F. Schlossman and E. L. Reinherz: Ta1, a novel 105 KD human T cell activation antigen defined by a monoclonal antibody. *J Immunol*, 133(3), 1250-6 (1984)

2. D. M. Nanus, D. Engelstein, G. A. Gastl, L. Gluck, M. J. Vidal, M. Morrison, C. L. Finstad, N. H. Bander and A. P. Albino: Molecular cloning of the human kidney differentiation antigen gp160: human aminopeptidase A. *Proc Natl Acad Sci U S A*, 90(15), 7069-73 (1993)
DOI: 10.1073/pnas.90.15.7069
PMid:8346219 PMCid:PMC47077

3. T. Tanaka, D. Camerini, B. Seed, Y. Torimoto, N. H. Dang, J. Kameoka, H. N. Dahlberg, S. F. Schlossman and C. Morimoto: Cloning and functional expression of the T cell activation antigen CD26. *J Immunol*, 149(2), 481-6 (1992)

4. I. De Meester, S. Korom, J. Van Damme and S. Scharpe: CD26, let it cut or cut it down. *Immunol Today*, 20(8), 367-75 (1999)
DOI: 10.1016/S0167-5699(99)01486-3

5. B. Fleischer: CD26: a surface protease involved in T-cell activation. *Immunol Today*, 15(4), 180-4 (1994)
DOI: 10.1016/0167-5699(94)90316-6

6. C. Morimoto and S. F. Schlossman: The structure and function of CD26 in the T-cell immune response. *Immunol Rev*, 161, 55-70 (1998)
DOI: 10.1111/j.1600-065X.1998.tb01571.x
PMid:9553764

7. A. von Bonin, J. Huhn and B. Fleischer: Dipeptidyl-peptidase IV/CD26 on T cells: analysis of an alternative T-cell activation pathway. *Immunol Rev*, 161, 43-53 (1998)
DOI: 10.1111/j.1600-065X.1998.tb01570.x
PMid:9553763

8. M. A. Thompson, K. Ohnuma, M. Abe, C. Morimoto and N. H. Dang: CD26/dipeptidyl peptidase IV as a novel therapeutic target for cancer and immune disorders. *Mini Rev Med Chem*, 7(3), 253-73 (2007)
DOI: 10.2174/138955707780059853
PMid:17346218

9. K. Ohnuma, N. H. Dang and C. Morimoto: Revisiting an old acquaintance: CD26 and its molecular mechanisms in T cell function. *Trends Immunol*, 29(6), 295-301 (2008)
DOI: 10.1016/j.it.2008.02.010
PMid:18456553

10. P. A. Havre, M. Abe, Y. Urasaki, K. Ohnuma, C. Morimoto and N. H. Dang: The role of CD26/dipeptidyl peptidase IV in cancer. *Front Biosci*, 13, 1634-45 (2008)
DOI: 10.2741/2787
PMid:17981655

11. P. Busek, J. Stremenova and A. Sedo: Dipeptidyl peptidase-IV enzymatic activity bearing molecules in human brain tumors--good or evil? *Front Biosci*, 13, 2319-26 (2008)

12. L. Sromova, P. Busek, L. Sedova and A. Sedo: Intraindividual changes of dipeptidyl peptidase-IV in peripheral blood of patients with rheumatoid arthritis are associated with the disease activity. *BMC Musculoskelet Disord*, 16, 244 (2015)

13. K. Ohnuma, N. Takahashi, T. Yamochi, O. Hosono, N. H. Dang and C. Morimoto: Role of CD26/dipeptidyl peptidase IV in human T cell activation and function. *Front Biosci*, 13, 2299-310 (2008)
DOI: 10.2741/2844
PMid:17981712

14. B. R. Blazar, W. J. Murphy and M. Abedi: Advances in graft-versus-host disease biology and therapy. *Nat Rev Immunol*, 12(6), 443-58 (2012)
DOI: 10.1038/nri3212
PMid:22576252 PMCid:PMC3552454

15. H. J. Deeg, D. Lin, W. Leisenring, M. Boeckh, C. Anasetti, F. R. Appelbaum, T. R. Chauncey, K. Doney, M. Flowers, P. Martin, R. Nash, G. Schoch, K. M. Sullivan, R. P. Witherspoon and R. Storb: Cyclosporine or cyclosporine plus methylprednisolone for prophylaxis of graft-versus-host disease: a prospective, randomized trial. *Blood*, 89(10), 3880-7 (1997)

16. A. H. Filipovich: Diagnosis and manifestations of chronic graft-versus-host disease. *Best Pract Res Clin Haematol*, 21(2), 251-7 (2008)
DOI: 10.1016/j.beha.2008.02.008
PMid:18503990

17. G. Socie and J. Ritz: Current issues in chronic graft-versus-host disease. *Blood*, 124(3), 374-84 (2014)
DOI: 10.1182/blood-2014-01-514752
PMid:24914139 PMCid:PMC4102710

18. J. W. Chien, S. Duncan, K. M. Williams and S. Z. Pavletic: Bronchiolitis obliterans syndrome after allogeneic hematopoietic stem cell transplantation-an increasingly recognized manifestation of chronic graft-versus-host disease. *Biol Blood Marrow Transplant*, 16(1 Suppl), S106-14 (2010)

19. A. Z. Dudek, H. Mahaseth, T. E. DeFor and D. J. Weisdorf: Bronchiolitis obliterans in chronic graft-versus-host disease: analysis of risk factors and treatment outcomes. *Biol Blood Marrow Transplant*, 9(10), 657-66 (2003)
DOI: 10.1016/S1083-8791(03)00242-8

20. C. Nakaseko, S. Ozawa, E. Sakaida, M. Sakai, Y. Kanda, K. Oshima, M. Kurokawa, S. Takahashi, J. Ooi, T. Shimizu, A. Yokota, F. Yoshiba, K. Fujimaki, H. Kanamori, R. Sakai, T. Saitoh, T. Sakura, A. Maruta, H. Sakamaki and S. Okamoto: Incidence, risk factors and outcomes of bronchiolitis obliterans after allogeneic stem cell transplantation. *Int J Hematol*, 93(3), 375-82 (2011)
DOI: 10.1007/s12185-011-0809-8
PMid:21424350

21. R. Zeiser and B. R. Blazar: Preclinical models of acute and chronic graft-versus-host disease: how predictive are they for

a successful clinical translation? *Blood*, 127(25), 3117-26 (2016)

22. R. Champlin, I. Khouri and S. Giralt: Graft-vs.-malignancy with allogeneic blood stem cell transplantation: a potential primary treatment modality. *Pediatr Transplant*, 3 Suppl 1, 52-8 (1999)
DOI: 10.1034/j.1399-3046.1999.00054.x

23. C. E. Rudd: T-cell signaling and immunopathologies. *Semin Immunopathol*, 32(2), 91-4 (2010)
DOI: 10.1007/s00281-010-0203-2
PMid:20238116

24. K. A. Markey, K. P. MacDonald and G. R. Hill: The biology of graft-versus-host disease: experimental systems instructing clinical practice. *Blood*, 124(3), 354-62 (2014)
DOI: 10.1182/blood-2014-02-514745
PMid:24914137 PMCid:PMC4102708

25. N. H. Dang, Y. Torimoto, K. Deusch, S. F. Schlossman and C. Morimoto: Comitogenic effect of solid-phase immobilized anti-1F7 on human CD4 T cell activation via CD3 and CD2 pathways. *J Immunol*, 144(11), 4092-100 (1990)

26. C. Morimoto, Y. Torimoto, G. Levinson, C. E. Rudd, M. Schrieber, N. H. Dang, N. L. Letvin and S. F. Schlossman: 1F7, a novel cell surface molecule, involved in helper function of CD4 cells. *J Immunol*, 143(11), 3430-9 (1989)

27. K. Ohnuma, T. Yamochi, M. Uchiyama, K. Nishibashi, N. Yoshikawa, N. Shimizu, S. Iwata, H. Tanaka, N. H. Dang and C. Morimoto: CD26 up-regulates expression of CD86 on antigen-presenting cells by means of caveolin-1. *Proc Natl Acad Sci U S A*, 101(39), 14186-91 (2004)
DOI: 10.1073/pnas.0405266101
PMid:15353589 PMCid:PMC521134

28. K. Ohnuma, T. Yamochi, M. Uchiyama, K. Nishibashi, S. Iwata, O. Hosono, H. Kawasaki, H. Tanaka, N. H. Dang and C. Morimoto: CD26 mediates dissociation of Tollip and IRAK-1 from caveolin-1 and induces upregulation of CD86 on antigen-presenting cells. *Mol Cell Biol*, 25(17), 7743-57 (2005)
DOI: 10.1128/MCB.25.17.7743-7757.2005
PMid:16107720 PMCid:PMC1190283

29. K. Ohnuma, M. Uchiyama, T. Yamochi, K. Nishibashi, O. Hosono, N. Takahashi, S. Kina, H. Tanaka, X. Lin, N. H. Dang and C. Morimoto: Caveolin-1 triggers T-cell activation via CD26 in association with CARMA1. *J Biol Chem*, 282(13), 10117-31 (2007)
DOI: 10.1074/jbc.M609157200
PMid:17287217

30. K. Ohnuma, M. Uchiyama, R. Hatano, W. Takasawa, Y. Endo, N. H. Dang and C. Morimoto: Blockade of CD26-mediated T cell costimulation with soluble caveolin-1-Ig fusion protein induces anergy in CD4+T cells. *Biochem Biophys Res Commun*, 386(2), 327-32 (2009)
DOI: 10.1016/j.bbrc.2009.06.027
PMid:19523449

31. B. Bengsch, B. Seigel, T. Flecken, J. Wolanski, H. E. Blum and R. Thimme: Human Th17 cells express high levels of enzymatically active dipeptidylpeptidase IV (CD26). *J Immunol*, 188(11), 5438-47 (2012)
DOI: 10.4049/jimmunol.1103801
PMid:22539793

32. R. Hatano, K. Ohnuma, J. Yamamoto, N. H. Dang, T. Yamada and C. Morimoto: Prevention of acute graft-versus-host disease by humanized anti-CD26 monoclonal antibody. *Br J Haematol*, 162(2), 263-77 (2013)
DOI: 10.1111/bjh.12378
PMid:23692598

33. K. Sato, H. Nagayama and T. A. Takahashi: Aberrant CD3- and CD28-mediated signaling events in cord blood T cells are associated with dysfunctional regulation of Fas ligand-mediated cytotoxicity. *J Immunol*, 162(8), 4464-71 (1999)

34. S. Kobayashi, K. Ohnuma, M. Uchiyama, K. Iino, S. Iwata, N. H. Dang and C. Morimoto: Association of CD26 with CD45RA outside lipid rafts attenuates cord blood T-cell activation. *Blood*, 103(3), 1002-10 (2004)
DOI: 10.1182/blood-2003-08-2691
PMid:14525771

35. L. D. Shultz, M. A. Brehm, J. V. Garcia-Martinez and D. L. Greiner: Humanized mice for immune system investigation: progress, promise and challenges. *Nat Rev Immunol*, 12(11), 786-98 (2012)
DOI: 10.1038/nri3311
PMid:23059428 PMCid:PMC3749872

36. K. Tezuka, R. Xun, M. Tei, T. Ueno, M. Tanaka, N. Takenouchi and J. Fujisawa:

An animal model of adult T-cell leukemia: humanized mice with HTLV-1-specific immunity. *Blood*, 123(3), 346-55 (2014)
DOI: 10.1182/blood-2013-06-508861
PMid:24196073

37. K. Ohnuma, R. Hatano, T. M. Aune, H. Otsuka, S. Iwata, N. H. Dang, T. Yamada and C. Morimoto: Regulation of pulmonary graft-versus-host disease by IL-26+CD26+CD4 T lymphocytes. *J Immunol*, 194(8), 3697-712 (2015)
DOI: 10.4049/jimmunol.1402785
PMid:25786689 PMCid:PMC4568737

38. P. L. Collins, M. A. Henderson and T. M. Aune: Lineage-specific adjacent *IFNG* and *IL26* genes share a common distal enhancer element. *Genes Immun*, 13(6), 481-8 (2012)
DOI: 10.1038/gene.2012.22
PMid:22622197 PMCid:PMC4180225

39. R. P. Donnelly, F. Sheikh, H. Dickensheets, R. Savan, H. A. Young and M. R. Walter: Interleukin-26: an IL-10-related cytokine produced by Th17 cells. *Cytokine Growth Factor Rev*, 21(5), 393-401 (2010)
DOI: 10.1016/j.cytogfr.2010.09.001
PMid:20947410 PMCid:PMC2997847

40. P. L. Collins, S. Chang, M. Henderson, M. Soutto, G. M. Davis, A. G. McLoed, M. J. Townsend, L. H. Glimcher, D. P. Mortlock and T. M. Aune: Distal regions of the human *IFNG* locus direct cell type-specific expression. *J Immunol*, 185(3), 1492-501 (2010)
DOI: 10.4049/jimmunol.1000124
PMid:20574006 PMCid:PMC2923829

41. J. A. Engelman, X. Zhang, F. Galbiati, D. Volonte, F. Sotgia, R. G. Pestell, C. Minetti, P. E. Scherer, T. Okamoto and M. P. Lisanti: Molecular genetics of the caveolin gene family: implications for human cancers, diabetes, Alzheimer disease, and muscular dystrophy. *Am J Hum Genet*, 63(6), 1578-87 (1998)
DOI: 10.1086/302172
PMid:9837809 PMCid:PMC1377628

42. C. J. Wu and J. Ritz: Revealing tumor immunity after hematopoietic stem cell transplantation. *Clin Cancer Res*, 15(14), 4515-7 (2009)
DOI: 10.1158/1078-0432.CCR-09-0873
PMid:19584145

43. D. Marguet, A. M. Bernard, I. Vivier, D. Darmoul, P. Naquet and M. Pierres: cDNA cloning for mouse thymocyte-activating molecule. A multifunctional ecto-dipeptidyl peptidase IV (CD26) included in a subgroup of serine proteases. *J Biol Chem*, 267(4), 2200-8 (1992)

44. S. Yan, D. Marguet, J. Dobers, W. Reutter and H. Fan: Deficiency of CD26 results in a change of cytokine and immunoglobulin secretion after stimulation by pokeweed mitogen. *Eur J Immunol*, 33(6), 1519-27 (2003)
DOI: 10.1002/eji.200323469
PMid:12778469

45. A. M. Zaki, S. van Boheemen, T. M. Bestebroer, A. D. Osterhaus and R. A. Fouchier: Isolation of a novel coronavirus from a man with pneumonia in Saudi Arabia. *N Engl J Med*, 367(19), 1814-20 (2012)
DOI: 10.1056/NEJMoa1211721
PMid:23075143

46. WHO Programmes and Projects. Emergencies: Middle East resipratory syndrome cornavirus (MERS-CoV). http://www.who.int/emergencies/mers-cov/en/ (2017)

47. Y. Mo and D. Fisher: A review of treatment modalities for Middle East Respiratory Syndrome. *J Antimicrob Chemother*, 71(12), 3340-3350 (2016)
DOI: 10.1093/jac/dkw338
PMid:27585965

48. A. Zumla, J. F. Chan, E. I. Azhar, D. S. Hui and K. Y. Yuen: Coronaviruses - drug discovery and therapeutic options. *Nat Rev Drug Discov*, 15(5), 327-47 (2016)
DOI: 10.1038/nrd.2015.37
PMid:26868298

49. S. van Boheemen, M. de Graaf, C. Lauber, T. M. Bestebroer, V. S. Raj, A. M. Zaki, A. D. Osterhaus, B. L. Haagmans, A. E. Gorbalenya, E. J. Snijder and R. A. Fouchier: Genomic characterization of a newly discovered coronavirus associated with acute respiratory distress syndrome in humans. *MBio*, 3(6) (2012)

50. S. Agnihothram, R. Gopal, B. L. Yount, Jr., E. F. Donaldson, V. D. Menachery, R. L. Graham, T. D. Scobey, L. E. Gralinski, M. R. Denison, M. Zambon and R. S. Baric: Evaluation of serologic and antigenic relationships between middle eastern respiratory syndrome coronavirus and

other coronaviruses to develop vaccine platforms for the rapid response to emerging coronaviruses. *J Infect Dis*, 209(7), 995-1006 (2014)
DOI: 10.1093/infdis/jit609
PMid:24253287 PMCid:PMC3952667

51. H. Mou, V. S. Raj, F. J. van Kuppeveld, P. J. Rottier, B. L. Haagmans and B. J. Bosch: The receptor binding domain of the new Middle East respiratory syndrome coronavirus maps to a 231-residue region in the spike protein that efficiently elicits neutralizing antibodies. *J Virol*, 87(16), 9379-83 (2013)
DOI: 10.1128/JVI.01277-13
PMid:23785207 PMCid:PMC3754068

52. N. M. Okba, V. S. Raj and B. L. Haagmans: Middle East respiratory syndrome coronavirus vaccines: current status and novel approaches. *Curr Opin Virol*, 23, 49-58 (2017)
DOI: 10.1016/j.coviro.2017.03.007
PMid:28412285

53. S. Jiang, L. Lu, L. Du and A. K. Debnath: A predicted receptor-binding and critical neutralizing domain in S protein of the novel human coronavirus HCoV-EMC. *J Infect*, 66(5), 464-6 (2013)
DOI: 10.1016/j.jinf.2012.12.003
PMid:23266463

54. S. Gierer, S. Bertram, F. Kaup, F. Wrensch, A. Heurich, A. Kramer-Kuhl, K. Welsch, M. Winkler, B. Meyer, C. Drosten, U. Dittmer, T. von Hahn, G. Simmons, H. Hofmann and S. Pohlmann: The spike protein of the emerging betacoronavirus EMC uses a novel coronavirus receptor for entry, can be activated by TMPRSS2, and is targeted by neutralizing antibodies. *J Virol*, 87(10), 5502-11 (2013)
DOI: 10.1128/JVI.00128-13
PMid:23468491 PMCid:PMC3648152

55. G. Lu, Y. Hu, Q. Wang, J. Qi, F. Gao, Y. Li, Y. Zhang, W. Zhang, Y. Yuan, J. Bao, B. Zhang, Y. Shi, J. Yan and G. F. Gao: Molecular basis of binding between novel human coronavirus MERS-CoV and its receptor CD26. *Nature*, 500(7461), 227-31 (2013)
DOI: 10.1038/nature12328
PMid:23831647

56. V. S. Raj, H. Mou, S. L. Smits, D. H. Dekkers, M. A. Muller, R. Dijkman, D. Muth, J. A. Demmers, A. Zaki, R. A. Fouchier, V. Thiel, C. Drosten, P. J. Rottier, A. D. Osterhaus, B. J. Bosch and B. L. Haagmans: Dipeptidyl peptidase 4 is a functional receptor for the emerging human coronavirus-EMC. *Nature*, 495(7440), 251-4 (2013)
DOI: 10.1038/nature12005
PMid:23486063

57. L. Jiang, N. Wang, T. Zuo, X. Shi, K. M. Poon, Y. Wu, F. Gao, D. Li, R. Wang, J. Guo, L. Fu, K. Y. Yuen, B. J. Zheng, X. Wang and L. Zhang: Potent neutralization of MERS-CoV by human neutralizing monoclonal antibodies to the viral spike glycoprotein. *Sci Transl Med*, 6(234), 234ra59 (2014)

58. J. Kameoka, T. Tanaka, Y. Nojima, S. F. Schlossman and C. Morimoto: Direct association of adenosine deaminase with a T cell activation antigen, CD26. *Science*, 261(5120), 466-9 (1993)
DOI: 10.1126/science.8101391
PMid:8101391

59. C. Gakis: Adenosine deaminase (ADA) isoenzymes ADA1 and ADA2: diagnostic and biological role. *Eur Respir J*, 9(4), 632-3 (1996)
DOI: 10.1183/09031936.96.09040632
PMid:8726922

60. W. A. Weihofen, J. Liu, W. Reutter, W. Saenger and H. Fan: Crystal structure of CD26/dipeptidyl-peptidase IV in complex with adenosine deaminase reveals a highly amphiphilic interface. *J Biol Chem*, 279(41), 43330-5 (2004)
DOI: 10.1074/jbc.M405001200
PMid:15213224

61. H. B. Rasmussen, S. Branner, F. C. Wiberg and N. Wagtmann: Crystal structure of human dipeptidyl peptidase IV/CD26 in complex with a substrate analog. *Nat Struct Biol*, 10(1), 19-25 (2003)
DOI: 10.1038/nsb882
PMid:12483204

62. K. Ohnuma, B. L. Haagmans, R. Hatano, V. S. Raj, H. Mou, S. Iwata, N. H. Dang, B. J. Bosch and C. Morimoto: Inhibition of Middle East respiratory syndrome coronavirus infection by anti-CD26 monoclonal antibody. *J Virol*, 87(24), 13892-9 (2013)
DOI: 10.1128/JVI.02448-13
PMid:24067970 PMCid:PMC3838260

63. H. A. Mohd, J. A. Al-Tawfiq and Z. A. Memish: Middle East Respiratory Syndrome

Coronavirus (MERS-CoV) origin and animal reservoir. *Virol J*, 13, 87 (2016)

64. Z. A. Memish, A. I. Zumla, R. F. Al-Hakeem, A. A. Al-Rabeeah and G. M. Stephens: Family cluster of Middle East respiratory syndrome coronavirus infections. *N Engl J Med*, 368(26), 2487-94 (2013)
DOI: 10.1056/NEJMoa1303729
PMid:23718156

65. C. Drosten, M. Seilmaier, V. M. Corman, W. Hartmann, G. Scheible, S. Sack, W. Guggemos, R. Kallies, D. Muth, S. Junglen, M. A. Muller, W. Haas, H. Guberina, T. Rohnisch, M. Schmid-Wendtner, S. Aldabbagh, U. Dittmer, H. Gold, P. Graf, F. Bonin, A. Rambaut and C. M. Wendtner: Clinical features and virological analysis of a case of Middle East respiratory syndrome coronavirus infection. *Lancet Infect Dis*, 13(9), 745-51 (2013)
DOI: 10.1016/S1473-3099(13)70154-3

66. B. Guery, J. Poissy, L. el Mansouf, C. Sejourne, N. Ettahar, X. Lemaire, F. Vuotto, A. Goffard, S. Behillil, V. Enouf, V. Caro, A. Mailles, D. Che, J. C. Manuguerra, D. Mathieu, A. Fontanet, S. van der Werf and M. E.-C. s. group: Clinical features and viral diagnosis of two cases of infection with Middle East Respiratory Syndrome coronavirus: a report of nosocomial transmission. *Lancet*, 381(9885), 2265-72 (2013)
DOI: 10.1016/S0140-6736(13)60982-4

67. R. P. Dong, K. Tachibana, M. Hegen, S. Scharpe, D. Cho, S. F. Schlossman and C. Morimoto: Correlation of the epitopes defined by anti-CD26 mAbs and CD26 function. *Mol Immunol*, 35(1), 13-21 (1998)
DOI: 10.1016/S0161-5890(98)80013-8

68. T. Inamoto, T. Yamada, K. Ohnuma, S. Kina, N. Takahashi, T. Yamochi, S. Inamoto, Y. Katsuoka, O. Hosono, H. Tanaka, N. H. Dang and C. Morimoto: Humanized anti-CD26 monoclonal antibody as a treatment for malignant mesothelioma tumors. *Clin Cancer Res*, 13(14), 4191-200 (2007)
DOI: 10.1158/1078-0432.CCR-07-0110
PMid:17634548

69. N. Wang, X. Shi, L. Jiang, S. Zhang, D. Wang, P. Tong, D. Guo, L. Fu, Y. Cui, X. Liu, K. C. Arledge, Y. H. Chen, L. Zhang and X. Wang: Structure of MERS-CoV spike receptor-binding domain complexed with human receptor DPP4. *Cell Res*, 23(8), 986-93 (2013)
DOI: 10.1038/cr.2013.92
PMid:23835475 PMCid:PMC3731569

70. E. Angevin, N. Isambert, V. Trillet-Lenoir, B. You, J. Alexandre, G. Zalcman, P. Vielh, F. Farace, F. Valleix, T. Podoll, Y. Kuramochi, I. Miyashita, O. Hosono, N. H. Dang, K. Ohnuma, T. Yamada, Y. Kaneko and C. Morimoto: First-in-human phase 1 of YS110, a monoclonal antibody directed against CD26 in advanced CD26-expressing cancers. *Br J Cancer*, 116(9), 1126-1134 (2017)
DOI: 10.1038/bjc.2017.62
PMid:28291776 PMCid:PMC5418443

71. J. C. Szepietowski and A. Reich: Pruritus in psoriasis: An update. *Eur J Pain*, 20(1), 41-6 (2016)
DOI: 10.1002/ejp.768
PMid:26415584

72. G. Yosipovitch, A. Goon, J. Wee, Y. H. Chan and C. L. Goh: The prevalence and clinical characteristics of pruritus among patients with extensive psoriasis. *Br J Dermatol*, 143(5), 969-73 (2000)
DOI: 10.1046/j.1365-2133.2000.03829.x
PMid:11069504

73. J. C. Szepietowski, A. Reich and B. Wisnicka: Pruritus and psoriasis. *Br J Dermatol*, 151(6), 1284 (2004)
DOI: 10.1111/j.1365-2133.2004.06299.x
PMid:15606540

74. S. E. Chang, S. S. Han, H. J. Jung and J. H. Choi: Neuropeptides and their receptors in psoriatic skin in relation to pruritus. *Br J Dermatol*, 156(6), 1272-7 (2007)
DOI: 10.1111/j.1365-2133.2007.07935.x
PMid:17535226

75. B. Amatya, G. Wennersten and K. Nordlind: Patients' perspective of pruritus in chronic plaque psoriasis: a questionnaire-based study. *J Eur Acad Dermatol Venereol*, 22(7), 822-6 (2008)
DOI: 10.1111/j.1468-3083.2008.02591.x
PMid:18422545

76. G. Stinco, G. Trevisan, F. Piccirillo, S. Pezzetta, E. Errichetti, N. di Meo, F. Valent and P. Patrone: Pruritus in chronic plaque psoriasis: a questionnaire-based study of 230 Italian patients. *Acta Dermatovenerol Croat*, 22(2), 122-8 (2014)

77. M. Nakamura, M. Toyoda and M. Morohashi: Pruritogenic mediators in psoriasis vulgaris: comparative evaluation of itch-associated cutaneous factors. *Br J Dermatol*, 149(4), 718-30 (2003)
DOI: 10.1046/j.1365-2133.2003.05586.x
PMid:14616362

78. A. S. Raut, R. H. Prabhu and V. B. Patravale: Psoriasis clinical implications and treatment: a review. *Crit Rev Ther Drug Carrier Syst*, 30(3), 183-216 (2013)
DOI: 10.1615/CritRevTherDrugCarrierSyst.2013005268
PMid:23614646

79. A. Thielitz, D. Reinhold, R. Vetter, U. Bank, M. Helmuth, R. Hartig, S. Wrenger, I. Wiswedel, U. Lendeckel, T. Kahne, K. Neubert, J. Faust, C. C. Zouboulis, S. Ansorge and H. Gollnick: Inhibitors of dipeptidyl peptidase IV and aminopeptidase N target major pathogenetic steps in acne initiation. *J Invest Dermatol*, 127(5), 1042-51 (2007)
DOI: 10.1038/sj.jid.5700439
PMid:16778789

80. M. Novelli, P. Savoia, M. T. Fierro, A. Verrone, P. Quaglino and M. G. Bernengo: Keratinocytes express dipeptidyl-peptidase IV (CD26) in benign and malignant skin diseases. *Br J Dermatol*, 134(6), 1052-6 (1996)
DOI: 10.1111/j.1365-2133.1996.tb07941.x
DOI: 10.1046/j.1365-2133.1996.d01-900.x
PMid:8763423

81. R. G. van Lingen, P. C. van de Kerkhof, M. M. Seyger, E. M. de Jong, D. W. van Rens, M. K. Poll, P. L. Zeeuwen and P. E. van Erp: CD26/dipeptidyl-peptidase IV in psoriatic skin: upregulation and topographical changes. *Br J Dermatol*, 158(6), 1264-72 (2008)
DOI: 10.1111/j.1365-2133.2008.08515.x
PMid:18384439

82. M. Lynch, A. M. Tobin, T. Ahern, D. O'Shea and B. Kirby: Sitagliptin for severe psoriasis. *Clin Exp Dermatol*, 39(7), 841-2 (2014)
DOI: 10.1111/ced.12408
PMid:25154439

83. T. Nishioka, M. Shinohara, N. Tanimoto, C. Kumagai and K. Hashimoto: Sitagliptin, a dipeptidyl peptidase-IV inhibitor, improves psoriasis. *Dermatology*, 224(1), 20-1 (2012)
DOI: 10.1159/000333358
PMid:22056790

84. K. Ohnuma, O. Hosono, N. H. Dang and C. Morimoto: Dipeptidyl peptidase in autoimmune pathophysiology. *Adv Clin Chem*, 53, 51-84 (2011)
DOI: 10.1016/B978-0-12-385855-9.00003-5
PMid:21404914

85. M. Diani, G. Altomare and E. Reali: T cell responses in psoriasis and psoriatic arthritis. *Autoimmun Rev*, 14(4), 286-92 (2015)
DOI: 10.1016/j.autrev.2014.11.012
PMid:25445403

86. J. Baliwag, D. H. Barnes and A. Johnston: Cytokines in psoriasis. *Cytokine*, 73(2), 342-50 (2015)
DOI: 10.1016/j.cyto.2014.12.014
PMid:25585875 PMCid:PMC4437803

87. M. P. Schon and W. H. Boehncke: Psoriasis. *N Engl J Med*, 352(18), 1899-912 (2005)
DOI: 10.1056/NEJMra041320
PMid:15872205

88. E. Komiya, R. Hatano, H. Otsuka, T. Itoh, H. Yamazaki, T. Yamada, N. H. Dang, M. Tominaga, Y. Suga, U. Kimura, K. Takamori, C. Morimoto and K. Ohnuma: A possible role for CD26/DPPIV enzyme activity in the regulation of psoriatic pruritus. *J Dermatol Sci*, 86(3), 212-221 (2017)
DOI: 10.1016/j.jdermsci.2017.03.005
PMid:28365081

89. K. Ohnuma, T. Saito, R. Hatano, O. Hosono, S. Iwata, N. H. Dang, H. Ninomiya and C. Morimoto: Comparison of two commercial ELISAs against an in-house ELISA for measuring soluble CD26 in human serum. *J Clin Lab Anal*, 29(2), 106-11 (2015)
DOI: 10.1002/jcla.21736
PMid:24687574

90. A. Sedo and R. Malik: Dipeptidyl peptidase IV-like molecules: homologous proteins or homologous activities? *Biochim Biophys Acta*, 1550(2), 107-16 (2001)

91. C. De Felipe, J. F. Herrero, J. A. O'Brien, J. A. Palmer, C. A. Doyle, A. J. Smith, J. M. Laird, C. Belmonte, F. Cervero and S. P. Hunt: Altered nociception, analgesia and aggression in mice lacking the receptor for substance P. *Nature*, 392(6674), 394-7 (1998)
DOI: 10.1038/32904
PMid:9537323

92. F. O. Nestle, P. Di Meglio, J. Z. Qin and B. J. Nickoloff: Skin immune sentinels in health

and disease. *Nat Rev Immunol*, 9(10), 679-91 (2009)
DOI: 10.1038/nri2622

93. T. Akiyama and E. Carstens: Neural processing of itch. *Neuroscience*, 250, 697-714 (2013)
DOI: 10.1016/j.neuroscience.2013.07.035
PMid:23891755 PMCid:PMC3772667

94. L. van der Fits, S. Mourits, J. S. Voerman, M. Kant, L. Boon, J. D. Laman, F. Cornelissen, A. M. Mus, E. Florencia, E. P. Prens and E. Lubberts: Imiquimod-induced psoriasis-like skin inflammation in mice is mediated via the IL-23/IL-17 axis. *J Immunol*, 182(9), 5836-45 (2009)
DOI: 10.4049/jimmunol.0802999
PMid:19380832

95. K. Sakai, K. M. Sanders, M. R. Youssef, K. M. Yanushefski, L. Jensen, G. Yosipovitch and T. Akiyama: Mouse model of imiquimod-induced psoriatic itch. *Pain*, 157(11), 2536-2543 (2016)
DOI: 10.1097/j.pain.0000000000000674
PMid:27437787 PMCid:PMC5069152

96. C. Remrod, S. Lonne-Rahm and K. Nordlind: Study of substance P and its receptor neurokinin-1 in psoriasis and their relation to chronic stress and pruritus. *Arch Dermatol Res*, 299(2), 85-91 (2007)
DOI: 10.1007/s00403-007-0745-x
PMid:17370082

97. B. Amatya, K. Nordlind and C. F. Wahlgren: Responses to intradermal injections of substance P in psoriasis patients with pruritus. *Skin Pharmacol Physiol*, 23(3), 133-8 (2010)
DOI: 10.1159/000270385
PMid:20051714

98. T. Miyagaki, M. Sugaya, H. Suga, S. Morimura, M. Kamata, H. Ohmatsu, H. Fujita, Y. Asano, Y. Tada, T. Kadono and S. Sato: Serum soluble CD26 levels: diagnostic efficiency for atopic dermatitis, cutaneous T-cell lymphoma and psoriasis in combination with serum thymus and activation-regulated chemokine levels. *J Eur Acad Dermatol Venereol*, 27(1), 19-24 (2013)
DOI: 10.1111/j.1468-3083.2011.04340.x
PMid:22077186

99. R. G. van Lingen, M. K. Poll, M. M. Seyger, E. M. de Jong, P. C. van de Kerkhof and P. E. van Erp: Distribution of dipeptidyl-peptidase IV on keratinocytes in the margin zone of a psoriatic lesion: a comparison with hyperproliferation and aberrant differentiation markers. *Arch Dermatol Res*, 300(10), 561-7 (2008)
DOI: 10.1007/s00403-008-0862-1
PMid:18496701

100. D. J. Drucker: Enhancing incretin action for the treatment of type 2 diabetes. *Diabetes Care*, 26(10), 2929-40 (2003)
DOI: 10.2337/diacare.26.10.2929
PMid:14514604

101. R. Barreira da Silva, M. E. Laird, N. Yatim, L. Fiette, M. A. Ingersoll and M. L. Albert: Dipeptidylpeptidase 4 inhibition enhances lymphocyte trafficking, improving both naturally occurring tumor immunity and immunotherapy. *Nat Immunol*, 16(8), 850-8 (2015)
DOI: 10.1038/ni.3201
PMid:26075911

102. P. Proost, E. Schutyser, P. Menten, S. Struyf, A. Wuyts, G. Opdenakker, M. Detheux, M. Parmentier, C. Durinx, A.-M. Lambeir, J. Neyts, S. Liekens, P. C. Maudgal, A. Billiau and J. Van Damme: Amino-terminal truncation of CXCR3 agonists impairs receptor signaling and lymphocyte chemotaxis, while preserving antiangiogenic properties. *Blood*, 98(13), 3554-3561 (2001)
DOI: 10.1182/blood.V98.13.3554
PMid:11739156

103. P. van der Bruggen, C. Traversari, P. Chomez, C. Lurquin, E. De Plaen, B. Van den Eynde, A. Knuth and T. Boon: A gene encoding an antigen recognized by cytolytic T lymphocytes on a human melanoma. *Science*, 254(5038), 1643-7 (1991)
DOI: 10.1126/science.1840703
PMid:1840703

104. M. Liu, S. Guo and J. K. Stiles: The emerging role of CXCL10 in cancer. *Oncol Lett*, 2(4), 583-589 (2011)

105. J. R. Groom and A. D. Luster: CXCR3 in T cell function. *Exp Cell Res*, 317(5), 620-31 (2011)
DOI:10.1016/j.yexcr.2010.12.017
PMid:21376175 PMCid:PMC3065205

106. M. A. Koch, G. Tucker-Heard, N. R. Perdue, J. R. Killebrew, K. B. Urdahl and D. J. Campbell: The transcription factor T-bet

controls regulatory T cell homeostasis and function during type 1 inflammation. *Nat Immunol*, 10(6), 595-602 (2009)
DOI: 10.1038/ni.1731
PMid:19412181 PMCid:PMC2712126

107. Z. Shi, Y. Okuno, M. Rifa'i, A. T. Endharti, K. Akane, K. Isobe and H. Suzuki: Human CD8+CXCR3+ T cells have the same function as murine CD8+CD122+ Treg. *Eur J Immunol*, 39(8), 2106-19 (2009)
DOI: 10.1002/eji.200939314
PMid:19609979

108. R. Hatano, K. Ohnuma, H. Otsuka, E. Komiya, I. Taki, S. Iwata, N. H. Dang, K. Okumura and C. Morimoto: CD26-mediated induction of EGR2 and IL-10 as potential regulatory mechanism for CD26 costimulatory pathway. *J Immunol*, 194(3), 960-72 (2015)
DOI: 10.4049/jimmunol.1402143
PMid:25548232

109. T. Okamura, K. Fujio, M. Shibuya, S. Sumitomo, H. Shoda, S. Sakaguchi and K. Yamamoto: CD4+CD25-LAG3+ regulatory T cells controlled by the transcription factor Egr-2. *Proc Natl Acad Sci U S A*, 106(33), 13974-9 (2009)
DOI: 10.1073/pnas.0906872106
PMid:19666526 PMCid:PMC2729005

110. B. Huard, P. Prigent, F. Pages, D. Bruniquel and F. Triebel: T cell major histocompatibility complex class II molecules down-regulate CD4+ T cell clone responses following LAG-3 binding. *Eur J Immunol*, 26(5), 1180-6 (1996)
DOI: 10.1002/eji.1830260533
PMid:8647185

111. L. Macon-Lemaitre and F. Triebel: The negative regulatory function of the lymphocyte-activation gene-3 co-receptor (CD223) on human T cells. *Immunology*, 115(2), 170-8 (2005)
DOI: 10.1111/j.1365-2567.2005.02145.x
PMid:15885122 PMCid:PMC1782137

112. L. T. Nguyen and P. S. Ohashi: Clinical blockade of PD1 and LAG3--potential mechanisms of action. *Nat Rev Immunol*, 15(1), 45-56 (2015)
DOI: 10.1038/nri3790
PMid:25534622

113. N. H. Dang, Y. Torimoto, S. F. Schlossman and C. Morimoto: Human CD4 helper T cell activation: functional involvement of two distinct collagen receptors, 1F7 and VLA integrin family. *J Exp Med*, 172(2), 649-52 (1990)
DOI: 10.1084/jem.172.2.649
PMid:2165129

114. V. J. Amatya, Y. Takeshima, K. Kushitani, T. Yamada, C. Morimoto and K. Inai: Overexpression of CD26/DPPIV in mesothelioma tissue and mesothelioma cell lines. *Oncol Rep*, 26(6), 1369-75 (2011)
DOI: 10.3892/or.2011.1449

115. K. Aoe, V. J. Amatya, N. Fujimoto, K. Ohnuma, O. Hosono, A. Hiraki, M. Fujii, T. Yamada, N. H. Dang, Y. Takeshima, K. Inai, T. Kishimoto and C. Morimoto: CD26 overexpression is associated with prolonged survival and enhanced chemosensitivity in malignant pleural mesothelioma. *Clin Cancer Res*, 18(5), 1447-56 (2012)
DOI: 10.1158/1078-0432.CCR-11-1990
PMid:22261805

116. T. Inamoto, T. Yamochi, K. Ohnuma, S. Iwata, S. Kina, S. Inamoto, M. Tachibana, Y. Katsuoka, N. H. Dang and C. Morimoto: Anti-CD26 monoclonal antibody-mediated G1-S arrest of human renal clear cell carcinoma Caki-2 is associated with retinoblastoma substrate dephosphorylation, cyclin-dependent kinase 2 reduction, $p27^{kip1}$ enhancement, and disruption of binding to the extracellular matrix. *Clin Cancer Res*, 12(11), 3470-7 (2006)
DOI: 10.1158/1078-0432.CCR-06-0361
PMid:16740772

117. M. Hayashi, H. Madokoro, K. Yamada, H. Nishida, C. Morimoto, M. Sakamoto and T. Yamada: A humanized anti-CD26 monoclonal antibody inhibits cell growth of malignant mesothelioma via retarded G2/M cell cycle transition. *Cancer Cell Int*, 16, 35 (2016)

118. ClinicalTrials.gov: Clinical Study of YS110 in Patients With Malignant Pleural Mesothelioma.https://www.clinicaltrials.gov/ct2/show/NCT03177668?term=YS110&cond=Mesotheliomas+Pleural&rank=1, (2017)

119. C. Durinx, H. Neels, J. C. Van der Auwera, K. Naelaerts, S. Scharpe and I. De Meester: Reference values for plasma dipeptidyl-peptidase IV activity and their association with other laboratory parameters. *Clin Chem Lab Med*, 39(2), 155-9 (2001)
DOI: 10.1515/CCLM.2001.026
PMid:11341750

120. D. J. Drucker and M. A. Nauck: The incretin system: glucagon-like peptide-1 receptor agonists and dipeptidyl peptidase-4 inhibitors in type 2 diabetes. *Lancet*, 368(9548), 1696-705 (2006)
DOI: 10.1016/S0140-6736(06)69705-5

121. T. Okamoto, S. Iwata, H. Yamazaki, R. Hatano, E. Komiya, N. H. Dang, K. Ohnuma and C. Morimoto: CD9 negatively regulates CD26 expression and inhibits CD26-mediated enhancement of invasive potential of malignant mesothelioma cells. *PLoS ONE*, 9(1), e86671 (2014)
DOI: 10.1371/journal.pone.0086671
PMid:24466195 PMCid:PMC3900581

122. E. Komiya, K. Ohnuma, H. Yamazaki, R. Hatano, S. Iwata, T. Okamoto, N. H. Dang, T. Yamada and C. Morimoto: CD26-mediated regulation of periostin expression contributes to migration and invasion of malignant pleural mesothelioma cells. *Biochem Biophys Res Commun*, 447(4), 609-15 (2014)
DOI: 10.1016/j.bbrc.2014.04.037
PMid:24747072

123. L. Morra and H. Moch: Periostin expression and epithelial-mesenchymal transition in cancer: a review and an update. *Virchows Arch*, 459(5), 465-75 (2011)
DOI: 10.1007/s00428-011-1151-5
PMid:21997759 PMCid:PMC3205268

124. J. Yamamoto, K. Ohnuma, R. Hatano, T. Okamoto, E. Komiya, H. Yamazaki, S. Iwata, N. H. Dang, K. Aoe, T. Kishimoto, T. Yamada and C. Morimoto: Regulation of somatostatin receptor 4-mediated cytostatic effects by CD26 in malignant pleural mesothelioma. *Br J Cancer*, 110(9), 2232-45 (2014)
DOI: 10.1038/bjc.2014.151
PMid:24743707 PMCid:PMC4007235

125. K. Ohnuma, R. Hatano, H. Yamazaki, Y. Kaneko, N. H. Dang and C. Morimoto: CD26-targeted therapy: a new horizon in malignant pleural mesothelioma management. In: *Horizons in Cancer Research*. Ed S. H. Wanatabe. Nova Science Publishers, Inc., Hauppauge, NY (2017)

126. K. Yamada, M. Hayashi, W. Du, K. Ohnuma, M. Sakamoto, C. Morimoto and T. Yamada: Localization of CD26/DPPIV in nucleus and its nuclear translocation enhanced by anti-CD26 monoclonal antibody with anti-tumor effect. *Cancer Cell Int*, 9, 17 (2009)

127. K. Yamada, M. Hayashi, H. Madokoro, H. Nishida, W. Du, K. Ohnuma, M. Sakamoto, C. Morimoto and T. Yamada: Nuclear localization of CD26 induced by a humanized monoclonal antibody inhibits tumor cell growth by modulating of POLR2A transcription. *PLoS One*, 8(4), e62304 (2013)
DOI: 10.1371/journal.pone.0062304
PMid:23638030 PMCid:PMC3639274

128. P. A. Havre, M. Abe, Y. Urasaki, K. Ohnuma, C. Morimoto and N. H. Dang: CD26 expression on T cell lines increases SDF-1-alpha-mediated invasion. *Br J Cancer*, 101(6), 983-91 (2009)
DOI: 10.1038/sj.bjc.6605236
PMid:19654580 PMCid:PMC2743358

129. D. Droz, D. Zachar, L. Charbit, J. Gogusev, Y. Chretein and L. Iris: Expression of the human nephron differentiation molecules in renal cell carcinomas. *Am J Pathol*, 137(4), 895-905 (1990)

130. T. Stange, U. Kettmann and H. J. Holzhausen: Immunoelectron microscopic demonstration of the membrane proteases aminopeptidase N/CD13 and dipeptidyl peptidase IV/CD26 in normal and neoplastic renal parenchymal tissues and cells. *Eur J Histochem*, 44(2), 157-64 (2000)

131. B. Bauvois, I. De Meester, J. Dumont, D. Rouillard, H. X. Zhao and E. Bosmans: Constitutive expression of CD26/dipeptidylpeptidase IV on peripheral blood B lymphocytes of patients with B chronic lymphocytic leukaemia. *Br J Cancer*, 79(7-8), 1042-8 (1999)

132. N. H. Dang, U. Aytac, K. Sato, S. O'Brien, J. Melenhorst, C. Morimoto, A. J. Barrett and J. J. Molldrem: T-large granular lymphocyte lymphoproliferative disorder: expression of CD26 as a marker of clinically aggressive disease and characterization of marrow inhibition. *Br J Haematol*, 121(6), 857-65 (2003)
DOI: 10.1046/j.1365-2141.2003.04365.x
PMid:12786796

133. A. Carbone, M. Cozzi, A. Gloghini and A. Pinto: CD26/dipeptidyl peptidase IV expression in human lymphomas is restricted to CD30-positive anaplastic large cell and a subset of T-cell non-Hodgkin's lymphomas. *Hum Pathol*, 25(12), 1360-5 (1994)
DOI: 10.1016/0046-8177(94)90098-1

134. A. Carbone, A. Gloghini, V. Zagonel, D. Aldinucci, V. Gattei, M. Degan, S. Improta, R. Sorio, S. Monfardini and A. Pinto: The expression of CD26 and CD40 ligand is mutually exclusive in human T-cell non-Hodgkin's lymphomas/leukemias. *Blood*, 86(12), 4617-26 (1995)

135. K. Sato and N. H. Dang: CD26: a novel treatment target for T-cell lymphoid malignancies? (Review). *Int J Oncol*, 22(3), 481-97 (2003)

136. U. Aytac, F. X. Claret, L. Ho, K. Sato, K. Ohnuma, G. B. Mills, F. Cabanillas, C. Morimoto and N. H. Dang: Expression of CD26 and its associated dipeptidyl peptidase IV enzyme activity enhances sensitivity to doxorubicin-induced cell cycle arrest at the G(2)/M checkpoint. *Cancer Res*, 61(19), 7204-10 (2001)

137. U. Aytac, K. Sato, T. Yamochi, T. Yamochi, K. Ohnuma, G. B. Mills, C. Morimoto and N. H. Dang: Effect of CD26/dipeptidyl peptidase IV on Jurkat sensitivity to G2/M arrest induced by topoisomerase II inhibitors. *Br J Cancer*, 88(3), 455-62 (2003)
DOI: 10.1038/sj.bjc.6600791
PMid:12569391 PMCid:PMC2747550

138. K. Sato, U. Aytac, T. Yamochi, T. Yamochi, K. Ohnuma, K. S. McKee, C. Morimoto and N. H. Dang: CD26/dipeptidyl peptidase IV enhances expression of topoisomerase IIα and sensitivity to apoptosis induced by topoisomerase II inhibitors. *Br J Cancer*, 89(7), 1366-74 (2003)
DOI: 10.1038/sj.bjc.6601253
PMid:14520473 PMCid:PMC2394325

139. T. Yamochi, T. Yamochi, U. Aytac, T. Sato, K. Sato, K. Ohnuma, K. S. McKee, C. Morimoto and N. H. Dang: Regulation of p38 phosphorylation and topoisomerase IIα expression in the B-cell lymphoma line Jiyoye by CD26/dipeptidyl peptidase IV is associated with enhanced *in vitro* and *in vivo* sensitivity to doxorubicin. *Cancer Res*, 65(5), 1973-83 (2005)
DOI: 10.1158/0008-5472.CAN-04-2611
PMid:15753397

140. T. Oravecz, M. Pall, G. Roderiquez, M. D. Gorrell, M. Ditto, N. Y. Nguyen, R. Boykins, E. Unsworth and M. A. Norcross: Regulation of the receptor specificity and function of the chemokine RANTES (regulated on activation, normal T cell expressed and secreted) by dipeptidyl peptidase IV (CD26)-mediated cleavage. *J Exp Med*, 186(11), 1865-72 (1997)
DOI: 10.1084/jem.186.11.1865
PMid:9382885 PMCid:PMC2199148

141. P. Proost, S. Struyf, D. Schols, G. Opdenakker, S. Sozzani, P. Allavena, A. Mantovani, K. Augustyns, G. Bal, A. Haemers, A. M. Lambeir, S. Scharpe, J. Van Damme and I. De Meester: Truncation of macrophage-derived chemokine by CD26/dipeptidyl-peptidase IV beyond its predicted cleavage site affects chemotactic activity and CC chemokine receptor 4 interaction. *J Biol Chem*, 274(7), 3988-93 (1999)
DOI: 10.1074/jbc.274.7.3988
PMid:9933589

142. R. Pang, W. L. Law, A. C. Chu, J. T. Poon, C. S. Lam, A. K. Chow, L. Ng, L. W. Cheung, X. R. Lan, H. Y. Lan, V. P. Tan, T. C. Yau, R. T. Poon and B. C. Wong: A subpopulation of CD26+ cancer stem cells with metastatic capacity in human colorectal cancer. *Cell Stem Cell*, 6(6), 603-15 (2010)
DOI: 10.1016/j.stem.2010.04.001
PMid:20569697

143. J. H. Jang, L. Baerts, Y. Waumans, I. De Meester, Y. Yamada, P. Limani, I. Gil-Bazo, W. Weder and W. Jungraithmayr: Suppression of lung metastases by the CD26/DPP4 inhibitor Vildagliptin in mice. *Clin Exp Metastasis*, 32(7), 677-87 (2015)
DOI: 10.1007/s10585-015-9736-z
PMid:26233333

144. U. Yamaguchi, R. Nakayama, K. Honda, H. Ichikawa, T. Hasegawa, M. Shitashige, M. Ono, A. Shoji, T. Sakuma, H. Kuwabara, Y. Shimada, M. Sasako, T. Shimoda, A. Kawai, S. Hirohashi and T. Yamada: Distinct gene expression-defined classes of gastrointestinal stromal tumor. *J Clin Oncol*, 26(25), 4100-8 (2008)
DOI: 10.1200/JCO.2007.14.2331
PMid:18757323

145. V. K. Hopsu-Havu and G. G. Glenner: A new dipeptide naphthylamidase hydrolyzing glycyl-prolyl-beta-naphthylamide. *Histochemie*, 7(3), 197-201 (1966)
DOI: 10.1007/BF00577838
PMid:5959122

146. C. A. Abbott, E. Baker, G. R. Sutherland and G. W. McCaughan: Genomic organization, exact localization, and tissue expression of

the human CD26 (dipeptidyl peptidase IV) gene. *Immunogenetics*, 40(5), 331-8 (1994) DOI: 10.1007/BF01246674 PMid:7927537

147. M. E. Morrison, S. Vijayasaradhi, D. Engelstein, A. P. Albino and A. N. Houghton: A marker for neoplastic progression of human melanocytes is a cell surface ectopeptidase. *J Exp Med*, 177(4), 1135-43 (1993) DOI: 10.1084/jem.177.4.1135 PMid:8096237

148. S. S. Farag, S. Srivastava, S. Messina-Graham, J. Schwartz, M. J. Robertson, R. Abonour, K. Cornetta, L. Wood, A. Secrest, R. M. Strother, D. R. Jones and H. E. Broxmeyer: *In vivo* DPP-4 inhibition to enhance engraftment of single-unit cord blood transplants in adults with hematological malignancies. *Stem Cells Dev*, 22(7), 1007-15 (2013) DOI: 10.1089/scd.2012.0636 PMid:23270493 PMCid:PMC3607909

149. P. Proost, S. Struyf, J. Van Damme, P. Fiten, E. Ugarte-Berzal and G. Opdenakker: Chemokine isoforms and processing in inflammation and immunity. *J Autoimmun* (2017)

150. K. Ohnuma, R. Hatano, T. Itoh, N. Iwao, N. H. Dang and C. Morimoto: Role of IL-26+CD26+CD4 T Cells in Pulmonary Chronic Graft-Versus-Host Disease and Treatment with Caveolin-1-Ig Fc Conjugate. *Crit Rev Immunol*, 36(3), 239-267 (2016) DOI: 10.1615/CritRevImmunol.2016018772 PMid:28008806

151. F. I. Ghani, H. Yamazaki, S. Iwata, T. Okamoto, K. Aoe, K. Okabe, Y. Mimura, N. Fujimoto, T. Kishimoto, T. Yamada, C. W. Xu and C. Morimoto: Identification of cancer stem cell markers in human malignant mesothelioma cells. *Biochem Biophys Res Commun*, 404(2), 735-42 (2011) DOI: 10.1016/j.bbrc.2010.12.054 PMid:21163253

152. H. Yamazaki, M. Naito, F. I. Ghani, N. H. Dang, S. Iwata and C. Morimoto: Characterization of cancer stem cell properties of CD24 and CD26-positive human malignant mesothelioma cells. *Biochem Biophys Res Commun*, 419(3), 529-36 (2012) DOI: 10.1016/j.bbrc.2012.02.054 PMid:22369943

153. H. Herrmann, I. Sadovnik, S. Cerny-Reiterer, T. Rulicke, G. Stefanzl, M. Willmann, G. Hoermann, M. Bilban, K. Blatt, S. Herndlhofer, M. Mayerhofer, B. Streubel, W. R. Sperr, T. L. Holyoake, C. Mannhalter and P. Valent: Dipeptidylpeptidase IV (CD26) defines leukemic stem cells (LSC) in chronic myeloid leukemia. *Blood*, 123(25), 3951-62 (2014) DOI: 10.1182/blood-2013-10-536078 PMid:24778155

154. S. Davies, A. Beckenkamp and A. Buffon: CD26 a cancer stem cell marker and therapeutic target. *Biomed Pharmacother*, 71, 135-8 (2015) DOI: 10.1016/j.biopha.2015.02.031 PMid:25960228

155. R. Hatano, T. Yamada, S. Matsuoka, S. Iwata, H. Yamazaki, E. Komiya, T. Okamoto, N. H. Dang, K. Ohnuma and C. Morimoto: Establishment of monoclonal anti-human CD26 antibodies suitable for immunostaining of formalin-fixed tissue. *Diagn Pathol*, 9, 30-42 (2014) DOI: 10.1186/1746-1596-9-30 PMid:24502396 PMCid:PMC3944398

156. K. Ohnuma, R. Hatano and C. Morimoto: DPP4 in anti-tumor immunity: going beyond the enzyme. *Nat Immunol*, 16(8), 791-2 (2015) DOI: 10.1038/ni.3210 PMid:26194276

Abbreviation: AA, amino acid; ADA, adenosine deaminase; ADCC, antibody-dependent cellular cytotoxicity; aGVHD, acute graft-versus-host disease; alloHSCT, allogeneic hematopoietic stem cell transplantation; AP-1, activator protein-1; APCs, antigen presenting cells; A20-luc, luciferase-transfected A20 cell; B6 WT, parental C57BL/6 mice; Cav-Ig, soluble Fc fusion proteins containing the N-terminal domain of caveolin-1; CB, cord blood; CD26KO, CD26 knockout; cGVHD, chronic graft-versus-host disease; CRC, colorectal cancer; CTL, cytotoxic T lymphocyte; CTLA-4, cytotoxic T-lymphocyte–associated antigen 4; ΔCNS-77 Tg mice, mice carrying human *IFNG* transgene with deleting *IL26* transcription; DPPIV, dipeptidyl peptidase IV; ECM, extracellular matrix; EGR2, early growth response 2; ELISA, enzyme-linked immunosorbent assay; EMT, epithelial to mesenchymal transition; ERK, extracellular signal-regulated kinase; FIH, first-in-human; GIST, gastrointestinal stromal tumors; GVHD,

graft-versus-host disease; GVL, graft-versus-leukemia; HuCB, human umbilical cord blood; IBD, inflammatory bowel diseases; i.d., intradermal injection; IFN, interferon; IL, interleukin; IMQ, imiquimod; JKT-hCD26WT, Jurkat cells transfected with full-length human CD26/DPPIV; LAG3, lymphocyte activation gene-3; LBL/ALL, lymphoblastic lymphoma/acute lymphoblastic leukemia: mAb, monoclonal antibody; MAPK, mitogen-activated protein kinase; MERS-CoV, Middle East respiratory syndrome coronavirus; MERS-CoV S1-Fc, S1 domain of MERS-CoV fused to the Fc region of human IgG; MPM, malignant pleural mesothelioma; NFAT, nuclear factor of activated T cells; NOG, NOD/Shi-*scid*IL2rγ^{null}; OB, obliterative bronchiolitis; PBL, peripheral blood lymphocyte; PD-1, programmed cell death 1; PSO, psoriasis; RA, rheumatoid arthritis; RBD, receptor binding domain; RCC, renal cell carcinoma; RECIST, response evaluation criteria in solid tumors; sCD26, soluble CD26; sDPPIV, soluble dipeptidyl peptidase IV; siRNA, small interfering RNA; SP, substance P; SSTR4, somatostatin receptor 4; Tg, transgenic; T-LGL, T-large granular lymphocyte; TME, tumor microenvironment; TNF, tumor necrosis factor; Tr1, Type 1 regulatory T cells; WHO, World Health Organization; 190-*IFNG* Tg mice, mice carrying human *IFNG* and *IL26* transgene

Key Words CD26, DPPIV, Caveolin-1, Humanized anti-CD26 monoclonal antibody, Graft-versus-host disease, Malignant pleural mesothelioma, Review

Send correspondence to: Kei Ohnuma, Department of Therapy Development and Innovation for Immune Disorders and Cancers, Graduate School of Medicine, Juntendo University, 2-1-1, Hongo, Bunkyo-ku, Tokyo 113-8421, Japan, Tel: 81-3-3868-2310, Fax: 81-3-3868-2310, E-mail: kohnuma@juntendo.ac.jp

Biochemical and Biophysical Research Communications 505 (2018) 787–793

Contents lists available at ScienceDirect

Biochemical and Biophysical Research Communications

journal homepage: www.elsevier.com/locate/ybbrc

A novel derivative (GTN024) from a natural product, komaroviquinone, induced the apoptosis of high-risk myeloma cells via reactive oxygen production and ER stress

Mikio Okayama [a, b], Shotaro Kitabatake [a], Mariko Sato [a], Kota Fujimori [a], Daiju Ichikawa [a], Maiko Matsushita [a], Yutaka Suto [c], Genji Iwasaki [c], Taketo Yamada [d], Fumiyuki Kiuchi [e], Maki Hirao [f], Hisako Kunieda [f], Makoto Osada [f], Shinichiro Okamoto [b], Yutaka Hattori [a, f, *]

[a] Clinical Physiology and Therapeutics, Keio University Faculty of Pharmacy, Tokyo, Japan
[b] Division of Hematology, Department of Internal Medicine, Keio University School of Medicine, Tokyo, Japan
[c] Faculty of Pharmacy, Takasaki University of Health and Welfare, Gunma, Japan
[d] Department of Pathology, Saitama Medical University, Saitama, Japan
[e] Division of Natural Medicines, Keio University Faculty of Pharmacy, Tokyo, Japan
[f] Department of Hematology, Tokyo Saiseikai Central Hospital, Tokyo, Japan

ARTICLE INFO

Article history:
Received 19 September 2018
Accepted 28 September 2018
Available online 5 October 2018

Keywords:
Multiple myeloma
Natural product
Apoptosis
Reactive oxygen species
ER stress

ABSTRACT

New drugs have significantly improved the survival of patients with multiple myeloma (MM), but the prognosis of MM patients with high-risk cytogenetic changes such as t(4; 14), t(14; 16) or del17p remains very poor. A natural product, komaroviquinone (KQN), was originally isolated from the perennial semi-shrub *Dracocephalum komarovi* and has anti-protozoal activity against *Trypanosoma cruzi*, the organism causing Chagas' disease. Here we demonstrate that a novel KQN-derivative, GTN024, has an anti-MM effect both *in vitro* and *in vivo*. GTN024 induced the apoptosis of MM cell lines including those with high-risk cytogenetic changes. GTN024 produced reactive oxygen species (ROS) and increased phosphorylated eIF2α. The ROS production and subsequent endoplasmic reticulum (ER) stress are thought to play a key role in GTN024-induced apoptosis, as the apoptosis was completely abrogated by anti-oxidant treatment. In a mouse xenograft model, an intraperitoneal injection of 20 mg/kg of GTN024 significantly delayed tumor growth. Hematological toxicity and systemic toxicity as indicated by weight loss were not observed. These results suggest that the novel KQN-derivative GTN024 could become a candidate drug for treating high-risk MM.

1. Introduction

Multiple myeloma (MM) is a B-cell neoplasm that causes clonal plasma cell proliferation in bone marrow and bone lesions. The 5-year prevalence rate of MM incidence in Japan is reported to be 9.7 per 100,000 persons [1]. New agents such as proteasome inhibitors and immunomodulatory drugs (IMiDs) have significantly improved the overall survival of MM patients [2–5], drugs from different categories such as a histone-deacetylase inhibitor [6], an anti-SLAMF7 antibody [7], and an anti-CD38 antibody [8] have also been reported to be effective for refractory MM in combination therapy with IMiDs and proteasome inhibitors.

Despite these advances, the survival of certain groups of MM patients remains unsatisfactory [9–11]. Those patients are known as having 'high-risk MM,' and their MM cells frequently possess chromosomal abnormalities such as t(4; 14), t(14; 16), del17p, and 1q21 amplification. The revised International Staging System indicates that the overall survival of the patients with high-risk cytogenic abnormalities is significantly short [12]. Another limitation of newly developed drugs is their toxicities [13,14], which impede the optimal drug efficacy and result in unsatisfactory treatment outcomes, especially among elderly patients. New therapeutic modalities that are effective for high-risk MM with less side effects are thus currently an unmet clinical need in MM treatment.

A series of anti-neoplastic drugs were developed from natural

* Corresponding author. Clinical Physiology and Therapeutics, Keio University Faculty of Pharmacy, Tokyo, Japan.
E-mail address: hattori-yt@pha.keio.ac.jp (Y. Hattori).

https://doi.org/10.1016/j.bbrc.2018.09.177
0006-291X/

products, and there are some reports describing anti-neoplastic activities of anti-protozoal agents. For example, nifurtimox, a drug for Chagas' disease, showed anti-tumor effects against neural tumor cells. Nifurtimox induced the apoptosis of neuroblastomas by inhibiting extracellular signal-regulated kinase (ERK) phosphorylation [15]. Artesunate, an anti-malaria drug, also showed anti-MM effects by inhibiting nuclear factor-kappa B (NFκB) function [16]. With these drugs, the anti-tumor activities were discovered as off-target effects in drug repositioning studies.

Komaroviquinone (KQN) is one of the natural products isolated from the perennial semi-shrub *Dracocephalum komarovi* (family Laminaceae), which shows anti-protozoal activities. Suto et al. reported the asymmetric synthesis of KQN [17]. In a study of the structure activity relationship study of KQN [17], a series of low-molecular-weight compounds were discovered to exhibit promising anti-protozoal activities against *Trypanosoma cruzi*, which is the causative pathogen of Chagas' disease [18]. It is also reported that KQN was reduced by *T. cruzi* old yellow enzyme (TcOYE) to form its semiquinone and produced reactive oxygen species (ROS), which showed trypanocidal activities [19]. A biomedical assay of both KQN and its derivatives demonstrated that the new KQN-derivative GTN024 had high anti-proliferation activities against MM cells [20]. In addition, in the above-cited structure-activity relationship study, GTN024 was shown to be readily accessible and a valuable compound for the further pharmacodynamic study of MM cells [20].

With this background, we carried out the present study to determine the anti-tumor effects of GTN024 on MM cell lines including those with high-risk cytogenetic changes, and we clarified this promising new drug's mode of action and safety.

2. Materials and methods

2.1. Cells

The human myeloma cell lines KMM1, KMS11, KMS21, KMS26, KMS27, KMS28 and KMS34 were kindly provided by Dr. T. Otsuki (Kawasaki Medical School, Kurashiki, Japan) [21]. The cell line MUM24 was established in our laboratory from a patient with thalidomide-resistant MM [22]. These cell lines were maintained in RPMI1640 medium (Sigma-Aldrich, St. Louis, MO, USA) containing 10% fetal bovine serum (FBS, Gibco, Life Technologies, Carlsbad, CA) and 1% penicillin-streptomycin (Pen Strep, Gibco). Chronosomal abnormalities were detected by the fluorescence *in situ* hybridization (FISH) analysis. (LSI medience, Tokyo).

2.2. Reagents

GTN024 (Fig. 1A) was prepared as described by Suto et al. [18]. In the present *in vitro* study, GTN024 was diluted in phosphate-buffered saline (PBS, Sigma-Aldrich) containing 1% Tween®80 (Otsuka Pharmaceutical, Tokyo) and 10% DMSO.

2.3. Patient's samples

Bone marrow samples were collected from MM patients treated at Tokyo Saiseikai Central Hospital. The collection of clinical samples was approved by ethical committee of Saiseikai Central Hospital (No. 28–66) and the Faculty of Pharmacy, Keio University (No. 170616–5, 180615–5). Written informed consent for their samples to be used was obtained from all patients. Cells were isolated by centrifugation with Lymphoprep™ (Axis-Shield, Oslo, Norway). Cells were labeled with CD138 MicroBeads (Miltenyi Biotec, Bergisch Gladbach, Germany). The magnetically labeled CD138-positive cells were purified by MACS Columns (Miltenyi Biotec).

2.4. Trypan blue exclusion assay

Cells (2×10^5 cells/mL) were seeded on six-well plates and cultured in various concentrations of GTN024 (0–20 μM) with or without 6 mM of *N*-acetyl cysteine (NAC, Sigma-Aldrich) or 3 mM of glutathione (GSH, Sigma-Aldrich) at 37 °C in 5% CO_2. The cells were stained with Trypan Blue Stain 0.4% (Gibco) and viable cells were counted by an automatic cell counter TC20™ (Bio-Rad, Hercules, CA). Viable cells were counted three times, and the average was calculated. The IC_{50} of GTN024 was calculated by approximation.

2.5. MTT assay

Collected clinical samples (6×10^4 cells/mL) were seeded on 96-well plates and cultured with various concentrations of GTN024 (0–30 μM) at 37 °C in 5% CO_2 for 48 h. The viability of the cells was calculated by MTT dye absorbance (Roche Diagnostics, Indianapolis, IN) according to the manufacturer's instructions.

2.6. Apoptosis detection assay

Cells (2×10^5 cells/mL) were seeded on six-well plates and cultured at 37 °C in 10 μM GTN024 for 72 h. Apoptotic cells were detected by an annexin V-FITC Apoptosis Detection Kit (BioVision, San Francisco, CA) following the manufacturer's protocol. Briefly, cells were collected and resuspended in 500 μL of 1 × Binding Buffer and stained with annexin V –FITC and propidium iodide (PI) for 5 min. The cells were analyzed using a BD™ LSRII flow cytometer (Becton Dickinson, Lincoln Park, NJ).

2.7. Detection of reactive oxygen species

Cells (2×10^5 cells/mL) were seeded on six-well plates and cultured at 37 °C with or without 6 mM NAC or 3 mM GSH for 2 h. Then, 20 μM GTN024 was added and incubated in 5% CO_2. After 72 h, 1 μM chloromethyl-dichlorodihydrofluorescein diacetate, acetyl ester (CM-H_2DCFDA, Invitrogen, Carlsbad, CA) was added and incubated for 30 min. The stained cells were analyzed using the BD LSRII flow cytometer.

2.8. Western blotting

Cells were cultured with GTN024 and lysed in 1% NP-40 buffer containing 1 mM PMSF, 1 mM Na_2PO_4, 20 mM NaF, 2 mM Na_2PO_7, and protease inhibitors (Complete Protease Inhibitor Mixture, Roche Diagnostics, Mannheim, Germany). After incubation for 10 min on ice, the lysates were centrifuged at 15,000 rpm for 10 min at 4 °C, and the supernatants were collected. The amount of protein was evaluated by BCA Protein Assay Kit (Thermo Fisher Scientific, Waltham, MA).

The lysates were mixed with Laemmli's buffer (1.33% SDS, 10% glycerol, 0.083 M Tris-HCl, 0.04% bromphenol blue, 2% 2-ME) and boiled for 5 min. The lysates were subjected onto 10% sodium dodecyl sulfate-polyacrylamide gel electrophoresis (SDS-PAGE), and transferred to a PVDF membrane. The membranes were blocked with 5% skim milk and then immunoblotted. Antibodies against eIF2α (Cell Signaling Technology, Danvers, MA), *p*-eIF2α (Cell Signaling Technology), β-actin (Santa Cruz Biotechnology, Santa Cruz, CA), and cleaved caspase-3 (Cell Signaling Technology) (diluted at 1:1000) was used. The second antigen-antibodies was a horseradish peroxidase (HRP)-coupled anti-rabbit, anti-mouse Ig antibody (diluted at 1:500). Antigen-antibody complexes were detected using enhanced chemiluminescence (Amersham, Arlington Heights, IL).

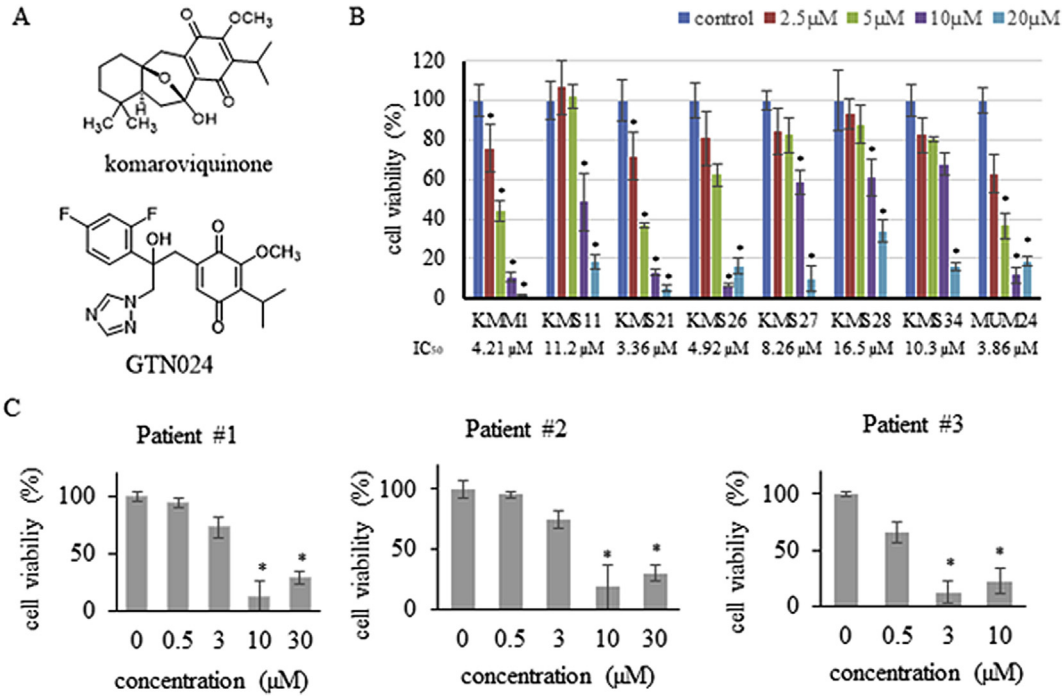

Fig. 1. GTN024 induced cell death in MM cell lines and MM patients. (A) The chemical structures of komaroviquinone and GTN024. (B) The inhibitory effects of GTN024 on MM cells with chromosomal abnormalities [22,35]. Cells were cultured with GTN024 for 48 h. The number of viable cells was counted by staining with trypan blue. Bars: means ± SD, n = 3. *p < 0.05 vs. control. (C) The inhibitory effects of GTN024 on MM clinical samples. Cells were collected from clinical bone marrow samples obtained from three MM patients. The viability of CD138$^+$ cells treated with GTN024 was measured by MTT assay. Bars: indicate means ± SD, n = 3. *p < 0.05 vs. control. (For interpretation of the references to color in this figure legend, the reader is referred to the Web version of this article.)

2.9. Toxicity assessment

To evaluate the toxicity of GTN024 *in vivo*, we intraperitoneally injected 0, 10, 20, or 40 mg/kg of GTN024 in 1% Tween®80 and 10% DMSO in saline to 5-wk-old male ICR mice (Clea, Tokyo) daily for three consecutive days. The body weights of the mice were measured every 3 days. We took peripheral blood samples with a heparinized hematocrit tube (Terumo, Tokyo) from the tail veins of the mice every 3 days. Blood samples were diluted 10 times by Türk's solution (Merck, Darmstadt, Germany), and the numbers of leukocytes and neutrophils were counted under a light microscope. All animal experiments were approved by the Ethics Committee for Animal Experiments at Keio University (Approval no. 12067-(2)).

2.10. In vivo tumor growth assay

KMS11 cells (3×10^7 cells) were inoculated into 5-wk-old male ICR/SCID mice (Clea) subcutaneously in the flank. When the resulting tumors reached 100 mm^3, 20 mg/kg of GTN024 (1% Tween®80, 10% DMSO in saline) was injected intraperitoneally daily for three consecutive days. The tumor volume was calculated by length × width^2 × 0.52 [23].

2.11. Histopathologic examination

Xenografted mice were sacrificed, and isolated tumors were fixed with 10% formalin and embedded in 5-μm pieces of paraffin. Sliced sections were stained with hematoxylin and eosin (H&E). Anti-human cleaved PARP polyclonal antibody (Cell Signaling Technology Japan, Tokyo), anti-human cleaved caspase-3 (Asp175) polyclonal antibody (Cell Signaling Technology Japan), anti-human Ki-67 monoclonal antibody (clone MIB-1) (Dako Japan, Tokyo), and anti-human PCNA polyclonal antibody (Atlas Antibodies, Stockholm, Sweden) were used for immunohistochemistry.

2.12. Statistical analysis

The significance of differences was determined using Student's *t*-test. The level of significance was set at $p < 0.05$.

3. Results

3.1. GTN024 inhibited the growth of MM cells

We examined the tumoricidal effects of GTN024 against various MM cell lines. GTN024 induced the cell death of all of the MM cell lines tested (KMM1, KMS11, KMS21, KMS26, KMS27, KMS28, KMS34, and MUM24) (Fig. 1B). IC_{50} varied from 3.36 μM (KMS21) to 16.5 μM (KMS28). One arm of chromosome 17 is deleted in KMM1, KMS11, KMS26, KMS34 and MUM24 cells, and KMS11, KMS26, KMS28, KMS34 and MUM24 also show t(4; 14) (our unpublished data).

We then examined whether GTN024 could induce cell death in CD138$^+$ cells obtained from three MM patients. Patient #1 and #2 had untreated MM and both of their MM cells had 1q21 amplification. Patient #3 had been treated with and showed resistance to bortezomib, lenalidomide, pomalidomide, ixazomib, and elotuzumab. Based on the results shown in Fig. 1C, their IC_{50} values in response to GTN024 were calculated as 5.09 μM (patient #1), 5.94 μM (patient #2), and 0.84 μM (patient #3).

3.2. Anti-MM effect via the ROS production of GTN024

We examined the ROS production in GTN024-treated MM cells. The flow cytometric analysis using CM-H_2DCFDA showed that GTN024 significantly induced ROS production in MM cells (Fig. 2A).

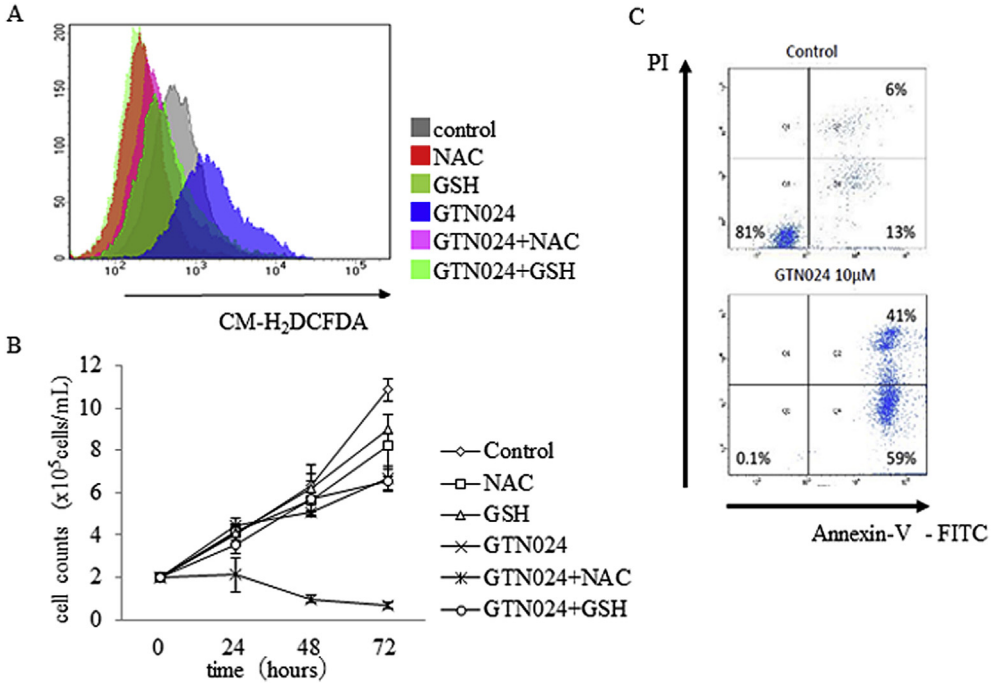

Fig. 2. GTN024 treatment resulted in ROS-mediated apoptotic cell death. (A) MUM24 cells (2×10^5 cells/mL) were incubated with or without NAC or GSH for 2 h and GTN024 was added. ROS levels were determined by staining with CM-H_2DCFDA. Stained cells were analyzed using a FACS BD LSRII. (B) MUM24 cells (2×10^5 cells/mL) were cultured with NAC or GSH for 2 h, and GTN024 was added. The number of viable cells was counted by staining with trypan blue. Bars: mean ± SD, n = 3. *$p < 0.05$ vs. control. (C) MUM24 cells (2×10^5 cells/mL) were cultured with 10 μM GTN024 for 72 h stained with Annexin V-FITC and propidium iodide (PI) followed by an analysis with the BD LSRII system.

We next examined whether the growth inhibitory effect of GTN024 depends on ROS production. As shown in Fig. 2B, the growth inhibition by GTN024 treatment was mostly abrogated when the MM cells were preincubated with anti-oxidants. The flow cytometric analysis also showed that the GTN024 treatment of MM cells increased the number of annexin V^+ cells, indicating that GTN024 induced apoptosis (Fig. 2C).

3.3. Excessive ER stress pathway appears to be the cause of GTN024's anti-MM activity

Since GTN024 showed tumoricidal effects in an ROS-dependent manner, we hypothesized that GTN024 would cause excessive endoplasmic reticulum (ER) stress. We observed that the phosphorylation of eIF2α was increased in GTN024-treated MM cells (Fig. 3A). We also observed an increased amount of cleaved caspase-3 following treatment with GTN024 (Fig. 3B).

3.4. Safety and the anti-MM effects of GTN024 in vivo

To determine the optimal dosage of GTN024 in the KMS11-xenografted mice model, we administered 10, 20, or 40 mg/kg day of GTN024 to ICR mice by intraperitoneal injection for three consecutive days (days 1–3). When mice were treated with 40 mg/kg day of GTN024, significant weight loss and bowel obstructions were observed. However, when 10 mg/kg day or 20 mg/kg day were given to mice, no loss of body weight was observed (Fig. 4A). No hematological toxicities were detected at any dosage levels (Fig. 4A). Given these results, we considered 20 mg/kg for three consecutive days as the maximal tolerated dose for mouse experiments.

To examine the growth-inhibitory effects of GTN024 *in vivo*, we intraperitoneally injected 20 mg/kg of GTN024 in KMS11-xenografted mice for three consecutive days. As shown in Fig. 4B, GTN024 significantly delayed tumor growth in xenografted mice. At 14 days after the first injection, the average tumor volume was 383 mm^3 in the GTN024-treated mice, and 843 mm^3 in the control mice ($p < 0.05$).

The H&E staining showed an agglutination of chromatin in the tumors of GTN024-treated mice (Fig. 4C). Cleaved-caspase-3-positive and PARP-positive cells were also significantly increased in the GTN024-treated tumors. In contrast, staining with MIB-1, a strong marker of cell proliferation, was weaker in the tumors of the GTN024-treated mice compared to those of the control mice (Fig. 4C).

4. Discussion

A number of novel drugs have been derived from natural products. For example, irinotecan, a derivative of camptothecin that was originally isolated from the deciduous tree *Camptotheca acuminata*, is now widely used as an anti-cancer agent for lung cancer and colorectal cancer [24]. Paclitaxel, which is derived from the tree *Taxus brevifolia*, induces the apoptosis of cancer cells via binding to β-tubulin, inducing depolymerization and stabilizing microtubules [25]. A variety of molecular-targeting agents have been developed, but their success is limited to a few malignant diseases such as chronic myelogenous leukemia.

Multiple myeloma is a genetically heterogenenous disease, and target molecules (such as a driver gene mutation) have not been discovered. More therapeutic options including novel compounds are needed for treating high-risk MM patients to improve their prognoses and quality of life. The exploitation of clinically effective drugs is time-consuming and involves significant costs. Therefore, natural products remain an important resource for drug development. In this study, we focused on a novel natural compound, KQN, and its derivative, GTN024 analogues.

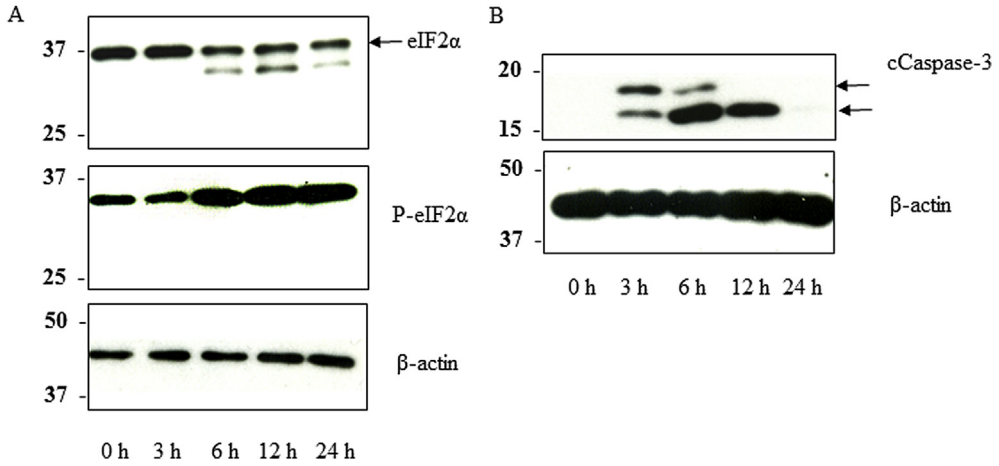

Fig. 3. GTN024 induced ER stress-mediated cell death in MUM24 cells. MUM24 cells were treated with GTN024 for 3, 6, 12, or 24 h. The cells were lysed and analyzed by immunoblotting against eIF2α, *p*-eIF2α, β-actin, and cleaved caspase-3. The lower band of eIF2α was considered as the degradation of eIF2α [36].

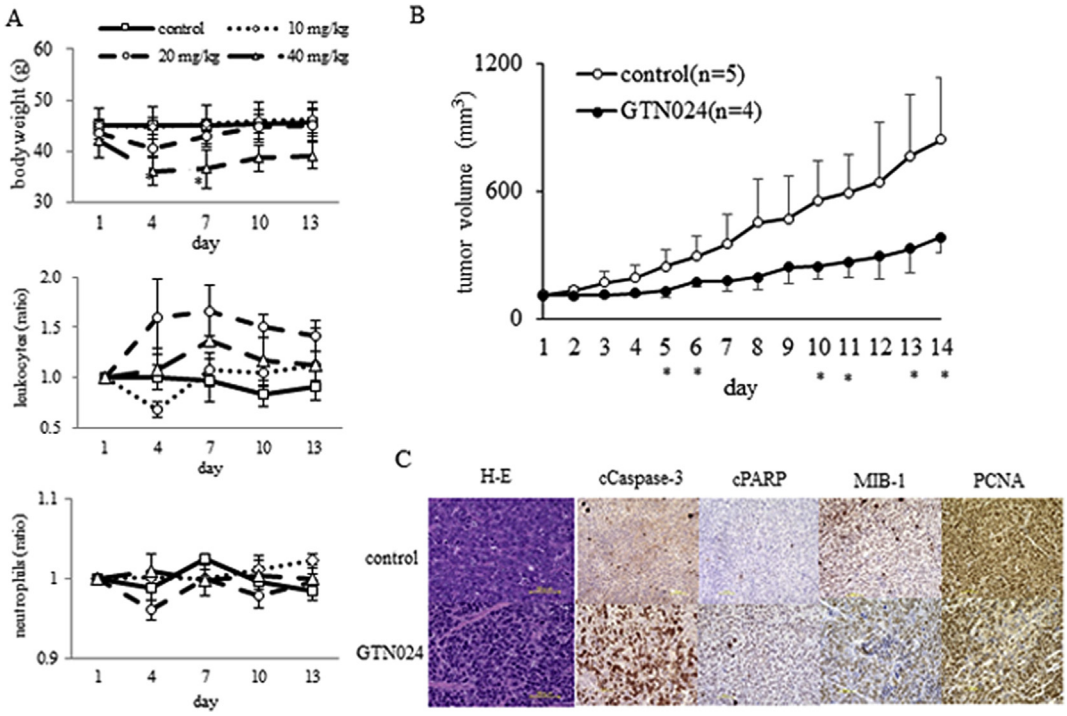

Fig. 4. Toxicity and anti-MM effects of GTN024 in the *in vivo* model. (A) ICR mice were treated with 10, 20, or 40 mg/kg of GTN024 for three consecutive days (days 1–3). Blood samples were collected from tail veins. Leukocyte and neutrophil numbers were counted after Türk's solution staining. Bars: mean ± SD, n = 3. *p < 0.05 vs. control. (B) Suppressed growth of MM cells in the xenograft mouse model by GTN024 20 mg/kg. GTN024 was given when xenografted tumor exceeded 100 mm^3. GTN024 20 mg/kg was given intraperitoneally on days 1–3. Bars: mean ± SD. *p < 0.05 (control vs. GTN024). (C) Stained xenografted tumor of a GTN024-treated mouse. Xenograft tumors in mice after treatment with or without GTN024 were collected and stained with H&E, anti-cleaved caspase-3, anti-cleaved PARP, anti-MIB-1, and anti-PCNA.

Suto et al. synthesized a series of KQN-related compounds. The above-cited structure-activity relationship study revealed that the hydroquinone moiety is necessary to potent anti-tumor effects of these compounds [20]. Among them, GTN024, which has a benzoquinone moiety, showed significant anti-MM effects, and was readily accessible because it has only a single chiral carbon [20]. We therefore conducted further research regarding GTN024.

Our present findings demonstrated that GTN024 had *in vitro* anti-MM effects against MM cell lines and clinical samples obtained from MM patients including those with high-risk chromosomal abnormalities, indicating that GTN024 is a promising candidate for treating MM patients with high-risk cytogenic changes.

As described in results, we concluded that 20 mg/kg for 3 days is the maximum tolerated dose for our mouse model. In our mouse xenograft model, significant anti-MM effects were produced by the same schedule of drug administration without severe toxicities. The results of the histopathological examination confirmed that GTN024 caused the apoptosis of xenografted tumors.

KQN, the mother compound of GTN024, was reduced by TcOYE to its semiquinone form, and the production of ROS is the key mechanism of anti-trypanocidal effects [18,19]. In the present study, we observed that GTN024 showed ROS production and

induced the apoptosis of MM cells, which were abrogated by antioxidants. We therefore speculate that the anti-MM effects of GTN024 are due mainly to the cytotoxicity by ROS. Several ROS-mediated compounds have also shown significant cytotoxicity against MM cells, via various pathways such as the inhibition of thioredoxin 1 by PX-12 [26], DNA damage by an ATR inhibitor [27], and the activation of p53 by CP-31398 [28]. It is thus apparent that ROS-mediated cytotoxicity plays an important role in treatments for MM.

MM cells are characterized by the excessive accumulation of unfolded M-protein. In this study, we focused on endoplasmic reticulum (ER) stress, because ROS cause the apoptosis of cells by an excessive ER response, which could be a therapeutic target in MM [29–32]. ROS induced ER stress via many signals including PERK and mitochondria pathway [33,34]. Here we focused on eIF2α, a key molecule of ER stress, and our findings showed an increased phosphorylation of eIF2α in MM cells by GTN024. We also observed increased level of cleaved caspase-3. These results suggested that ROS-mediated ER stress is a putative target pathway of GTN024-induced apoptosis.

In conclusion, we developed GTN024 from a natural product, KQN, and our present results demonstrated the induction of the apoptosis of MM cells with high-risk cytogenic abnormalities *in vitro* and *in vivo*. The major merits of using GTN024 in MM treatments are as follows. First, GTN024 showed cytotoxicity to MM cells with high-risk chromosomal changes that are resistant to currently available drugs. Some of the cell lines used in this study are resistant to lenalidomide or dexamethasone [22,23]. MUM24 cells were established from a thalidomide-resistant patient [22]. Second, in our mouse xenograft model, GTN024 significantly inhibited tumor growth without eminent hematological or systemic side effects when the mice were treated with 10–20 mg/kg of GTN024. Third, GTN024 induced apoptosis via ROS-mediated excessive ER stress, to which MM cells were highly vulnerable. We therefore propose that GTN024 is a promising candidate compound for the treatment of high-risk MM.

Acknowledgements

We thank for Prof. Otsuki for the kind gift of MM cell lines. We also thank Shogo Mori, Koya Kakimoto, and Sayaka Motonaga for doing the growth-inhibition assay. This work was supported in part by a Grant-in-Aid for Scientific Research and a grant from the Private University Strategic Research Base Development Program of the Ministry of Education, Culture, Sports, Science and Technology (MEXT) of Japan (to Y.H.); grants-in-aid from the Translational Research Network Program, Japan Agency for Medical Research and Development (AMED), #15lm0103010j0002 and #16lm0103010j0003 (Y.H.); and International Myeloma Foundation Japan's grants (M.M.), and Japanese Society of Myeloma (JSM) Research Award (D.I.).

Transparency document

Transparency document related to this article can be found online at https://doi.org/10.1016/j.bbrc.2018.09.177.

References

[1] K. Yamabe, S. Inoue, C. Hiroshima, Epidemiology and burden of multiple myeloma in Japan, Value Health 18 (2015). A449.
[2] S.K. Kumar, A. Dispenzieri, M.Q. Lacy, et al., Continued improvement in survival in multiple myeloma: changes in early mortality and outcomes in older patients, Leukemia 28 (2014) 1122–1128.
[3] D.S. Siegel, T. Martin, M. Wang, et al., A phase 2 study of single-agent carfilzomib (PX-171-003-A1) in patients with relapsed and refractory multiple myeloma, Blood 120 (2012) 2817–2825.
[4] S.K. Kumar, J.G. Berdeja, R. Niesvizky, et al., Safety and tolerability of ixazomib, an oral proteasome inhibitor, in combination with lenalidomide and dexamethasone in patients with previously untreated multiple myeloma: an open-label phase 1/2 study, Lancet Oncol. 15 (2014) 1503–1512.
[5] X. Leleu, M. Attal, B. Arnulf, et al., Pomalidomide plus low-dose dexamethasone is active and well tolerated in bortezomib and lenalidomide-refractory multiple myeloma: intergroupe Francophone du Myélome 2009-02, Blood 121 (2013) 1968–1975.
[6] M. Dimopoulos, D.S. Siegel, S. Lonial, et al., Vorinostat or placebo in combination with bortezomib in patients with multiple myeloma (VANTAGE 088): a multicentre, randomised, double-blind study, Lancet Oncol. 14 (2013) 1129–1140.
[7] S. Lonial, M. Dimopoulos, A. Palumbo, et al., Elotuzumab therapy for relapsed or refractory multiple myeloma, N. Engl. J. Med. 373 (2015) 621–631.
[8] T. Plesner, H.T. Arkenau, P. Gimsing, et al., Phase 1/2 study of daratumumab, lenalidomide, and dexamethasone for relapsed multiple myeloma, Blood 128 (2016) 1821–1828.
[9] S. Usmani, T. Ahmadi, Y. Ng, et al., Analysis of real-world data on overall survival in multiple myeloma patients with ≥3 prior lines of therapy including a proteasome inhibitor (PI) and an immunomodulatory drug (IMiD), or double refractory to a PI and an IMiD, Oncology 21 (2016) 1355–1361.
[10] R. Fonseca, P.L. Bergsagel, J. Drach, et al., International Myeloma Working Group molecular classification of multiple myeloma: spotlight review, Leukemia 23 (2009) 2210–2221.
[11] N. Grzasko, M. Hus, A. Pluta, et al., Additional genetic abnormalities significantly worsen poor prognosis associated with 1q21 amplification in multiple myeloma patients, Hematol. Oncol. 31 (2013) 41–48.
[12] P.R. Greipp, J. San Miguel, B.G. Durie, et al., International staging system for multiple myeloma, J. Clin. Oncol. 23 (2005) 3412–3420.
[13] M.V. Mateos, P.G. Richardson, R. Schilag, et al., Bortezomib plus melphalan and prednisone compared with melphalan and prednisone in previously untreated multiple myeloma: updated follow-up and impact of subsequent therapy in the phase III VISTA trial, J. Clin. Oncol. 28 (2010) 2259–2266.
[14] M.A. Dimopoulos, C. Chen, A. Spencer, et al., Long-term follow-up on overall survival from the MM-009 and MM-010 phase III trials of lenalidomide plus dexamethasone in patients with relapsed or refractory multiple myeloma, Leukemia 23 (2009) 2147–2152.
[15] M. Du, L. Zhang, K.A. Scorsone, et al., Nifurtimox is effective against neural tumor cells and is synergistic with buthionine sulfoximine, Sci. Rep. 6 (2016) 27458.
[16] S. Li, F. Xue, Z. Cheng, et al., Effect of artesunate on inhibiting proliferation and inducing apoptosis of SP2/0 myeloma cells through affecting NFkappaB p65, Int. J. Hematol. 90 (2009) 513–521.
[17] Y. Suto, K. Kaneko, N. Yamagiwa, et al., A short and efficient asymmetric synthesis of komaroviquinone, Tetrahedron Lett. 51 (2010) 6329–6330.
[18] Y. Suto, J. Nakajima-Shimada, N. Yamagiwa, et al., Synthesis and biological evaluation of quinones derived from natural product komaroviquinone as anti-Trypanosoma cruzi agents, Bioorg. Med. Chem. Lett 25 (2015) 2967–2971.
[19] N. Uchiyama, Z. Kabututu, B.K. Kubata, et al., Antichagasic activity of komaroviquinone is due to generation of reactive oxygen species catalyzed by Trypanosoma cruzi old yellow enzyme, Antimicrob. Agents Chemother. 49 (2005) 5123–5126.
[20] Y. Suto, M. Sato, K. Fujimori, et al., Synthesis and biological evaluation of the natural product komaroviquinone and related compounds aiming at a potential therapeutic lead compound for high-risk multiple myeloma, Bioorg. Med. Chem. Lett 27 (2017) 4558–4563.
[21] M. Namba, T. Ohtsuki, M. Mori, et al., Establishment of five human myeloma cell lines, In Vitro Cell. Dev. Biol. 25 (1989) 723–729.
[22] Y. Hattori, W. Du, T. Yamada, et al., A myeloma cell line established from a patient refractory to thalidomide therapy revealed high-risk cytogenetic abnormalities and produced vascular endothelial growth factor, Blood Canc. J. 3 (2013) e115.
[23] W. Du, Y. Hattori, T. Yamada, et al., NK4, an antagonist of hepatocyte growth factor (HGF), inhibits growth of multiple myeloma cells: molecular targeting of angiogenic growth factor, Blood 109 (2007) 3042–3049.
[24] P.B. Mullan, J.E. Quinn, P.M. Gilmore, et al., BRCA1 and GADD45 mediated G2/M cell cycle arrest in response to antimicrotuble agents, Oncogene 20 (2001) 6123–6131.
[25] W.B. Derry, L. Wilson, M.A. Jordan, Substoichiometric binding of taxol suppresses microtubule dynamics, Biochemistry 34 (1995) 2203–2211.
[26] P.V. Raninga, G. Di Trapani, S. Vuckovic, et al., Inhibition of thioredoxin 1 leads to apoptosis in drug-resistant multiple myeloma, Oncotarget 6 (2015) 15410–15424.
[27] F. Cottini, T. Hideshima, R. Suzuki, et al., Synthetic lethal approaches exploiting DNA damage in aggressive myeloma, Cancer Discov. 5 (2015) 972–987.
[28] Y. Arihara, K. Takeda, Y. Kamihara, et al., Small molecule CP-31398 induces reactive oxygen species-dependent apoptosis in human multiple myeloma, Oncotarget 8 (2017) 65889–65899.
[29] M. Ri, Endoplasmic-reticulum stress pathway-associated mechanisms of action of proteasome inhibitors in multiple myeloma, Int. J. Hematol. 104 (2016) 273–280.
[30] M. Sperandio, A.P.D. Demasi, E.F. Martinez, et al., 15d-PGJ$_2$ as an endoplasmic

reticulum stress manipulator in multiple myeloma in vitro and in vivo, Exp. Mol. Pathol. 102 (2017) 434–445.
[31] S. Bustany, J. Cahu, P. Guardiola, et al., CyclinD1 sensitizes myeloma cells to endoplasmic reticulum stress-mediated apoptosis by activating the unfolded protein response pathway, BMC Canc. 15 (2015) 262.
[32] S. Manni, A. Brancalion, L.Q. Tubi, et al., Protein kinase CK2 protects multiple myeloma cells from ER stress-induced apoptosis and from the cytotoxic effect of HSP90 inhibition through regulation of the unfolded protein response, Clin. Canc. Res. 18 (2012) 1888–1900.
[33] S. Moriya, S. Komatsu, K. Yamasaki, et al., Targeting the integrated networks of aggresome formation, proteasome, and autophagy potentiates ER stress-mediated cell death in multiple myeloma cells, Int. J. Oncol. 46 (2015) 474–486.
[34] W. Rozpedek, D. Pytel, B. Mucha, et al., The Role of the PERK/eIF2α/ATF4/CHOP signaling pathway in tumor progression during endoplasmic reticulum stress, Curr. Mol. Med. 16 (2016) 533–544.
[35] H. Shiheido, F. Terada, N. Tabata, et al., A phtalimide derivative that inhibits centrosomal clustering is effective on multiple myeloma, PloS One 7 (2012), e38878.
[36] W.E. Marissen, Y. Guo, A.A. Thomas, et al., Identification of caspase 3-mediated cleavage and functional alteration of eukaryotic initiation factor 2alpha in apoptosis, J. Biol. Chem. 275 (2000) 9314–9323.

Signaling between pancreatic β cells and macrophages via S100 calcium-binding protein A8 exacerbates β-cell apoptosis and islet inflammation

Received for publication, July 29, 2017, and in revised form, February 27, 2018 Published, Papers in Press, March 1, 2018, DOI 10.1074/jbc.M117.809228

Hideaki Inoue[‡], Jun Shirakawa[‡1], Yu Togashi[‡2], Kazuki Tajima[‡2], Tomoko Okuyama[‡2], Mayu Kyohara[‡], Yui Tanaka[‡], Kazuki Orime[‡§], Yoshifumi Saisho[¶], Taketo Yamada[‖], Kimitaka Shibue[§], Rohit N. Kulkarni[§3], and Yasuo Terauchi[‡4]

From the [‡]Department of Endocrinology and Metabolism, Graduate School of Medicine, Yokohama-City University, 3-9 Fuku-ura, Kanazawa-ku, Yokohama 236-0004, Japan, the Departments of [¶]Internal Medicine and [‖]Pathology, School of Medicine, Keio University, Tokyo 108-8345, Japan, and the [§]Section of Islet Cell and Regenerative Biology, Joslin Diabetes Center, Department of Medicine, Brigham and Women's Hospital, Harvard Stem Cell Institute, Harvard Medical School, Boston, Massachusetts 02138

Edited by Jeffrey E. Pessin

Chronic low-grade inflammation in the pancreatic islets is observed in individuals with type 2 diabetes, and macrophage levels are elevated in the islets of these individuals. However, the molecular mechanisms underlying the interactions between the pancreatic β cells and macrophages and their involvement in inflammation are not fully understood. Here, we investigated the role of S100 calcium-binding protein A8 (S100A8), a member of the damage-associated molecular pattern molecules (DAMPs), in β-cell inflammation. Co-cultivation of pancreatic islets with unstimulated peritoneal macrophages in the presence of palmitate (to induce lipotoxicity) and high glucose (to induce glucotoxicity) synergistically increased the expression and release of islet-produced S100A8 in a Toll-like receptor 4 (TLR4)-independent manner. Consistently, a significant increase in the expression of the *S100a8* gene was observed in the islets of diabetic db/db mice. Furthermore, the islet-derived S100A8 induced TLR4-mediated inflammatory cytokine production by migrating macrophages. When human islet cells were co-cultured with U937 human monocyte cells, the palmitate treatment up-regulated S100A8 expression. This S100A8-mediated interaction between islets and macrophages evoked β-cell apoptosis, which was ameliorated by TLR4 inhibition in the macrophages or S100A8 neutralization in the pancreatic islets. Of note, both glucotoxicity and lipotoxicity triggered S100A8 secretion from the pancreatic islets, which in turn promoted macrophage infiltration of the islets. Taken together, a positive feedback loop between islet-derived S100A8 and macrophages drives β-cell apoptosis and pancreatic islet inflammation. We conclude that developing therapeutic approaches to inhibit S100A8 may serve to prevent β-cell loss in patients with diabetes.

Activation of the innate immune system and circulating levels of acute-phase inflammatory proteins play important roles in the onset and development of type 2 diabetes (1–3). Evidence of chronic inflammation has been demonstrated in the adipose tissue, liver, vascular endothelial cells, circulating leukocytes, and pancreatic islets in obese and/or diabetic humans (4–8). Chronic islet inflammation evokes a decline in the β-cell mass by promoting β-cell apoptosis, which is a hallmark of type 2 diabetes (9, 10).

It has been reported that macrophages are elevated in the pancreatic islets in patients with type 2 diabetes (11). Chronic hyperglycemia promotes amyloid formation in the islets by inducing the secretion of islet amyloid polypeptide (12), production of reactive oxygen species in β cells (13), and formation of advanced glycation end products (14, 15). These conditions lead to activation of the NLRP3 inflammasomes, IL-1β secretion, macrophage infiltration of the β cells, and pro-apoptotic processes (12, 16). Thus, islet inflammation is closely related to β-cell failure and apoptosis in diabetes. A previous study showed that the co-culture of MIN6 insulinoma cells with RAW264.7 macrophage cells in the presence of palmitate increased the expression of inflammatory genes in the MIN6 cells and decreased insulin secretion (17). However, the precise mechanisms involved in the mutual interaction between the pancreatic β cells and macrophages in diabetes remain unclear.

In this study, we identified *S100a8* as an up-regulated gene after chronic glucose stimulation, which reflects a state of sustained hyperglycemia, in the pancreatic islets. S100A8 is a small calcium-binding protein that is found at high levels in the extracellular milieu under inflammatory conditions. Furthermore, the S100A8 protein is known to be associated with various chronic inflammatory diseases and both type 1 and type 2 diabetes (18, 19). S100A8 is thought to be a member of the damage-associated molecular pattern molecules and stimulates macrophages (20–23). Consequently, to test the

This work was supported by Grant-in-Aid for Scientific Research (B) 16H05329 (to Y. Terauchi) from the Ministry of Education, Culture, Sports, Science, and Technology (MEXT) of Japan, a grant-in-aid from the Japan Foundation for Applied Enzymology (to J. S.), and a Junior Scientist Development Grant supported by Novo Nordisk Pharma Ltd. (to J. S.). The authors declare that they have no conflicts of interest with the contents of this article. The content is solely the responsibility of the authors and does not necessarily represent the official views of the National Institutes of Health.

This article contains Tables S1–S3.

[1] To whom correspondence may be addressed. Tel.: 81-45-787-2639; Fax: 81-45-781-5379. E-mail: jshira-tky@umin.ac.jp.

[2] These authors contributed equally to this work.

[3] Supported by National Institutes of Health Grants RO1 DK67536 and DK103215.

[4] To whom correspondence may be addressed. Tel.: 81-45-787-2639; Fax: 81-45-781-5379. E-mail: terauchi-tky@umin.ac.jp.

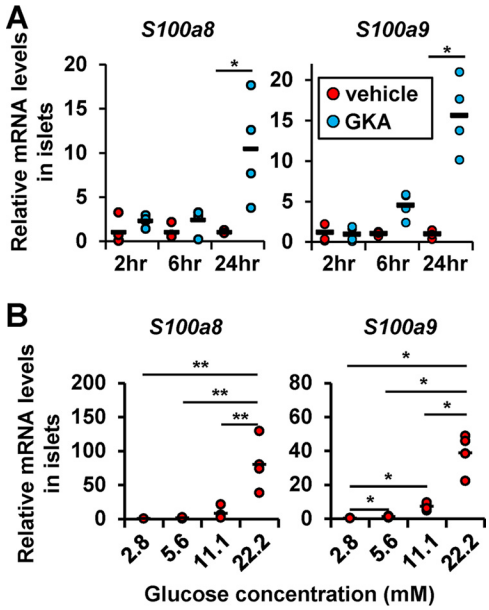

Figure 1. Glucose stimulation up-regulated S100A8/A9 expression in the islets. *A*, mRNA expression levels in the islets stimulated with GKA Cpd A (glucokinase activator; 30 μmol/liter) for 2, 6, or 24 h. *Horizontal bars*, mean values. *, $p \leq 0.05$ *versus* other groups ($n = 4$/group). *B*, mRNA expression levels in islets cultured in the presence of 2.8, 5.6, 11.1, or 22.2 mmol/liter glucose for 24 h. *Horizontal bars*, mean values. *, $p \leq 0.05$; **, $p \leq 0.01$ ($n = 4$/group).

hypothesis that S100A8 contributes to islet inflammation, we established a co-culture system with freshly isolated primary pancreatic islets and resident peritoneal macrophages to investigate the role(s) of S100A8 in the sustenance of islet inflammation.

Results

S100A8/A9 expression in the islets was up-regulated by chronic glucose stimulation

Chronic hyperglycemia induces β-cell apoptosis, in part, through continuous glucokinase activation (24). We previously identified the target genes of glucokinase by examining the gene expression profiles of glucokinase activator (GKA)[5]-treated isolated islets (NCBI GEO database GSE41248) (25). Among them, *S100a8* and *S100a9* (*S100a8/a9*) expression showed the greatest increase following chronic glucokinase activation of the islets (90- and 254-fold increase, respectively). We validated the gene expression changes in isolated islets stimulated with a glucokinase activator (Fig. 1*A*) and confirmed that glucose stimulation increased the expression of *S100a8/a9* in the islets in a concentration-dependent manner (Fig. 1*B*). Thus, S100A8 expression was induced by high glucose in the islets without macrophages.

S100A8/A9 expression in the islets was enhanced by co-culture with macrophages in the presence of palmitate

We co-cultured islets with macrophages using co-culture inserts (Fig. 2*A*) and observed that the islet expression of *S100a8*, *S100a9*, *Il-1b*, *Tnf-a*, *Il-6*, and *Ccl2* was increased in the presence of macrophages (Fig. 2*B*). The absence of elevated expression of the macrophage markers, *Cd11b* and *F4/80*, suggested that it was unlikely that there was contamination of the co-cultured islet samples with macrophages (Fig. 2*C*). The expression of *S100a8* and *S100a9*, but not of *Il-1b*, *Tnf-a*, *Il-6*, or *Ccl2*, was enhanced in the islets co-cultured with macrophages in the presence of the saturated fatty acid palmitate (16:0) (Fig. 2*B*). We confirmed the secretion of S100A8, but not of S100A9, by ELISAs in the supernatant of islets co-cultured with macrophages in the presence of palmitate (Fig. 2*D*). Notably, secretion of S100A8 from the macrophages was not affected by the concentration of glucose or palmitate (Fig. 2*E*). S100A8 proteins were predominantly expressed in the mouse pancreatic islets, but not in acinar cells (Fig. 2*F*).

To test the possibility that the adipocyte-derived fatty acids contributed to the macrophage-mediated islet inflammation *in vivo*, we added isolated white adipocytes from the epididymal fat to the co-culture of islets with macrophages and examined islet gene expression. As expected, the adipocytes and macrophages synergistically increased the expression of *S100a8* and *S100a9* in the islets, and this was not associated with elevation of the expression of macrophage or adipocyte markers (Fig. 3*A*). Palmitate has been reported to induce islet inflammation through the TLR4/MyD88 pathway (17). Islets obtained from TLR4-knockout mice and co-cultured with WT macrophages in the presence of palmitate showed a significant increase in the expression of *S100a8/a9* (Fig. 3*B*). These results suggest that TLR4-mediated signaling was not required for the S100A8 production induced by macrophage-derived factors and palmitate in the co-cultured islets.

Glucotoxicity further enhanced the induction of S100A8/A9 in co-cultured islets

Chronic high ambient glucose concentration has been shown to accelerate inflammation in various tissues in diabetes (26, 27). We undertook experiments under normal glucose (5.6 mmol/liter) conditions and under high glucose (11.1 mmol/liter) conditions to mimic the environment in diabetes. The protein expression of S100A8/A9 in the co-cultured islets was enhanced following culture in the presence of 11.1 mmol/liter glucose (high concentration) (Fig. 4*A*). S100A8 secretion from islets co-cultured with macrophages in the presence of palmitate was also enhanced by glucose stimulation (Fig. 4*B*). High glucose enhanced palmitate-induced *S100a8* and *S100a9* gene expression, whereas expression of other inflammatory or macrophage markers in the co-cultured islets was not influenced by the glucose concentration (Fig. 4*C*). In addition, inflammatory gene expression in the macrophages was up-regulated by the ambient glucose level (Fig. 4*D*).

We next examined the expression of *S100a8/a9* in the islets of the db/db mouse, an established model of diabetes. Six- and 12-week-old db/db mice exhibited morbid obesity, severe hyperglycemia, and irregular α/β-cell distribution within the islets; however, the ratio of β to α cells and the proportion of apoptotic β cells were not altered in the db/db mice compared with control db/+ mice (Table S1 and Fig. 5 (*A* and *B*)). Isolated pancreatic islets from db/db mice, at both 6 and 12 weeks of age,

[5] The abbreviations used are: GKA, glucokinase activator; TLR, Toll-like receptor; TUNEL, TdT-mediated dUTP nick-end labeling; ER, endoplasmic reticulum.

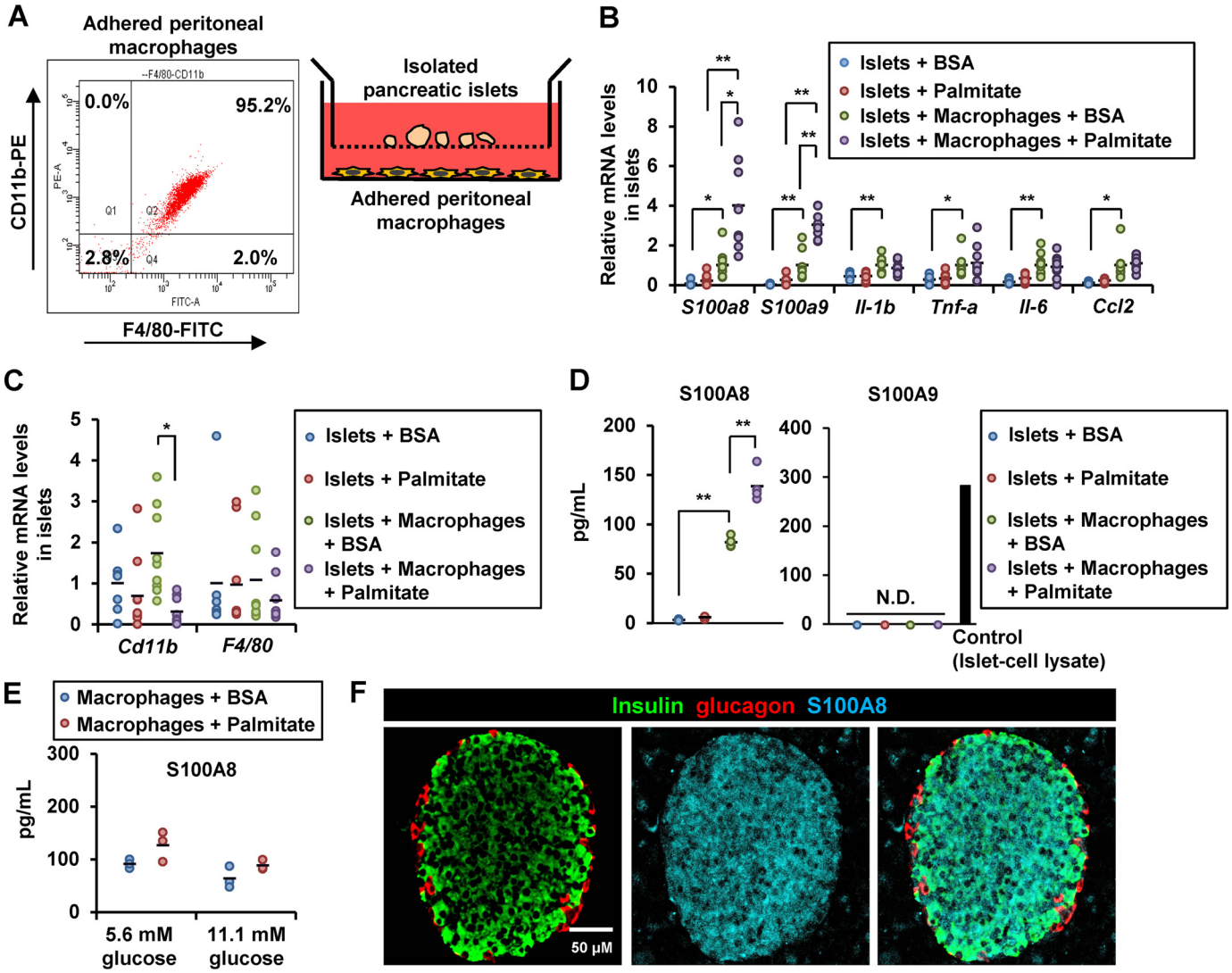

Figure 2. Chronic stimulation with high concentrations of glucose, palmitate, and macrophages induced S100A8/A9 expression in the pancreatic islets. *A*, illustration of co-cultured islets and macrophages (*right*). Flow cytometry of the adherent peritoneal macrophages (*left*). *B–D*, isolated mouse pancreatic islets (50 islets) were co-cultured with peritoneal macrophages (1×10^5 cells) in the presence of BSA (0.5%) or palmitate (500 μmol/liter). *B* and *C*, mRNA expression levels in islets co-cultured with macrophages in the presence/absence of palmitate for 24 h. *Horizontal bars*, mean values. *, $p \leq 0.05$; **, $p \leq 0.01$ ($n = 9$). *D*, secreted S100A8 protein (*left*) and S100A9 protein (*right*) levels in the supernatant obtained from co-culture of islets with macrophages in the presence/absence of palmitate for 48 h. *Horizontal bars*, mean values. *N.D.*, not detected; **, $p \leq 0.01$ ($n = 4$). *E*, secreted S100A8 protein levels in the supernatant of macrophages cultured in the presence of 5.6 or 11.1 mmol/liter glucose with/without palmitate for 48 h. *Horizontal bars*, mean values ($n = 3$/group). *F*, pancreatic sections from 8-week-old male WT C57BL/6J mice were stained with antibodies to insulin (*green*), glucagon (*red*), and S100A8 (*blue*). Scale bar, 50 μm.

showed higher levels of expression of *S100a8/a9*, of the inflammatory cytokine gene *Il-6*, and of the macrophage marker *F4/80* compared with db/+ islets (Fig. 5*C*).

Factors from the islets, but not from macrophages, activated the macrophages in co-culture via TLR4

In macrophages co-cultured with islets in the presence of palmitate, expression of *Tnf-a*, *Ccl2*, *Il-1b*, *Il-6*, *Il-12*, *Il-22*, *Il-23*, and *Il-24* genes were elevated (Fig. 6*A*). IL-23 and IL-24 are potent inducers of oxidative and ER stress in β cells (28). No increase in the expression of *S100a8/a9* genes was observed in the macrophages co-cultured with the islets in the presence of palmitate or in the presence of high ambient glucose (Fig. 6*B*). This implies that the production of S100A8 induced by co-culture with macrophages was predominantly derived from the islets. The aforementioned increase in the cytokine gene expression was blunted by the TLR4-inhibitory peptide VIPER (Fig. 6*C*). These results suggest that a humoral factor derived from the co-cultured islets stimulated the macrophages via TLR4.

Because S100A8 is reported as a ligand of TLR4, we examined whether S100A8 induces inflammation in the co-cultured macrophages. Treatment with the recombinant S100A8-GST peptide increased the expression of the *Tnf-a*, *Ccl2*, *Il-1b*, *Il-6*, *Il-12*, *Il-22*, and *Il-23* genes in the macrophages and prompted macrophage migration (Fig. 7, *A* and *B*). Neutralization of S100A8 using an antibody significantly reduced the migration of the macrophages induced by co-culture with islets (Fig. 7*C*). Neutralization of S100A8 with an antibody also reduced the cytokine expression of the macrophages induced by co-culture

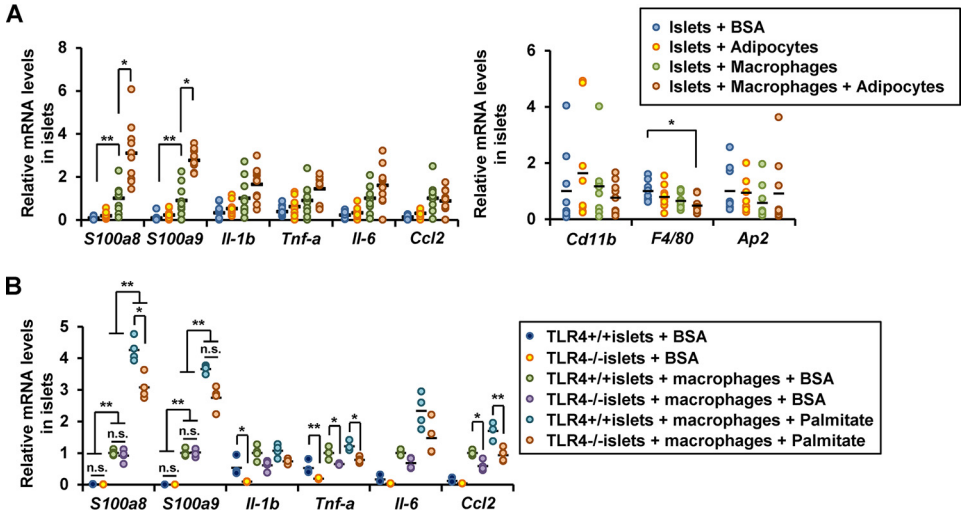

Figure 3. TLR4-independent S100A8 production induced by macrophage-derived factors and palmitate in the co-cultured islets. *A*, isolated pancreatic islets (50 islets) were co-cultured with white adipocytes in the presence of BSA (0.5%) or palmitate (500 μmol/liter) for 24 h. mRNA expression levels in co-cultured islets. *Horizontal bars*, mean values. *, $p \leq 0.05$; **, $p \leq 0.01$ ($n = 9$). *B*, mRNA expression levels in TLR4$^{+/+}$ or TLR4$^{-/-}$ islets co-cultured with TLR4$^{+/+}$ macrophages in the presence of BSA (0.5%) or palmitate (500 μmol/liter) for 24 h. *Horizontal bars*, mean values. *, $p \leq 0.05$; **, $p \leq 0.01$ ($n = 6$).

of the macrophages with islets in the presence of palmitate (Fig. 7*D*). Inhibition of TLR4 with VIPER or TAK-242 attenuated the migration of the macrophages and the cytokine expression in these cells induced by purified S100A8-GST peptide (Fig. 7, *E* and *F*). TLR4$^{-/-}$ macrophages exhibited a significant decrease of cytokine expression following co-culture with islets in the presence of palmitate as compared with TLR4$^{+/+}$ macrophages (Fig. 7*G*). Taken together, S100A8 leads to the up-regulation of inflammation mediators in macrophages via TLR4.

Co-cultivation of islets with macrophages in the presence of palmitate coordinately promoted β-cell apoptosis via islet-derived S100A8 and macrophages

Exogenous *S100a8/a9* expression induced by adenoviral transduction was also influenced by the ambient glucose levels (Fig. 8*A*), suggesting that glucose stimulation possibly enhanced translation or stabilized the S100A8/A9 mRNA or protein. Overexpression of S100A8/S100A9 exerted no effect on glucose-induced insulin secretion from the islets (Fig. 8*B*) or on the degree of apoptosis in the islets (Fig. 8*C*). S100A8 overexpression in the MIN6K8 β cells slightly decreased insulin secretion from the cells, and conversely, *S100a8* knockdown was capable of restoring the insulin secretion, even in the absence of macrophages (Fig. 8*D*). In the presence of macrophages, however, S100A8 overexpression increased insulin secretion, whereas *S100a8* knockdown tended to decrease insulin secretion in S100A8-overexpressing MIN6K8 β cells (Fig. 8*E*).

To assess the effects of the co-cultivation on the islets, β-cell apoptosis was evaluated. Co-culturing with macrophages increased the number of apoptotic β cells, and palmitate enhanced macrophage-induced β-cell apoptosis (Fig. 9*A*). The combination of glucose stimulation further induced apoptosis of β cells in the presence of macrophages (Fig. 9*A*). The apoptosis-associated Bax protein expression level, but not that of the necrosis-associated HMGB1 protein, increased in the islets co-cultured with macrophages in the presence of palmitate and ambient high glucose levels (Fig. 9*B*). The TLR4-inhibitory peptides VIPER and TAK-242 showed a tendency to reduce β-cell apoptosis caused by co-culturing of the islets with macrophages (Fig. 9, *C* and *D*). Furthermore, neutralization of S100A8 with an antibody specific to S100A8 significantly reduced the degree of β-cell apoptosis in the islets co-cultured with macrophages (Fig. 9, *C* and *D*).

Expression of S100A8 in human islets

Next, investigation of human islets revealed that expression of S100A8 was significantly enhanced after stimulation with GKA in both nondiabetes and type 2 diabetes donors (Fig. 10*A*). Co-existence of human monocyte U937 cell line and palmitate significantly up-regulated the expression of *S100A8* in human islets (Fig. 10*B*). We also explored the localization of S100A8 in human islets. Immunohistochemical staining for S100A8 was predominantly detected in β cells in the islets (Fig. 10*C*). The degree of β-cell apoptosis in the human islets co-cultured with U937 cells and palmitate tended to be decreased by the S100A8-specific neutralizing antibody (Fig. 10*D*). Further study is warranted to clarify the pathological significance of S100A8 in human islet inflammation.

Discussion

The results of the present study identified S100A8 as an endogenous islet-derived secretory peptide that is induced by a combination of infiltrating macrophages, palmitate (lipotoxicity), and high glucose (glucotoxicity), resulting in the activation of macrophages and potentiation of islet inflammation and β-cell death through a positive feedback loop (Fig. 11). The current results are consistent with a recent report suggesting that the serum level of the S100A8/A9 complex is a sensitive marker of acute inflammation associated with islet transplant rejection (29).

Several studies have shown that TLR4 signaling and MyD88 signaling in β cells play important roles in the development of islet inflammation (17, 30, 31). However, TLR4 stimulation did not induce S100A8/A9 production in the islets, whereas

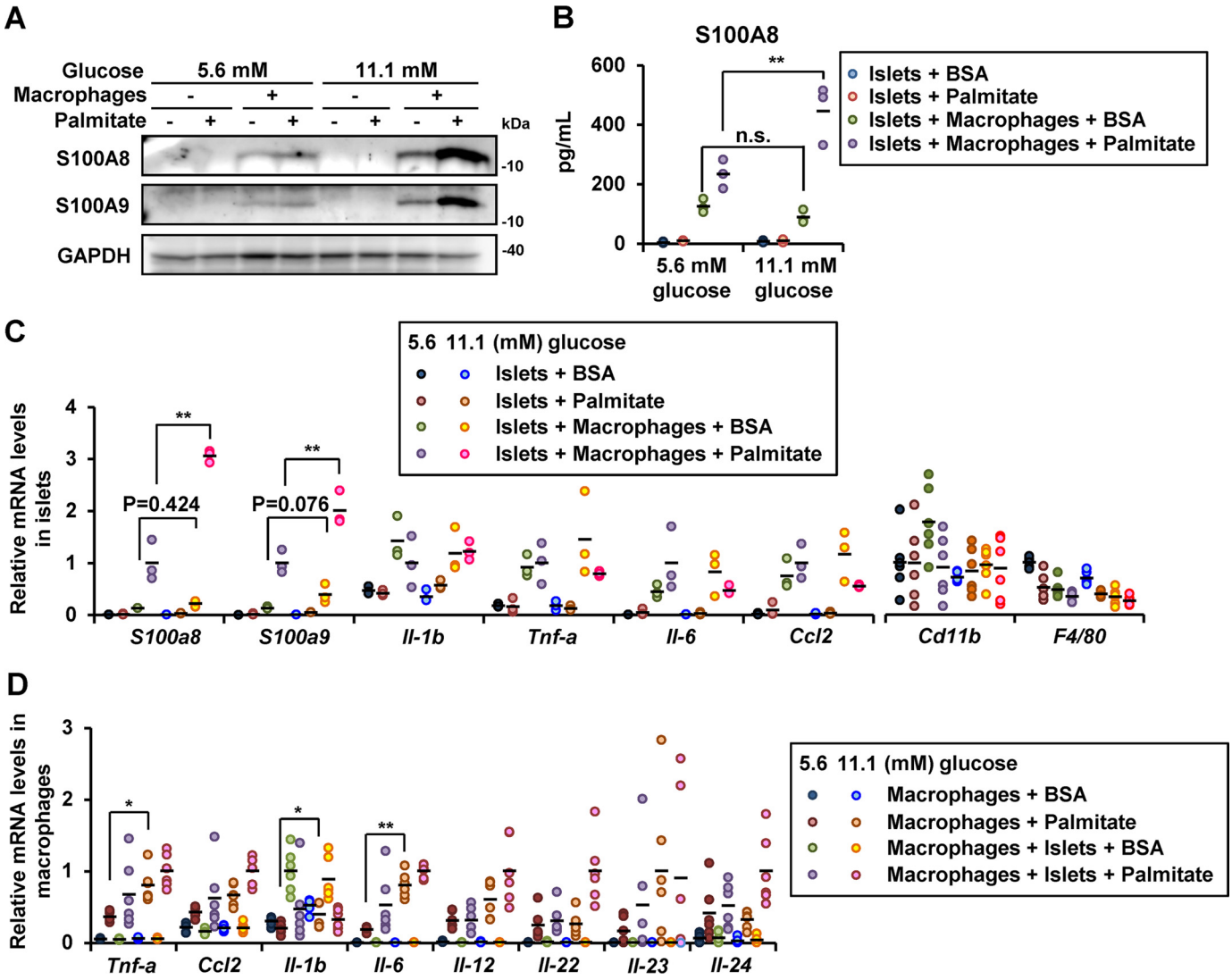

Figure 4. Increased ambient glucose concentrations enhanced the expressions of S100A8/A9 in co-cultured islets with macrophages. Isolated pancreatic islets (200 islets for *A* and *B*, 50 islets for *C* and *D*) were co-cultured with peritoneal macrophages (5×10^5 cells for *A* and *B*, 1×10^5 cells for *C* and *D*) in medium containing BSA in the presence/absence of palmitate. *A*, isolated islets were co-cultured with macrophages in the presence of 5.6 or 11.1 mmol/liter of glucose with/without palmitate for 48 h. Total cell extracts from the islets were subjected to immunoblotting as indicated. *B*, secreted S100A8 protein levels in the supernatant from a co-culture of islets with macrophages in the presence/absence of palmitate and 5.6 or 11.1 mmol/liter glucose for 48 h. *Horizontal bars*, mean values. *n.s.*, not significant; **, $p \leq 0.01$ ($n = 3$). *C*, mRNA expression levels in islets co-cultured with macrophages in the presence of 5.6 or 11.1 mmol/liter glucose with/without palmitate for 24 h. *Horizontal bars*, mean values. **, $p \leq 0.01$ ($n = 6$). *D*, mRNA expression levels in macrophages co-cultured with islets in the presence of 5.6 or 11.1 mmol/liter glucose with/without palmitate for 24 h. *Horizontal bars*, mean values. *, $p \leq 0.05$; **, $p \leq 0.01$ ($n = 6$).

S100A8 protein from the islets acted as a ligand for the TLR4 expressed in macrophages. Because TLR4 and RAGE (receptor for advanced glycation end products) receptors are also expressed in the pancreatic β cells (17), it was suggested that S100A8 also exerts direct effects on the β cells. TLR4 stimulation by S100A8 triggered the release of the inflammatory cytokines *Il-12*, *Il-23*, and *Il-24* from the macrophages, which resulted in β-cell apoptosis. Further production of S100A8 may evoke inflammation of the surrounding islets, neighboring tissues, or feeding vessels. TNFα, CCL2, and IL-1β are known to induce islet inflammation through the NF-κB pathway (3), and IL-23 and IL-24 have been shown to be potent inducers of oxidative and ER stress in β cells (28). The expression of these cytokines was also induced in the macrophages following stimulation with S100A8 in the present study.

Overexpression of S100A8/A9 had no inhibitory effect on insulin secretion from isolated islets (Fig. 8*B*). We also report that S100A8 *per se* impaired insulin secretion from MIN6K8 β cells in the absence of macrophages (Fig. 8*D*). However, overexpression of S100A8 enhanced insulin secretion from MIN6K8 β cells in the presence of macrophages (Fig. 8*E*). Overexpression of S100A8 has been reported in ductal adenocarcinoma of the pancreas, and it has been suggested that a peptide metabolite of S100A8 released from pancreatic cancer possibly suppresses insulin secretion to induce diabetes (32). Further research is required to clarify the effects of S100A8 on insulin secretion under similar pathophysiological conditions.

Our results suggested that S100A8 did not act directly to induce β-cell apoptosis, but via a mutual interaction with

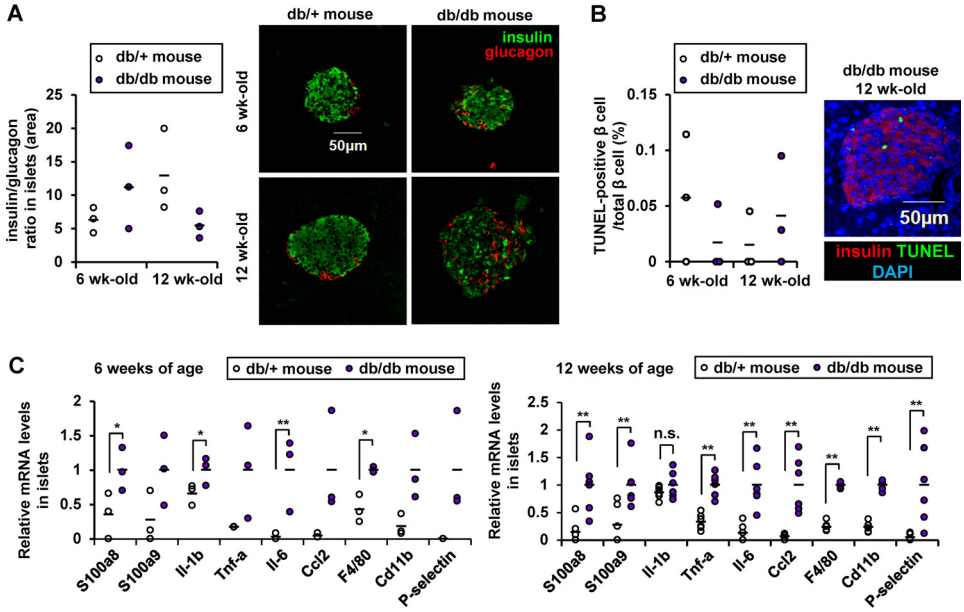

Figure 5. Increased S100A8/A9 expressions in diabetic islets. *A*, quantification of β-cell mass as a proportion of the total α-cell mass in the islet. *Horizontal bars*, mean values ($n = 6$). *B*, the proportion of TUNEL-positive cells is shown as a percentage of the total number of insulin-positive cells in the sections. *Horizontal bars*, mean values ($n = 5$). *Scale bar*, 50 μm. *C*, mRNA expression levels in islets from 6- or 12-week-old db/db or db/+ mice. *Horizontal bars*, mean values. *n.s.*, not significant; *, $p \leq 0.05$; **, $p \leq 0.01$ ($n = 6$).

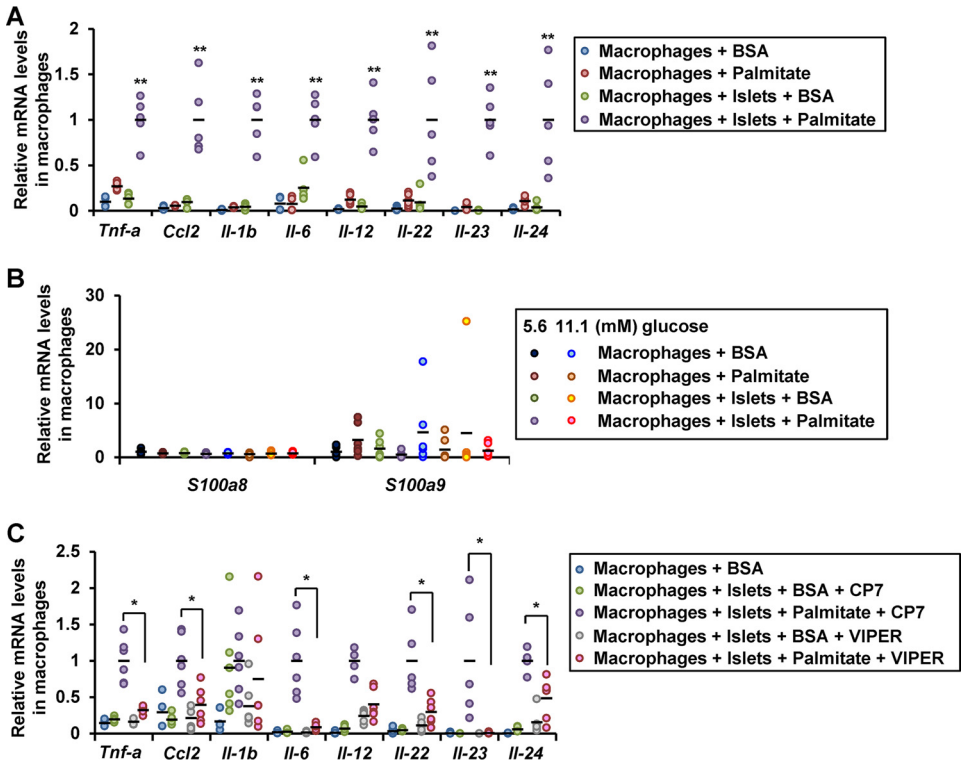

Figure 6. Activation of the macrophages in co-culture with islets via TLR4. Peritoneal macrophages (1×10^5 cells) were co-cultured with isolated pancreatic islets (50 islets) in a medium containing BSA (0.5%) in the presence/absence of palmitate. *A* and *B*, mRNA expression levels in macrophages co-cultured with islets for 24 h. *Horizontal bars*, mean values. **, $p \leq 0.01$ ($n = 5$). *C*, mRNA expression levels in macrophages co-cultured with islets in the presence of the TLR4 inhibitory peptide VIPER or the control peptide CP7 for 24 h. *Horizontal bars*, mean values. *, $p \leq 0.05$ ($n = 5$).

macrophages. S100A8 in β cells probably triggers destruction of the β-cell membrane, because S100A8 and S100A9 have the ability to form oligomers and induce amyloid deposition (33). Because S100A9 protein was detected in the islets but not in the culture medium, the contribution of S100A9 in our experimental conditions remains unclear. S100A9 protein, a heterodimerization partner of S100A8, possibly plays an essential role in the protein expression of S100A8 protein, as indicated by previous studies that found that S100A8 was not detectable in S100A9-KO peripheral tissues (20, 34).

Glucokinase-mediated induction of S100A8 production seems specific to pancreatic β cells, as deduced from the results

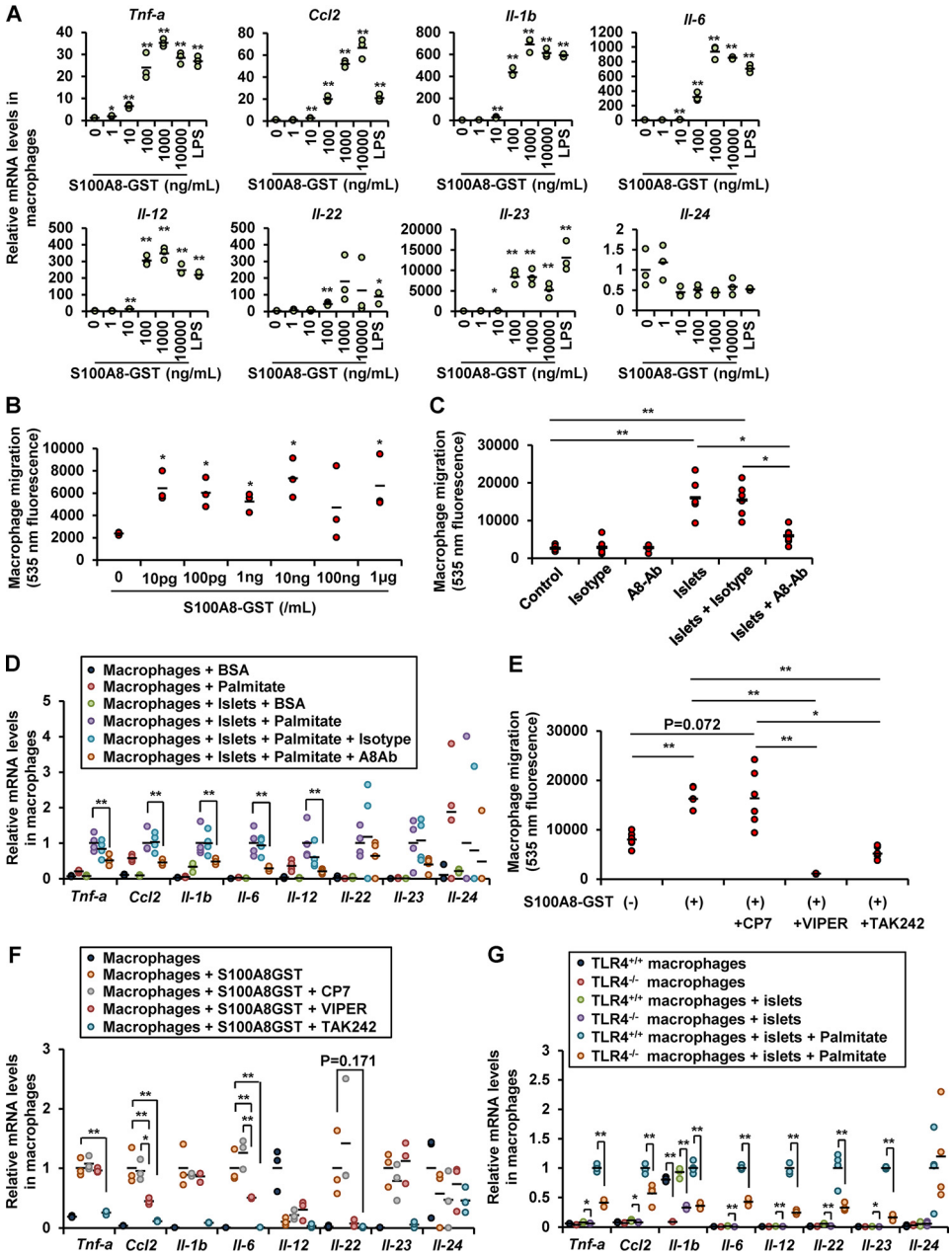

Figure 7. Islet-derived S100A8 activated macrophage migration and inflammation. *A*, mRNA expression levels in peritoneal macrophages (1×10^5 cells) stimulated with S100A8-GST peptide for 24 h. *Horizontal bars*, mean values. *, $p \leq 0.05$; **, $p \leq 0.01$ *versus* 0 ng/ml control ($n = 3$). *B*, fluorescence intensity of Calcein-AM–labeled macrophages migrating in response to S100A8-GST peptide stimulation for 24 h. *Horizontal bars*, mean values. *, $p \leq 0.05$ *versus* 0 ng/ml control ($n = 3$). *C*, fluorescence intensity of migrated Calcein-AM–labeled macrophages migrating in response to co-culture with islets in the presence of anti-S100A8 neutralizing antibody (10 μg/ml) or IgG_{2B} isotype control for 48 h. *Horizontal bars*, mean values. *, $p \leq 0.05$; **, $p \leq 0.01$ ($n = 6$). *D*, mRNA expression levels in macrophages co-cultured with the islets with/without palmitate in the presence of anti-S100A8 neutralizing antibody or IgG_{2B} isotype control. *Horizontal bars*, mean values. **, $p \leq 0.01$ ($n = 4$). *E*, fluorescence intensity of migrated Calcein-AM–labeled macrophages in response to co-culture with islets in the presence of recombinant S100A8 peptide and the TLR4-inhibitory peptide VIPER or TAK-242 (100 nmol/liter) for 24 h. *Horizontal bars*, mean values. *, $p \leq 0.05$; **, $p \leq 0.01$ ($n = 6$). *F*, mRNA expression levels in S100A8-stimulated macrophages cultured in the presence of the TLR4 inhibitory peptide VIPER or TAK-242 for 24 h. *Horizontal bars*, mean values. *, $p \leq 0.05$; **, $p \leq 0.01$ ($n = 3$). *G*, mRNA expression levels in $TLR4^{+/+}$ or $TLR4^{-/-}$ macrophages co-cultured with $TLR4^{+/+}$ islets in the presence of palmitate for 24 h. *Horizontal bars*, mean values. *, $p \leq 0.05$; **, $p \leq 0.01$ ($n = 4$).

of previous studies carried out in other organs (35–37). Glucokinase activation enhances adaptive β-cell proliferation and prevents β-cell apoptosis induced by glucotoxicity or ER stress (25, 38, 39). However, chronic glucokinase activation and high glucose act to trigger β-cell apoptosis (24, 39). There is considerable debate about the role of glucokinase in the protection of β cells from the S100A8-mediated positive feedback loop of islet inflammation under glucolipotoxicity. Additional studies are necessary to confirm the production of S100A8 in human β cells from obese or diabetic subjects.

In summary, our studies support the identification of S100A8 as a secretory protein to promote β-cell apoptosis and constitute an important step in the development of approaches to protect β cells in patients with diabetes.

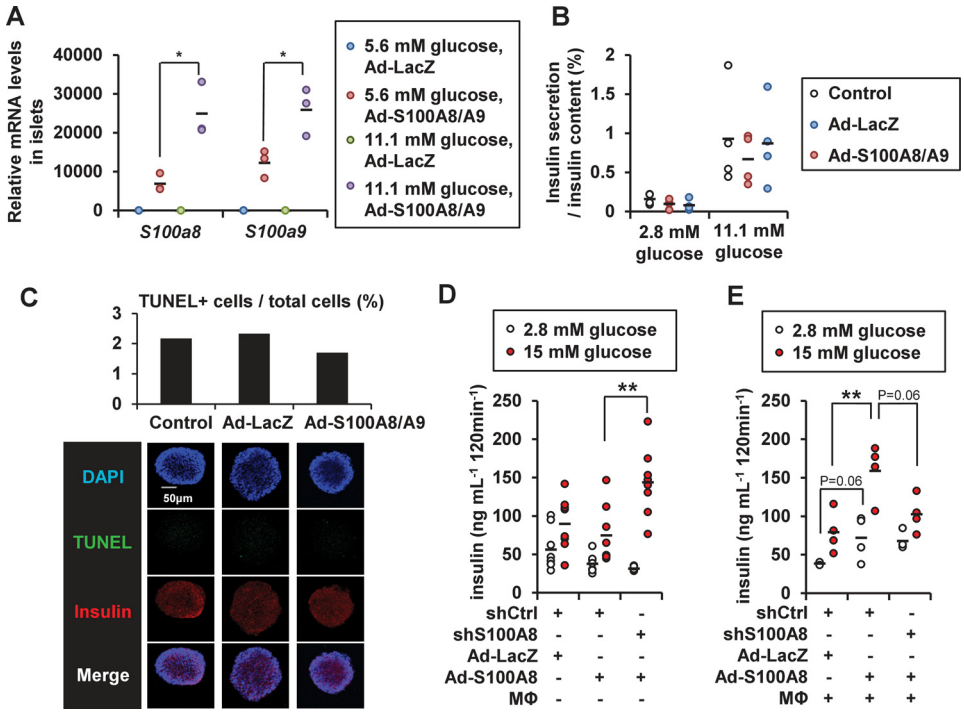

Figure 8. Effects of S100A8 on insulin secretion from pancreatic islets. *A*, islets were treated with adenoviral LacZ or adenoviral S100A8/A9 for 48 h. The mRNA expression levels in the adenoviral S100A8/A9-transduced islets (50 islets) cultured in the presence of 5.6 or 11.1 mmol/liter glucose are shown. *Horizontal bars*, mean values. *, $p \leq 0.05$ ($n = 3$). *B*, glucose-stimulated insulin secretion analysis from the adenoviral S100A8/A9-transduced islets (50 islets). *Horizontal bars*, mean values ($n = 4$). *C*, TUNEL assay in the adenoviral S100A8/A9-transduced islets (200 islets). *Horizontal bars*, mean values. *D* and *E*, glucose-stimulated insulin secretion analysis from shRNA-treated MIN6K8 cells. MIN6K8 cells were cultured for 24 h for adenoviral S100A8 transduction with/without peritoneal macrophages. *D*, without macrophages. *Horizontal bars*, mean values. **, $p \leq 0.01$ ($n = 8$). *E*, with macrophages. *Horizontal bars*, mean values. **, $p \leq 0.01$ ($n = 4$).

Experimental procedures

Animals and animal care

Animal handling procedures were in accordance with institutional animal care and use committee protocols approved by Yokohama City University. Animals were housed in rooms maintained at a constant room temperature (25 °C) under a 12-h light (07:00 h)/12-h dark (19:00 h) cycle, and the animals were given free access to food and water. C57BL/6J mice were purchased from CLEA Japan (Tokyo, Japan). All of the mice used in this study belonged to the C57BL/6J background. db/db mice and db/+ mice (BKS.Cg-*Lepr*^{db}/*Lepr*^{db} and BKS.Cg-*Lepr*^{db}/*Dock7*^{m}) were purchased from Charles River Laboratories Japan (Yokohama, Japan). TLR4$^{-/-}$ mice were purchased from Oriental Bio Service (Kyoto, Japan).

Reagents, viruses, and cells

The S100A8 and S100A9 ELISA kits were purchased from Cloud-Clone Corp. (Houston, TX). GKA Cpd A was purchased from Merck (Darmstadt, Germany). Collagenase L was purchased from Nitta-Gelatin (Osaka, Japan). Thapsigargin was purchased from Sigma. Collagenase XI and LPS were purchased from Sigma-Aldrich. The TLR4 peptide inhibitor VIPER (40) was purchased from Novus Biologicals, LLC (Littleton, CO). TAK-242 was purchased from Chemscene, LLC (Monmouth Junction, NJ). D-Mannoheptulose was purchased from Carbosynth Ltd. (Compton, Berkshire, UK). Adenoviruses containing S100A8, S100A9, or LacZ were generated using the Virapower adenoviral expression system (Invitrogen). Five micrograms of adenoviral constructs were digested with PacI, and the linearized DNA was transfected into HEK293A cells. The adenovirus produced by these cells was then collected and subjected to three cycles of freezing and thawing to release the adenovirus. The resulting adenovirus was stored at −80 °C for later use. Viral titers were determined by plaque assays using cultured HEK293A cells, according to the manufacturer's instructions. Monoclonal rat IgG_{2B} anti-mouse S100A8 antibody and monoclonal rat IgG_{2B} isotype control were purchased from R&D Systems (Abingdon, UK). Calcein-AM was purchased from Dojindo Laboratories (Kumamoto, Japan). The MIN6K8 cell line was provided by Dr. Susumu Seino (Kobe University). Lentivirus particles expressing short hairpin RNA for S100A8 were purchased from Santa Cruz Biotechnology, Inc.

Isolation and co-culture of islets, resident peritoneal macrophages, and white adipocytes

Islets and peritoneal macrophages were isolated as described elsewhere (41, 42). The proportion of F4/80- and CD11b-positive macrophages was more than 90%, as confirmed by flow cytometry (Fig. 2*A*). Adipocytes were prepared by collagenase digestion (Nitta Gelatin) of epididymal fat tissue, as described previously (43). Glucose-stimulated insulin secretion from the islets was induced as described previously (44). The co-culture was performed at 37 °C in a Krebs–Ringer bicarbonate HEPES buffer, pH 7.4, containing 0.2% BSA. Isolated pancreatic islets and peritoneal macrophages were plated in a Netwell insert

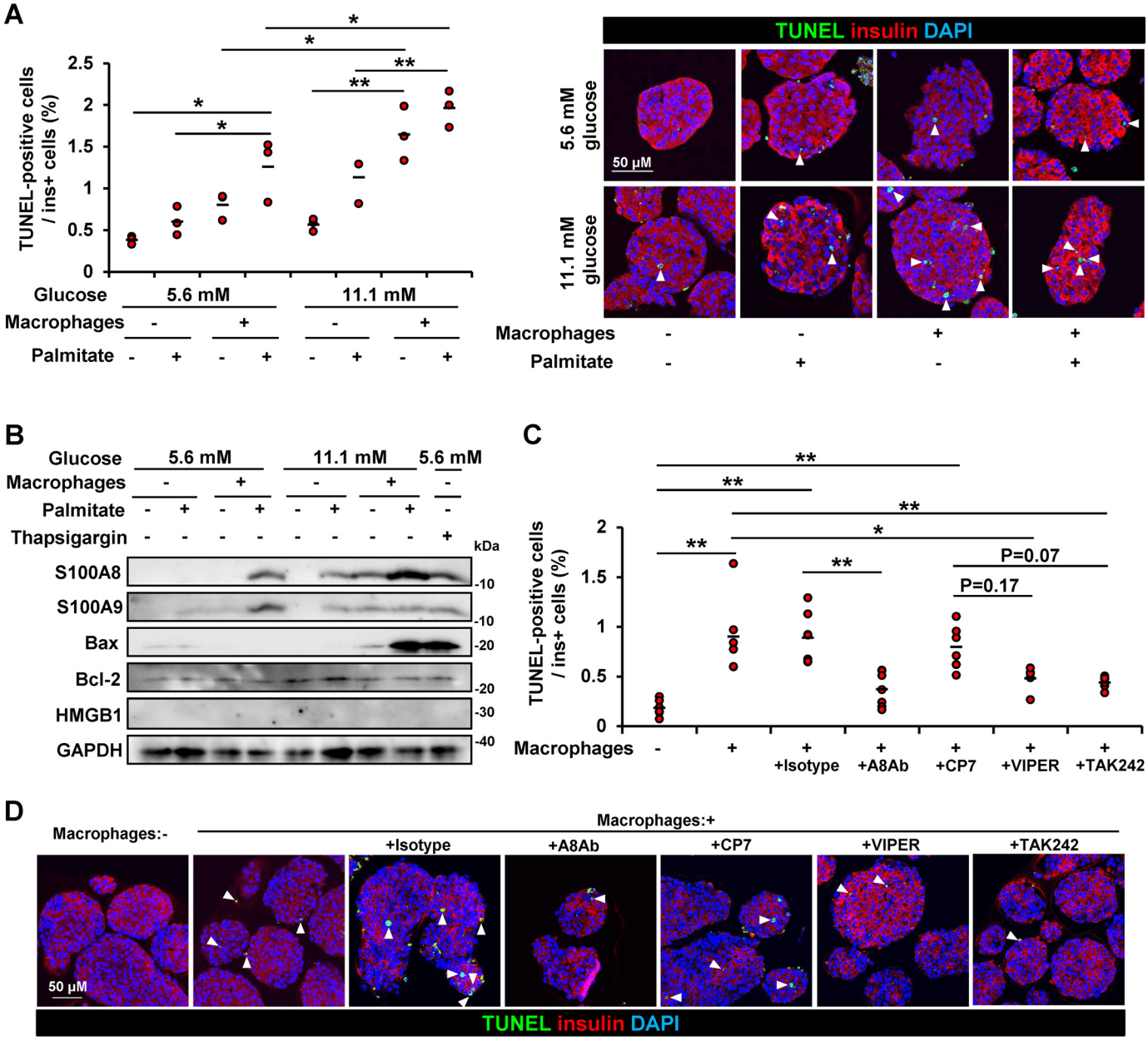

Figure 9. S100A8-stimulated macrophages induced β-cell apoptosis. Isolated pancreatic islets (200 islets) were co-cultured with peritoneal macrophages (5×10^5 cells) in medium containing BSA in the presence/absence of palmitate for 48 h. *A* and *C*, the islets were subjected to the TUNEL assay. The proportion of TUNEL-positive β cells is shown as a percentage of the co-cultured islets. Insulin is stained *red*, nuclei are stained *blue*, and TUNEL-positive nuclei are stained *green*. *A*, *left*, co-cultivation in the presence of 5.6 or 11.1 mmol/liter glucose. *Horizontal bars*, mean values. *, $p \leq 0.05$; **, $p \leq 0.01$ ($n = 3$). *Right*, representative images. *B*, isolated islets were co-cultured with macrophages in the presence of 5.6 or 11.1 mmol/liter glucose with/without palmitate for 48 h. Total cell extracts from the islets were subjected to immunoblotting as indicated. *C*, isolated islets were co-cultured with macrophages in the presence of 11.1 mmol/liter glucose with palmitate for 24 h. Co-cultivation in the presence of anti-S100A8 neutralizing antibody, IgG_{2B} isotype control, the control peptide CP7, the TLR4 inhibitory peptide VIPER, or the TLR4 inhibitor TAK-242. *Horizontal bars*, mean values. *, $p \leq 0.05$; **, $p \leq 0.01$ ($n = 6$). *D*, representative images of *C*.

with a 74-μm mesh size polyester membrane (Corning, Inc.) and in the bottom wells, respectively, and the cultures were incubated for 24 or 48 h in RPMI1640 containing fatal bovine serum, Krebs–Ringer bicarbonate containing BSA, or 500 μmol/liter palmitate (Fig. 2*A*). Adipocytes (from 25 mg of epididymal fat) were co-cultured above the co-culture Netwell insert.

Real-time PCR

Total RNA isolation from pancreatic islets, cDNA synthesis, and quantitative PCR were performed as described previously (25, 45). Data were normalized according to the expression level of β-actin, 18S rRNA, or GAPDH. The primers used for the real-time PCR are listed in Table S2.

Immunohistochemical analysis

Pancreases and islets were fixed and immunostained as reported previously (25, 45). Pancreatic tissue sections were immunostained with antibodies to S100A8 (Santa Cruz Biotechnology, Abcam), S100A9 (Abcam), insulin (Santa Cruz Biotechnology), or glucagon (Abcam). Alexa Fluor 488-, 555-, and 647-conjugated secondary antibodies (Invitrogen) were used

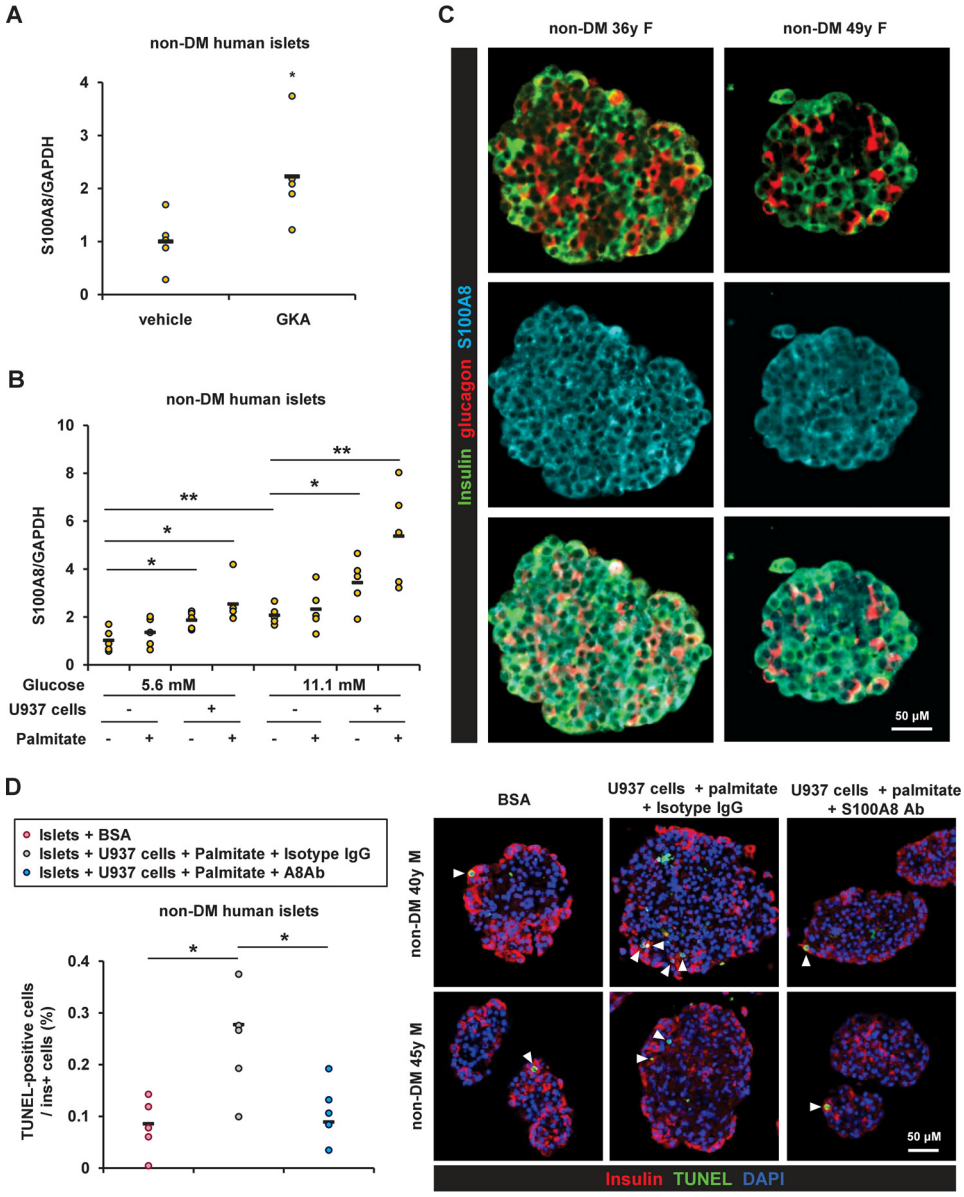

Figure 10. The expression of S100A8 was induced by glucose stimulation, monocytes, and palmitate in human islets. *A*, mRNA expression levels in human islets from nondiabetes (*non-DM*) donors after stimulation with GKA Cpd A (glucokinase activator; 30 μmol/liter) for 24 h. *Horizontal bars*, mean values. *, $p \leq 0.05$; **, $p \leq 0.01$ ($n = 5$). *B*, mRNA expression levels in human islets co-cultured with U937 human monocyte cell line (1×10^5 cells) in the presence of BSA (0.5%) or palmitate (500 μmol/liter) for 24 h. *Horizontal bars*, mean values. *, $p \leq 0.05$; **, $p \leq 0.01$ ($n = 5$). *C*, embedded human islets from nondiabetes donors were stained with antibodies to insulin (*green*), glucagon (*red*), and S100A8 (*blue*). *Scale bar*, 50 μm. *D*, human islets from nondiabetes donors were co-cultured with U937 cells in the presence of 11.1 mmol/liter glucose with palmitate for 24 h. They were co-cultivated in the presence of anti-S100A8 neutralizing antibody or IgG_{2B} isotype control. The proportion of TUNEL-positive β cells is shown as a percentage of the co-cultured islets. *Horizontal bars*, mean values. *, $p \leq 0.05$ ($n = 5$).

for the fluorescence microscopic analysis. β-cell apoptosis was evaluated using a TdT-mediated dUTP nick-end labeling (TUNEL) assay of the co-cultured β cells. Co-cultured islets (200 islets) were attached to poly-L-lysine–coated coverslips (Falcon) and subjected to a TUNEL assay using the ApopTag *in situ* detection kit (EMD Millipore, MA). All of the images were acquired using a FluoView FV1000-D confocal laser-scanning microscope (Olympus, Tokyo, Japan).

Immunoblotting

For immunoblotting, isolated islets (200 islets) were lysed in radioimmune precipitation buffer (Cell Signaling Technology, Danvers, MA) with complete protease inhibitor mixture (Roche Diagnostics). After centrifugation, the extracts were subjected to immunoblotting with antibodies. The primary antibodies used were Calgranulin A (S100A8), Calgranulin B (S100A9), Bcl-2–associated X protein (BAX), Bcl-2 (Santa Cruz Biotechnology), high-mobility group box 1 (HMGB1), and glyceraldehyde-3 phosphate dehydrogenase (GAPDH) (Abcam).

GST-fused proteins

GST-fused constructs comprising the mouse S100A8 and S100A9 proteins were generated in pGEX4T-1 and were received as kind gifts from Dr. Sachie Hiratsuka and Dr. Yoshihiro Maru (Department of Pharmacology, Tokyo Women's Medical University) (46). The proteins were

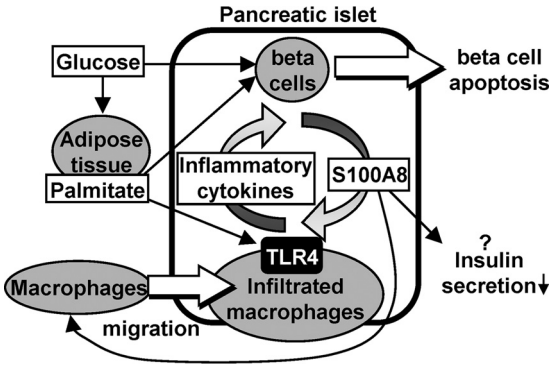

Figure 11. An illustrative model of islet inflammation–induced β-cell apoptosis via S100A8 in diabetes. A combination of infiltrating macrophages, saturated fatty acids (palmitate), and hyperglycemia augmented the production of S100A8. S100A8 secreted from the islets induced further macrophage migration and inflammation through TLR4. This positive feedback loop potentiates islet inflammation and β-cell death.

expressed in *Escherichia coli* BL21 and purified on a GSH-Sepharose column.

Macrophage migration assay

The migrated macrophages were labeled with Calcein-AM (WAKO, Osaka, Japan) and measured using an ARVO™ MX plate reader (PerkinElmer Life Sciences) at an excitation wavelength of 485 nm and emission filter of 535 nm. The migration of macrophages was evaluated using 8-μm pore Falcon BD FluoroBlok™ inserts and plates (BD Biosciences) with isolated pancreatic islets (50 islets) or S100A8-GST in the presence or absence of anti-S100A8 antibody, isotype control IgG2b, VIPER/CP7, or TAK-242. Macrophages were seeded onto the insert mesh and incubated for 24 or 48 h at 37 °C under 5% CO_2.

Human islets

Human islets were obtained from the Integrated Islet Distribution Program (National Institutes of Health). All studies and protocols used were approved by the Joslin Diabetes Center's Committee on Human Studies (approval CHS#5-05). Details of human islets are described in Table S3. Upon receipt, islets were cultured overnight in Miami Medium 1A (Cellgro). Co-culture was performed at 37 °C in final wash/culture medium (Cellgro) or RPMI1640 medium. Cadaveric human islets and U937 human monocyte cell line (ATCC) were plated in a Netwell insert with a 74-μm mesh size polyester membrane (Corning) and in the bottom wells, respectively.

Statistical analyses

All experiments were independently repeated at least three times. *Horizontal bars* indicate mean values. Statistical analyses were conducted using IBM SPSS Statistics version 19. Equality of variances was determined by using an F-test or Levene's test. Statistical comparisons between groups were analyzed for significance by an unpaired two-tailed Student's t test and one-way analysis of variance with post hoc Tukey tests for a parametric test or Welch's t test or Games–Howell test for a nonparametric test. Differences were considered significant at $p < 0.05$.

Author contributions—J. S. designed the research; H. I., J. S., Y. Togashi, K. T., T. O., M. K., Y. Tanaka, K. O., Y. S., and T. Y., performed the experiments; K. O., K. S., and R. N. K contributed to human islet studies. H. I., J. S., Y. Togashi, K. T., T. O., and Y. Terauchi analyzed the data; H. I., J. S., R. N. K., and Y. Terauchi wrote and edited the manuscript.

Acknowledgments—We thank Dr. Yoshihiro Maru and Dr. Sachie Hiratsuka (Tokyo Women's Medical University) for kindly gifting us the pGEX4T-1-S100A8 and -S100A9 plasmids and Dr. Susumu Seino (Kobe University) for providing the MIN6K8 cells. We also thank Mitsuyo Kaji, Eri Sakamoto (Yokohama City University), and Hiroko Madokoro (Keio University) for excellent technical assistance and Misa Katayama for excellent secretarial assistance.

References

1. Donath, M. Y., Schumann, D. M., Faulenbach, M., Ellingsgaard, H., Perren, A., and Ehses, J. A. (2008) Islet inflammation in type 2 diabetes: from metabolic stress to therapy. *Diabetes Care* **31,** S161–S164 CrossRef Medline
2. Pickup, J. C., Mattock, M. B., Chusney, G. D., and Burt, D. (1997) NIDDM as a disease of the innate immune system: association of acute-phase reactants and interleukin-6 with metabolic syndrome X. *Diabetologia* **40,** 1286–1292 CrossRef Medline
3. Donath, M. Y., and Shoelson, S. E. (2011) Type 2 diabetes as an inflammatory disease. *Nat. Rev. Immunol.* **11,** 98–107 CrossRef Medline
4. Xu, H., Barnes, G. T., Yang, Q., Tan, G., Yang, D., Chou, C. J., Sole, J., Nichols, A., Ross, J. S., Tartaglia, L. A., and Chen, H. (2003) Chronic inflammation in fat plays a crucial role in the development of obesity-related insulin resistance. *J. Clin. Invest.* **112,** 1821–1830 CrossRef Medline
5. Cai, D., Yuan, M., Frantz, D. F., Melendez, P. A., Hansen, L., Lee, J., and Shoelson, S. E. (2005) Local and systemic insulin resistance resulting from hepatic activation of IKK-β and NF-κB. *Nat. Med.* **11,** 183–190 CrossRef Medline
6. Brownlee, M. (2001) Biochemistry and molecular cell biology of diabetic complications. *Nature* **414,** 813–820 CrossRef Medline
7. Morigi, M., Angioletti, S., Imberti, B., Donadelli, R., Micheletti, G., Figliuzzi, M., Remuzzi, A., Zoja, C., and Remuzzi, G. (1998) Leukocyte-endothelial interaction is augmented by high glucose concentrations and hyperglycemia in a NF-κB-dependent fashion. *J. Clin. Invest.* **101,** 1905–1915 CrossRef Medline
8. Eguchi, K., and Manabe, I. (2013) Macrophages and islet inflammation in type 2 diabetes. *Diabetes Obes. Metab.* **15,** 152–158 CrossRef Medline
9. Donath, M. Y., and Halban, P. A. (2004) Decreased beta-cell mass in diabetes: significance, mechanisms and therapeutic implications. *Diabetologia* **47,** 581–589 CrossRef Medline
10. Donath, M. Y., Størling, J., Maedler, K., and Mandrup-Poulsen, T. (2003) Inflammatory mediators and islet beta-cell failure: a link between type 1 and type 2 diabetes. *J. Mol. Med.* **81,** 455–470 CrossRef Medline
11. Ehses, J. A., Perren, A., Eppler, E., Ribaux, P., Pospisilik, J. A., Maor-Cahn, R., Gueripel, X., Ellingsgaard, H., Schneider, M. K., Biollaz, G., Fontana, A., Reinecke, M., Homo-Delarche, F., and Donath, M. Y. (2007) Increased number of islet-associated macrophages in type 2 diabetes. *Diabetes* **56,** 2356–2370 CrossRef Medline
12. Masters, S. L., Dunne, A., Subramanian, S. L., Hull, R. L., Tannahill, G. M., Sharp, F. A., Becker, C., Franchi, L., Yoshihara, E., Chen, Z., Mullooly, N., Mielke, L. A., Harris, J., Coll, R. C., Mills, K. H., *et al.* (2010) Activation of the NLRP3 inflammasome by islet amyloid polypeptide provides a mechanism for enhanced IL-1β in type 2 diabetes. *Nat. Immunol.* **11,** 897–904 CrossRef Medline
13. Zhou, R., Tardivel, A., Thorens, B., Choi, I., and Tschopp, J. (2010) Thioredoxin-interacting protein links oxidative stress to inflammasome activation. *Nat. Immunol.* **11,** 136–140 CrossRef Medline

14. Vlassara, H., and Palace, M. R. (2002) Diabetes and advanced glycation endproducts. *J. Int. Med.* **251,** 87–101 CrossRef Medline
15. Zhu, Y., Shu, T., Lin, Y., Wang, H., Yang, J., Shi, Y., and Han, X. (2011) Inhibition of the receptor for advanced glycation endproducts (RAGE) protects pancreatic beta-cells. *Biochem. Biophys. Res. Commun.* **404,** 159–165 CrossRef Medline
16. Maedler, K., Sergeev, P., Ris, F., Oberholzer, J., Joller-Jemelka, H. I., Spinas, G. A., Kaiser, N., Halban, P. A., and Donath, M. Y. (2002) Glucose-induced beta cell production of IL-1β contributes to glucotoxicity in human pancreatic islets. *J. Clin. Invest.* **110,** 851–860 CrossRef Medline
17. Eguchi, K., Manabe, I., Oishi-Tanaka, Y., Ohsugi, M., Kono, N., Ogata, F., Yagi, N., Ohto, U., Kimoto, M., Miyake, K., Tobe, K., Arai, H., Kadowaki, T., and Nagai, R. (2012) Saturated fatty acid and TLR signaling link beta cell dysfunction and islet inflammation. *Cell Metab.* **15,** 518–533 CrossRef Medline
18. Bouma, G., Lam-Tse, W. K., Wierenga-Wolf, A. F., Drexhage, H. A., and Versnel, M. A. (2004) Increased serum levels of MRP-8/14 in type 1 diabetes induce an increased expression of CD11b and an enhanced adhesion of circulating monocytes to fibronectin. *Diabetes* **53,** 1979–1986 CrossRef Medline
19. Burkhardt, K., Schwarz, S., Pan, C., Stelter, F., Kotliar, K., Von Eynatten, M., Sollinger, D., Lanzl, I., Heemann, U., and Baumann, M. (2009) Myeloid-related protein 8/14 complex describes microcirculatory alterations in patients with type 2 diabetes and nephropathy. *Cardiovasc. Diabetol.* **8,** 10 CrossRef Medline
20. Vogl, T., Tenbrock, K., Ludwig, S., Leukert, N., Ehrhardt, C., van Zoelen, M. A., Nacken, W., Foell, D., van der Poll, T., Sorg, C., and Roth, J. (2007) Mrp8 and Mrp14 are endogenous activators of Toll-like receptor 4, promoting lethal, endotoxin-induced shock. *Nat. Med.* **13,** 1042–1049 CrossRef Medline
21. Foell, D., and Roth, J. (2004) Proinflammatory S100 proteins in arthritis and autoimmune disease. *Arthritis Rheum.* **50,** 3762–3771 CrossRef Medline
22. Riva, M., Källberg, E., Björk, P., Hancz, D., Vogl, T., Roth, J., Ivars, F., and Leanderson, T. (2012) Induction of nuclear factor-κB responses by the S100A9 protein is Toll-like receptor-4-dependent. *Immunology* **137,** 172–182 CrossRef Medline
23. Sunahori, K., Yamamura, M., Yamana, J., Takasugi, K., Kawashima, M., Yamamoto, H., Chazin, W. J., Nakatani, Y., Yui, S., and Makino, H. (2006) The S100A8/A9 heterodimer amplifies proinflammatory cytokine production by macrophages via activation of nuclear factor κB and p38 mitogen-activated protein kinase in rheumatoid arthritis. *Arthritis Res. Ther.* **8,** R69 CrossRef Medline
24. Tornovsky-Babeay, S., Dadon, D., Ziv, O., Tzipilevich, E., Kadosh, T., Schyr-Ben Haroush, R., Hija, A., Stolovich-Rain, M., Furth-Lavi, J., Granot, Z., Porat, S., Philipson, L. H., Herold, K. C., Bhatti, T. R., Stanley, C., *et al.* (2014) Type 2 diabetes and congenital hyperinsulinism cause DNA double-strand breaks and p53 activity in beta cells. *Cell Metab.* **19,** 109–121 CrossRef Medline
25. Shirakawa, J., Togashi, Y., Sakamoto, E., Kaji, M., Tajima, K., Orime, K., Inoue, H., Kubota, N., Kadowaki, T., and Terauchi, Y. (2013) Glucokinase activation ameliorates ER stress-induced apoptosis in pancreatic beta-cells. *Diabetes* **62,** 3448–3458 CrossRef Medline
26. Dasu, M. R., and Jialal, I. (2011) Free fatty acids in the presence of high glucose amplify monocyte inflammation via Toll-like receptors. *Am. J. Physiol. Endocrinol. Metab.* **300,** E145–E154 CrossRef Medline
27. Dasu, M. R., Devaraj, S., Zhao, L., Hwang, D. H., and Jialal, I. (2008) High glucose induces toll-like receptor expression in human monocytes: mechanism of activation. *Diabetes* **57,** 3090–3098 CrossRef Medline
28. Hasnain, S. Z., Borg, D. J., Harcourt, B. E., Tong, H., Sheng, Y. H., Ng, C. P., Das, I., Wang, R., Chen, A. C., Loudovaris, T., Kay, T. W., Thomas, H. E., Whitehead, J. P., Forbes, J. M., Prins, J. B., and McGuckin, M. A. (2014) Glycemic control in diabetes is restored by therapeutic manipulation of cytokines that regulate beta cell stress. *Nat. Med.* **20,** 1417–1426 CrossRef Medline
29. Ikemoto, M., Matsumoto, S., Egawa, H., Okitsu, T., Iwanaga, Y., Umemoto, S., Itoh, H., Murayama, H., and Fujita, M. (2007) A case with transient increases in serum S100A8/A9 levels implying acute inflammatory responses after pancreatic islet transplantation. *Ann. Clin. Biochem.* **44,** 570–572 CrossRef Medline
30. Böni-Schnetzler, M., Boller, S., Debray, S., Bouzakri, K., Meier, D. T., Prazak, R., Kerr-Conte, J., Pattou, F., Ehses, J. A., Schuit, F. C., and Donath, M. Y. (2009) Free fatty acids induce a proinflammatory response in islets via the abundantly expressed interleukin-1 receptor I. *Endocrinology* **150,** 5218–5229 CrossRef Medline
31. Gao, Q., Ma, L. L., Gao, X., Yan, W., Williams, P., and Yin, D. P. (2010) TLR4 mediates early graft failure after intraportal islet transplantation. *Am. J. Transplant.* **10,** 1588–1596 CrossRef Medline
32. Basso, D., Greco, E., Padoan, A., Fogar, P., Scorzeto, M., Fadi, E., Bozzato, D., Moz, S., Navaglia, F., Zambon, C. F., Seraglia, R., De Carlo, E., Valerio, A., Reggiani, C., Pedrazzoli, S., and Plebani, M. (2011) Altered intracellular calcium fluxes in pancreatic cancer induced diabetes mellitus: Relevance of the S100A8 N-terminal peptide (NT-S100A8). *J. Cell. Physiol.* **226,** 456–468 CrossRef Medline
33. Vogl, T., Gharibyan, A. L., and Morozova-Roche, L. A. (2012) Pro-inflammatory S100A8 and S100A9 proteins: self-assembly into multifunctional native and amyloid complexes. *Int. J. Mol. Sci.* **13,** 2893–2917 CrossRef Medline
34. Manitz, M. P., Horst, B., Seeliger, S., Strey, A., Skryabin, B. V., Gunzer, M., Frings, W., Schönlau, F., Roth, J., Sorg, C., and Nacken, W. (2003) Loss of S100A9 (MRP14) results in reduced interleukin-8-induced CD11b surface expression, a polarized microfilament system, and diminished responsiveness to chemoattractants *in vitro*. *Mol. Cell. Biol.* **23,** 1034–1043 CrossRef Medline
35. Sekimoto, R., Fukuda, S., Maeda, N., Tsushima, Y., Matsuda, K., Mori, T., Nakatsuji, H., Nishizawa, H., Kishida, K., Kikuta, J., Maijima, Y., Funahashi, T., Ishii, M., and Shimomura, I. (2015) Visualized macrophage dynamics and significance of S100A8 in obese fat. *Proc. Natl. Acad. Sci. U.S.A.* **112,** E2058–E2066 CrossRef Medline
36. Averill, M. M., Kerkhoff, C., and Bornfeldt, K. E. (2012) S100A8 and S100A9 in cardiovascular biology and disease. *Arterioscler. Thromb. Vasc. Biol.* **32,** 223–229 CrossRef Medline
37. Perera, C., McNeil, H. P., and Geczy, C. L. (2010) S100 Calgranulins in inflammatory arthritis. *Immunol. Cell Biol.* **88,** 41–49 CrossRef Medline
38. Oh, Y. S., Lee, Y. J., Park, K., Choi, H. H., Yoo, S., and Jun, H. S. (2014) Treatment with glucokinase activator, YH-GKA, increases cell proliferation and decreases glucotoxic apoptosis in INS-1 cells. *Eur. J. Pharm. Sci.* **51,** 137–145 CrossRef Medline
39. Roma, L. P., Duprez, J., and Jonas, J. C. (2015) Glucokinase activation is beneficial or toxic to cultured rat pancreatic islets depending on the prevailing glucose concentration. *Am. J. Physiol. Endocrinol. Metab.* **309,** E632–E639 CrossRef Medline
40. Lysakova-Devine, T., Keogh, B., Harrington, B., Nagpal, K., Halle, A., Golenbock, D. T., Monie, T., and Bowie, A. G. (2010) Viral inhibitory peptide of TLR4, a peptide derived from vaccinia protein A46, specifically inhibits TLR4 by directly targeting MyD88 adaptor-like and TRIF-related adaptor molecule. *J. Immunol.* **185,** 4261–4271 CrossRef Medline
41. Shirakawa, J., Amo, K., Ohminami, H., Orime, K., Togashi, Y., Ito, Y., Tajima, K., Koganei, M., Sasaki, H., Takeda, E., and Terauchi, Y. (2011) Protective effects of dipeptidyl peptidase-4 (DPP-4) inhibitor against increased beta cell apoptosis induced by dietary sucrose and linoleic acid in mice with diabetes. *J. Biol. Chem.* **286,** 25467–25476 CrossRef Medline
42. Zhang, X., Goncalves, R., and Mosser, D. M. (2008) The isolation and characterization of murine macrophages. *Curr. Protoc. Immunol.* Chapter 14, Unit 14.11 CrossRef Medline
43. Shirakawa, J., Fujii, H., Ohnuma, K., Sato, K., Ito, Y., Kaji, M., Sakamoto, E., Koganei, M., Sasaki, H., Nagashima, Y., Amo, K., Aoki, K., Morimoto, C., Takeda, E., and Terauchi, Y. (2011) Diet-induced adipose tissue inflammation and liver steatosis are prevented by DPP-4 inhibition in diabetic mice. *Diabetes* **60,** 1246–1257 CrossRef Medline
44. Shirakawa, J., Okuyama, T., Yoshida, E., Shimizu, M., Horigome, Y., Tuno, T., Hayasaka, M., Abe, S., Fuse, M., Togashi, Y., and Terauchi, Y. (2014) Effects of the antitumor drug OSI-906, a dual inhibitor of IGF-1 receptor

and insulin receptor, on the glycemic control, beta-cell functions, and beta-cell proliferation in male mice. *Endocrinology* **155,** 2102–2111 CrossRef Medline

45. Shirakawa, J., Fernandez, M., Takatani, T., El Ouaamari, A., Jungtrakoon, P., Okawa, E. R., Zhang, W., Yi, P., Doria, A., and Kulkarni, R. N. (2017) Insulin signaling regulates the FoxM1/PLK1/CENP-A pathway to promote adaptive pancreatic beta cell proliferation. *Cell Metab.* **25,** 868–882.e5 CrossRef Medline
46. Hiratsuka, S., Watanabe, A., Aburatani, H., and Maru, Y. (2006) Tumour-mediated upregulation of chemoattractants and recruitment of myeloid cells predetermines lung metastasis. *Nat. Cell Biol.* **8,** 1369–1375 CrossRef Medline

Signaling between pancreatic β cells and macrophages via S100 calcium-binding protein A8 exacerbates β-cell apoptosis and islet inflammation

Hideaki Inoue, Jun Shirakawa, Yu Togashi, Kazuki Tajima, Tomoko Okuyama, Mayu Kyohara, Yui Tanaka, Kazuki Orime, Yoshifumi Saisho, Taketo Yamada, Kimitaka Shibue, Rohit N. Kulkarni and Yasuo Terauchi

J. Biol. Chem. 2018, 293:5934-5946.
doi: 10.1074/jbc.M117.809228 originally published online March 1, 2018

Case Report

Necrotizing enterocolitis associated with *Clostridium butyricum* in a Japanese man

Yukio Sato,[1,2] Dai Kujirai,[1,2] Katsura Emoto,[3,4] Toshiaki Yagami,[5] Taketo Yamada,[3,4,6] Manabu Izumi,[7] Masaki Ano,[8] Kenichi Kase,[1] and Kenji Kobayashi[1,9]

[1]Department of Emergency Medicine, Saiseikai Utsunomiya Hospital, Tochigi, Japan, [2]Department of Emergency and Critical Care Medicine, Keio University School of Medicine, Tokyo, Japan, [3]Department of Pathology, Saiseikai Utsunomiya Hospital, Tochigi, Japan, [4]Department of Pathology, Keio University School of Medicine, Tokyo, Japan, [5]Department of Radiology, Saiseikai Utsunomiya Hospital, Tochigi, Japan, [6]Department of Pathology, Saitama Medical University, Saitama, Japan, [7]Department of General Internal Medicine, Saiseikai Utsunomiya Hospital, Tochigi, Japan, [8]Department of Critical Care Medicine, Saiseikai Utsunomiya Hospital, Tochigi, Japan, and [9]Department of Surgery, Saiseikai Utsunomiya Hospital, Tochigi, Japan

Case: Necrotizing enterocolitis (NEC) caused by *Clostridium butyricum* is common in neonates; however, a case of NEC in adults has not been previously reported. An 84-year-old Japanese man developed *C. butyricum*-related NEC during hospitalization for treatment of stab wounds to the left side of the neck and lower abdomen, without organ damage, and concomitant pneumonia.

Outcome: The patient developed acute onset of emesis accompanied by shock during his admission; partial resection of the small intestine was carried out due to necrosis. Pathologic findings showed mucosal necrosis and extensive vacuolation with gram-positive rods in the necrotic small intestine. Blood culture tests revealed *C. butyricum* infection. The patient's condition improved after the surgery. He was moved to a rehabilitation hospital on day 66.

Conclusion: This study suggests that hospitalized adult patients who receive antibiotic treatment are at risk for NEC.

Key words: Adult, Asia, *Clostridium butyricum*, enterocolitis, necrotizing

INTRODUCTION

SEVERAL STRAINS OF *Clostridium butyricum* have been cultured from the stool of healthy children and adults.[1] One of those strains, MIYAIRI 588, is used widely as a probiotic in Asia, including Japan.[2] It has been reported that it inhibited the cytotoxicity of *Clostridium difficile* in an *in vitro* study and reduced *C. difficile* toxin A in an *in vivo* study.[3,4] However, some of these strains produce endotoxins and cause necrotizing enterocolitis (NEC) in neonates.[5] The only toxin *C. butyricum* has been reported to produce is analogous to the type E botulinum neurotoxin secreted by *Clostridium botulinum*.[6] After the first report of NEC due to *C. butyricum* type E in an infant,[7] many similar cases have been reported, including two cases of intestinal botulism involving adolescents,[8] and one case of sepsis in an adult.[9] Additionally, cases of food-borne botulism caused by *C. butyricum* have been reported.[10] However, a case of NEC due to *C. butyricum* in an adult has not been reported to date.

Corresponding: Yukio Sato, MD, PhD, Department of Emergency & Critical Care Medicine, Keio University School of Medicine, 35 Shinanomachi, Shinjuku-ku, Tokyo 1608582, Japan. Email: yukiosato@a6.keio.jp.
Received 24 Oct, 2017; accepted 25 Dec, 2017; online publication 23 Jan, 2018
Funding Information
No funding information provided.

CASE

AN 84-YEAR-OLD MAN visited our hospital owing to a neck (left) and abdominal penetrating injury by a short sword in a suicide attempt. The patient had a medical history of cerebral infarction and paroxysmal atrial fibrillation on apixaban. He lived in his home with his family and had no recent history of hospitalization or admission to a nursing home.

On examination, his vital signs were normal except for disturbed consciousness: Glasgow coma scale score, 6; blood pressure, 158/92 mmHg; respiratory rate, 18 breaths/

min; heart rate, 72 b.p.m.; and body temperature, 35.9°C. A short sword had been inserted into the left lateral neck. There was no exit wound. There was another stab wound in the middle of the lower abdomen. There were no hard signs of bleeding around either wound. There were no peritoneal signs. Otherwise, the physical examination was unremarkable. Laboratory examination showed: white cell count, 13,000/μL; neutrophils, 11,180/μL; lymphocytes, 1,300/μL; hemoglobin, 12.3 g/dL; platelet count, 33.6 × 10^4/μL; activated partial thromboplastin time, 27.8 s; prothrombin time – international normalized ratio, 1.27; and fibrinogen level, 377 mg/dL.

On image examination, a chest radiograph did not indicate a hemopneumothorax, and a focused assessment with sonography for trauma did not indicate fluid in the chest or abdominal cavities (Fig. 1A). To examine the trajectory of the sword, a cervical radiograph was carried out (Fig. 1B). Neck and chest radiographs did not show any free air in the soft tissue. A whole body computed tomography (CT) scan with i.v. contrast revealed the sword penetrating through the left thoracic cavity from the left side of the neck and an injury in the lower abdomen. There was s.c. emphysema with signs of pneumothorax. The peritoneum was penetrated; however, there were no free air or free fluid in the abdominal cavity (Fig. 1C,D). It was difficult to ascertain whether the left subclavian artery was injured because of an artifact on the CT images generated by the sword; therefore, emergency exploratory thoracotomy and laparotomy were carried out.

During the surgery, no organ damage was found, and the sword was removed safely. The patient was treated in the intensive care unit after surgery; however, he needed continuous mechanical ventilation owing to respiratory failure. Subsequently, the patient developed ventilator-associated pneumonia due to methicillin-resistant *Staphylococcus aureus* on postoperative day (POD) 13 and was treated using meropenem 1.0 g/day and vancomycin 2 g/day i.v. until POD 23. The patient was extubated on POD 20. The patient was transferred from the intensive care unit and moved to the step-down unit on POD 21. As ambulation and oral intake were difficult, due to a continuously disturbed mental state, enteral feeding was continued. On POD 36, the patient presented with sudden onset of vomiting, with hypoxemia and shock. On examination before intubation, generalized abdominal tenderness with peritoneal signs was recognized. Laboratory examination showed: white blood count, 11,240/μL; neutrophils, 10,453/μL; lymphocytes, 674/μL; hemoglobin 7.4 g/dL; platelet count, 34.5 × 10^4/μL; activated partial thromboplastin time, 33.6 s; prothrombin time – international normalized ratio, 1.38; and C-reactive protein, 3.21 mg/dL. Niveau formation was observed on the chest radiograph obtained after intubation. A whole-body CT scan showed portal vein gas and pneumatosis cystoides intestinalis, suggesting ischemic enteritis (Fig. 2). Consequently,

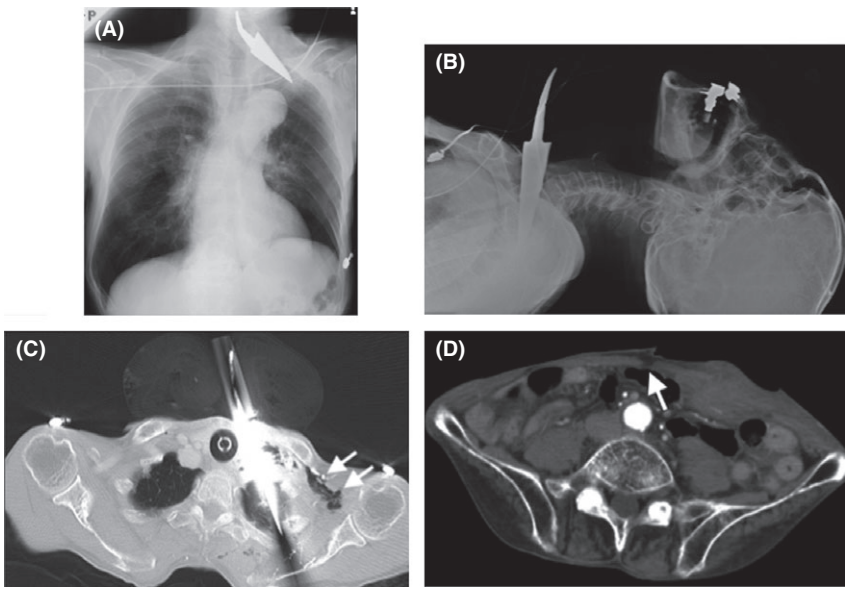

Fig. 1. Radiographs and whole body computed tomography (CT) scans taken on admission of an 84-year-old man with self-inflicted stab wounds to the neck and abdomen. A, Radiograph of the chest. B, Radiograph of the neck. C, CT image of the chest. Arrows indicate the air leakage. D, CT image of the abdomen. The arrow indicates the injury to the posterior layer of the rectus sheath.

the patient was brought to the operating room for the emergent exploratory laparotomy. Despite the patient's age, arteriosclerosis suggesting ischemic enteritis was not observed. One hundred and twenty centimeters of jejunum and ileum was resected, located 70 cm away from the ligament of Treitz; the first 20 cm was necrotic, the next 30 cm looked pale, suggesting ischemia, and the last 70 cm was necrotic (Fig. 3A). Mesenterium at the region was congested with blood. The remaining intact tracts, comprising 170 cm in total, were stapled by functional end-to-end anastomosis. Histopathologic examination of the resected intestine showed extensive mucosal necrosis, innumerable gram-positive bacilli, and associated vacuolation and epithelial regeneration (Fig. 3B–D). The findings suggested NEC. In addition, *C. butyricum*, a gram-positive bacillus, was concurrently isolated from two cultured blood samples drawn just before the partial enterectomy. We also reconfirmed that the blood culture samples obtained on POD 42 were sterile. An antibiotic, meropenem 1.0 g/day, was given for 2 weeks, starting at onset of shock, and had a susceptibility

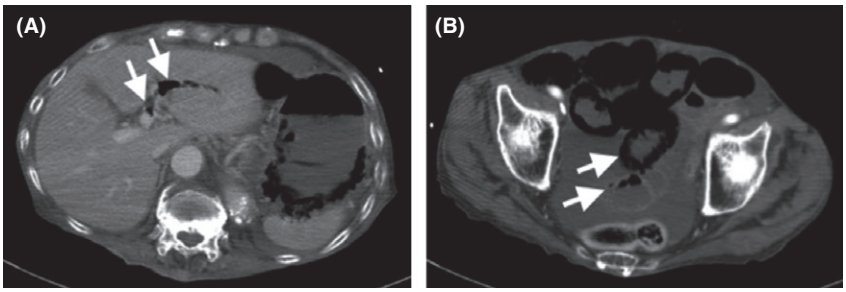

Fig. 2. Whole body computed tomography scan of an 84-year-old man with self-inflicted stab wounds to the neck and abdomen, taken when the patient presented with vomiting. A, Image of the upper abdomen. Arrows indicate portal vein gas. B, Image of the lower abdomen. Arrows indicate pneumatosis cystoides intestinalis.

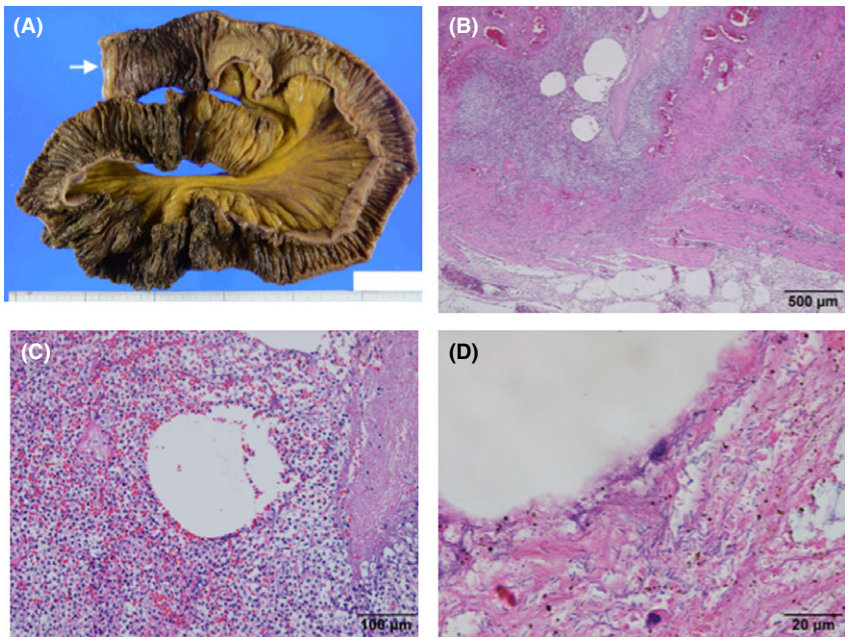

Fig. 3. Histological observation of the resected small intestine of an 84-year-old man with necrotizing enterocolitis associated with *Clostridium butyricum*, using hematoxylin–eosin staining with a macro image. A, Macro image of resected tract. Arrow indicates the oral side. B, Severe inflammation, several vacuoles, congestion, and hemorrhage in the muscularis propria and subserosal layer indicate gas gangrene. Scale bar, 500 μm. C, Vacuoles are surrounded by acute severe inflammation and considered as gas accumulation. Scale bar, 100 μm. D, Observation by oil immersion lens reveals numerous bacilli adjacent to vacuoles. Scale bar, 20 μm.

to *C. butyricum*. The patient recovered and was moved to a rehabilitation hospital on POD 66 following his first surgery.

DISCUSSION

NECROTIZING ENTEROCOLITIS CAUSED by *C. butyricum* is common in preterm neonates, and can be life-threatening.[5] However, to the best of our knowledge, no such cases have been reported in adults.

In the present case, we initially suspected ischemic enteritis; however, surgical and pathological findings suggested NEC. In addition to the lack of obvious obstruction of vessels on surgery, histopathology results indicated that *C. butyricum* isolation from the patient's blood samples resulted from mucosal breakdown and transmigration of these bacteria into the bloodstream. These findings indicated that pathogenic *C. butyricum* infection in the gut resulted in septic shock, leading to ischemia of the small intestine. With regard to the route of infection, in this case, the initial exploratory laparotomy for the stab wound did not involve any bowel injuries; therefore it was not related to the development of NEC. We hypothesized that the patient was a *C. butyricum* carrier, and treatment with several antibiotics for methicillin-resistant *Staphylococcus aureus* pneumonia might have resulted in the microbial substitution. Nevertheless, the invasion route is still unclear. In addition, a previous report suggested that lactose fermentation is involved in the pathogenesis of NEC.[11] However, the enteral nutrient administered to this patient did not include lactose. Moreover, the patient had been admitted for 30 days before the development of NEC. During that period, no outbreak of this kind of bacterial infection was observed in our hospital, thus, excluding the possibility of nosocomial infection.[7] Therefore, the course of *C. butyricum* infection remains unclear.

Regarding the differential diagnosis, we discussed the possibility of the following three diseases. Neutropenic enterocolitis, also known as typhlitis, is confused with NEC; however, our patient's background was completely different to reported cases.[12] Although its cause is still unclear, it basically occurs in patients with neutropenia, such as leukemic patients receiving chemotherapy. The patient did not have any medical history suggesting neutropenia. In addition, a test for antibodies against HIV yielded negative results. The possibility of non-occlusive mesenteric ischemia (NOMI) was definitely difficult to rule out, because of similar traits between both diseases: ischemia and infection.[13] Moreover, segmental and discontinuous necrosis in a region perfused by the superior mesenteric artery can be typically observed in NOMI, although it was difficult to confirm that necrotic and ischemic regions were completely continuous in our case. Nonetheless, if our case was NOMI, the innumerable bacteria propagated in such a short period would have been incongruous, as the patient had no risk factors at the onset, such as cardiac failure, low flow states, multi-organ dysfunction, or vasopressors.[14] The probability of ischemic enteritis was low because there was no arteriosclerosis, and it typically occurs in a region perfused by the inferior mesenteric artery. Thus, based on the above reasons, we diagnosed NEC.

Regarding the prevention of adult NEC, a clonal strain was found to be circulating in neonatal intensive care unit, during an outbreak of NEC in preterm neonates.[5,7,15] Therefore, it is necessary for medical and nursing staff to control infection effectively, even in adult care units. In addition, although prediction is difficult, a risk for developing NEC, owing to microbial substitution, could be considered during treatment with antibiotics in the same manner as consideration for *C. difficile* colitis.

Limitations of this study include the inability to assess the neurogenic symptoms (vision impairment and dysphagia) of the patient, because of his continuous disturbed mental state. Furthermore, gene sequencing to confirm the type of strain isolated could not be carried out.

CONCLUSION

WE PRESENT A rare case of successful management of a hospitalized elderly patient with NEC associated with *C. butyricum*. The present case suggests that hospitalized adults who receive antibiotic therapy carry a risk of critical illness associated with pathogenic *C. butyricum*.

ACKNOWLEDGEMENTS

WE WOULD LIKE to thank Editage for English language editing.

DISCLOSURE

Approval of the research protocol: N/A.
Informed consent: Informed consent was obtained from the subject.
Registry and the registration no. of the study/trial: N/A.
Animal studies: N/A.
Conflict of interest: T.Y. was supported by grants from Kissei Pharmaceutical Co., Ltd. and Nichirei Biosciences Inc. The other authors have no conflict of interest.

REFERENCES

1 Benno Y, Sawada K, Mitsuoka T. The intestinal microflora of infants: composition of fecal flora in breast-fed and bottle-fed infants. Microbiol. Immunol. 1984; 28: 975–86.

2 Isa K, Oka K, Beauchamp N *et al.* Safety assessment of the Clostridium butyricum MIYAIRI 588(R) probiotic strain including evaluation of antimicrobial sensitivity and presence of Clostridium toxin genes *in vitro* and teratogenicity *in vivo*. Hum. Exp. Toxicol. 2016; 35: 818–32.

3 Woo TD, Oka K, Takahashi M *et al.* Inhibition of the cytotoxic effect of Clostridium difficile *in vitro* by Clostridium butyricum MIYAIRI 588 strain. J. Med. Microbiol. 2011; 60: 1617–25.

4 Imase K, Takahashi M, Tanaka A *et al.* Efficacy of Clostridium butyricum preparation concomitantly with Helicobacter pylori eradication therapy in relation to changes in the intestinal microbiota. Microbiol. Immunol. 2008; 52: 156–61.

5 Cassir N, Benamar S, Khalil JB *et al.* Clostridium butyricum strains and Dysbiosis linked to necrotizing enterocolitis in preterm neonates. Clin. Infect. Dis. 2015; 61: 1107–15.

6 Popoff MR, Dodin A. Survey of neuraminidase production by Clostridium butyricum, Clostridium beijerinckii, and Clostridium difficile strains from clinical and nonclinical sources. J. Clin. Microbiol. 1985; 22: 873–6.

7 Howard FM, Flynn DM, Bradley JM, Noone P, Szawatkowski M. Outbreak of necrotising enterocolitis caused by Clostridium butyricum. Lancet 1977; 2: 1099–102.

8 Fenicia L, Franciosa G, Pourshaban M, Aureli P. Intestinal toxemia botulism in two young people, caused by Clostridium butyricum type E. Clin. Infect. Dis. 1999; 29: 1381–7.

9 Gardner EM, Kestler M, Beieler A, Belknap RW. Clostridium butyricum sepsis in an injection drug user with an indwelling central venous catheter. J. Med. Microbiol. 2008; 57: 236–9.

10 Meng X, Karasawa T, Zou K *et al.* Characterization of a neurotoxigenic Clostridium butyricum strain isolated from the food implicated in an outbreak of food-borne type E botulism. J. Clin. Microbiol. 1997; 35: 2160–2.

11 Bousseboua H, Le Coz Y, Dabard J *et al.* Experimental cecitis in gnotobiotic quails monoassociated with Clostridium butyricum strains isolated from patients with neonatal necrotizing enterocolitis and from healthy newborns. Infect. Immun. 1989; 57: 932–6.

12 Rodrigues FG, Dasilva G, Wexner SD. Neutropenic enterocolitis. World J. Gastroenterol. 2017; 23: 42–7.

13 Zachariah SK. Adult necrotizing enterocolitis and non occlusive mesenteric ischemia. J. Emerg. Trauma Shock. 2011; 4: 430–2.

14 Bala M, Kashuk J, Moore EE *et al.* Acute mesenteric ischemia: guidelines of the World Society of Emergency Surgery. World J. Emerg. Surg. 2017; 12: 38.

15 Benamar S, Cassir N, Merhej V *et al.* Multi-spacer typing as an effective method to distinguish the clonal lineage of Clostridium butyricum strains isolated from stool samples during a series of necrotizing enterocolitis cases. J. Hosp. Infect. 2017; 95: 300–5.

European Journal of Radiology 101 (2018) 124–128

Contents lists available at ScienceDirect

European Journal of Radiology

journal homepage: www.elsevier.com/locate/ejrad

Research article

Low-dose chest computed tomography screening of subjects exposed to asbestos

Katsuya Kato[a], Kenichi Gemba[b], Kazuto Ashizawa[c], Hiroaki Arakawa[d], Satoshi Honda[e], Naomi Noguchi[f], Sumihisa Honda[c], Nobukazu Fujimoto[g,*], Takumi Kishimoto[h]

[a] Department of Diagnostic Radiology 2, Kawasaki Medical School, General Medical Center, 2-1-80 Nakasange, Okayama, 7008505, Japan
[b] Department of Respiratory Medicine, Chugoku-chuo Hospital, 148-13 Oazakamiiwanari, Miyukicho, Fukuyama, 7200001, Japan
[c] Department of Clinical Oncology, Nagasaki University Graduate School of Medicine, 1-7-1 Sakamoto, Nagasaki, 8528102, Japan
[d] Department of Radiology, Dokkyo Medical University, 880, Kita-Kobayashi, Mibu, Tochigi, 3210293, Japan
[e] Department of Radiology, Okayama Rosai Hospital, 1-10-25 Chikkomidorimachi, Okayama, 7028055, Japan
[f] Department of Radiology, Tamano Mitsui Hospital, 3-2-1 Tama, Tamano, 7060012, Japan
[g] Department of Medical Oncology, Okayama Rosai Hospital, 1-10-25 Chikkomidorimachi, Okayama, 7028055, Japan
[h] Department of Internal Medicine, Okayama Rosai Hospital, 1-10-25 Chikkomidorimachi, Okayama, 7028055, Japan

ARTICLE INFO

Keywords:
Asbestos
Low-dose CT
Screening
Lung cancer
Mesothelioma

ABSTRACT

Objectives: The primary aim was to reveal the prevalence of lung cancer (LC) and malignant pleural mesothelioma (MPM) in subjects with past asbestos exposure (AE). We also examined pulmonary or pleural changes correlated with the development of LC.

Materials and methods: This was a prospective, multicenter, cross-sectional study. There were 2132 subjects enrolled between 2010 and 2012. They included 96.2% men and 3.8% women, with a mean age of 76.1 years; 78.8% former or current smokers; and 21.2% never smokers. We screened subjects using low-dose computed tomography (CT). The CT images were taken with a CT dose Index of 2.7 mGy. The evaluated CT findings included subpleural curvilinear shadow/subpleural dots, ground glass opacity or interlobular reticular opacity, traction bronchiectasia, honeycombing change, parenchymal band, emphysema changes, pleural effusion, diffuse pleural thickening, rounded atelectasis, pleural plaques (PQs), and tumor formation.

Results: The PQs were detected in most of subjects (89.4%) and emphysema changes were seen in 46.0%. Fibrotic changes were detected in 565 cases (26.5%). A pathological diagnosis of LC was confirmed in 45 cases (2.1%) and MPM was confirmed in 7 cases (0.3%). The prevalence of LC was 2.5% in patients with a smoking history, which was significantly higher than that in never smokers (0.7%, $p = 0.027$). The prevalence of LC was 2.8% in subjects with emphysema changes, which was higher than that of subjects without those findings (1.6%); although, the difference was not statistically significant ($p = 0.056$). The prevalence of LC in subjects with both fibrotic plus emphysema changes was 4.0%, which was significantly higher than that of subjects with neither of those findings (1.8%, $p = 0.011$). Logistic regression analysis revealed smoking history, fibrotic plus emphysema changes, and pleural effusion as significant explanatory variables.

Conclusions: Smoking history, fibrotic plus emphysema changes, and pleural effusion were correlated with the prevalence of LC.

1. Introduction

Asbestos was commonly used during the 20th century and remains prevalent in many developing countries [1]. Asbestos causes pathological changes in the lung or the pleura including asbestosis, pleural plaques (PQs), benign asbestos pleural effusion [2], diffuse pleural thickening, and malignant neoplasms such as malignant pleural mesothelioma (MPM) and lung cancer (LC) [3,4]. According to the World Health Organization, > 107,000 people die each year from asbestos-related diseases due to occupational exposure [1]. These diseases usually develop after long latency periods of 40–50 years [5]. Thus, there will be more LC or MPM developing in the next few decades,

Abbreviations: AE, asbestos exposure; CT, computed tomography; LC, lung cancer; LDCT, low-dose computed tomography; MPM, malignant pleural mesothelioma; PQs, pleural plaques; SCLS/DOTS, subpleural curvilinear shadow/subpleural dots

* Corresponding author.
E-mail address: nobufujimot@gmail.com (N. Fujimoto).

https://doi.org/10.1016/j.ejrad.2018.02.017
Received 8 August 2017; Received in revised form 11 December 2017; Accepted 12 February 2018

despite that asbestos use was banned in Japan in 2004. Subjects with histories of asbestos exposure (AE) in Japan are examined by annual chest X-ray; however, it is established that chest X-ray is not an efficient method forLC screening [6,7]. Thus, there is a need to establish a more useful screening strategy for subjects.

Mass screening of high-risk groups to detect LC could potentially be beneficial. Multidetector computed tomography (CT) has made high-resolution volumetric imaging possible during a single breath hold with acceptable levels of radiation exposure [8]. There were several reports that low-dose helical CT of the lung detected more nodules and LCs, including early-stage, than chest X-ray [9]. Recently, the National Lung Screening Trial, which recruited subjects at high-risk for LC, demonstrated that low-dose CT (LDCT) screening could decrease the death rate due to LC by about 20% compared with screening using chest X-ray [7]. In addition, there are some recent reports that LDCT screening is useful to detect LC at the earlier stages [10–12].

In the current study, we performed LDCT screening for subjects with histories of AE. The primary aim of the study was to reveal the prevalence of LC and MPM in the subjects. In addition, we focused on other pulmonary or pleural changes, such as fibrotic or emphysema changes and plaques, to determine what findings correlated with the prevalence of LC.

2. Materials and methods

2.1. Study approval

This study was conducted in compliance with the principles of the Declaration of Helsinki. This study was carried out according to The Ethical Guidelines for Epidemiological Research by the Japanese Ministry of Education, Culture, Sports, Science, and Technology, and the Ministry of Health, Labour, and Welfare. This study was approved by the Japan Health, Labour, and Welfare Organization and the institutional review boards of each institution. Patient confidentiality was strictly maintained and written informed consent was obtained from the subjects.

2.2. Subjects

This was a prospective, multicenter, cross-sectional study to reveal the prevalence of LC and MPM, and the prevalence of CT findings due to AE. The inclusion criteria of the subjects are 1) those who had engaged in asbestos-product manufacturing for more than 1 year, 2) those who had engaged in other industries related to AE for more than 10 years, or 3) those who had engaged in industries related to AE and demonstrated pleural plaques on chest X-ray or CT (regardless of the duration of AE). There were 2132 subjects enrolled in this study between 2010 and 2012. They included 2050 (96.2%) men and 82 (3.8%) women, with a mean (range) age of 76.1 (51–101) years. There were 502 subjects from Okayama Rosai Hospital, 392 from Chiba Rosai Hospital, 370 from Tamano Mitsui Hospital, 313 from Kinki Chuo Chest Medical Center, 214 from Kagawa Rosai Hospital, 196 from Toyama Rosai Hospital, 96 from Yamaguchi-Ube Medical Center, and 49 from Hokkaido Chuo Rosai Hospital. The occupational categories associated with AE are shown in Fig. 1. The main categories included 612 subjects (28.7%) in shipbuilding, 260 (12.2%) in chemical manufacturing, 259 (12.2%) in asbestos-product manufacturing, and 245 (11.5%) in construction. The smoking history was obtained from 2095 subjects and revealed 1651 (78.8%) former or current smokers and 444 (21.2%) never smokers.

2.3. CT acquisition and analysis

The CT images were taken in each institution with a median (range) CT dose Index of 2.7 (2.4–2.8) mGy. 2 mm thick images were obtained and stored in Digital Imaging and Communications in the Medicine format. The evaluated CT findings included pulmonary fibrotic changes, such as subpleural curvilinear shadow/subpleural dots (SCLS/DOTS), ground glass opacity or interlobular reticular opacity, traction bronchiectasia, honeycombing change, and parenchymal band (Fig. 2). Other evaluated findings were emphysema change, pleural effusion, diffuse pleural thickening, rounded atelectasis, PQs with or without calcification, and tumor formation. The CT images were taken with the subject in a prone position to differentiate slight pulmonary changes on the dorsal portion of the lungs from gravitational effects. Images were analyzed independently on the monitor, based on a quality standard, agreed on by two reference radiologists who were blinded to the clinical and demographic information of the subject and the results of one another's assessments. If there was a difference between the interpretations of the two radiologists, more rigorous interpretation was adopted with regard to emphysema changes, pleural effusion, diffuse pleural thickening, PQs, and tumor formation. For fibrotic changes, a third radiologist made the second-round interpretation and gave the final decision. When LC or MPM was suspected in subjects, further examinations such as bronchoscopy, needle biopsy, thoracentesis, and/or surgery were performed in the clinical practice.

This was a cross sectional study with only one CT performed in each subject. No follow up was performed for patients with a negative CT.

2.4. Statistical analysis

Comparisons between independent groups were performed using the chi-square test and the Mann-Whitney *U* test was used for non-parametric analysis. The average values were compared using the *t*-test. Overall survival of LC patients was obtained by using Kaplan-Meier methods. Logistic regression analysis was conducted as a multivariate analysis. Statistical calculations were performed using SPSS statistical package version 22.0 (IBM, Armonk, USA).

3. Results

3.1. CT findings

The CT findings of the 2132 subjects are summarized in Table 1. The PQs were detected in the majority of subjects (89.4%) and emphysema changes in about half of the subjects (46.0%). Fibrotic changes (at least one of: SCLS/DOTS, ground glass opacity or interlobular reticular opacity, traction bronchiectasia, honeycombing change, and parenchymal band) were detected in 565 cases (26.5%). There were 116 cases (5.4%) with suspected LC, including 101 with possible LC and 15 with definite LC.

The pathological diagnosis of LC was confirmed in 45 cases (2.1%), 44 men and 1 woman. Median (range) age at the diagnosis was 73 (60–87) years old. There were 31(68.9%) adenocarcinoma, 10(22.2%) squamous cell carcinoma, 3(6.7%) small cell carcinoma, and 1(2.2%) adenosquamous carcinoma. According to the International Association for the Study of Lung Cancer staging (7th Edition), there were 13 Stage IA, 14 Stage IB, 4 Stage IIA, 3 Stage IIB, 4 Stage IIIA, 2 Stage IIIB, and 1 Stage IV patients. Median overall survival (95% confidence interval) of these 13 patients was 26.8 (4.01–71.93) months.

Pleural effusion was detected in 45 subjects. Among them, LC was diagnosed in six cases including four adenocarcinomas and two squamous cell carcinomas. Pleural carcinomatosis was revealed in 2 of the 4 cases of adenocarcinoma. Another two subjects with adenocarcinoma and one of the 2 subjects with squamous cell carcinoma underwent thoracic surgery, suggesting they had post-operative pleural effusion. There were 16 subjects (0.8%) with suspected MPM and the pathological diagnosis was confirmed in seven cases (0.3%) including 4 cases of epithelioid, 2 cases of biphasic, and 1 case of sarcomatous subtype.

3.2. CT characteristics of LC cases

We examined the specific characteristics of patients in whom LC

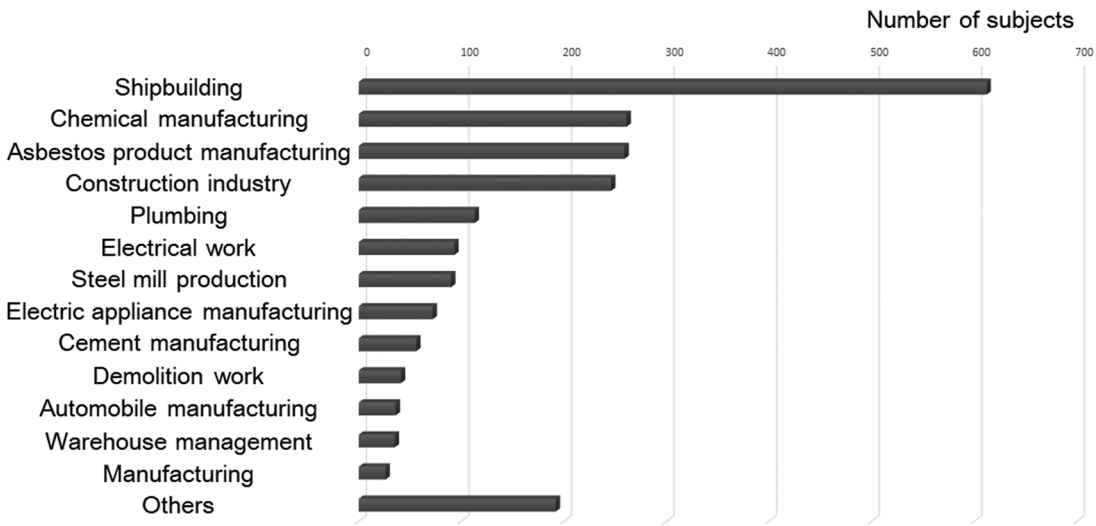

Fig. 1. Occupational categories of the enrolled subjects.

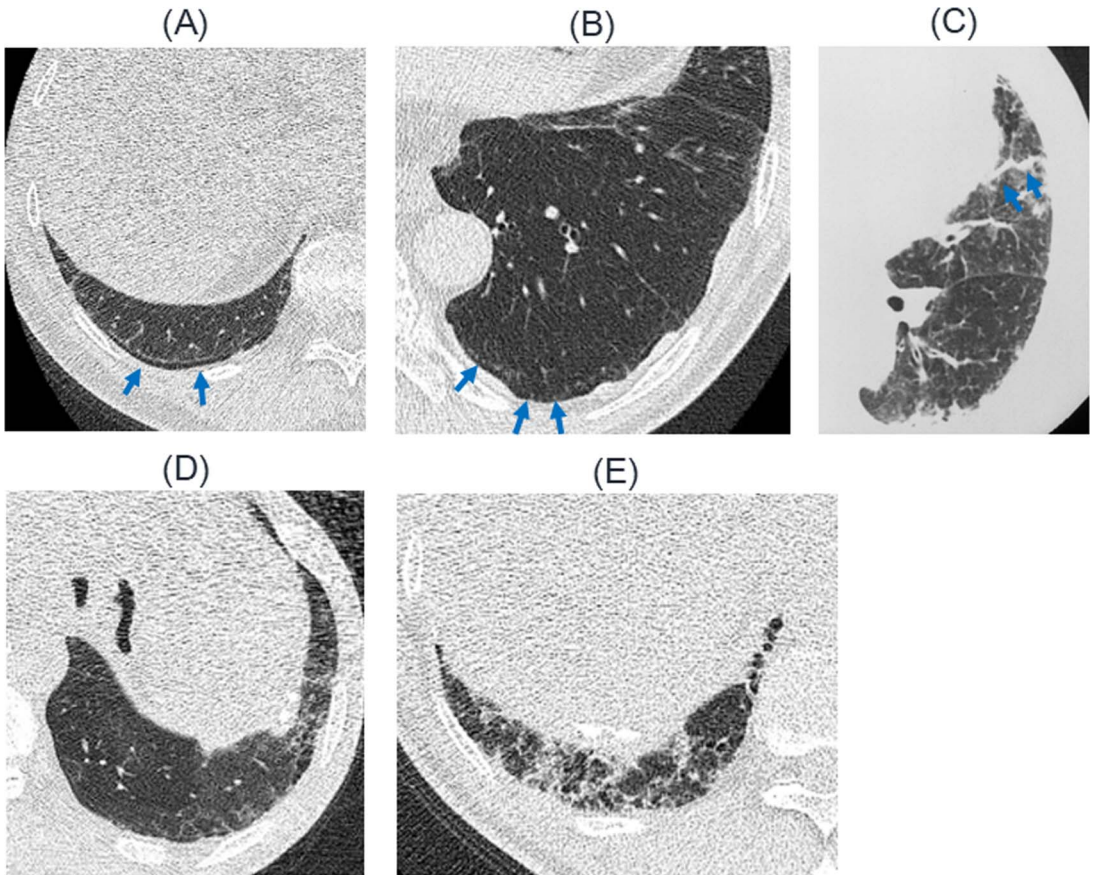

Fig. 2. Examples of pulmonary CT findings. (A) Subpleural curvilinear shadow, (B) subpleural dots, (C) parenchymal band, (D) ground-glass opacity, and (E) intralobular reticular opacities.

was detected. There was no significant difference in the prevalence when comparing genders, 2.1% (44/2050) in men and 1.2% (1/82) in women ($p = 0.567$). The prevalence of LC was 2.5% (42/1651) in patients with a smoking history, which was significantly higher than the prevalence in never smokers (0.7%, $p = 0.027$).

The associations between CT findings and the prevalence of LC are shown in Table 2. There was no difference concerning the prevalence of LC in those with and without PQs (2.1% and 2.2%, respectively, $p = 0.910$). The prevalence of LC was 2.8% in subjects with emphysema changes, which was higher than that of subjects without those findings (1.6%); although, this difference was not statistically significant ($p = 0.056$). The prevalence of LC in subjects with both emphysema changes and fibrotic changes was 4.0%, which was significantly higher than that of subjects with neither of those findings (1.8%, $p = 0.011$). The prevalence of LC was significantly higher in subjects with pleural effusion.

Logistic regression analysis was conducted using smoking history, fibrotic plus emphysema change, and pleural effusion as explanatory variables, and revealed that all of them were statistically significant (Table 3).

Table 1
CT findings of enrolled subjects.

Findings	Cases	%
Pleural plaques	1906	89.4
Emphysematous changes	980	46.0
Ground glass opacity/Interlobular reticular opacity	482	22.6
Subpleural curvilinear shadow/Subpleural dots	297	13.9
Diffuse pleural thickening	292	13.7
Parenchymal band	287	13.5
Traction bronchiectasia	186	8.7
Rounded atelectasis	70	3.3
Pleural effusion	45	2.1
Honeycombing change	42	2.0

Table 2
Associations between CT findings and the prevalence of lung cancer.

Findings		Lung Cancer (−)	Lung Cancer (+)	Total	P
Subpleural curvilinear shadow/subpleural dots (SCLS/DOTS)	+	289	8	297	
	−	1798	37	1835	0.451
Ground glass opacity/ interlobular reticular opacity	+	469	13	482	
	−	1618	32	1650	0.309
Traction bronchiectasia	+	182	4	186	
	−	1905	41	1946	0.968
Honeycombing change	+	40	2	42	
	−	2047	43	2090	0.277
Parenchymal band	+	282	5	287	
	−	1805	40	1845	0.641
Emphysema changes	+	953	27	980	
	−	1134	18	1152	0.056
Pleural effusion	+	38	7	45	
	−	2049	38	2087	< 0.001
Diffuse pleural thickening	+	287	5	292	
	−	1800	40	1840	0.61
Rounded atelectasis	+	70	0	70	
	−	2017	45	2062	0.212
Fibrotic[a] plus emphysema change	+	315	13	328	
	−	1772	32	1804	0.011

[a] Either of traction bronchiectasia, honeycombing change, or parenchymal band.

Table 3
Logistic regression analyses concerning the risk of lung cancer.

	Exp(ß)	95% C.I.[a]	*p*-value
Smoking	0.270	0.082–0.891	0.032
Fibrotic[b] plus emphysema changes	1.954	0.999–3.824	0.050
Pleural effusion	10.238	4.221–24.833	< 0.001

[a] C.I. confidence interval.
[b] Either of traction bronchiectasia, honeycombing change, or parenchymal band.

4. Discussion

Asbestos is one of the risk factors for LC as well as MPM; therefore, a strategy should be established for medical checkups among subjects with past AE. In the current study, we screened subjects with occupational AE using LDCT. The primary aim was to reveal the prevalence of LC and MPM, and the secondary aim was to examine what findings correlated with the prevalence of LC to determine the subjects at high-risk for LC. For this reason, we focused on slight pulmonary or pleural changes such as SCLS/DOTS, ground glass opacity or interlobular reticular opacity, in addition to emphysema changes or PQs. To our knowledge, this is the largest study (> 2000 subjects) evaluating subjects with past AE.

In the current study, PQs were detected in 89.4% of the enrolled subjects. In previous reports of CT screening of subjects with AE [13–18], the detection rates of PQs varied from 32 to 81% [13,15–18]. The high detection rate of PQs in the current study supports the confirmed history of AE for the enrolled subjects. As a result, 45 cases (2.1%) of LC and 7 cases (0.3%) of MPM were detected. The prevalence of LC in the current study was higher than that of previous studies using LDCT screening in Japan [10,11]. These findings suggest that subjects with past AE are a high-risk population for LC. There is another report of CT screening of subjects with AE that found the prevalence of LC was 4.28% in the high-risk group of subjects with AE and a heavy smoking history [19]. Smoking and AE are independent risk factors for LC and raise the incidence in a synergistic manner [20]. Subjects with past AE should be screened with LDCT, especially those with a smoking history.

We examined the prevalence of pulmonary CT findings, including pulmonary fibrotic changes in subjects with AE. Pulmonary fibrotic changes were found in 26.5% of the subjects. There are previous reports of radiologic findings of subjects with AE [16,18]. In those reports, pulmonary fibrotic changes were found in 6–24% of the subjects. There is another report that some sort of pulmonary fibrotic change was detected in 27% of subjects with a smoking history [21]. Many subjects in the current study had a history of smoking, so it is unclear whether these slight fibrotic changes are specific to AE or due to other causes, such as smoking. In either case, the prevalence of LC was higher in subjects with fibrotic changes, such as traction bronchiectasis and honeycomb fibrosis. In addition, the prevalence of LC was significantly higher in subjects with both fibrotic and emphysema changes. Multivariate analysis revealed smoking history, fibrotic plus emphysema changes, and pleural effusion as significant explanatory variables. These findings suggest that subjects with AE and these factors are at high-risk for LC.

There were 7 subjects with MPM detected in the current study. In previous studies, two cases of MPM were identified in 516 AE individuals [13] and no case was detected in 1045 AE workers [17]. Unlike LC, the treatment outcome of MPM is poor even when cases are diagnosed in the earlier stages [22]. The usefulness of LDCT for the early diagnosis and improvement of treatment outcome in MPM should be addressed and investigated in future studies.

There are limitations to the current study. It is a cross-sectional study. The causal connection between LC and some CT pulmonary findings were suggested; however, these should be clarified in a future prospective study.

5. Conclusions

We demonstrated that smoking history, fibrotic plus emphysema changes, and pleural effusion were correlated with the prevalence of LC. Future studies are warranted to examine the utility of LDCT screening for subjects with AE to improve the prognosis of LC.

Conflict of interest

None.

Funding

This research was funded by the Ministry of Health, Labour, and Welfare of Japan. It is one of the research and development dissemination projects related to the nine fields of occupational injuries and illnesses of the Japan Health, Labour, and Welfare Organization.

Role of the funding source

The sponsors had no involvement in the study design; collection, analysis, and interpretation of the data; writing of the manuscript; or

the decision to submit the manuscript for publication.

Acknowledgements

The authors would like to thank all the participants in this study.

References

[1] L. Stayner, L.S. Welch, R. Lemen, The worldwide pandemic of asbestos-related diseases, Annu. Rev. Public Health 34 (2013) 205–216.
[2] N. Fujimoto, K. Gemba, K. Aoe, K. Kato, T. Yokoyama, I. Usami, K. Onishi, K. Mizuhashi, T. Yusa, T. Kishimoto, Clinical investigation of benign asbestos pleural effusion, Pulm. Med. (2015) 416179, http://dx.doi.org/10.1155/2015/416179.
[3] Asbestos, asbestosis, and cancer: the Helsinki criteria for diagnosis and attribution, Scand. J. Work Environ. Health 23 (1997) 311–316.
[4] G. Hillerdal, Pleural plaques and risk for bronchial carcinoma and mesothelioma. A prospective study, Chest 105 (1994) 144–150.
[5] K. Gemba, N. Fujimoto, K. Kato, K. Aoe, Y. Takeshima, K. Inai, T. Kishimoto, National survey of malignant mesothelioma and asbestos exposure in Japan, Cancer Sci. 103 (2012) 483–490.
[6] P.M. Marcus, E.J. Bergstralh, R.M. Fagerstrom, D.E. Williams, R. Fontana, W.F. Taylor, P.C. Prorok, Lung cancer mortality in the Mayo Lung Project: impact of extended follow-up, J. Natl. Cancer Inst. 92 (2000) 1308–1316.
[7] D.R. Aberle, A.M. Adams, C.D. Berg, W.C. Black, J.D. Clapp, R.M. Fagerstrom, I.F. Gareen, C. Gatsonis, P.M. Marcus, J.D. Sicks, National lung screening trial research team, reduced lung-cancer mortality with low-dose computed tomographic screening, N. Engl. J. Med. 365 (2011) 395–409.
[8] D.P. Naidich, C.H. Marshall, C. Gribbin, R.S. Arams, D.I. McCauley, Low-dose CT of the lungs: preliminary observations, Radiology 175 (1990) 729–731.
[9] V.P. Doria-Rose, E. Szabo, Screening and prevention of lung cancer, in: K.H. Kernstine, K. Reckamp (Eds.), Lung Cancer: A Multidisciplinary Approach to Diagnosis and Management, Demos Medical Publishing, New York, 2010, pp. 53–72.
[10] S. Sone, S. Takashima, F. Li, Z. Yang, T. Honda, Y. Maruyama, M. Hasegawa, T. Yamanda, K. Kubo, K. Hanamura, K. Asakura, Mass screening for lung cancer with mobile spiral computed tomography scanner, Lancet 351 (1998) 1242–1245.
[11] M. Kaneko, K. Eguchi, H. Ohmatsu, R. Kakinuma, T. Naruke, K. Suemasu, N. Moriyama, Peripheral lung cancer: screening and detection with low-dose spiral CT versus radiography, Radiology 201 (1996) 798–802.
[12] C.I. Henschke, D.I. McCauley, D.F. Yankelevitz, D.P. Naidich, G. McGuinness, O.S. Miettinen, D.M. Libby, M.W. Pasmantier, J. Koizumi, N.K. Altorki, J.P. Smith, Early Lung Cancer Action Project: overall design and findings from baseline screening, Lancet 354 (1999) 99–105.
[13] H.C. Roberts, D.A. Patsios, N.S. Paul, M. DePerrot, W. Teel, H. Bayanati, F. Shepherd, M.R. Johnston, Screening for malignant pleural mesothelioma and lung cancer in individuals with a history of asbestos exposure, J. Thorac. Oncol. 4 (2009) 620–628.
[14] T. Vierikko, R. Jarvenpaa, T. Autti, P. Oksa, M. Huuskonen, S. Kaleva, J. Laurikka, S. Kajander, K. Paakkola, S. Saarelainen, E.R. Salomaa, A. Tossavainen, P. Tukiainen, J. Uitti, T. Vehmas, Chest CT screening of asbestos-exposed workers: lung lesions and incidental findings, Eur. Respir. J. 29 (2007) 78–84.
[15] G. Mastrangelo, M.N. Ballarin, E. Bellini, R. Bizzotto, F. Zannol, F. Gioffre, M. Gobbi, G. Tessadri, L. Marchiori, G. Marangi, S. Bozzolan, J.H. Lange, F. Valentini, P. Spolaore, Feasibility of a screening programme for lung cancer in former asbestos workers, Occup. Med. (Lond.) 58 (2008) 175–180.
[16] C. Paris, A. Martin, M. Letourneux, P. Wild, Modelling prevalence and incidence of fibrosis and pleural plaques in asbestos-exposed populations for screening and follow-up: a cross-sectional study, Environ. Health 7 (2008) 30.
[17] G. Fasola, O. Belvedere, M. Aita, T. Zanin, A. Follador, P. Cassetti, S. Meduri, V. Pangher, G. Pignata, V. Rosolen, F. Barbone, F. Grossi, Low-dose computed tomography screening for lung cancer and pleural mesothelioma in an asbestos-exposed population: baseline results of a prospective, nonrandomized feasibility trial—an Alpe-adria Thoracic Oncology Multidisciplinary Group Study (ATOM 002), Oncologist 12 (2007) 1215–1224.
[18] M. Remy-Jardin, A. Sobaszek, A. Duhamel, I. Mastora, C. Zanetti, J. Remy, Asbestos-related pleuropulmonary diseases: evaluation with low-dose four-detector row spiral CT, Radiology 233 (2004) 182–190.
[19] M. Das, G. Muhlenbruch, A.H. Mahnken, K.G. Hering, H. Sirbu, W. Zschiesche, L. Knol, M.K. Felten, T. Kraus, R.W. Gunther, J.E. Wildberger, Asbestos Surveillance Program Aachen (ASPA): initial results from baseline screening for lung cancer in asbestos-exposed high-risk individuals using low-dose multidetector-row CT, Eur. Radiol. 17 (2007) 1193–1199.
[20] M. Akira, S. Yamamoto, Y. Inoue, M. Sakatani, High-resolution CT of asbestosis and idiopathic pulmonary fibrosis, AJR Am. J. Roentgenol. 181 (2003) 163–169.
[21] M. Remy-Jardin, J. Remy, B. Gosselin, V. Becette, J.L. Edme, Lung parenchymal changes secondary to cigarette smoking: pathologic-CT correlations, Radiology 186 (1993) 643–651.
[22] K. Gemba, N. Fujimoto, K. Aoe, K. Kato, Y. Takeshima, K. Inai, T. Kishimoto, Treatment and survival analyses of malignant mesothelioma in Japan, Acta Oncol. 52 (2013) 803–808.

Nagamatsu et al. BMC Cancer (2018) 18:350
https://doi.org/10.1186/s12885-018-4293-x

BMC Cancer

RESEARCH ARTICLE Open Access

Quality of life of survivors of malignant pleural mesothelioma in Japan: a cross sectional study

Yasuko Nagamatsu[1], Isao Oze[2], Keisuke Aoe[3], Katsuyuki Hotta[4], Katsuya Kato[5], Junko Nakagawa[6], Keiko Hara[6], Takumi Kishimoto[7] and Nobukazu Fujimoto[8*]

Abstract

Background: Previous studies have indicated that people with malignant pleural mesothelioma (MPM) have a poor quality of life (QOL); however, information about the QOL of people with MPM in Japan is anecdotal. The aims of this study were to investigate the QOL of survivors of MPM in Japan and to determine the factors that correlate with their QOL.

Methods: This was a cross sectional study. The included patients were those diagnosed with MPM in Japan. We created a self-administered questionnaire consisting of 64 questions. The questionnaires were sent to hospitals and patient advocacy groups, distributed to the patients, completed, and sent back to the researchers by postal mail. QOL was assessed with the European Organization for Research and Treatment of Cancer 16 questionnaire (QLQ) and the short version of the core domains of the Comprehensive Quality of Life Outcome questionnaire (CoQoLo).

Results: In total, 133 questionnaires were collected. The QLQ assessments demonstrated that the survivors of MPM most frequently complained of fatigue, pain, sleep disturbances, and dyspnea. The symptom scales were acceptable, but the functional scales were significantly poorer for the patients with poor performance statuses (PSs). The short CoQoLo assessment was very unfavorable for 'Being free from physical pain.' Being a long-term survivor and a survivor with a poor PS were significantly correlated with poor global health status.

Conclusions: Survivors of MPM have impaired function, a variety of symptoms, and lower QOL. Survivors of MPM, even those in good physical condition, need broad support.

Keywords: Asbestos, CoQoLo, Mesothelioma, Palliative care, Quality of life, Questionnaire

Background

The World Health Organization (WHO) reported that 107,000 people die from occupational exposure to asbestos each year, and the WHO advocates for the elimination of asbestos-related diseases [1, 2]. Mesothelioma is a rare malignancy caused by asbestos exposure that affects the pleura, peritoneum, and pericardium [3]. Malignant pleural mesothelioma (MPM), which is the most common mesothelioma, is almost always fatal [4]. The overall median survival time and 2-year survival rate of patients with resectable disease, who have undergone trimodal treatment composed of induction chemotherapy followed by extrapleural pneumonectomy and postoperative radiation therapy, are 19.9 months and 42.9%, respectively [5], and the median overall survival of patients with advanced surgically unresectable disease who received cisplatin and pemetrexed is approximately 12 months [6]. Additionally, MPM causes debilitating physical symptoms, such as pain, dyspnea, fatigue, and loss of appetite [7, 8]. The British Thoracic Society Standards of Care Committee recommends that palliative care and symptom control be central to any management plan for mesothelioma patients [9]. Recently, maintaining patients' quality of life (QOL) has become more important in the treatment of MPM because of its poor prognosis. The Australian guidelines were

* Correspondence: nobufujimot@gmail.com
[8]Department of Medical Oncology, Okayama Rosai Hospital, 1-10-25 Chikkomidorimachi, Okayama 7028055, Japan
Full list of author information is available at the end of the article

developed by employing questions about the QOL of the patient, interventions, comparisons, and outcomes [4]. The QOL has been assessed in studies of treatments for MPM, such as chemotherapy [10], pleurectomy [11], and extrapleural pneumonectomy [12]. There are previous reports that MPM impairs the QOL of patients and their care givers [13, 14]. Kao et al. reported that health-related QOL is associated with survival in MPM patients [15].

Japan is one of the world's largest importers and users of asbestos [16, 17], and the number of deaths due to MPM reached 1500 in 2015 [18]. A total of 100,000 deaths are expected in Japan in the next 40 years [19]. Previous research has demonstrated that patients with MPM in Japan exhibit different care needs in the different stages of the disease. A previous study reported a lack of information about their disease and treatment options upon diagnosis, pain and deteriorated physical condition after extrapleural pneumonectomy, uncomfortable symptoms from chemotherapy, shock of the recurrence of the disease, uncontrolled symptoms in the terminal stage, anxiety and anger about developing disease due to asbestos, and burden of legal procedures in all stages [20]. Nurses who care for patients with MPM also experienced difficulties, such as struggling with care, failure to introduce palliative care, limited support for patients with decision making, difficulty in dealing with families, unsuccessful communication, and emotional distress after being with patients with MPM [21]. Previous studies indicate that people with MPM have a poor QOL. Moore et al. reported that support groups can provide an important source of information and support for patients with MPM and their family members [22]. However, information about the QOL of people with MPM in Japan is anecdotal.

This study investigated the QOL of patients with MPM in Japan and determined factors that correlated with their QOL.

Methods

Study design

This was a cross-sectional study. The inclusion criteria were 1) patients who were diagnosed with MPM and 2) those who could respond to self-administered questionnaires written in Japanese. No exclusion criteria were applied. A request for cooperation was sent to all hospitals designated to promote quality oncologic care by the Japanese Ministry of Health and Welfare. Based on their agreements, the questionnaires were sent to the hospitals and distributed to patients with MPM. Questionnaires were also sent to 15 branches of a patient advocacy group (Patients and Family Support Group in Japan) for distribution to survivors of MPM. Completed questionnaires were returned to the researchers by postal mail.

QOL assessment

A self-administered questionnaire was developed that consisted of 64 questions about QOL and collected information about the patients' age, gender, duration of their disease, and treatments received. The questionnaire also asked whether the patient had received worker's compensation or support from the asbestos-related health damage relief system and whether the patient had contact with a patient advocacy group. QOL was assessed with the European Organization for Research and Treatment of Cancer questionnaire (EORTC-QLQ C30; QLQ) [23] and the short version of the core domains of the Comprehensive Quality of Life Outcome questionnaire (CoQoLo) [24]. These measures were included in the distributed questionnaire.

The QLQ is a validated, patient-rated, core questionnaire for assessing the health-related QOL of cancer patients. The questionnaire incorporates 5 functional scales (physical, role, cognitive, emotional, and social), symptom scales (fatigue, pain, and nausea and vomiting), a global health and QOL scale, and single items for assessing additional symptoms commonly reported by cancer patients (i.e., dyspnea, loss of appetite, sleep disturbances, constipation, and diarrhea) as well as the perceived functional influence of the disease and its treatment. All items are scored on a 4-point Likert scale (1 = not at all, 2 = a little, 3 = quite a bit, 4 = very much) except for the global health and QOL scale, which uses a modified 7-point linear analog scale (from 1 = very poor to 7 = excellent). The scores for each scale and single-item measures were averaged and linearly transformed into a score ranging from 0 to 100. A high score for the Global Health Status/QOL represents health-related QOL, whereas high scores for the functional and symptom scales and single items represent worse functional ability or significant symptomatology.

The CoQoLo consists of 10 subscales and 28 items and has been validated for Japanese cancer patients. The CoQoLo assesses the QOL of patients with advanced cancer in the terminal stage to support a 'good death' based on the patient's perspective [24]. In the current study, we applied the short version of the CoQoLo (short CoQoLo) to minimize the burden on participants. The short CoQoLo includes the following 10 items that assess physical and psychological comfort: staying in the patient's favorite place, maintaining hope and pleasure, good relationships with the medical staff, not being a burden to others, good relationships with family, independence, environmental comfort, being respected as an individual, and having a fulfilling life. These items were

answered on a 7-point Likert scale (from 1 = completely disagree to 7 = completely agree).

Statistical analysis

The scores on the QLQ were calculated using a previously described scoring procedure [25]. The Likert scales for each item on the short CoQoLo were used to score each item. A multiple regression analysis was assessed to estimate the correlations between the QOL scores and the clinical and social factors that potentially affected the factors for the QOL scores. Age was categorized as less than 60 years, 60–69 years, 70–79 years, and 80 years or older. Sex, receiving surgery, receiving chemotherapy, receiving radiotherapy, receiving supportive care, receiving compensation, and membership in an advocacy group were treated as dichotomous variables. The years from diagnosis were divided into categories of less than 2 years and two or more years. A p value less than 0.05 was considered statistically significant. The statistical analyses were performed using STATA version 14.2 (STATA corporation, College Station, TX, USA).

Results

Collection of questionnaires

Requests for cooperation were sent to 422 cancer hospitals, and 64 (15.2%) agreed to participate. The main reason for nonparticipation was the absence of patients with MPM. In February 2016, 438 questionnaires were distributed throughout the hospitals to patients with MPM. By the end of April 2016, 88 patients had returned the questionnaires to the researchers by postal mail. Additionally, 94 questionnaires were mailed to survivors of MPM through a patient advocacy group in March 2016. Among these, 45 (47.9%) were returned. In total, 133 questionnaires were collected.

Characteristics of the participants

The characteristics of the participants are presented in Table 1. Overall, 83.5% were male, and the mean age was 69.3 years. The mean (± standard deviation) duration of MPM was 31.0 (± 43.6) months, 55.6% of the patients had undergone surgery, 83.5% had received chemotherapy, 28.6% had received radiotherapy, and 45.9% had received palliative care. Either worker's compensation or assistance from the asbestos-related health damage relief system was received by 74.4%, and 36.8% were members of a patient advocacy group.

Table 1 Sociodemographics of the participants

	N (133)	Percent
Sex		
Male	111	83.5
Female	22	16.5
Age		
≤ 59	17	12.8
60–69	56	42.1
70–79	47	35.3
≥ 80	13	9.8
Duration of disease (months)		
0–11	49	36.8
12–23	35	26.3
24–35	17	12.8
36–47	6	4.5
48–60	6	4.5
≥ 61	20	15.0
Performance status		
0	19	14.3
1	66	49.6
2	21	15.8
3	25	18.8
4	2	1.5
Received treatment	0	0
Surgery	57	55.6
Extra pleural pneumonectomy	31	
Pleurectomy decortication	23	
Unknown	3	
Chemotherapy	111	83.5
Radiotherapy	38	28.6
Palliative Care	61	45.9
Compensated (there is some overlap)	99	74.4
Workmen's accident compensation insurance	58	
The asbestos-related health damage relief system	61	
Patient and family support group membership	49	36.8

QOL assessment in MPM survivors

The QOL scores are presented in Table 2. The mean global QOL score was 47.9, and the mean scores for the 5 functional scales, i.e., physical, role, cognitive, emotional, and social function, were 64.4, 54.1, 64.5, 70.1, and 67.0, respectively. Regarding the symptom scales, the mean scores for fatigue, pain, nausea and vomiting, dyspnea, appetite loss, sleep disturbance, constipation and diarrhea were 50.8, 34.7, 12.9, 50.1, 38.3, 36.1, 38.1, and 14.8, respectively. The scores on the symptom scales and functional scales were significantly worse among those with poor performance statuses (PSs).

The results of the short CoQoLo assessment revealed favorable scores for 'Trusting physician' (5.8), 'Being dependent in daily activities' (5.4), 'Being valued as a person' (5.4), 'Being able to stay at one's favorite place' (5.3), and 'Spending enough time with one's family' (5.0). The scores were not very favorable

Table 2 Quality of life scores of the survivors with MPM

EORTC QLQ C-30	Mean	SD	Short CoQoLo	Mean	SD
Global QOL	47.9	24.9	Total score	48.9	9.7
Physical functioning	64.4	25.8	Being free from physical pain	3.8	1.9
Role functioning	54.1	30.3	Being able to stay at one's favorite place	5.3	1.4
Emotional functioning	70.1	24.8	Having some pleasure in daily life	4.4	1.7
Cognitive functioning	64.5	25.7	Trusting physician	5.8	1.5
Social functioning	67.0	28	Feeling like the cause of trouble for others	4.0	1.8
Fatigue	50.8	26.4	Spending enough time with one's family	5.0	1.6
Nausea & Vomiting	12.9	21.7	Being dependent in daily activities	5.4	1.6
Pain	34.7	29.0	Living in calm circumstances	5.4	1.4
Dyspnea	50.1	29.0	Being valued as a person	5.4	1.3
Insomnia	36.1	30.9	Feeling that one's life was complete	4.4	1.7
Appetite loss	38.3	34.7			
Constipation	38.1	34.6			
Diarrhea	14.8	23.0			
Financial difficulties	33.1	31.9			

for 'Having some pleasure in daily life' (4.4), 'Feeling that one's life was complete' (4.4), 'Feeling like the cause of trouble for others' (4.0), and 'Being free from physical pain' (3.8). The mean total score across the 10 items was 48.9.

Clinical factors correlated with QOL

The correlations between the QOL scores and the clinical factors are presented in Table 3. The score for the global health status on the QLQ among female survivors was 10.89 points higher than that among males. Long-term survivors (≥ 2 years from diagnosis) and survivors with poor PSs were significantly correlated with poor global health status. The total score on the core domain of the short CoQoLo was also significantly lower among the long-term survivors and survivors with poor PSs.

Discussion

In this cross-sectional study, we intended to clarify the QOL of survivors with MPM at various stages of their disease, including diagnosis and during and after cancer treatment. To our knowledge, this is the first study in Japan to focus on the assessment of QOL of patients with MPM and to include a considerable number of long-term survivors.

The QLQ assessment in the current study indicated that emotional function and social function were relatively impaired in survivors of MPM, and the survivors complained more frequently of fatigue and dyspnea. Arber et al. reported that patients with MPM receive insufficient psychosocial support at the time of the diagnosis [26]. Previous reports on the QOL of patients with MPM during systemic chemotherapy revealed impairments on QOL scales that were similar to the results reported here [10]. Another study that included patients with MPM who were treated with either chemotherapy or best supportive care produced consistent impairments of QOL [27]. Although the current study included subjects with poorer PSs, the results are quite similar to those of the previous studies and support the notion that patients with MPM experience diverse, overlapping symptoms that are often difficult to control [21, 28]. The QLQ scores reported in the current study were similar to those reported in previous studies of patients with MPM in other countries [10, 11].

The short CoQoLo assessment revealed relatively favorable scores concerning items such as 'Trusting physician', 'Being dependent in daily activities', 'Being valued as a person', 'Being able to stay at one's favorite place', and 'Spending enough time with one's family'. However, the score for 'Being free from physical pain' was not favorable, which suggests that pain is an important element of QOL in patients with MPM.

The results of the multiple regression analysis of the QLQ indicated that a longer duration from diagnosis and a poor PS were factors correlated with impaired QOL. The results of multivariate regression analysis of the short CoQoLo scores also indicated that impaired QOL was correlated with poor PS and a longer duration from the diagnosis. A better QOL in patients with better PSs has been widely reported in previous studies [10, 11, 29]. The current study includes a considerable number of people who had survived for more than 2 years. We speculate that MPM can be cured in only a few cases; therefore, a

Table 3 Multiple regression analysis of the QLQ-C30 and CoQoLo scores

	QLQ-C30; Global health status			CoQoLo; Core domain total		
	Coefficient	95% CI	*p*-value	Coefficient	95% CI	*p*-value
Age at survey						
−59	0			0		
60–69	−3.08	−14.48, 8.33	0.594	2.44	−2.69, 7.56	0.348
70–79	−4.55	−16.52, 7.43	0.454	2.25	−3.13, 7.63	0.409
80-	1.10	−14.83, 17.03	0.891	4.97	− 2.19, 12.13	0.172
Sex						
Male	0			0		
Female	10.89	1.30, 20.48	0.026	4.03	−0.28, 8.34	0.067
Years from diagnosis						
< 2	0			0		
≥ 2	−10.36	−18.53, −2.19	0.011	−4.73	−8.40, − 1.06	0.012
Treatment						
Surgery						
(−)	0			0		
(+)	4.99	−3.30, 13.27	0.235	1.10	−2.62, 4.82	0.558
Chemotherapy						
(−)	0			0		
(+)	−5.75	−15.50, 4.00	0.245	0.65	−3.73, 5.04	0.768
Radiation						
(−)	0			0		
(+)	1.25	−2.56, 5.06	0.65	1.25	−2.56, 5.06	0.65
Palliative care						
(−)	0			0		
(+)	−2.63	−5.93, 0.66	0.116	−2.63	−5.92, 0.66	0.116
Performance Status						
0	0			0		
1	−16.55	−27.26, −5.84	0.003	−3.54	−8.36, 1.26	0.147
2	−34.49	−47.69, −21.28	0.000	−7.64	−13.57, − 1.71	0.012
3	−40.97	−53.78, −28.15	0.000	−11.42	−17.18, − 5.67	0.000
4	−73.01	− 102.99, − 43.02	0.000	−24.09	− 37.56, −10.62	0.001
Compensation						
Not approved	0			0		
Approved	5.86	−2.98, 14.70	0.192	1.75	−2.22, 5.72	0.385
Patient advocacy group						
Non-member	0			0		
Member	0.97	−7.47, 9.41	0.821	0.15	−3.64, 3.95	0.936

prolonged clinical course would result in more severe and continuous struggles with the disease.

Several studies have been performed from a qualitative perspective, focusing on the MPM patient's perspective, suggesting that patients living with MPM undergo a traumatic shock and a "Damocles' syndrome" characterized by intense fears of death and anxiety along with the awareness of the absence of effective treatments [30]. There are other studies performed with semi-structured interviews, those seem to suggest that the reduced QOL of these cancer patients is strictly related with the severity of symptoms, the poor prognosis, along with the awareness of the "unnatural" origin of MPM, the ethical issues connected to the human responsibilities in the

contamination, and intense worries for the beloved ones who will survive [14, 26, 31, 32]. From a clinical point of view of the subjective experience of patients living with the disease, specific tailored psychological interventions should be developed in the understanding of the in-depth psychological functioning of these patients.

This study has some limitations. First, the current study included a small convenience sample. We recruited as many patients as possible from the hospitals that provide oncological care and through a patient advocacy group in Japan. Our results may not be representative of the general population of patients with MPM; however, our participants may at least be representative of survivors to a certain extent. Second, our participants had a relatively longer duration of disease, had received surgery, chemotherapy, and/or palliative care, and had better PSs. The data from the patients in the terminal stage and from those with poor general conditions may have been missed due mainly to the difficulty of accessing such people. The QOL of our participants might be better than those of the general population of patients with MPM, which indicates that the QOL of patients with MPM on site may be more impaired. Finally, this study was a cross-sectional study of prevalent cases. A longitudinal study of incident cases is warranted to identify the factors that affect the QOL of incident cases of MPM and to develop systems for the desired support and care.

Conclusions

Survivors of MPM have impaired function, experience a variety of symptoms, and have a lower QOL. The duration of disease and a poor PS correlated with impaired QOL. Survivors of MPM, even those in good physical condition, need broader support.

Abbreviations

CoQoLo: Comprehensive quality of life outcome; EORTC: European Organization for Research and Treatment of Cancer; MPM: Malignant pleural mesothelioma; PS: Performance status; QOL: Quality of life; WHO: World Health Organization

Acknowledgements

We thank Ms. Riwa Koni for her support as a liaison nurse.

Funding

This study was supported by the Research and Development and the Dissemination of Projects Related to the Nine Fields of Occupational Injuries and Illnesses of the Japan Labour Health and Welfare Organization. This work is also supported by grants-in-aid from the Ministry of Health, Labor and Welfare, Japan.

Availability of data and materials

The datasets used and analyzed in the current study are available from the corresponding author on reasonable request.

Authors' contributions

YN and IO made substantial contributions to the conception and design; YN, KA, JN, and KH made substantial contributions to the acquisition of the data; YN, IO, KA, KH, KK, and TK made substantial contributions to the analysis and interpretation of the data; YN and NF were involved in drafting the manuscript; and NF provided the final approval of the version to be published. All authors read and approved the final manuscript.

Ethics approval and consent to participate

This study was approved by the institutional review board of Okayama Rosai Hospital (approval no. 2017–22). This study was also approved by the institutional review board of each hospital or institution that distributed the questionnaire to their patients according to their policy. The study was conducted based on the ethical principles of avoiding harm, voluntary participation, anonymity, and protection of privacy and personal information. The purpose, procedures, and confidentiality of the study were explained in written format. The participants were informed that nonparticipation would not disadvantage them. Return of the answered questionnaire was considered to constitute the patient's consent.

Consent for publication

Not applicable.

Competing interests

The authors declare that they have no competing interests.

Publisher's Note

Springer Nature remains neutral with regard to jurisdictional claims in published maps and institutional affiliations.

Author details

[1]Graduate School of Nursing Science, St. Luke's International University, 10-1 Akashicho, Chuo-ku, Tokyo 1040044, Japan. [2]Division of Molecular and Clinical Epidemiology, Aichi Cancer Center Research Institute, 1-1 Kanokoden, Chigusa-ku, Nagoya 4648681, Japan. [3]National Hospital Organization Yamaguchi-Ube Medical Center, Department of Medical Oncology, 685 Higashikiwa, Ube 7550241, Japan. [4]Center for Innovative Clinical Medicine, Okayama University Hospital, 2-5-1 Shikatacho, Okayama 7008558, Japan. [5]Department of Radiology, Kawasaki General Medical Center, 2-6-1 Nakasange, Okayama 7008505, Japan. [6]Department of Nursing, Okayama Rosai Hospital, 1-10-25 Chikkomidorimachi, Okayama 7028055, Japan. [7]Department of Medicine, Okayama Rosai Hospital, 1-10-25 Chikkomidorimachi, Okayama 7028055, Japan. [8]Department of Medical Oncology, Okayama Rosai Hospital, 1-10-25 Chikkomidorimachi, Okayama 7028055, Japan.

Received: 17 October 2017 Accepted: 22 March 2018
Published online: 27 March 2018

References

1. World Health Organization. Chrysotile asbestos. 2014. www.who.int/ipcs/assessment/.../chrysotile_asbestos_summary.pdf
2. World Health Organization. Elimination of asbestos-related diseases. 2006. whqlibdoc.who.int/hq/2006/WHO_SDE_OEH_06.03_eng.pdf.
3. Kao SC, Reid G, Lee K, Vardy J, Clarke S, van Zandwijk N. Malignant mesothelioma. Intern Med J. 2010;40:742–50.
4. van Zandwijk N, Clarke C, Henderson D, Musk AW, Fong K, Nowak A, et al. Guidelines for the diagnosis and treatment of malignant pleural mesothelioma. J Thorac Dis. 2013;5:254–307.
5. Hasegawa S, Okada M, Tanaka F, Yamanaka T, Soejima T, Kamikonya N, et al. Trimodality strategy for treating malignant pleural mesothelioma: results of a feasibility study of induction pemetrexed plus cisplatin followed by extrapleural pneumonectomy and postoperative hemithoracic radiation (Japan mesothelioma interest group 0601 trial). Int J Clin Oncol. 2016;21:523–30.
6. Vogelzang NJ, Rusthoven JJ, Symanowski J, Denham C, Kaukel E, Ruffie P, et al. Phase III study of pemetrexed in combination with cisplatin versus cisplatin alone in patients with malignant pleural mesothelioma. J Clin Oncol. 2003;21:2636–44.
7. Bibby AC, Tsim S, Kanellakis N, Ball H, Talbot DC, Blyth KG, et al. Malignant pleural mesothelioma: an update on investigation, diagnosis and treatment. Eur Respir Rev. 2016;25:472–86.
8. Mercadante S, Degiovanni D, Casuccio A. Symptom burden in mesothelioma patients admitted to home palliative care. Curr Med Res Opin. 2016;32:1985–8.

9. British Thoracic Society Standards of Care Committee. BTS statement on malignant mesothelioma in the UK, 2007. Thorax. 2007;62(Suppl 2):ii1–ii19.
10. Nowak AK, Stockler MR, Byrne MJ. Assessing quality of life during chemotherapy for pleural mesothelioma: feasibility, validity, and results of using the European Organization for Research and Treatment of Cancer Core quality of life questionnaire and lung Cancer module. J Clin Oncol. 2004;22:3172–80.
11. Mollberg NM, Vigneswaran Y, Kindler HL, Warnes C, Salgia R, Husain AN, et al. Quality of life after radical pleurectomy decortication for malignant pleural mesothelioma. Ann Thorac Surg. 2012;94:1086–92.
12. Rena O, Casadio C. Extrapleural pneumonectomy for early stage malignant pleural mesothelioma: a harmful procedure. Lung Cancer. 2012;77:151–5.
13. Granieri A, Tamburello S, Tamburello A, Casale S, Cont C, Guglielmucci F, et al. Quality of life and personality traits in patients with malignant pleural mesothelioma and their first-degree caregivers. Neuropsychiatr Dis Treat. 2013;9:1193–202.
14. Guglielmucci F, Franzoi IG, Bonafede M, Borgogno FV, Grosso F, Granieri A. "the less I think about it, the better I feel": a thematic analysis of the subjective experience of malignant mesothelioma patients and their caregivers. Front Psychol. 2018;9:205.
15. Kao SC, Vardy J, Harvie R, Chatfield M, van Zandwijk N, Clarke S, et al. Health-related quality of life and inflammatory markers in malignant pleural mesothelioma. Support Care Cancer. 2013;21:697–705.
16. Furuya S, Takahashi K, Movahed M, Jiang Y. National asbestos profile of Japan based on the national asbestos profile by the ILO and the WHO. 2013. http://envepi.med.uoeh-u.ac.jp/NAPJ.pdf
17. Furuya S, Takahashi K. Experience of Japan in achieving a total ban on asbestos. Int J Environ Res Public Health. 2017;14:1261. https://doi.org/10.3390/ijerph14101261.
18. Ministry of Health, Labour and Welfare, Japan. Vital statistics in Japan. 2016. http://www.mhlw.go.jp/toukei/saikin/hw/jinkou/tokusyu/chuuhisyu15/dl/chuuhisyu.pdf (in Japanese).
19. Murayama T, Takahashi K, Natori Y, Kurumatani N. Estimation of future mortality from pleural malignant mesothelioma in Japan based on an age-cohort model. Am J Ind Med. 2006;49:1–7.
20. Nagamatsu Y, Horinouchi S, Natori Y. The stages and difficulties of patients with malignant pleural mesothelioma. J Hum Care Stud. 2012;12:69–81.
21. Nagamatsu Y, Horinouchi S, Natori Y. Difficulties faced by nurses in careing for patients with malignant pleural mesothelioma. J Hum Care Stud. 2012;13:1–13.
22. Moore S, Teehan C, Cornwall A, Ball K, Thomas J. 'Hands of Time': the experience of establishing a support group for people affected by mesothelioma. Eur J Cancer Care (Engl). 2008;17:585–92.
23. Aaronson NK, Ahmedzai S, Bergman B, Bullinger M, Cull A, Duez NJ, et al. The European Organization for Research and Treatment of Cancer QLQ-C30: a quality-of-life instrument for use in international clinical trials in oncology. J Natl Cancer Inst. 1993;85:365–76.
24. Miyashita M, Wada M, Morita T, Ishida M, Onishi H, Tsuneto S, et al. Development and validation of the comprehensive quality of life outcome (CoQoLo) inventory for patients with advanced cancer. BMJ Support Palliat Care. 2015; https://doi.org/10.1136/bmjspcare-2014-000725.
25. Fayers PM, Aaronson NK, Bjordal K, Groenvold M, Curran D, Bottomley A, on behalf of the EORTC Quality of Life Group. EORTC QLQ-C30 Scoring Manual (3rd edition). 2001. https://wiki.nci.nih.gov/download/.../EORTC_QLQ_C30%20_scoring_Manual.pdf
26. Arber A, Spencer L. It's all bad news': the first 3 months following a diagnosis of malignant pleural mesothelioma. Psychooncology. 2013;22:1528–33.
27. Arnold DT, Hooper CE, Morley A, White P, Lyburn ID, Searle J, et al. The effect of chemotherapy on health-related quality of life in mesothelioma: results from the SWAMP trial. Br J Cancer. 2015;112:1183–9.
28. Wood H, Connors S, Dogan S, Peel T. Individual experiences and impacts of a physiotherapist-led, non-pharmacological breathlessness programme for patients with intrathoracic malignancy: a qualitative study. Palliat Med. 2013;27:499–507.
29. Moore A, Parker RJ, Wiggings J. Malignant mesothelioma. Orphanet J Rare Dis. 2008;3:34.
30. Clayson H, Seymour J, Noble B. Mesothelioma from the patient's perspective. Hematol Oncol Clin North Am. 2005;19:1175–90. viii
31. Hughes N, Arber A. The lived experience of patients with pleural mesothelioma. Int J Palliat Nurs. 2008;14:66–71.
32. Guglielmucci F, Franzoi IG, Barbasio CP, Borgogno FV, Granieri A. Helping traumatized people survive: a psychoanalytic intervention in a contaminated site. Front Psychol. 2014;5:1419.

Current Trial Report

A Phase II Trial of First-Line Combination Chemotherapy With Cisplatin, Pemetrexed, and Nivolumab for Unresectable Malignant Pleural Mesothelioma: A Study Protocol

Nobukazu Fujimoto,[1] Keisuke Aoe,[2] Toshiyuki Kozuki,[3] Isao Oze,[4] Katsuya Kato,[5] Takumi Kishimoto,[6] Katsuyuki Hotta[7]

Abstract

Background: The purpose of this study is to assess the efficacy and safety of combination chemotherapy with cisplatin, pemetrexed, and nivolumab for unresectable malignant pleural mesothelioma (MPM). **Patients and Methods:** Patients with untreated, advanced, or metastatic MPM who meet the inclusion and exclusion criteria will be included. A total of 18 patients will be enrolled from 4 Japanese institutions within 1 year. Combination chemotherapy with cisplatin (75 mg/m^2), pemetrexed (500 mg/m^2), and nivolumab (360 mg/person) is administered every 3 weeks for a total of 4 to 6 cycles. Then, maintenance therapy with nivolumab will be administered until disease progression, unacceptable toxicities, or the patient's condition meets the withdrawal criteria. The primary end point is the centrally reviewed overall response rate. The secondary end points include the disease control rate, overall survival, progression-free survival, and adverse events. **Conclusion:** This phase II trial evaluating first-line combination chemotherapy for unresectable MPM commenced in January 2018. This is the first prospective trial to evaluate the effect of an anti-programmed death-1 antibody combined with cisplatin and pemetrexed for unresectable MPM.

Clinical Lung Cancer, Vol. ■, No. ■, ■-■

Keywords: Asbestos, Immune checkpoint inhibitor, Maintenance, Programmed death-1, Prospective study

Introduction

Malignant pleural mesothelioma (MPM) is a highly aggressive tumor that arises from mesothelial-lined surfaces and has a poor survival rate.[1] MPM occurs more frequently in men (80%) than in women, and the peak age of onset is between 60 and 80 years old.[2] The industrial use of asbestos has been banned in Japan since 2006, but the incidence of MPM is expected to continue to increase for the next few decades because of the past usage of asbestos.[3] Treatment of MPM is challenging. Most of the cases are diagnosed at an advanced stage and are treated with systemic chemotherapy. Combination chemotherapy with cisplatin and pemetrexed is the standard treatment regimen; however, the median overall survival (OS) is only approximately 12 .months.[4] Recently, the additional use of bevacizumab improved OS when used with cisplatin and pemetrexed in unresectable MPM.[5] However, the prolongation of the OS was <3 months. In addition, it can be administered only to bevacizumab-eligible patients. On the basis of these facts, cisplatin and pemetrexed is still considered the standard treatment regimen, thus, additional treatment options are urgently needed.

Nivolumab is a human monoclonal antibody that targets the programmed death (PD)-1 cluster of differentiation 279 cell surface membrane receptor. Binding of PD-1 to its ligands, PD ligands 1 and 2, results in the downregulation of lymphocyte activation.

This trial is registered in the UMIN Clinical Trials Registry: UMIN000030892.

[1]Department of Medical Oncology, Okayama Rosai Hospital, Okayama, Japan
[2]Department of Medical Oncology, National Hospital Organization Yamaguchi-Ube Medical Center, Ube, Japan
[3]Department of Thoracic Oncology, National Hospital Organization Shikoku Cancer Center, Matsuyama, Japan
[4]Division of Molecular and Clinical Epidemiology, Aichi Cancer Center Research Institute, Nagoya, Japan
[5]Department of Diagnostic Radiology 2, Kawasaki Medical School, Okayama, Japan
[6]Department of Medicine, Okayama Rosai Hospital, Okayama, Japan
[7]Center of Innovative Clinical Medicine, Okayama University Hospital, Okayama, Japan

Submitted: Mar 25, 2018; Revised: Apr 12, 2018; Accepted: May 1, 2018

Address for correspondence: Nobukazu Fujimoto, MD, PhD, Department of Medical Oncology, Okayama Rosai Hospital, 1-10-25 Chikkomidorimachi, Okayama 7028055, Japan
Fax: +81-86-2623391; e-mail contact: nobufujimot@gmail.com

https://doi.org/10.1016/j.cllc.2018.05.001

Figure 1 Overview of the Study Design

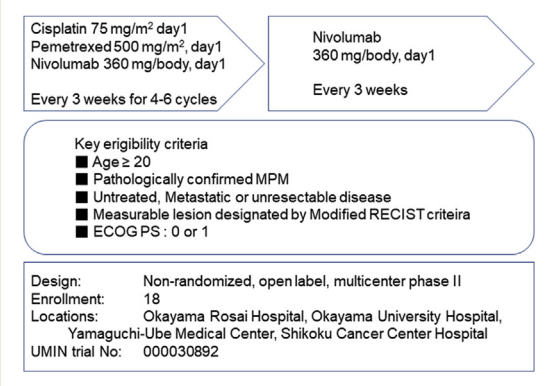

Abbreviations: ECOG = Eastern Cooperative Oncology Group; MPM = malignant pleural mesothelioma; PS = performance status; RECIST = Response Evaluation Criteria in Solid Tumors.

Nivolumab inhibits the interaction between PD-1 and its ligands, promotes immune responses, and triggers antitumor activity. It has already been approved by the Ministry of Health, Labor, and Welfare, Japan for multiple types of cancer including malignant melanoma, non−small-cell lung cancer, and gastric cancer in Japan. Additionally, a phase II trial showed there was a favorable response with nivolumab for previously treated MPM.[6]

A recent report indicated that platinum drugs enhance the effector immune response through modulation of PD-ligand 1.[7] These encouraging results might extend to the first-line treatment of MPM with the hope of enhancing the antitumor response, particularly in combination with the current standard chemotherapy. Unfortunately, no prospective clinical trial is being conducted to evaluate the combination of nivolumab and cisplatin/pemetrexed. Thus, we launched the current trial to assess combination chemotherapy with cisplatin, pemetrexed, and nivolumab for MPM.

Table 1 Key Inclusion Criteria

1. Age: older than 20 years at the date of informed consent
2. Pathologically-confirmed pleural malignant mesothelioma
3. Advanced or metastatic malignant pleural mesothelioma that is untreated and unresectable
4. Patients who have a measurable lesion designated according to modified RECIST criteria
5. Tumor sample available to test for programmed death-ligand 1 expression
6. Eastern Cooperative Oncology Group performance status is 0 or 1
7. Life expectancy is ≥90 days
8. Oxygen saturation measured using pulse oximeter is ≥94%
9. Meet the defined lab value criteria
10. Females of childbearing potential who agree to prevent pregnancy and lactation for at least 5 months after the last administration of nivolumab
11. Men who agree to contraception for at least 7 months after the last administration of nivolumab
12. Patients who understand the study contents and provide written consent by their own free will

Abbreviation: RECIST = Response Evaluation Criteria in Solid Tumors.

Table 2 Key Exclusion Criteria

1. History of anaphylaxis induced by any drug
2. Autoimmune disease
3. Double cancer
4. Metastasis to the brain or meninges
5. Interstitial lung disease or pulmonary fibrosis
6. Diverticulitis or peptic ulcer
7. Pleural effusion that requires drainage every 2 weeks or more
8. Pericardial effusion or ascites that requires drainage
9. Uncontrollable cancer pain
10. Transient ischemic attack, cerebrovascular accident, thrombosis, or thromboembolism within 180 days
11. Uncontrollable severe cardiovascular disease
12. Anticoagulant therapy
13. Uncontrollable diabetes
14. Receiving treatment for a systemic infection
15. Obviously positive for human immunodeficiency virus
16. HTLV-1 antibody-positive, HBs antigen-positive, or HCV antibody-positive. Either HBs antigen positive or HBc antibody-positive and HBV-DNA detection if HBs antigen is negative
17. History of treatment for T-cell regulation
18. Surgery with local or surface anesthesia within 14 days
19. Surgery with general anesthesia within 28 days
20. Pleurodesis within 14 days
21. Pleurodesis treated with picibanil within 28 days
22. Adhesion surgery of the pericardium or peritoneum
23. Radiation therapy for pain relief within 14 days
24. Radiopharmaceutical therapy within 56 days
25. Administration of unapproved drugs within 28 days or an unapproved antibody within 90 days
26. Administration of systemic adrenal cortical hormone or immunosuppressive agents
27. Women who are or might be pregnant or lactating
28. Patients who are incapable of giving consent (for example, because of dementia)
29. Any other inadequacy for this study

Abbreviations: HB = hepatitis B; HBV = hepatitis B virus; HCV = hepatitis C virus; HTLV = human T-cell leukemia virus.

Patients and Methods

Objectives/End Points

This study will assess the efficacy and safety of the first-line combination therapy of cisplatin, pemetrexed, and nivolumab for advanced or metastatic MPM. The primary end point is the centrally reviewed overall response rate. The secondary end points include efficacy evaluated according to the: (1) response rate assessed by investigators; (2) disease control rate; (3) OS; (4) progression-free survival; (5) duration of response; and (6) time to response. Safety and adverse events will also be evaluated.

Study Design/Study Setting

This is a single-arm, prospective, nonrandomized, noncomparative, open-label, multicenter, phase II trial. Figure 1 shows an overview of the study design.

Eligibility Criteria

All patients who meet the main inclusion and exclusion criteria (Tables 1 and 2) will be invited for screening. Written informed

consent must be obtained by an investigator from the patient before any screening or inclusion procedure. This study will be conducted in compliance with the principles of the Declaration of Helsinki, and the protocol was approved by the institutional review board of each of the participating hospitals.

Intervention

Treatment is composed of 2 sequential phases: the combination phase and the maintenance phase. In the former, cisplatin (75 mg/m^2), pemetrexed (500 mg/m^2), and nivolumab (360 mg/person) will be administered intravenously. Nivolumab was kindly provided by Ono Pharmaceutical Co, Ltd. This treatment will be repeated every 3 weeks with a total of 4 to 6 cycles. If patients have not progressed during the combination phase, maintenance therapy with nivolumab will be administered until disease progression, unacceptable toxicities, or the patient's condition meets the withdrawal criteria.

Nivolumab was administered at a dose of 240 mg/person biweekly in recent clinical trials[6,8] including the one for MPM that showed encouraging clinical utility and acceptable toxicity profile.[6] Both of cisplatin and pemetrexed are usually administered every 3 weeks. Under the consideration of practical utility and dose intensity, we planned to administer nivolumab every 3 weeks with the dose of 360 mg/person. The combination of nivolumab (10 mg/kg) and pemetrexed/cisplatin every 3 weeks showed an acceptable toxicity profile and encouraging antitumor activity in patients with advanced non−small-cell lung cancer.[9] On the basis of these findings, nivolumab will be administered at a dose of 360 mg/person, every 3 weeks, in the current study.

Outcome Measurement/Follow-up

Response is evaluated using the modified Response Evaluation Criteria in Solid Tumors.[10] The OS is defined as the duration from study registration until the date of death or the last patient visit.

Statistical Considerations

The target number of patients is 18 for the current phase II study. If we assume that there would be 6 to 12 patients with a response, the response rate would be 33.3% to 66.7%. In this case, the estimated accuracy indicates the range between the point estimate of the response rate and the lower confidence limit (2-sided 95% confidence coefficient on the basis of exact test) would be 18% to 22%. An OS curve will be constructed using the Kaplan−Meier product limit method.

Discussion

There is a medical need for improved treatments for MPM. This study is, to our knowledge, the first clinical trial to evaluate the effect of combining an immune checkpoint inhibitor and platinum-based chemotherapy for MPM. In addition, to our knowledge, this is the first investigator-initiated prospective clinical trial evaluating systemic chemotherapy for MPM that complies with Good Clinical Practice in Japan.

Conclusion

A phase II trial of first-line combination chemotherapy for unresectable MPM commenced in January 2018. This study is, to our knowledge, the first prospective trial to evaluate the effect of an anti−PD-1 antibody combined with cisplatin and pemetrexed for unresectable MPM.

Acknowledgments

This study is supported by a grant from Ono Pharmaceutical Co, Ltd, and also by grants-in-aid from the Ministry of Health, Labor, and Welfare, Japan. Nivolumab was kindly provided by Ono Pharmaceutical Co, Ltd.

Disclosure

Dr Fujimoto has received consultancy fees from Boehringer Ingelheim, Bristol-Myers Squibb, Kyorin, and Kissei, and received honoraria or research funding from Hisamitsu, Chugai, Ono, Taiho, Boehringer Ingelheim, Bristol-Myers Squibb, Novartis, GlaxoSmithKline, and MSD. Dr Aoe has received consultancy fees from Boehringer Ingelheim, Bristol-Myers Squibb, Ono, and received honoraria or research funding from Ono, Bristol-Myers Squibb, Novartis, MSD, AstraZeneca, and Eli Lilly. Dr Kozuki has received honoraria or research funding from Chugai, AstraZeneca, Eli Lilly, Pfizer, Ono, Boehringer Ingelheim, Bristol-Myers Squibb, Kyowa, Taiho, MSD, Merck, and Nippon Kayaku. Dr Hotta has received honoraria or research funding from AstraZeneca, Ono, Boehringer Ingelheim, Nippon Kayaku, Taiho, Chugai, Astellas, Novartis, Bristol-Myers Squibb, Eli Lilly, and MSD. The remaining authors have stated that they have no conflicts of interest.

References

1. Gemba K, Fujimoto N, Aoe K, et al. Treatment and survival analyses of malignant mesothelioma in Japan. *Acta Oncol* 2013; 52:803-8.
2. Gemba K, Fujimoto N, Kato K, et al. National survey of malignant mesothelioma and asbestos exposure in Japan. *Cancer Sci* 2012; 103:483-90.
3. Robinson BW, Lake RA. Advances in malignant mesothelioma. *N Engl J Med* 2005; 353:1591-603.
4. Vogelzang NJ, Rusthoven JJ, Symanowski J, et al. Phase III study of pemetrexed in combination with cisplatin versus cisplatin alone in patients with malignant pleural mesothelioma. *J Clin Oncol* 2003; 21:2636-44.
5. Zalcman G, Mazieres J, Margery J, et al. Bevacizumab for newly diagnosed pleural mesothelioma in the Mesothelioma Avastin Cisplatin Pemetrexed Study (MAPS): a randomised, controlled, open-label, phase 3 trial. *Lancet* 2016; 387:1405-14.
6. Goto Y, Okada M, Kijima T, et al. A phase II study of nivolumab: a multicenter, open-label, single arm study in malignant pleural mesothelioma (MERIT). *J Thorac Oncol* 2017; 12(11 suppl 2):S1883.
7. Hato SV, Khong A, de Vries IJ, Lesterhuis WJ. Molecular pathways: the immunogenic effects of platinum-based chemotherapeutics. *Clin Cancer Res* 2014; 20:2831-7.
8. Zhao X, Suryawanshi S, Hruska M, et al. Assessment of nivolumab benefit-risk profile of a 240-mg flat dose relative to a 3-mg/kg dosing regimen in patients with advanced tumors. *Ann Oncol* 2017; 28:2002-8.
9. Kanda S, Goto K, Shiraishi H, et al. Safety and efficacy of nivolumab and standard chemotherapy drug combination in patients with advanced non-small-cell lung cancer: a four-arm phase Ib study. *Ann Oncol* 2016; 27:2242-50.
10. Byrne MJ, Nowak AK. Modified RECIST criteria for assessment of response in malignant pleural mesothelioma. *Ann Oncol* 2004; 15:257-60.

Utility of Survivin, BAP1, and Ki-67 immunohistochemistry in distinguishing epithelioid mesothelioma from reactive mesothelial hyperplasia

KEI KUSHITANI[1], VISHWA JEET AMATYA[1], AMANY SAYED MAWAS[2], RUI SUZUKI[1], YOSHIHIRO MIYATA[3], MORIHITO OKADA[3], KOUKI INAI[1], TAKUMI KISHIMOTO[4] and YUKIO TAKESHIMA[1]

[1]Department of Pathology, Institute of Biomedical and Health Sciences, Hiroshima University, Hiroshima 734-8551, Japan; [2]Department of Pathology and Clinical Pathology, Faculty of Veterinary Medicine, South Valley University, Qena 83523, Egypt; [3]Department of Surgical Oncology, Research Center for Radiation Casualty Medicine, Research Institute for Radiation Biology and Medicine, Hiroshima University, Hiroshima 734-8551; [4]Department of Internal Medicine, Okayama Rosai Hospital, Okayama 702-8055, Japan

Received June 30, 2017; Accepted November 20, 2017

DOI: 10.3892/ol.2018.7765

Abstract. Histological distinction between epithelioid mesothelioma (EM) and reactive mesothelial hyperplasia (RMH) can be challenging. The aim of this study was to assess the diagnostic utility of Survivin, Ki-67, and loss of BRCA1-associated protein 1 (BAP1) expressions in distinguishing EM from RMH using immunohistochemistry. Formalin-fixed, paraffin-embedded specimens from 78 cases of EM and 80 cases of RMH were immunohistochemically examined for Survivin, BAP1, and Ki-67. In addition, receiver operating characteristic curve analyses were performed to establish the cut-off values for Survivin and Ki-67 labelling indices. Survivin (cut-off value: 5%) had 67.7% sensitivity and 100% specificity, while Ki-67 (cut-off value: 10%) had 85.1% sensitivity and 87.5% specificity, and BAP1 had 66.2% sensitivity and 100% specificity for the differentiation of EM from RMH. Among the combinations of two markers, the combination of Survivin and BAP1 (Survivin-positive and/or BAP1-loss finding) had the highest diagnostic accuracy (sensitivity: 89.8%; specificity: 100%; accuracy: 95.3%). We recommend using the combination of Survivin and BAP1 to distinguish EM from RMH.

Introduction

Malignant mesothelioma (MM) is a relatively rare but highly aggressive malignant neoplasm arising from mesothelial cells of the pleura, peritoneum, pericardium, and tunica vaginalis. It is well-correlated with occupational and environmental asbestos exposure. (1,2) The incidence of MM has increased in many countries; (3) in Japan, mortality due to MM has increased since the 1990s, and is predicted to peak in the 2030s (4).

Epithelioid mesothelioma (EM) must be differentiated from reactive mesothelial hyperplasia (RMH), which is a non-neoplastic condition frequently caused by pleuritis, peritonitis, or serosal invasion of other cancers. Due to the close resemblance of EM to RMH, differentiation by routine histological observation alone can be challenging.

Various established and novel immunohistochemical markers have been utilized to distinguish EM from other malignancies (5-8) and RMH (6,9-17) Multiple potential immunohistochemical markers, including Ki-67, desmin, epithelial membrane antigen (EMA), p53, glucose transporter 1, insulin-like growth factor 2 messenger RNA binding protein-3 and BRCA1-associated protein 1 (BAP1) have been evaluated. However, despite the use of these immunohistochemical markers, the distinction between EM and RMH remains challenging in some cases.

Recently, detection of *p16 (CDKN2A)* homozygous deletion (*p16* HD) using fluorescence *in situ* hybridization (FISH) has been used to differentiate MM from RMH, with 100% specificity. However, the sensitivity of this marker for pleural EM varies between 45 and 86%, while its sensitivity for peritoneal EM ranges from 14 to 41% in different laboratories (10,18-20). In our unpublished experience, *p16* HD (detected by FISH) was present in 63.2% (12/19) of EM cases, but absent in all RMH cases (0/20). Although the detection of *p16* HD using FISH may be considered highly specific, its sensitivity in differentiating EM from RMH is not very high. In addition, FISH analysis cannot be applied in all cases or in all pathology laboratories, given its high cost and stringent experimental requirements.

We recently reported that phorbol 12-myristate-13-acetate-induced protein-1 (PMAIP-1; Noxa) and baculoviral IAP repeat-containing 5 (BIRC5; Survivin) mRNA expression levels are significantly higher in EM than in non-neoplastic pleural tissue, and discussed the utility of anti-Noxa antibody

Correspondence to: Professor Yukio Takeshima, Department of Pathology, Institute of Biomedical and Health Sciences, Hiroshima University, 1-2-3 Kasumi, Minami-ku, Hiroshima 734-8551, Japan
E-mail: ykotake@hiroshima-u.ac.jp

Key words: BAP1, immunohistochemistry, Ki-67, mesothelioma, reactive mesothelial hyperplasia, survivin

for the distinction between EM and RMH (21). However, the utility of Survivin IHC for the differentiation of benign and malignant mesothelial proliferation has not yet been assessed.

Here, we studied the utility of Survivin and Ki-67 expressions along with the loss of BAP1 expression in distinguishing benign from malignant mesothelial proliferation.

Materials and methods

Patients and histological samples. We used formalin-fixed, paraffin-embedded (FFPE) specimens from 78 patients with a definite histological diagnosis of EM who had undergone thoracoscopic pleural biopsy, pleurectomy/decortication, extrapleural pneumonectomy, or autopsy between 2000 and 2016. FFPE histological samples from surgical specimens obtained from 80 patients with a histological diagnosis of RMH were obtained via thoracoscopic biopsy, laparoscopic biopsy, or surgical resection between 2005 and 2016. These samples were retrieved from the archives of the Department of Pathology at Hiroshima University (Hiroshima, Japan). Each of the tumour specimens was independently reviewed by three pathologists (K.K., V.J.A, and Y.T.), and all cases of mesothelioma were diagnosed according to currently accepted World Health Organization Histological Criteria (6,22).

The tissue samples were retrieved from the archive of the Department of Pathology at Hiroshima University's Institute of Biomedical and Health Sciences. The collection of tissue specimens for this study was carried out in accordance with the 'Ethics Guidelines for Human Genome/Gene Research' enacted by the Japanese Government. Ethical approval was obtained from the institutional ethics review committee (Hiroshima University E-974). All experimental procedures were in accordance with the with ethical guidelines.

Immunohistochemical procedures. Immunohistochemical staining of sections from the FFPE tissue samples was performed using Ventana BenchMark GX (Roche Diagnostics, Basel, Switzerland). In brief, after deparaffinization using EZ-Prep (Roche Diagnostics) and antigen retrieval using Cell Conditioning 1 buffer at 95˚C for 32 min, sections were incubated with primary antibodies. The primary antibodies were anti-Survivin (cat. no. AF886, polyclonal, dilution of 1:200; R&D systems, Minneapolis, MN, USA), anti-BAP1 (C-4, dilution of 1:50; Santa Cruz Biotechnology, Inc., Dallas, TX, USA), and anti-Ki-67 (MIB-1, dilution of 1:25; Dako, Glostrup, Denmark). Incubation with secondary antibodies and detection was performed using the Ventana UltraView Universal DAB Detection kit.

Nuclear staining of Survivin, BAP1, and Ki-67 in EM or RMH cells with the same or higher intensity than internal positive controls was regarded as positive staining. Negative staining of BAP1 was defined as completely absent nuclear staining in the target cells in the presence of a positive internal control such as lymphocytes or stromal cells. Although some cases had weak cytoplasmic positivity for Survivin and BAP1, we have not included cases with only cytoplasmic positivity for Survivin and BAP1 for evaluation in this study. Immunoreactivity of Survivin and Ki-67 was evaluated using a labelling index (% of positive cells) in the 'hot spot' exhibiting the highest number of positive cells compared to the rest of the lesion. We evaluated at least 100 (maximum 500) EM or RMH cells in high power fields (x400). Counting of labelling indices of Survivin and Ki-67 was performed by three pathologists (K.K., V.J.A, and Y.T.) independently; the mean of three numbers was then calculated.

Statistical analysis. Receiver operating characteristic (ROC) curve analysis was performed to establish the cut-off values for the Survivin and Ki-67 labelling indices. The cut-off points were determined based on the Youden index. All statistical analyses were performed using EZR (Saitama Medical Center, Jichi Medical University, Saitama, Japan), a graphical user interface for R (The R Foundation for Statistical Computing, Vienna, Austria). More precisely, it is a modified version of R commander designed to add statistical functions frequently used in biostatistics (23).

Sensitivity, specificity, positive predictive values, negative predictive values, and diagnostic accuracies were calculated for each marker and combinations of two markers.

Results

Survivin expression and cut-off value. Representative immunohistochemical staining images for EM and RMH are shown in Fig. 1. Survivin expression was significantly higher in EM than in RMH. The mean of the Survivin labelling indices in EM [mean, 9.3; range, 0-24.5, standard deviation (SD), 6.5] was significantly higher than that in RMH (mean, 1.2; range, 0-4.0, SD, 1.2) (t-test, P-value <0.001). Distributions of the Survivin labelling indices in EM and RMH are shown in Fig. 2A.

The cut-off value for the Survivin IHC assay led by the result of ROC analysis was 4.000 (Fig. 2B). Based on the ROC analysis, and in consideration of convenience in practical pathological diagnosis, we set the cut-off value for the Survivin IHC assay at 5%. Immunoreactivity of Survivin was classified as negative (positivity of less than 5% of the mesothelioma cells or non-neoplastic mesothelial cells) or positive (positivity of over 5% of the mesothelioma or mesothelial cells).

Forty-two of 62 (67.7%) EM cases were positive for Survivin. In contrast, none of the RMH cases were positive for Survivin (Table I).

Ki-67 expression and cut-off value. Representative immunohistochemical staining images for EM and RMH are shown in Fig. 3. Ki-67 expression was also significantly higher in EM than in RMH. The mean of the Ki-67 labelling indices in EM (mean, 32.6; range, 1.0-90.0; SD, 22.1) was significantly higher than that in RMH (mean, 3.5; range, 0-20.0, SD, 4.2) (t-test, P-value <0.001). Distributions of the Ki-67 labelling indices in EM and RMH are shown in Fig. 4A.

The cut-off value for the Ki-67 IHC assay led by the result of ROC analysis was 10.333 (Fig. 4B). Based on the ROC analysis, and in consideration of convenience in practical pathological diagnosis, we set the cut-off value for the Ki-67 IHC assay at 10%. Immunoreactivity of Ki-67 was classified as negative (positivity of less than 10% of the mesothelioma cells or non-neoplastic mesothelial cells) or positive (positivity of over 10% of the mesothelioma or mesothelial cells).

Fifty-seven of 67 (85.1%) EM cases and 7 of 56 (12.5%) RMH cases were positive for Ki-67 (Table I).

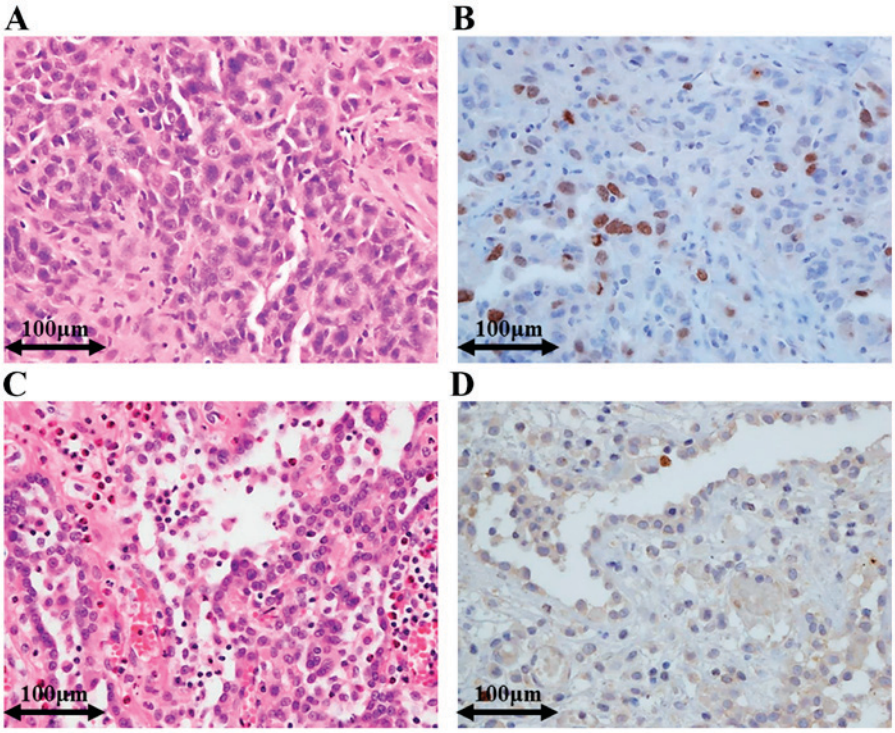

Figure 1. Representative histological images of Survivin IHC. (A) EM with H&E staining. (B) Survivin IHC in EM; labelling index, 18.1. (C) RMH with H&E stain. (D) Survivin IHC in RMH; labelling index, 1.3. IHC, immunohistochemistry; EM, epithelioid mesothelioma; RMH, reactive mesothelial hyperplasia; H&E, haematoxylin and eosin.

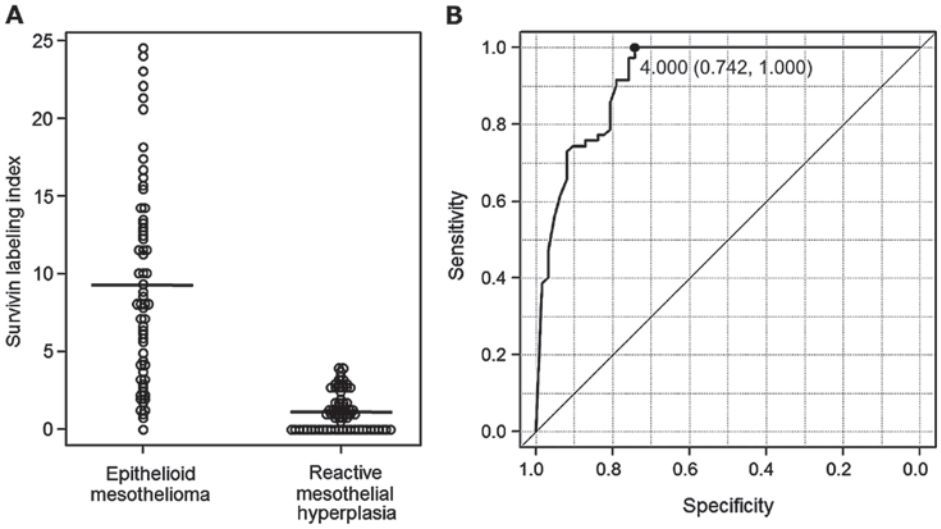

Figure 2. (A) Distribution of Survivin labelling index in epithelioid mesothelioma and reactive mesothelial hyperplasia. The horizontal line in the dot chart shows the mean. (B) ROC analysis. ROC curve was estimated using Survivin labelling index. Cut-off value based on the Youden index is also shown. ROC, receiver operating characteristic.

BAP1 expression. Loss of nuclear BAP1 expression was observed in 49 of 74 (66.2%) cases of EM (Table I). Almost all cases without BAP1 expression had a homogenous expression loss pattern. No heterogeneous loss patterns were observed. In contrast, nuclear BAP1 expression was preserved in all 78 RMH cases (Table I). Representative immunohistochemical staining images for EM and RMH are shown in Fig. 5.

Utilities of each marker and combinations of two markers. The sensitivity and specificity of each marker and combinations of two markers for the distinction between EM and RMH are shown in Table II. Among three single markers and six combination patterns of two markers, 'Survivin-positive and/or BAP1-loss' finding showed the highest diagnostic accuracy (95.3%).

Discussion

Accurate histopathological differentiation between MM and RMH is extremely important, not only for clinical management, but also for the appropriate operation of the public

Table I. Immunohistochemical findings of Survivin, Ki-67, and BAP1 in epithelioid mesothelioma and reactive mesothelial hyperplasia.

Immunohistochemical data	Epithelioid mesothelioma			Reactive mesothelial hyperplasia		
	n (%)	Negative	Positive	n (%)	Negative	Positive
Survivin expression	42/62 (67.7)	20	42	0/70	70	0
Ki-67 expression	57/67 (85.1)	10	57	7/56 (12.5)	49	7
BAP1-loss	49/74 (66.2)	25	49	0/78	78	0

BAP1, BRCA1-associated protein 1.

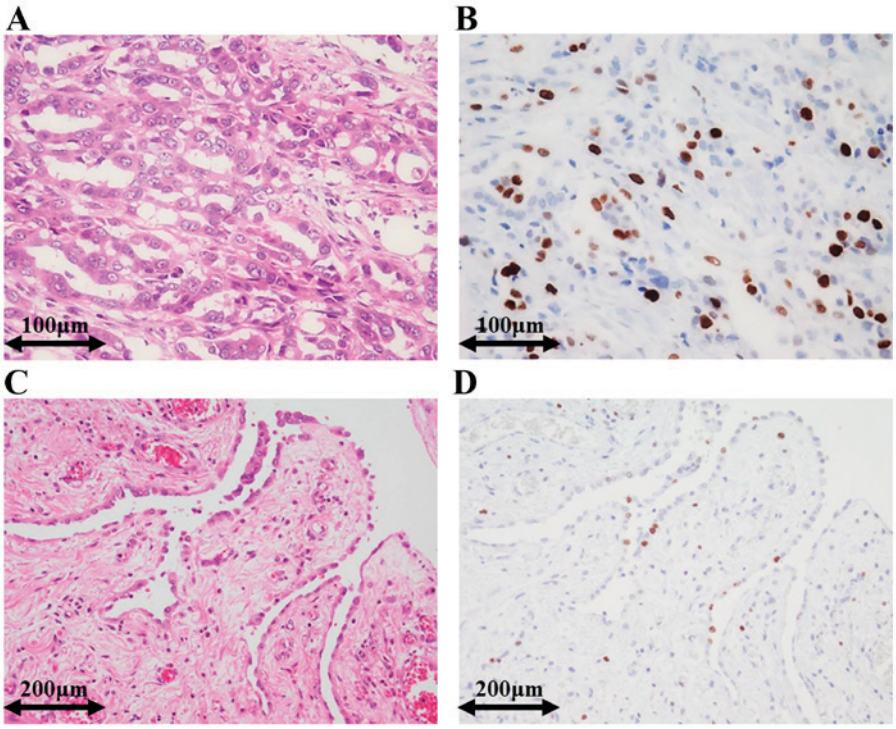

Figure 3. Representative histological images of Ki-67 IHC. (A) EM with H&E stain. (B) Ki-67 IHC in EM; labelling index, 35.0. (C) RMH with H&E stain. (D) Ki-67 IHC in RMH; labelling index, 8.7. IHC, immunohistochemistry; EM, epithelioid mesothelioma; RMH, reactive mesothelial hyperplasia; H&E, haematoxylin and eosin.

compensation system for victims of environmental and occupational asbestos exposure and their dependents. To obtain a better marker for EM, we evaluated the diagnostic utilities of Survivin, BAP1, and Ki-67 in differentiating EM from RMH. We found that the sensitivity and specificity of the nuclear Survivin labelling index following the use of a properly determined cut-off value was appropriate in distinguishing EM from RMH. The utility of Survivin IHC for the differentiation between benign and malignant mesothelial proliferation has not been reported to date. To the best of our knowledge, this is the first report evaluating the utility of Survivin IHC in differentiating EM from RMH.

Survivin is the smallest member of the inhibitor of apoptosis (IAP) family, and is expressed highly in most human foetal tissues and cancers. However, it is completely absent in terminally-differentiated tissues. Survivin functions as a regulator of both cell division and apoptosis. The function of Survivin differs according to cellular localization. Cytosolic Survivin is believed to function as an apoptotic suppressor, while nuclear Survivin is postulated to regulate cell division (24). Overexpression of Survivin is associated with tumour progression and poor prognosis in many types of human malignancies, including MM (25,26). In fact, several reports indicate that Survivin is a promising marker for the diagnosis of malignant pleural effusion (27). Survivin has also been reported to be associated with anti-tumour activity and outcomes of chemotherapy in MM, and is a new therapeutic target for the treatment of MM (28-30).

While the Survivin labelling indices of the EM cases in our study were similar to those reported by Meerang *et al* (25), they were significantly lower than those reported by Hmeljak *et al* (median, 67; mean, 63; range, 9.7-94.9; SD, 20.8) (26). This discrepancy in Survivin expression may be due to differences in staining technique, source of antibodies used for analysis,

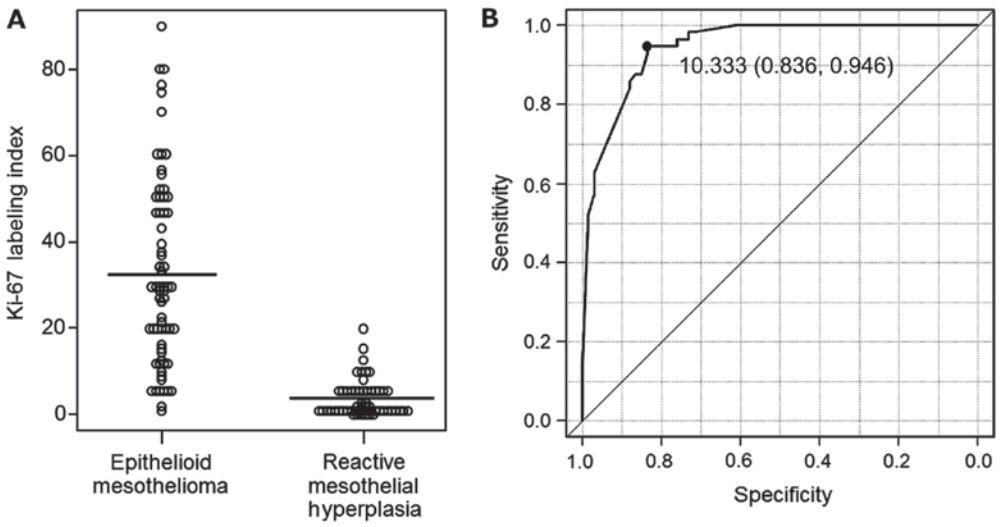

Figure 4. (A) Distributions of Ki-67 labelling index in epithelioid mesothelioma and reactive mesothelial hyperplasia. The horizontal line in the dot chart shows the mean. (B) ROC analysis. ROC curve was estimated using Ki-67 labelling index. Cut-off value based on the Youden index is also shown. ROC, receiver operating characteristic.

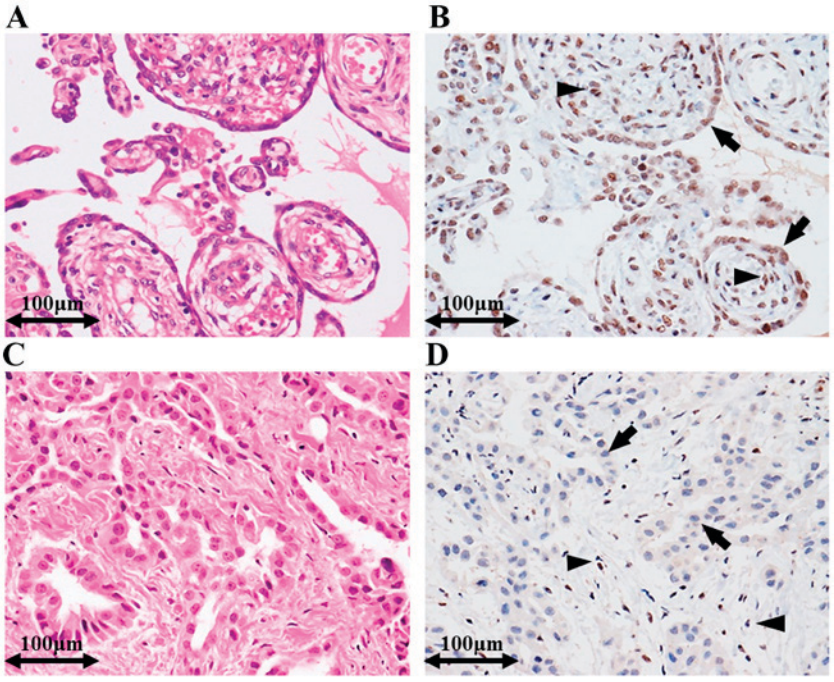

Figure 5. Representative histological images of BAP1 IHC. (A) RMH with H&E stain. (B) BAP1 IHC in RMH. Nuclear staining of the mesothelial cells (arrows) demonstrated the same intensity as that of internal positive controls (arrowheads; stromal cells). (C) EM with H&E stain. (D) BAP1 IHC in EM. Nuclear staining was not observed in tumour cells (loss of expression). Strong nuclear staining was observed in internal positive controls (arrowheads; stromal cells). IHC, immunohistochemistry; EM, epithelioid mesothelioma; RMH, reactive mesothelial hyperplasia; H&E, haematoxylin and eosin; BAP1, BRCA1-associated protein 1.

and the quantification technique. In our study, we used fully automated immunohistochemical staining utilising equipment from Roche for reproducible results. We also used commercially available antibodies from reputable sources and evaluated nuclear reactivity alone. Evaluation of nuclear reactivity was reproducible and was independently confirmed by 3 pathologists.

Several studies have determined that germline mutations in the gene for *BAP1* predispose individuals to developing various tumours, including MM, cutaneous melanocytic tumours, uveal melanoma, lung adenocarcinoma, and meningioma (31). These studies suggest that germline mutations in *BAP1* result in a 'tumour predisposition syndrome' linking BAP1 to many other cancers. Somatic mutations in the *BAP1* gene have also been relatively frequently reported in MMs, uveal melanomas, and renal cell carcinomas (31). BAP1 is encoded by the *BAP1* gene, which is located on the short arm of chromosome 3 (3p21). BAP1 is a deubiquitinase targeting histones and the host cell factor-1 transcriptional co-factor, and plays a role in transcriptional regulation, chromatin modulation, cell cycle

Table II. Sensitivity, specificity, PPVs, NPVs and diagnostic accuracies of each marker and combinations of two markers for the differential diagnosis between epithelioid mesothelioma and reactive mesothelial hyperplasia.

Immunohistochemical findings	Sensitivity (%)	Specificity (%)	PPV (%)	NPV (%)	Accuracy (%)
Survivin-positive	67.7	100.0	100.0	77.8	84.8
BAP1-loss	66.2	100.0	100.0	75.7	83.6
Ki-67-positive	85.1	87.5	89.1	83.1	86.2
Survivin-positive and/or BAP1-loss	89.8	100.0	100.0	92	95.3
Both Survivin-positive and BAP1-loss	39.0	100	100.0	65.7	71.9
Survivin-positive and/or Ki-67-positive	91.1	86.3	87.9	89.8	88.8
Both Survivin-positive and Ki-67-positive	66.1	100.0	100.0	72.9	82.2
BAP1-loss and/or Ki-67-positive	96.9	92.1	94.3	95.9	94.8
Both BAP1-loss and Ki-67-positive	53.8	100	100.0	64.3	74.8

PPV, positive predictive values; NPV, negative predictive values; BAP1, BRCA1-associated protein 1.

regulation, and DNA repair (31,32). Several different alterations in the *BAP1* gene have been described, including large deletions of exons leading to loss of the N-terminal region, or to premature protein termination, focal deletions, frameshift mutations due to insertions or deletions, splice site mutations, and base substitutions leading to nonsense and missense mutations. Frameshift mutations and missense and nonsense substitutions are the most common sequence alterations. Truncating mutations frequently result in loss of the nuclear localization signal and/or the C-terminal protein-binding domain, while missense mutations interfere with the ubiquitin hydrolase function of BAP1 (31). As the detection of these alterations in *BAP1* has been made possible in recent years using immunohistochemistry (IHC), immunohistochemical detection of BAP1 loss has also been reported to be useful in distinguishing MM from RMH. However, the sensitivity of this assay in differentiating MM from RMH does not exceed 70% (10-13). Several studies indicate that the loss of nuclear BAP1 expression as assessed by IHC is closely correlated with genetic alterations in BAP1 (33-35).

In the present study, the frequency of BAP1 loss in EM was 66.2% (49/74), similar to those found in previous reports (10-13). Recently, Hida *et al* reported a focal heterogeneous BAP1 staining pattern in mesothelioma cases (10). However, in our study, almost all EM cases had either a uniform positive staining pattern or completely negative staining for BAP1. There were some EM cases that appeared to have focal staining for BAP1; however, careful observation of these cases under high power magnification confirmed that these focal positive cells were in fact inflammatory cells infiltrating into the mesothelioma or stromal cells. We classified such cases as cases with no loss of BAP1 expression. This may be the reason for the observed heterogeneous BAP1 staining pattern in mesothelioma. However, other reasons, such as differences in staining techniques and improper processing of the tumour, may also contribute to apparent differences between studies.

The specificity of a Survivin labelling index of over 5% and a loss of BAP1 expression was 100%. However, sensitivity of Survivin labelling index (67.7%) and loss of BAP1 expression (66.2%) alone are not sufficient for differential diagnosis. Although diagnostic accuracies of Survivin (84.8%) and BAP1 (83.6%) as single markers were inferior to that of EMA (95.5%), (21) the diagnostic accuracy of the combination of Survivin and BAP1 (Survivin-positive and/or BAP1-loss) was 95.3%, which was almost similar to EMA. Recently, Shinozaki-Ushiku *et al* proposed using a combination of BAP1 and enhancer of zeste homolog 2 (EZH2) expression to differentiate between MM from RMH; the sensitivity of this combination was 90%, while the specificity was absolute (36). The sensitivity (89.8%) and specificity (100%) of the combination of Survivin and BAP1 IHC in this study was comparable to those of previous reports (36).

A positive correlation between nuclear Survivin and Ki-67 labelling indices was previously reported by Meerang *et al* (25). We observed a similar correlation between Survivin and Ki-67 labelling indices in our study (data not shown). Although this correlation was present in both EM and RMH, it was more conspicuous in EM. Ki-67 protein is present during all active phases of the cell cycle (G1, S, G2, and mitosis), but is absent in resting cells (G0). Therefore, Ki-67 is well known as a so-called 'proliferation marker', and the Ki-67 labelling index is often correlated with the clinical course of cancer (37,38). On the other hand, nuclear Survivin plays important roles in the regulation of mitosis. Survivin expression is found to be dominant only in the G2/M phase, and Survivin is known to localize to components of the mitotic spindle during the metaphase and anaphase of mitosis (39,40). Therefore, both nuclear Survivin and Ki-67 may be considered proliferation markers. We can thus explain both the high expression of Survivin and Ki-67 in EM compared to RMH, and the positive correlation between the nuclear Survivin and Ki-67 labelling indices.

Although various studies have reported the usefulness of Ki-67 IHC in differentiating EM from RMH, (14-17) it is not routinely utilized for the confirmation of mesothelioma due to its low sensitivity and specificity.

The sensitivity, specificity, and diagnostic accuracy of Ki-67 (85.1, 87.5, and 86.2%, respectively) in this study were almost the same or slightly higher compared with previous reports (14,15,17). These values were relatively high but not sufficient for differential diagnosis by single marker. However, the diagnostic accuracy

of the combination of Ki-67 and BAP1 was 94.8%, which was almost the same as that of the combination of Survivin and BAP1.

We evaluated the utility of Survivin, BAP1, and Ki-67 IHC in distinguishing EM from RMH. Based on our results, 'Survivin-positive and/or BAP1-loss' finding strongly suggest EM, therefore we recommend the use of a combination of Survivin and BAP1. In addition, further evaluation of the Ki-67 labelling index may be useful for accurate differential diagnosis.

Acknowledgements

The authors would like to thank the Technical Centre of Hiroshima University for technical assistance. This study was funded in part by the Japanese Ministry of Health, Labour, and Welfare.

References

1. Robinson BW, Musk AW and Lake RA: Malignant mesothelioma. Lancet 366: 397-408, 2005.
2. Roggli VL, Sharma A, Butnor KJ, Sporn T and Vollmer RT: Malignant mesothelioma and occupational exposure to asbestos: A clinicopathological correlation of 1445 cases. Ultrastruct Pathol 26: 55-65, 2002.
3. Delgermaa V, Takahashi K, Park EK, Le GV, Hara T and Sorahan T: Global mesothelioma deaths reported to the World Health Organization between 1994 and 2008. Bull World Health Organ 89: 716-724, 2011.
4. Murayama T, Takahashi K, Natori Y and Kurumatani N: Estimation of future mortality from pleural malignant mesothelioma in Japan based on an age-cohort model. Am J Ind Med 49: 1-7, 2006.
5. Churg A, Roggli V, Galateau-Salle F, Cagle PhT, Gibbs AR, Hasleton PhS, Henderson DW, Vignaud JM, Inai K, Praet M, *et al*: Tumours of the pleura. In: WHO Classification of Tumours of the Lung, Pleura, Thymus and Heart. Travis WD, Brambilla E, Burke AP, Marx A and Nicholson AG (eds). IARC Press, Lyon, pp153-181, 2015.
6. Husain AN, Colby T, Ordonez N, Krausz T, Attanoos R, Beasley MB, Borczuk AC, Butnor K, Cagle PT, Chirieac LR, *et al*: Guidelines for pathologic diagnosis of malignant mesothelioma: 2012 update of the consensus statement from the International Mesothelioma Interest Group. Arch Pathol Lab Med 137: 647-667, 2013.
7. Ordóñez NG: Application of immunohistochemistry in the diagnosis of epithelioid mesothelioma: A review and update. Hum Pathol 44: 1-19, 2013.
8. Kushitani K, Amatya VJ, Okada Y, Katayama Y, Mawas AS, Miyata Y, Okada M, Inai K, Kishimoto T and Takeshima Y: Utility and pitfall of immunohistochemistry in the differential diagnosis between epithelioid mesothelioma and poorly differentiated lung squamous cell carcinoma. Histopathology 70: 375-384, 2017.
9. Minato H, Kurose N, Fukushima M, Nojima T, Usuda K, Sagawa M, Sakuma T, Ooi A, Matsumoto I, Oda M, *et al*: Comparative immunohistochemical analysis of IMP3, GLUT1, EMA, CD146, and desmin for distinguishing malignant mesothelioma from reactive mesothelial cells. Am J Clin Pathol 141: 85-93, 2014.
10. Hida T, Hamasaki M, Matsumoto S, Sato A, Tsujimura T, Kawahara K, Iwasaki A, Okamoto T, Oda Y, Honda H and Nabeshima K: BAP1 immunohistochemistry and p16 FISH results in combination provide higher confidence in malignant pleural mesothelioma diagnosis: ROC analysis of the two tests. Pathol Int 66: 563-570, 2016.
11. Hwang HC, Sheffield BS, Rodriguez S, Thompson K, Tse CH, Gown AM and Churg A: Utility of BAP1 immunohistochemistry and p16 (CDKN2A) FISH in the diagnosis of malignant mesothelioma in effusion cytology specimens. Am J Surg Pathol 40: 120-126, 2016.
12. McGregor SM, Dunning R, Hyjek E, Vigneswaran W, Husain AN and Krausz T: BAP1 facilitates diagnostic objectivity, classification, and prognostication in malignant pleural mesothelioma. Hum Pathol 46: 1670-1678, 2015.
13. Cigognetti M, Lonardi S, Fisogni S, Balzarini P, Pellegrini V, Tironi A, Bercich L, Bugatti M, Rossi G, Murer B, *et al*: BAP1 (BRCA1-associated protein 1) is a highly specific marker for differentiating mesothelioma from reactive mesothelial proliferations. Mod Pathol 28: 1043-1057, 2015.
14. Kimura F, Okayasu I, Kakinuma H, Satoh Y, Kuwao S, Saegusa M and Watanabe J: Differential diagnosis of reactive mesothelial cells and malignant mesothelioma cells using the cell proliferation markers minichromosome maintenance protein 7, geminin, topoisomerase II alpha and Ki-67. Acta Cytol 57: 384-390, 2013.
15. Kimura F, Kawamura J, Watanabe J, Kamoshida S, Kawai K, Okayasu I and Kuwao S: Significance of cell proliferation markers (Minichromosome maintenance protein 7, topoisomerase IIalpha and Ki-67) in cavital fluid cytology: Can we differentiate reactive mesothelial cells from malignant cells? Diagn Cytopathol 38: 161-167, 2010.
16. Hasteh F, Lin GY, Weidner N and Michael CW: The use of immunohistochemistry to distinguish reactive mesothelial cells from malignant mesothelioma in cytologic effusions. Cancer Cytopathol 118: 90-96, 2010.
17. Taheri ZM, Mehrafza M, Mohammadi F, Khoddami M, Bahadori M and Masjedi MR: The diagnostic value of Ki-67 and repp86 in distinguishing between benign and malignant mesothelial proliferations. Arch Pathol Lab Med 132: 694-697, 2008.
18. Churg A, Sheffield BS and Galateau-Salle F: New markers for separating benign from malignant mesothelial proliferations: Are we there yet? Arch Pathol Lab Med 140: 318-321, 2016.
19. Hiroshima K, Wu D, Hasegawa M, Koh E, Sekine Y, Ozaki D, Yusa T, Walts AE, Marchevsky AM, Nabeshima K, *et al*: Cytologic differential diagnosis of malignant mesothelioma and reactive mesothelial cells with fish analysis of p16. Diagn Cytopathol 44: 591-598, 2016.
20. Walts AE, Hiroshima K, McGregor SM, Wu D, Husain AN and Marchevsky AM: BAP1 immunostain and CDKN2A (p16) FISH analysis: Clinical applicability for the diagnosis of malignant mesothelioma in effusions. Diagn Cytopathol 44: 599-606, 2016.
21. Kushitani K, Amatya VJ, Mawas AS, Miyata Y, Okada M and Takeshima Y: Use of anti-noxa antibody for differential diagnosis between epithelioid mesothelioma and reactive mesothelial hyperplasia. Pathobiology 83: 33-40, 2016.
22. Travis WD, Brambilla E, Nicholson AG, Yatabe Y, Austin JHM, Beasley MB, Chirieac LR, Dacic S, Duhig E, Flieder DB, *et al*: The 2015 World Health Organization Classification of Lung Tumors: Impact of genetic, clinical and radiologic advances since the 2004 classification. J Thorac Oncol 10: 1243-1260, 2015.
23. Kanda Y: Investigation of the freely available easy-to-use software 'EZR' for medical statistics. Bone Marrow Transplant 48: 452-458, 2013.
24. Garg H, Suri P, Gupta JC, Talwar GP and Dubey S: Survivin: A unique target for tumor therapy. Cancer Cell Int 16: 49, 2016.
25. Meerang M, Bérard K, Friess M, Bitanihirwe BK, Soltermann A, Vrugt B, Felley-Bosco E, Bueno R, Richards WG, Seifert B, *et al*: Low merlin expression and high survivin labeling index are indicators for poor prognosis in patients with malignant pleural mesothelioma. Mol Oncol 10: 1255-1265, 2016.
26. Hmeljak J, Erčulj N, Dolžan V, Pižem J, Kern I, Kovač V, Cemažar M and Cör A: Is survivin expression prognostic or predictive in malignant pleural mesothelioma? Virchows Arch 462: 315-321, 2013.
27. Chen S, Wang Y, An L, Fei ZT and Li T: The diagnostic value of survivin in malignant pleural effusion: A meta-analysis. Clin Chim Acta 441: 142-147, 2015.
28. Bertino P, Panigada M, Soprana E, Bianchi V, Bertilaccio S, Sanvito F, Rose AH, Yang H, Gaudino G, Hoffmann PR, *et al*: Fowlpox-based survivin vaccination for malignant mesothelioma therapy. Int J Cancer 133: 612-623, 2013.
29. De Cesare M, Cominetti D, Doldi V, Lopergolo A, Deraco M, Gandellini P, Friedlander S, Landesman Y, Kauffman MG, Shacham S, *et al*: Anti-tumor activity of selective inhibitors of XPO1/CRM1-mediated nuclear export in diffuse malignant peritoneal mesothelioma: The role of survivin. Oncotarget 6: 13119-13132, 2015.
30. Goričar K, Kovač V, Franko A, Dodič-Fikfak M and Dolžan V: Serum survivin levels and outcome of chemotherapy in patients with malignant mesothelioma. Dis Markers 2015: 316739, 2015.
31. Murali R, Wiesner T and Scolyer RA: Tumours associated with BAP1 mutations. Pathology 45: 116-126, 2013.
32. Scheuermann JC, de Ayala Alonso AG, Oktaba K, Ly-Hartig N, McGinty RK, Fraterman S, Wilm M, Muir TW and Müller J: Histone H2A deubiquitinase activity of the Polycomb repressive complex PR-DUB. Nature 465: 243-247, 2010.

33. Bott M, Brevet M, Taylor BS, Shimizu S, Ito T, Wang L, Creaney J, Lake RA, Zakowski MF, Reva B, *et al*: The nuclear deubiquitinase BAP1 is commonly inactivated by somatic mutations and 3p21.1 losses in malignant pleural mesothelioma. Nat Genet 43: 668-672, 2011.
34. Testa JR, Cheung M, Pei J, Below JE, Tan Y, Sementino E, Cox NJ, Dogan AU, Pass HI, Trusa S, *et al*: Germline BAP1 mutations predispose to malignant mesothelioma. Nat Genet 43: 1022-1025, 2011.
35. Yoshikawa Y, Sato A, Tsujimura T, Emi M, Morinaga T, Fukuoka K, Yamada S, Murakami A, Kondo N, Matsumoto S, *et al*: Frequent inactivation of the BAP1 gene in epithelioid-type malignant mesothelioma. Cancer Sci 103: 868-874, 2012.
36. Shinozaki-Ushiku A, Ushiku T, Morita S, Anraku M, Nakajima J and Fukayama M: Diagnostic utility of BAP1 and EZH2 expression in malignant mesothelioma. Histopathology 70: 722-733, 2017.
37. Scholzen T and Gerdes J: The Ki-67 protein: From the known and the unknown. J Cell Physiol 182: 311-322, 2000.
38. Brown DC and Gatter KC: Monoclonal antibody Ki-67: Its use in histopathology. Histopathology 17: 489-503, 1990.
39. Altieri DC: Validating survivin as a cancer therapeutic target. Nat Rev Cancer 3: 46-54, 2003.
40. Kim JY, Chung JY, Lee SG, Kim YJ, Park JE, Yoo KS, Yoo YH, Park YC, Kim BG and Kim JM: Nuclear interaction of Smac/DIABLO with survivin at G2/M arrest prompts docetaxel-induced apoptosis in DU145 prostate cancer cells. Biochem Biophys Res Commun 350: 949-954, 2006.

腫瘍内科，22(2)：190-197，2018

Lecture

解説

抗CD26抗体*

大沼　圭**　波多野　良**　森本幾夫**

Key Words：CD26, dipeptidyl peptidase IV, malignant mesothelioma, YS110, monoclonal antibody

はじめに

CD26分子はdipeptidyl peptidase IV(DPPIV)酵素を有するT細胞活性化分子である．われわれはCD26分子のcDNAの単離および単クローン抗体(monoclonal antibody；mAb)の樹立を世界に先駆けて行い，当分野の研究では世界の最先端にいる[1]．この研究過程で悪性中皮腫細胞株JMNがCD26を発現していることを見出し[2]，また，CD26は正常中皮細胞で発現はないが，上皮型悪性中皮腫組織では8割以上に発現していることを発見した[3]．われわれは，それまで樹立してきたCD26マウスmAbのエピトープをもとにして，親和性および生物学的活性が非常に高いヒト化CD26抗体をin silicoで設計し，小スケールから大スケールで生産可能なヒト化CD26 mAb(YS110)を開発樹立した[4]．このヒト化CD26抗体を用いた研究により，CD26は悪性中皮腫細胞の増殖，浸潤に重要な役割を果たし，CD26抗体がその機能を強く抑制することを*in vitro*および*in vivo*実験で明らかにし，悪性中皮腫の新規治標的として大変有望な分子であることを示した[4)~7)]．悪性中皮腫は化学療法，外科的治療および放射線療法を組み合わせても，最初の症状発現から10～17か月以内に死に至る予後不良な疾患である．悪性胸膜中皮腫(malignant pleural mesothelioma；MPM)の8割以上は過去のアスベストばく露が原因とされ，日本を含むアジア諸国および欧米では今後ますます患者数が増加すると予測されている．しかし，現時点では悪性中皮腫に対する有効な治療法はなく，新規かつ有効な治療法開発は急務である．本稿では，われわれの研究室が世界に向けて発信しているヒト化CD26抗体によるがん治療について，その作用機序およびFirst-in-human(FIH)第I相臨床試験の成績について紹介する．

CD26分子について

CD26分子は766アミノ酸残基よりなり，N末端が細胞質内に存在する，いわゆるII型の膜糖タンパク質である(図1)．630番目のセリン残基を中心として，セリンプロテアーゼであるDPPIV酵素活性をもっており，基質となるペプチドのN末端から2番目のプロリンあるいはアラニンをそのC末端側で切断する．このCD26分子はTa1というマウスmAbと反応するヒト末梢血T細胞表面抗原として報告され，その後，活性化T細胞に強く発現することから，T細胞活性化抗原として確立された[8)9)]．静止期のヒト末梢血T細胞のCD26をフローサイトメーターで解析すると，3相性のヒストグラムを示し，このうちCD26強陽性の細胞集団($CD26^{high}$ T細胞)は，$CD29^{+}$ $CD45RO^{+}$のメモリーT細胞サブセットである．$CD26^{high}$ T細胞は，破傷風キソイドのようなメモ

* Anti-CD26 monoclonal antibody.

** Kei OHNUMA, M.D., Ph.D., Ryo HATANO, Ph.D. & Chikao MORIMOTO, M.D., Ph.D.: 順天堂大学大学院医学研究科免疫病・がん先端治療学講座〔〒113-8421 東京都文京区本郷2-1-1〕; Department of Therapy Development and Innovation for Immune Disorders and Cancers, Graduate School of Medicine, Juntendo University, Tokyo 113-8421, JAPAN

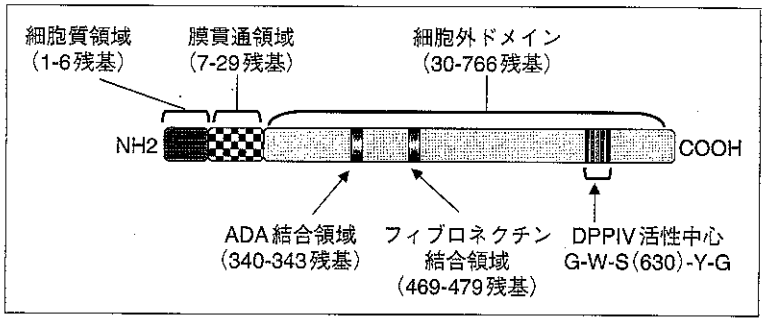

図1　ヒトCD26分子の模式図

ヒトCD26/DPPIV分子は766アミノ酸残基よりなるII型の膜糖タンパク質である．N末端から1～6番目のアミノ酸残基が細胞質内領域で，T細胞ではCARMA1と結合して細胞内シグナル伝達を担っている．7～29番目のアミノ酸残基は細胞膜貫通領域である．細胞外領域の340～343番目のアミノ酸残基はADA結合部位，469～479番目はフィブロネクチン結合部位である．DPPIV酵素活性は630番目のセリン残基(S)を中心にその前後のアミノ酸残基グリシン(G)・トリプトファン(W)・チロシン(Y)・グリシン(G)が，基質ポケット構造の底部を形成している．また，630番目のセリンおよび705番目のアスパラギ酸，740番目のヒスチジンは酵素活性に必須の三つ組み構造残基(catalytic triad)である．

リー抗原に対して最も強く反応して増殖活性を示し，メモリー抗原応答の主要なエフェクター細胞である．また，血管内皮細胞間の遊走能を強く示し，炎症部位への移動，集積をきたし，炎症局所において炎症のエフェクターT細胞としても重要な役割を発揮すると考えられている．CD26^{high}T細胞はIL-2やIFN-γなどのサイトカインを分泌するTh1型のリンパ球とされ，さらに，B細胞の免疫グロブリン産生を誘導する．このように，CD26^{high}T細胞は炎症のエフェクター細胞として，関節リウマチやバセドウ病などの自己免疫疾患の末梢血T細胞でその発現が増加し，また，これら疾患の炎症局所や遅延型過敏反応の部位でもCD26^{high}T細胞の集簇が認められる[1]．

一方，マウスのCD26分子はthymocyte activating molecule(THAM)として発見され，胸腺細胞中CD4$^-$CD8$^-$のdouble negative細胞に強発現しており，静止期，活性化T細胞，B細胞，NK細胞はともに弱陽性であり，ヒトCD26とマウスCD26の免疫系での役割は異なるものであることが示唆されている．C57BL/6バックグラウンドをもつCD26ノックアウトマウス(CD26$^{-/-}$KOマウス)は正常表現型で生存するが，脾臓ではCD4T細胞の減少とNK細胞の増加を認め，末梢血液ではCD4NKT細胞が著明に減少している．さらに，CD26$^{-/-}$KOマウスの脾臓細胞は，IL-4，IgG，IgEの産生能が低下し，一方，IL-10，IFN-γの産生能が増加していた[10]．CD26の構造は種を超えて強く保存されており，高いホモロジーを示す．ヒトCD26とラット，マウスCD26との相同性はそれぞれ85%，86%である．しかしヒトCD26はアデノシンデアミナーゼ(adenosine deaminase；ADA)の結合タンパクであるがラット，マウスCD26はADAに結合しない．

われわれは，永らく不明であったヒトT細胞上のCD26の共刺激シグナル伝達の分子メカニズムを解明した．すなわち，CD26陽性T細胞のメモリー応答における共刺激リガンドとして抗原提示細胞(APC)のCaveolin-1を同定し，CD26およびカベオリンの直下のシグナル分子を解明し，CD26-カベオリン系がT細胞のメモリー応答において新たな共刺激系であることを示した[1]．CD26が，抗原を取込んだAPC上のCaveolin-1と結合してリン酸化し，APCのCD86の発現上昇を誘導すること，またCaveolin-1の82～101番目のアミノ酸残基がCD26のDPPIV酵素活性中心との結合に関与していることを明らかにした．すなわち，T細胞のCD26とメモリー抗原を取り込んだAPCのCaveolin-1が互いに接触してimmunological synapseを形成しメモリー抗原に対するT細胞の増殖反応がもたらされる．さらに，

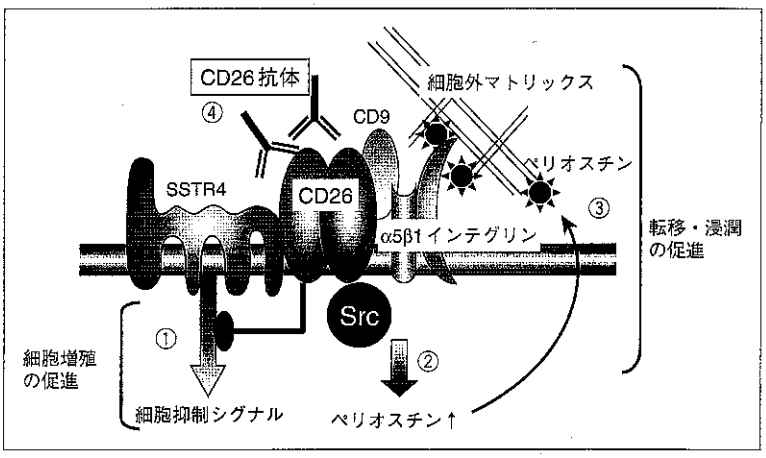

図2　CD26分子を含む細胞表面分子複合体による悪性中皮腫細胞の制御メカニズム

①SSTR4はCD26と結合することにより，細胞制御シグナルが阻害されるため，悪性中皮腫細胞の増殖能が増す．②また，CD26分子複合体によってSrcが活性化され，ペリオスチンの転写が増加する．③増加したペリオスチンががん微小環境に蓄積してインテグリント結合し，悪性中皮腫細胞の転移浸潤が促進される．以上のサイクルがCD26分子を中心として発現するため，CD26陽性悪性中皮腫細胞は増殖，浸潤，転移能が増す．④CD26抗体のメカニズムの1つとして，これらの機能をブロックして，抗腫瘍効果を発揮すると推察される．

（文献[31] p. 145, Figure 4より改変）

CD26によってAPC内で惹起されるCaveolin-1下流のシグナル伝達機構としてCaveolin-1, Tollip, IRAK-1複合体がNF-κBが活性化してCD86の発現増強が誘導され，CD26-カベオリンという新たな免疫活性化経路を明らかにした．

一方，がん細胞におけるCD26分子シグナル伝達においても，われわれは詳細に明らかにした．まず，CD26陽性T細胞腫瘍株やヒトT細胞クローンをCD26抗体で処理すると細胞増殖を抑制し，この時にcyclin dependent kinase inhibitor（CDKI）の$p21^{Cip1}$が誘導され細胞周期を止めることを見出した．また，T細胞腫瘍株を移植した免疫不全マウスの系でもCD26抗体の*in vivo*投与で腫瘍細胞は壊死に陥り，抗体投与マウスは長期生存した[11]．さらに，悪性中皮腫細胞におけるCD26の細胞内シグナル分子同定を目的として，CD26の細胞内ドメインの機能を喪失させるため，CD10の細胞内ドメインに置換した遺伝子組み換えCD26-CD10キメラ体を作製して悪性中皮腫細胞に発現させたところ，ネイティブなCD26を発現したMPMに比べ，細胞増殖・遊走・浸潤能が著しく低下した．細胞膜タンパク質を抽出し，CD26細胞内ドメイン結合分子を質量分析法で解析したところ，CD26細胞質ドメインに会合するタンパク質としてソマトスタチン受容体4（SSTR4）を同定した[5]．さらに，ネイティブCD26発現MPMでは，CD26陰性あるいはキメラ体発現MPMに比べ，細胞外マトリックスタンパク質であるペリオスチンの発現が著しく増加していること[7]，また，CD26はテトラスパン分子CD9およびインテグリンとの相互作用がその浸潤に重要であることを見出した[6]．すなわち，CD26分子は悪性中皮腫細胞表面おいて巨大な分子複合体を構成し，表面分子と細胞内および細胞外を相互につなげるプラットフォームを形成していることを明らかにした（図2）．

さらにわれわれは，CD26分子は悪性中皮腫におけるがん幹細胞の重要なマーカーであることを明らかにしている．すなわち，悪性中皮腫のSP（side-population），CD9，CD24，およびCD26陽性細胞集団は非対称性分裂を示すとともに連続移植可能な性質を有し，がん幹細胞の新たなマーカーであることを明らかにした[12]．さらに，種々の悪性中皮腫細胞株を用いて網羅的解析を行っ

たところ，CD26陽性がん幹細胞はIGFBP3およびIGFBP7を高発現しており，従来のCD24陽性がん幹細胞とは異なる遺伝子発現およびEGFシグナル活性化メカニズムを有していることを明らかにした[13]．

CD26抗体療法

1．前臨床試験

上述したように，CD26分子は悪性中皮腫の新規治療標的として臨床応用できる有望な分子であることを強く示唆している．そこで，われわれは，実験室で用いたCD26マウスmAbのCDR（complementary determining region；相補性決定領域）を解析し，親和性の高いヒト化抗体の作製に必要なCDRおよびFR（framework；枠組み構造）のアミノ酸配列をin silicoでデザインし，高親和性で高い生物学的活性を示すIgG1型ヒト化CD26抗体（YS110）を作製した．ヒト化CD26抗体は*in vivo*でJMN細胞株の増殖を抑制し，移植した免疫不全マウスの系においてもヒト化CD26抗体投与により，腫瘍縮小，生存延長，肺への転移抑制などをもたらすことを見出し，CD26分子が悪性中皮腫の治療ターゲットになる可能性が示唆された[4]．悪性中皮腫はその病理組織型により上皮型，混合型，肉腫型の3種類に分類される．そこで，われわれは広島大学医学部病理学・井内教授との共同研究により，152症例の悪性中皮腫患者病理組織でのCD26発現の検討を行った．その結果，CD26は正常中皮細胞ではまったく発現せず，また，肉腫型ではほとんど発現がみられなかったが，上皮型では約8割が陽性，混合型では約4割が陽性であり，上皮型悪性中皮腫に有意にCD26が発現することを明らかにした[14]．さらに，CD26陽性中皮腫細胞株を免疫不全マウスの胸腔内に接種し，胸腔内でびまん性に中皮腫細胞が進展し，胸壁に浸潤するとともに，心嚢や対側胸壁にも転移浸潤するヒト中皮腫浸潤・増殖モデルマウスの作製に成功した．このモデルマウスにヒト化CD26抗体を週2回，4週間腹腔内投与したところ，コントロールIgG投与群と比べて，心外膜，対側胸壁への転移浸潤が著明に抑制され，さらに原発腫瘍そのものもほとんど消失した．このようにヒト化CD26抗体YS110は本モデルにおいても有効性を示したことから，悪性中皮腫での新規治療法として臨床応用できる可能性を強く示唆した．

われわれはこれまでにYS110の抗腫瘍作用メカニズムとして，抗体依存性細胞傷害（ADCC）活性・補体依存性細胞傷害（CDC）活性などの間接的作用に加えて，CD26陽性腫瘍に抗体が結合することによる直接的な作用があることを明らかにしてきた[4)11)15)16)]．がん細胞の細胞膜上のCD26にヒト化CD26抗体が結合すると，CDKIである$p21^{Cip1}$や$p27^{Kip1}$の発現が上昇し，S期の細胞を減少させるとともにG2/M期で細胞周期を遅延させることが明らかになっている[4)11)15)16)]．さらにCD26抗体とCD26の複合体が膜から細胞質，さらに核内へと移行し，RNA polymeraseである*POLR2A*遺伝子の転写領域下流に結合することで*POLA2A*の転写を抑制し増殖を抑制する[17]．このように細胞増殖や生存プログラムに重要な役割を果たす*POLR2A*遺伝子機能を抑制することで，細胞増殖を抑制することを明らかにした．また，CD26はコラーゲンやフィブロネクチンなどの細胞外マトリックスとも結合してがん細胞の浸潤・転移を促進しているが，腎がん細胞では，CD26抗体により細胞外マトリックスとの接着が阻害され，このことからCD26抗体が腎がんをはじめとするCD26陽性腫瘍の浸潤・転移の抑制にも働くことが示唆された[16]．さらに，CD26抗体は悪性中皮腫以外のCD26陽性腫瘍である腎がん，白血病において，*in vivo*担がんマウスで検討を行ったところ，著明な腫瘍抑制効果を示した[11)16)18)]．

以上のように，YS110について有望な基礎実験データが得られたことから，開発ステージをさらに進めるため，毒性試験を行うカニクイザルの組織におけるCD26との交差反応性，および，良好なヒト化抗体生産細胞株の構築などの観点からYS110抗体産生クローンを選択した．このYS110の安全性を調べるため，カニクイザルを用いて10 mg/kg～100 mg/kgの単回静脈内点滴投与において特記すべき副作用と思われる変化は認められず，さらに毎週1回3か月間に及ぶ反復投与長期毒性試験においてもその安全性を確認した．また，CD3，CD4，CD8陽性T細胞はいずれの群

でも投与期間中および投与後56日間は特に変化は認められなかった．さらに，CD25，CD26陽性T細胞についても同様に変化はなかった．

2．FIH第I相臨床試験

われわれは，化学療法抵抗性の悪性中皮腫およびそのほかCD26陽性悪性腫瘍をターゲットにした第I相臨床試験をフランスGustave-Roussy Institute Hospital, Cochin Hospital, Lyon Hospital, Caen Hospital, Dijon Hospitalの5施設で実施した[19]．0.1～6.0 mg/kgの6容量・3例または6例/コホートからなり，第4コホートの途中までは隔週投与で1か月間計3回の投与，その後ヒト化CD26抗体の血中濃度をさらに上げるためプロトコールを変更して，1か月間毎週計5回投与を行い投与終了2週後にmodified RESISTにてその有効性を評価した．化学療法剤抵抗性悪性腫瘍141症例のCD26発現をスクリーニングして20%以上病理組織標本においてCD26陽性の場合にその対象症例とした．総計33例の化学療法抵抗性の固形がんで，23例が進行性悪性中皮腫，10例が腎がんであった．結果は，13例がProgressive Disease(PD)，13例がStable Disease(SD)，7例が評価不能であった．さらに，悪性中皮腫の評価可能例19例中10例がSDと評価され，5例が6か月以上SDを継続し，1例が3か月以上SDを継続し，有効性を示唆するデータも得られた．安全性に関して注射後反応が2例あったが，ステロイドの前投薬でこの副反応はみられなくなった．加えて，免疫不全をはじめとして特記すべき有害事象は認められず，安全性も実証された[19]．以上の結果により，YS110は，悪性中皮腫の第I相臨床試験に使用された薬剤25種類のうち，FAK阻害薬，c-KIT阻害薬に並んで3つの有望な薬剤の1つに選ばれ[20]，さらに，Lancet誌の腫瘍学専門誌「The LANCET Oncology」にて紹介された[21]．現在，本邦においても，MPM患者を対象とした国内第I/II相試験が進行している(ClinicalTrials.gov Identifier, NCT03177668)．

CD26抗体療法の多彩な作用機序について

CD26の機能の一つにDPPIV酵素活性があり，生体内でさまざまな生理活性物質がその基質となることが知られている．血糖コントロールにかかわるインクレチンもDPPIVの基質であり，DPPIV阻害薬は経口血糖降下薬として臨床応用されている．免疫系においては，CXCL10などのケモカインもDPPIVによる切断を受けその細胞遊走活性が不活化される[22)23]．CXCL10は活性化T細胞に発現する受容体CXCR3に結合してT細胞の遊走を促進し，炎症巣やがん組織に免疫反応を誘導するケモカインである．最近，経口血糖降下薬のDPPIV阻害薬投与によりケモカインCXCL10の分解を抑制した結果，腫瘍特異的活性リンパ球であるCXCR3陽性T細胞が腫瘍周囲に集簇し，その結果，腫瘍の増殖抑制をもたらすことが，担がんマウスモデルによって証明された[24]．CD26抗体はDPPIV酵素活性自体に直接は影響しないが，CD26抗体投与により血中の可溶性CD26の量が顕著に低下し，DPPIV酵素活性も同様に低下することが示されている[19)25]．DPPIV酵素活性の低下により特にCXCL10のケモカインの切断と不活性化が抑えられ，CXCR3陽性T細胞が腫瘍組織に遊走しやすくなり，腫瘍細胞を破壊する可能性が考えられている(図3)[26]．

さて，がん細胞には免疫系からの攻撃を逃れるさまざまな機構が備わっている[27]．たとえば，制御性リンパ球・樹状細胞などから分泌される免疫制御因子TGF-β，IL-10が腫瘍免疫を抑制し，腫瘍細胞上のMHCクラスIの発現低下が生じて腫瘍特異的細胞傷害性T細胞が無力化され，さらにCTLA-4，PD-1，LAG3などの免疫チェックポイント分子がT細胞表面に発現誘導され，その結果，抗腫瘍性T細胞機能が抑制される[27]．現在，臨床現場では，CTLA-4抗体やPD-1/PD-L1抗体による免疫チェックポイント阻害により抗腫瘍免疫効果を亢進させる治療が行われ，著明な効果を上げている[28]．一方，われわれは，CD4Tリンパ球の中に，CD26分子シグナルによりIL-10およびLAG-3分子の発現が上昇するサブセットを同定し，CD26分子が免疫チェックポイント分子としても機能していることを発見した[29]．さらに，米国のグループも，ヒトCD4陽性制御性T細胞におけるCD26陽性サブセットはT細胞受容

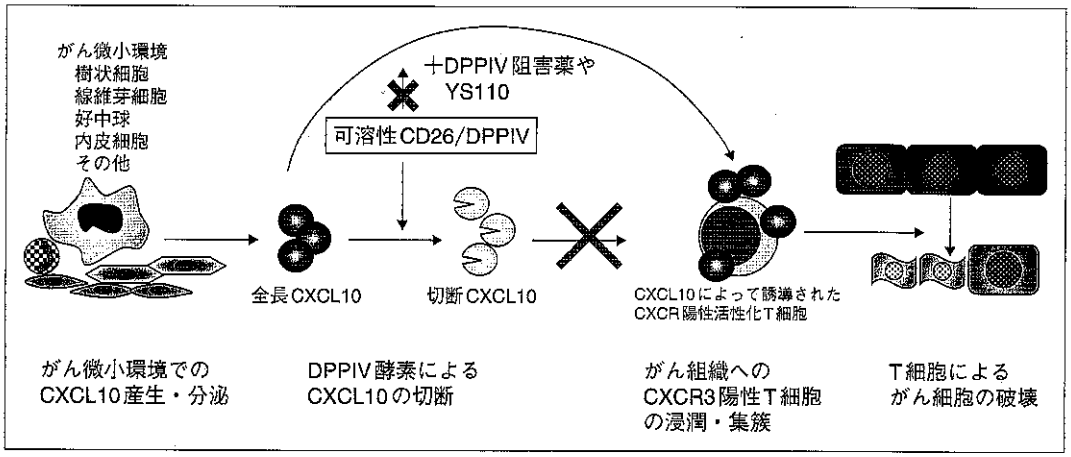

図3　DPPIV阻害薬によるT細胞依存性抗腫瘍効果のメカニズム
がん微小環境で産生分泌されるCXCL10はその受容体CXCR3に結合して活性化T細胞をがん組織に誘導するが，血液などの生体内に存在する可溶性CD26/DPPIVによりCXCL10は切断され不活化されるため，T細胞の遊走が抑制される．しかし，DPPIV阻害薬やYS110による可溶性CD26/DPPIVの低下によりCXCL10の不活化が抑制されることにより，活性化T細胞の遊走が促進され，がん組織におけるT細胞依存性抗腫瘍効果が増強される．
（文献[32] p. 792, Figure 1より改変）

体刺激において最もIL-10を強く産生する制御性T細胞であることを見出し，われわれの結果を支持するデータを報告している[30]．このように，ヒトCD4T細胞に強いCD26共刺激シグナルが伝達すると代表的抑制性サイトカインのIL-10の強産生および免疫チェックポイント分子のLAG-3分子の発現が誘導されることが明らかとなり，がん微小環境においてCD26分子は，IL-10高産生，LAG-3分子の高発現を通じて免疫チェックポイント分子として機能している可能性が示唆された．その結果，CD26抗体の投与によりこれら免疫チェックポイントが阻害され抗腫瘍免疫をさらに促進するものと考えられる[26)29)]．

おわりに

CD26分子の免疫系およびがんの機能およびヒト化CD26抗体YS110の前臨床でのデータおよびフランスでの第I相臨床試験の結果を説明した．本抗体はすでに，本邦でも治療抵抗性の悪性中皮腫を対象として国内第I/II相臨床試験を実施している．さらに，われわれは臨床試験と並行して，YS110のエピトープとは交叉しない新たな抗ヒトCD26モノクローナル抗体を樹立し，パラフィン固定病理組織標本やフローサイトメトリー，ELISAなどの検査できわめて良好な性能を示すコンパニオン診断薬を開発した．このコンパニオン診断薬の開発により，YS110治療中あるいは治療後においても標的分子の精密なモニタリングが可能となり，薬効と副反応の監視を厳密に行える基盤が整った．

CD26分子は悪性中皮腫以外にも非小細胞性肺がん，肝がん，大腸がん，腎がんなど幅広く発現しており，これらの細胞株においても担がんマウスの系でヒト化抗体の有効性を確認しており，さらに化学療法剤との相乗作用の結果も得ている．CD26抗体は直接的な抗がん作用以外にも免疫チェックポイント阻害など非常にユニークな機能を有しており，今後その対象を拡大させていく予定で，がんに苦しむ患者さんに少しでも役立つことを願っている．

文　献

1) Ohnuma K, Dang NH, Morimoto C. Revisiting an old acquaintance : CD26 and its molecular mechanisms in T cell function. Trends Immunol 2008 ; 29 : 295.
2) Dang NH, Torimoto Y, Schlossman SF, Morimoto C. Human CD4 helper T cell activation : functional involvement of two distinct collagen receptors, 1F7 and VLA integrin family. J Exp Med 1990 ; 172 :

649.

3) Aoe K, Amatya VJ, Fujimoto N, et al. CD26 overexpression is associated with prolonged survival and enhanced chemosensitivity in malignant pleural mesothelioma. Clin Cancer Res 2012 ; 18 : 1447.

4) Inamoto T, Yamada T, Ohnuma K, et al. Humanized anti-CD26 monoclonal antibody as a treatment for malignant mesothelioma tumors. Clin Cancer Res 2007 ; 13 : 4191.

5) Yamamoto J, Ohnuma K, Hatano R, et al. Regulation of somatostatin receptor 4-mediated cytostatic effects by CD26 in malignant pleural mesothelioma. Br J Cancer 2014 ; 110 : 2232.

6) Okamoto T, Iwata S, Yamazaki H, et al. CD9 negatively regulates CD26 expression and inhibits CD26-mediated enhancement of invasive potential of malignant mesothelioma cells. PLoS One 2014 ; 9 : e86671.

7) Komiya E, Ohnuma K, Yamazaki H, et al. CD26-mediated regulation of periostin expression contributes to migration and invasion of malignant pleural mesothelioma cells. Biochem Biophys Res Commun 2014 ; 447 : 609.

8) Eguchi K, Ueki Y, Shimomura C, et al. Increment in the Ta1^{+} cells in the peripheral blood and thyroid tissue of patients with Graves' disease. J Immunol 1989 ; 142 : 4233.

9) Morimoto C, Torimoto Y, Levinson G, et al. 1F7, a novel cell surface molecule, involved in helper function of CD4 cells. J Immunol 1989 ; 143 : 3430.

10) Yan S, Marguet D, Dobers J, et al. Deficiency of CD26 results in a change of cytokine and immunoglobulin secretion after stimulation by pokeweed mitogen. Eur J Immunol 2003 ; 33 : 1519.

11) Ho L, Aytac U, Stephens LC, et al. In vitro and in vivo antitumor effect of the anti-CD26 monoclonal antibody 1F7 on human CD30+ anaplastic large cell T-cell lymphoma Karpas 299. Clin Cancer Res 2001 ; 7 : 2031.

12) Ghani FI, Yamazaki H, Iwata S, et al. Identification of cancer stem cell markers in human malignant mesothelioma cells. Biochem Biophys Res Commun 2011 ; 404 : 735.

13) Yamazaki H, Naito M, Ghani FI, et al. Characterization of cancer stem cell properties of CD24 and CD26-positive human malignant mesothelioma cells. Biochem Biophys Res Commun 2012 ; 419 : 529.

14) Amatya VJ, Takeshima Y, Kushitani K, et al. Overexpression of CD26/DPPIV in mesothelioma tissue and mesothelioma cell lines. Oncol Rep 2011 ; 26 : 1369.

15) Ohnuma K, Ishii T, Iwata S, et al. G1/S cell cycle arrest provoked in human T cells by antibody to CD26. Immunology 2002 ; 107 : 325.

16) Inamoto T, Yamochi T, Ohnuma K, et al. Anti-CD26 monoclonal antibody-mediated G1-S arrest of human renal clear cell carcinoma Caki-2 is associated with retinoblastoma substrate dephosphorylation, cyclin-dependent kinase 2 reduction, p27^{kip1} enhancement, and disruption of binding to the extracellular matrix. Clin Cancer Res 2006 ; 12 : 3470.

17) Yamada K, Hayashi M, Du W, et al. Localization of CD26/DPPIV in nucleus and its nuclear translocation enhanced by anti-CD26 monoclonal antibody with anti-tumor effect. Cancer Cell Int 2009 ; 9 : 17.

18) Havre PA, Abe M, Urasaki Y, et al. The role of CD26/dipeptidyl peptidase IV in cancer. Front Biosci 2008 ; 13 : 1634.

19) Angevin E, Isambert N, Trillet-Lenoir V, et al. First-in-human phase 1 of YS110, a monoclonal antibody directed against CD26 in advanced CD26-expressing cancers. Br J Cancer 2017 ; 116 : 1126.

20) Raphael J, Le Teuff G, Hollebecque A, et al. Efficacy of phase 1 trials in malignant pleural mesothelioma : description of a series of patients at a single institution. Lung Cancer 2014 ; 85 : 251.

21) Das M. Monoclonal antibody YS110 for refractory solid tumours. Lancet Oncol 2017 ; 18 : e247.

22) Ohnuma K, Hosono O, Dang NH, Morimoto C. Dipeptidyl peptidase in autoimmune pathophysiology. Adv Clin Chem 2011 ; 53 : 51.

23) Ohnuma K, Morimoto C. DPP4 (dipeptidyl-peptidase 4). Atlas Genet Cytogenet Oncol Haematol 2013 ; 17 : 301.

24) Barreira da Silva R, Laird ME, Yatim N, et al.

Dipeptidylpeptidase 4 inhibition enhances lymphocyte trafficking, improving both naturally occurring tumor immunity and immunotherapy. Nat Immunol 2015 ; 16 : 850.

25) Ohnuma K, Hatano R, Aune TM, et al. Regulation of pulmonary graft-versus-host disease by IL-26+CD26+CD4 T lymphocytes. J Immunol 2015 ; 194 : 3697.

26) Ohnuma K, Hatano R, Morimoto C. DPP4 in antitumor immunity : going beyond the enzyme. Nat Immunol 2015 ; 16 : 791.

27) Joyce JA, Fearon DT. T cell exclusion, immune privilege, and the tumor microenvironment. Science 2015 ; 348 : 74.

28) Sharma P, Allison JP. The future of immune checkpoint therapy. Science 2015 ; 348 : 56.

29) Hatano R, Ohnuma K, Otsuka H, et al. CD26-mediated induction of EGR2 and IL-10 as potential regulatory mechanism for CD26 costimulatory pathway. J Immunol 2015 ; 194 : 960.

30) Hua J, Davis SP, Hill JA, Yamagata T. Diverse gene expression in human regulatory T cell subsets uncovers connection between regulatory T cell genes and suppressive function. J Immunol 2015 ; 195 : 3642.

31) Ohnuma K, Hatano R, Yamazaki H, et al. CD26-Targeted Therapy : A New Horizon in Malignant Pleural Mesothelioma Management. In : Watanabe HS. Horizons in Cancer Research Volume 64. New York : Nova Science Publishers, Inc ; 2017. pp. 129-161.

32) Ohnuma K, Hatano R, Morimoto C. DPP4 in antitumor immunity : going beyond the enzyme. Nat Immunol 2015 : 16 : 791.

* * *

原　著

胸膜中皮腫患者の経時的ケアニーズとQOL向上のための支援

野村伽奈子[1)]，亀谷友理恵[1)]，原　桂子[1)]，中川　淳子[1)]
池元　友子[1)]，菊地　馨[1)]，岸本　卓巳[2)]，藤本　伸一[2)]
[1)]岡山労災病院看護部
[2)]岡山労災病院アスベスト研究センター

（平成29年8月16日受付）

要旨：【背景】悪性胸膜中皮腫（中皮腫）は急激に進行する悪性疾患であり，患者の主観的なニーズとクオリティオブライフ（QOL）向上のための支援を迅速に提供することが求められる．しかし，中皮腫における経時的な患者のケアニーズやQOL向上のためのケアについて調査した研究はほとんどない．

【方法】中皮腫と診断され岡山労災病院で治療中の入院患者のうち，研究内容を説明し同意を得られた患者に半構成的面接を行った．グラウンデッド・セオリー・アプローチに基づき，まず研究参加者の語った内容を元に逐語記録を作成し，診断，治療選択，治療開始，入院中など，病気の進行にそって経時的にQOL向上のために必要な支援について分析した．

【結果】参加者は60～80歳代の男性4名．分析の結果，138コード，33サブカテゴリー，14カテゴリーが抽出された．ケアニーズについては，1）先行きの見えない不安に戸惑う，2）先行きの見えない不安を乗り越えていく，3)先行きのみえない不安に戸惑いながらも残された時間を生きるという3つのプロセスに構造化され，先行きの見えない不安とともに生きるという中核カテゴリーが抽出された．

【まとめ】中皮腫が希少疾患であるための様々な苦悩が語られ，病気のことを知りたい，誰かに聞いてもらいたいという思いが強くみられた．中皮腫のケアにおいては，患者が知りたい情報を提供し，支援するサポート体制を充実させることが必要である．また残された時間の過ごし方や自己実現に向けての希望は様々であり，その思いを引き出し実現に向けての支援を行うことが重要である．

（日職災医誌，66：164―171，2018）

―キーワード―
アスベスト，胸膜中皮腫，クオリティオブライフ

I．はじめに

胸膜中皮腫（中皮腫）は胸膜に発生する悪性腫瘍であり，そのほとんどがアスベスト（石綿）ばく露によっておこる．2015年の我が国の中皮腫による死亡は約1,500件である[1)]が，今後も患者数は増加し2000年から40年間で男性だけでも10万人が死亡するとの予測もある[2)]．中皮腫はごく早期の外科療法以外に根治療法がなく，5年生存率は3.7％と極めて予後が悪い[3)]．また進行が速いため病気と向き合う期間が短く，肺がんと比べて痛みや呼吸困難の出現頻度も高い[4)]．我が国は大量の石綿を消費してきたが，欧米に比べて中皮腫の発生が遅れたため，本疾患に関する情報が少なく，そのため看護の歴史も浅い．以上のようなことから看護師は中皮腫に関する知識が不足しており，肺がん患者と同様のケアを行っているのが現状である．当院は石綿関連疾患研究施設であり，中皮腫患者が多く在院する．しかし，中皮腫と診断された患者がどのような思いを抱え，どのような支援を望んでいるのかを把握しきれないまま病状が進行してしまい，患者，家族が，周囲からの孤独や，医療従事者から見捨てられたと感じているケースを経験する．

長松らは，急速に進行する中皮腫においては，患者のケアに際し高度に専門的な知識と技術を要するとした上で，看護師の知識と経験不足によって効果的なケアを適切なタイミングで提供できず，結果として患者への支援に失敗し看護師自身の心身の負担が増していると報告し

表1　研究参加者の概要と特徴

	年齢	性別	石綿ばく露歴	病期 (IMIG 分類)	主症状	面接実施時までの治療内容	病脳期間	補償・救済申請状況
A氏	61	男	化学工場にて職業性石綿ばく露歴あり	IV	胸痛	カルボプラチン＋ペメトレキセド4コース施行後．外科的治療について検討中．	約5カ月間	救済法認定
B氏	65	男	配管作業にて職業性石綿ばく露歴あり	III	なし	シスプラチン＋ペメトレキセド4コース，ゲムシタビン2コース施行後．新規薬剤の治験参加中．	約14カ月間	労災補償認定
C氏	81	男	建設業にて職業性石綿ばく露歴あり	II	胸痛	カルボプラチン＋ペメトレキセド施行中．	約1カ月間	労災補償申請中
D氏	72	男	石綿ばく露歴なし	III	なし	シスプラチン＋ペメトレキセド4コース施行後．新規薬剤の治験参加中．	約9カ月間	救済法申請中

ている[5]．また秋山は，中皮腫患者への訪問看護の経験から，急速に症状が進む中でクオリティオブライフ(QOL)を維持しながらその人らしく過ごせるための調整が不足していると指摘している[6]．

近年，早期からの緩和ケア導入や先を見越したケアプラン作成が患者の緊張と症状の緩和に有効で，医療者との信頼関係構築やより良いエンドオブライフケアを可能にすることが実証されている．また川合ら[7]は，がん患者の真の訴えと患者の QOL 向上に必要な日常生活支援を，患者の主観的観点から具体的に理解することが重要だとしている．このように，がん患者のケアにおいては，患者の主観的なニーズと QOL 向上のための支援をいち早く察知し，迅速に提供することが求められる．しかしながら，中皮腫について経時的な患者のケアニーズや QOL 向上のためのケアについて調査した研究はほとんどない．そこで，中皮腫患者の QOL 向上のためのケアニーズを明らかにすることは，今後の看護ケアの向上に資すると考え本研究に取り組んだ．本研究の目的は，中皮腫患者がどのような思いを抱えているのかを知り，患者の QOL 向上のためのケアニーズを明らかにすることである．

II. 研究方法

1. 研究デザイン

半構成的面接法を用いた質的帰納的研究．

2. 研究対象

中皮腫と診断され岡山労災病院で治療中の入院患者のうち，研究内容を説明し，同意を得られた患者．

3. データ収集方法と分析方法

インタビューガイドを用いた半構成的面接調査で研究対象者に診断から現時点まで時系列に沿って，体験，その時の気持ち，困ったこと，支えとなったあるいは，してほしかったケアについて自由に語ってもらった．インタビューは治療開始前など患者の体調を十分に配慮し時期を決定した．一度の面接所要時間は30分以内で研究対象者の同意を得て IC レコーダーに録音した．分析はグラウンデッド・セオリー・アプローチに基づき実施した．まず研究参加者の語った内容を元に逐語記録を作成し，診断，治療選択，治療開始，入院中など，病気の進行にそって経時的に QOL 向上のために必要な支援について分析した．

4. 倫理的配慮

本研究は岡山労災病院の倫理委員会での承認を受けて実施した．研究への参加は自由意志によるもので，拒否・中断が可能であり，研究参加者が中断を希望する場合は，直ちにデータを廃棄することとした．インタビューは個室・面談室を使用しプライバシーの保護に努めた．またデータは個人を特定しない形で使用し厳重に管理した．

III. 結　果

1. 研究参加者の概要と特徴（表1）

平成28年4月から8月の間に，4名の患者に面接調査を行った．すべて男性であり，そのうち2名は岡山県外から受診していた．4名中3名に石綿ばく露歴があった．

2. 分析結果

文中の【】はカテゴリー，［］はサブカテゴリー，〈〉はコード，「」は研究参加者の発言を表す．本研究では14カテゴリー，33サブカテゴリーが生成された．それらの関連を中皮腫患者のストーリーラインとして概念図（図1)を作成した．分析の結果，中皮腫患者のケアニーズについては，1）先行きの見えない不安に戸惑う，2）先行きの見えない不安を乗り越えていく，3)先行きのみえない不安に戸惑いながらも残された時間を生きる，4)先行きの見えない不安とともに生きるプロセスという4つに構造化された．

1）先行きの見えない不安に戸惑うプロセス（表2）

中皮腫と告知をうけた患者は初期症状からは重篤な病気であることが予測できず，「まさか自分が」と【予期せぬ事態がおとずれ深刻さに戸惑う】，根治療法がなく予後不良な疾患に罹患したことに対し，C氏は「これで終わりという感じ」，B氏は「もう1，2年で死ぬと思った」と語り，【死に至る病になった絶望と孤独】を感じていた．そして，中皮腫における【情報，治療法，施設が限られるという現実】に直面し，患者本人が避け難い【アスベス

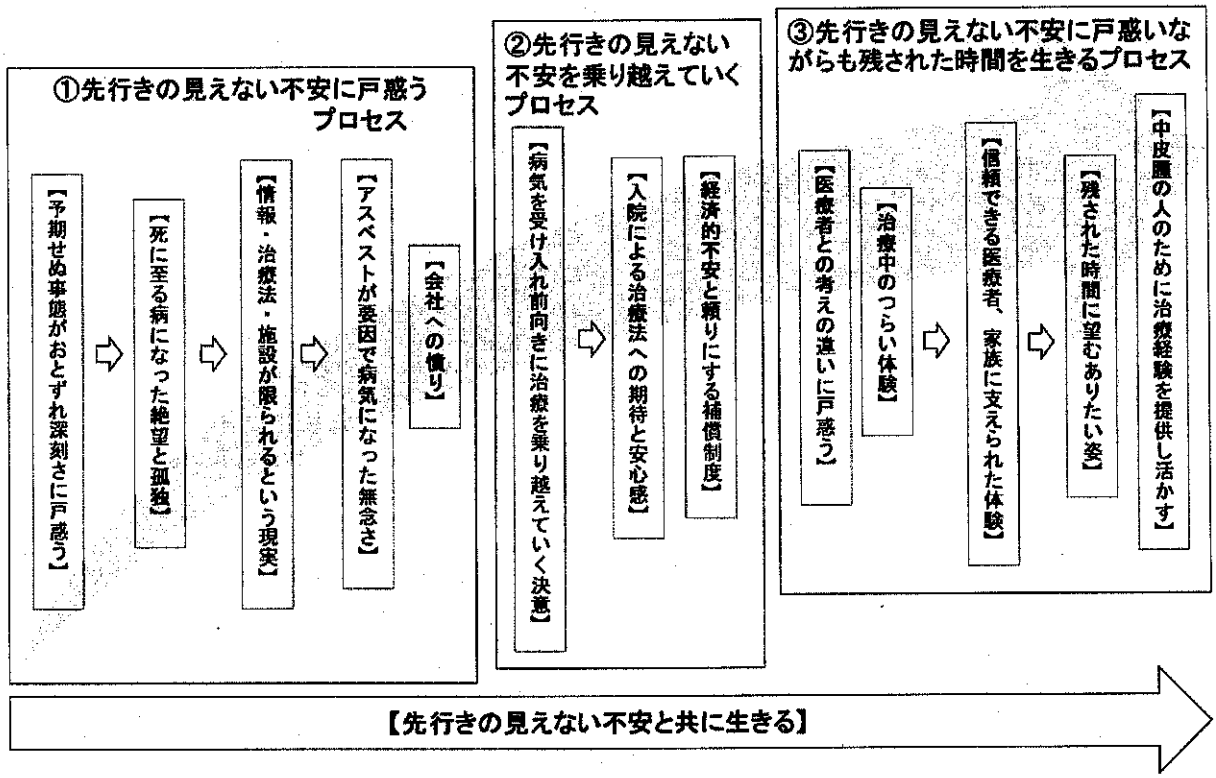

図1　胸膜中皮腫患者の先行きの見えない不安に対する概念図
グラウンデッド・セオリー・アプローチに基づき，患者へのインタビュー内容を文章化した．その上で特徴的な単語などをコード化し分類した．

トが要因で病気になった無念さ】と，やり場のない【会社への憤り】を感じていた．その中でも中皮腫特有といえる【情報，治療法，施設が限られるという現実】に着目すると，自ら<インターネットを使って情報収集>するものの，A氏は「患者向けの情報が少ない」，D氏は「専門的な物が多く分かりにくい」，C氏は「専門的なことが何も分からないからこちらからは聞けない」など，患者にとって有用な情報が得られず，また周りに中皮腫を知る人がいないため<他の患者の経験を知る機会が少ない>など，[少ない情報への戸惑い]がみられた．また，<馴染みの薄い病院で治療することへの不安>や<治療先の選択，治療に致るまでに1カ月の時間を要した>など[治療のできる施設が限られる]ことや，「手術の成功率は50%以下，1番効果の見込める化学療法でも20%くらいしかないと言われた」と[選択できる治療法が少ない現実]に不安を感じていた．

2) 先行きの見えない不安を乗り越えていくプロセス（表3）

先行きの見えない不安に戸惑いながらも【病気を受け入れ，前向きに治療を乗り越えていく決意】をし【入院による治療法への期待と安心感】を強く感じていた．また，今後の予測がつかないため医療費や交通費に対して【経済的不安と頼りにする補償制度】への思いが明らかとなった．

また中皮腫患者は【入院による治療法への期待と安心感】を強く感じていた．治療法が少なく，治療できる施設が限られているという状況の中で，ようやく治療を受けられるという思いで入院し，A氏は「専門の病院と聞いたから安心している」，C氏は「病院を信頼して頑張る」など，専門の病院で<治療が受けられることへの安堵感>や，B氏から「今，自分にはこれ(治験)しかないので，もうやるしかない」や，D氏からは「新しい薬や選択肢が増えれば希望が湧く」と<新しい治療で病状が少しでも軽くなることを願う>といった，[治療への期待]が語られた．

3) 先行きの見えない不安に戸惑いながらも残された時間を生きるプロセス（表4）

治療への期待を持って入院するが，A氏は「先生に治療に耐えられるように見えないと言われた」，B氏は「前の病院の先生に見放されたような気もする」など【医療者との考えの違いに戸惑う】思いがみられた．そして化学療法や手術など治療後の副作用や予後に対する不安，前医での【治療中のつらい体験】を表出した．その中で，【信頼できる医療者，家族に支えられた体験】が支えとなり，【残された時間に望むありたい姿】を考え，【中皮腫の人のために治療経験を提供し活かす】という思いが明らかとなった．

また中皮腫患者は，【信頼できる医療者，家族に支えられた体験】から，【残された時間に望むありたい姿】を見出していた．A氏は「専門の看護師が適切なアドバイス

表2　先行きの見えない不安に戸惑うプロセス

カテゴリー	サブカテゴリー	コード
予期せぬ事態がおとずれ深刻さに戸惑う	今まで体験したことのない息苦しさや体調の変化に戸惑う	自覚はないが息苦しく歩けなくなりしゃがみ込む 寝た方が良いと感じる初めての苦しさの体験 少し散歩したり階段を上がるだけで感じる息苦しさ すぐに落ち着くが孫と遊ぼうとすると動けない 今まで感じたことがない前触れのない息苦しさ いつもと違う体調の変化に戸惑う 胸水が溜まり横になるだけでひどく咳がでる
	診断され事態が深刻だと気付き戸惑う	普段と違うことに気付きすぐに病院へ行った 咳と息切れの原因が病院へ行き初めて分かった 何かあるかもしれないという説明 入院が必要なほど深刻な状況 名前は知っていたが正式な病名を聞き戸惑い落ち込む
	予期せぬ事態を受け入れられない気持ち	まさか自分がという戸惑いと受け入れられない気持ち 風邪だと思っていたら病気になり戸惑う 自分がなるとは予想していなかった アスベストとの関係性が全くないことへの戸惑い 中皮腫になった原因が分からないことに戸惑い受け入れられない
死に至る病になった絶望と孤独	死に至る病になった絶望	中皮腫と聞いて1，2年で死ぬと思い戸惑う 常に付きまとう死への恐怖 家族はさみしいと思っていないと思う 死に至る病になった絶望
	中皮腫の告知におびやかされる命	中皮腫について調べると恐怖心を抱いた 病気が根絶できないということを悟る 自分が重篤な病気と知って大変なことだと思った これで終わりかもしれないというショック
	自分だけがなってしまった中皮腫	身近な人に中皮腫の人はいなかった どうして自分だけがなったという無念さ
情報・治療法・施設が限られるという現実	中皮腫についての知識は診断を受けるまでなかった	父親が同じ病気だったからある程度知っている 中皮腫は厳しい病気という程度の認識で詳しく知らない 診断を受けるまでに中皮腫が予後の悪い病気ということは知っていた 中皮腫についてより裁判や補償のことの方が印象強い
	少ない情報への戸惑い	中皮腫という病気に対する患者向けの情報が少なく不安が強い 中皮腫のことは診断後アスベストと深く関係がある病気と知る インターネットを使って疾患の情報収集 情報不足による治療選択への戸惑い 他の患者の経験を知る機会が少ない 家族が調べてセカンドオピニオンについて知る
	治療のできる施設が限られる	治療先の選択，治療に至るまでに一カ月の時間を要した 馴染みの薄い病院で治療をすることへの不安 療養環境の選択に対する心配 ここでの治療が終わったら家から近い前の病院へ戻りたい
	選択できる治療法が少ない現実	中皮腫の手術は難しいため薬で治療すると勧められる 抗がん剤の効果がなくなり新たな治療法を選択 リスクが高いため手術という選択肢はない 選択できる治療法が少なく治療効果が悪いという事実
アスベストが要因で病気になった無念さ	職場環境が要因で病気になった無念さ	職場が要因で病気になったことに対する無念さ
	アスベストの現場で働いてきた記憶	アスベストは研究室にいるときに使う程度 20年くらいアスベストを取り扱っている職場で働いた 朝から晩まで働いた記憶
	アスベストにばく露したと思われる父親の職場	幼少期に数回父親の職場に行った思い出 父親の作業服から石綿ばく露した疑い 父親と同じ職場だった中皮腫の叔父さんと自分は同じ症状
会社への憤り	アスベストを取り扱う会社への怒り	昔は会社への怒りがあった
	会社の補償制度への不満	労災申請に会社は消極的な態度 会社の補償制度への不満
	仕事に対する感謝の思い	仕事内容に不満なく定年まで働けたことへの感謝の思い 叔父の経営する会社なので恩義があり補償について言うつもりはない 会社に対しては怒りよりもお世話になったという感謝の思いの方が強い

表3　先行きの見えない不安を乗り越えていくプロセス

カテゴリー	サブカテゴリー	コード
病気を受け入れ前向きに治療を乗り越えていく決意	治療を乗り越えていく決意	医師と相談し納得した治療をしたいという強い思い 選択した治療に対する意気込みの強さ，決意 どんな不安があっても乗り越える覚悟 手術で完治する期待が大きくリスクはあるが耐えれるという思い 根絶することは難しいと理解していて病気が少しでも良くなることを願う 病気を受け入れ前向きに頑張ってみようと思う治療への決意
	病気を受け入れ前向きに過ごそうとする意志	受け入れようとする気持ち 病気に対する理解も増し前向きに過ごそうとする意志 病気になったのは仕方のないことと受け入れようとする思い
	頼りにする補償制度	労災認定，補償制度は申請中 労災補償制度があり経済的負担はない 認定に関してはスムーズに受け入れられたのでストレスはない
入院による治療法への期待と安心感	入院による安心感	入院生活はいざという時に安心できる 治療に対しての期待が高く遠方からの通院でも苦痛はない 入院していた方が安心で療養生活の苦痛は少ない
	治療への期待	受け入れられない気持ちと治療への期待 治療が受けられることへの安堵感 新しい治療法が増えることに希望を持ち支えられる 新たな治療法の選択・期待 治療の効果が高いため期待する気持ち 新しい治療で病状が少しでも軽くなることを願う 治療が合ったおかげで現在は十分に生活できる体調 現治療法を決意したいことへの満足感
経済的不安と頼りにする補償制度	治療費や家族の生活費等の経済的不安	経済的不安があり早く働きたいという思い 今後の予測がつかない

をくれた」，D氏は「看護師が専門的に教えてくれ，献身的にしてくれて安心」などと，＜看護師が専門的，献身的に対応してくれて安心した＞など中皮腫のことをよく理解して関わる看護師が支えになっていることを表出した．また，C氏は「先生を信頼している．任せている」，D氏は「先生に頼らないとどうにもならない」など，＜病院，医師への期待，安心感＞を表出した．またA氏は「何かあったら家族が調べてくれる」，B氏は「息子が補償に詳しいので任せている」などと，［頼りになる家族の支え］を表出した．このように患者にとって【信頼できる医療者，家族に支えられた体験】は大きな心の支えになっていたほか，「やり残したことがないようにしたい，自分のデータを参考に胸膜中皮腫の人がちょっとでも気分が楽になってくれたらありがたい」と＜残された時間の大切さ＞や，情報が少ない中皮腫患者ために＜情報提供を惜しまない＞ことで【中皮腫の人のために治療経験を提供し活かす】という，【残された時間に望むありたい姿】を表出した．

4) 先行きの見えない不安とともに生きるプロセス（表5）

すべてのプロセスに共通してみられたのが【先行きの見えない不安と共に生きる】であり，これを中核カテゴリーとした．＜予期せぬ事態（診断）＞から＜中皮腫という病気に対する情報が少ない＞こと，＜選択できる治療法が少なく，治療しているのに改善されない症状＞，＜予後への不安＞などが表出され，それぞれのプロセスでつきまとう［先行きのみえない不安］と戦いともに生きていることが明らかになった．

Ⅳ. 考　　察

本研究では，中皮腫が希少疾患であることによると思われる様々な苦悩が表出された．研究参加者からは，病気のことを知りたい，誰かに聞いてもらいたいという思いが強くみられた．鶴若らは[8]「語る行為には，語ることによる意味の生成が含まれている．人間は自分が置かれている状況や経験を，物語を作るようにして意味づける」と述べている．患者は語ることによって，今までの自分の経験や思いを整理することができ，この先の自分のことを考えることができるといえる．また，長松は中皮腫患者との関わりについて「中皮腫患者が体験する恐怖に耳を傾け，必要な時に支援の手を差し伸べること，患者と家族にとって医療従事者が示す情熱と共感は，何よりも重要な意味をもつ」と述べている[9]．中皮腫患者に十分に思いを語ってもらうことで，そこに至るまでの背景やそれに伴う苦悩を知り理解することがより重要であるといえる．

また，選択できる治療法が少なく，治療できる施設が限られるという問題に直面した中皮腫患者は，ようやく治療が開始できるということが希望となり，治療に対して前向きに強い期待感を持っていた．新たな治療法への

表4　先行きの見えない不安に戸惑いながらも残された時間を生きるプロセス

カテゴリー	サブカテゴリー	コード
医療者との考えの違いに戸惑う	医療者との気持ちのズレに戸惑う	医師の治療に対する考え方の違いに戸惑う 見放されたという思い 前医との関係も大切にしたい 医療者との気持ちのズレ
	他者から見た自分に対する不満	他人から第一印象で弱々しく見られた 自分のことを理解してもらえていないことへの不満
治療中のつらい体験	治療中のつらい体験	口に合わない病院食 化学療法による副作用を体験し苦痛 初回の副作用が強すぎて通常クール通り治療が行えなかった 便秘による食欲低下
	副作用に対する不安	化学療法による身体的変化 薬が効かないのは精神的な要因が関与している 副作用に対する不安・苦痛
信頼できる医療者，家族に支えられた体験	療養生活で医療者に支えられた体験	病院，医療者への信頼や安心感がある 看護師の丁寧親切な対応，日常会話，優しさに支えられた体験 療養生活の支えは身近な看護師 専門，認定看護師の存在 医療者との関係性やサポート体制があり安心できる 看護師が専門的，献身的に対応してくれて安心した 体調が変化したときの対処法を具体的に指示してほしいという要望
	信頼できる医師の存在	病院・医師への期待，安心感 医師が病状に合わせた治療法や治療先を探してくれたという安心感 医師との信頼関係は良好 一番の心配は医師との信頼関係を失うこと 見放されたくないという思い
	頼りになる家族の支え	家族の支えが頼りで，不安がある時は側にいてほしい 何かあれば家族がサポートしてくれる安心感 家族が心配してくれているということが支えになっている 家族が面会に来ると安心する
残された時間に望むありたい姿	自己を肯定し治療に励む	自分の体力に自信がある 免疫力を上げるための行い
	残された時間に望むありたい姿	残された時間の大切さ 前向きに生きたいという気持ち 人に迷惑をかけなくて良いと思うほどの体調 人の手を借りずに生活できる状態を長く保ちたい 友人との時間が今の楽しみ 死ぬまでにやり残したことがないようにしたい
中皮腫の人のために治療経験を提供し活かす	中皮腫の人のために治療経験を提供し活かす	起こりえる状況の記録整理 情報が少ない中皮腫の人の為自分のデータを提供する 情報提供をおしまない 今までの治療の経験を活かそうとしている

表5　先行きの見えない不安とともに生きるプロセス

カテゴリー	サブカテゴリー	コード
先行きの見えない不安と共に生きる	先行きの見えない不安	予期せぬ事態（診断） 診断を受けて病気についてすぐ知りたい気持ち 中皮腫という病気に対する情報が少ない 死に至る病になった絶望 何かあるかもしれないという説明 なかなか診断がつかず何か大きな病気になっているのではという不安 前医では治療が出来ず大きな病院へ紹介された 病気が根絶できないということを悟る 自分が重篤な病気と知って大変なことだと思った 選択できる治療法が少なく，治療しているのに改善されない症状 化学療法による身体的変化 家にいると体調を気にして不安になる 術後の経過や日常生活に対する不安 予後への不安

期待も高まっていた．このことから中皮腫の診療にあたる施設の看護師は，患者の前向きな思いを支えるように，患者の知りたい情報を提供できる専門知識が求められ，また医師や他職種と情報共有し，サポート体制を充実させることが必要である．

中皮腫患者は周りの人に自分のことを理解してもらえないという孤独感や，疾患や治療に伴う副作用などの苦痛を体験し，体調の変化に不安を抱えている．その中で，残された時間を懸命に前向きに生きようとしており，家族や医療従事者の存在が患者の支えであることが明らかになった．残された時間をどのように過ごしたいかは人によって異なるが，自己実現に向けての思いを引き出し，実現に向けて支援を行うことが重要である．

V. 結　論

中皮腫患者は絶えず先行きの見えない不安とともに生きている．患者に思いを十分語ってもらうことでその不安を具体化し，ケアニーズを明らかにすることができる．看護師をはじめとする医療従事者は，胸膜中皮腫という疾患を十分に理解した上で個々の患者のケアニーズを察知し，それに対するベストサポートを提供する必要がある．

謝辞：本研究のインタビューに参加してくださった患者様，ご指導をしてくださった山陽大学教授富岡美佳先生，聖路加国際大学大学院看護学研究科准教授長松康子先生に感謝致します．

本研究は，労災疾病臨床研究補助金事業「胸膜中皮腫に対する新規治療法の臨床導入に関する研究」(研究代表者　藤本伸一)の一部として行った．

利益相反：利益相反基準に該当無し

文　献

1) 厚生労働省：アスベスト(石綿)情報　都道府県別にみた中皮腫による死亡数の年次推移（平成7年から28年）．2017.

2) Murayama T, Takahashi K, Natori Y, Kurumatani N: Estimation of future mortality from flexural malignant mesothelioma in Japan based on an age-cohort model. Am J Ind Med 49: 1—7, 2006.

3) 三浦溥太郎：中皮腫—臨床，石綿ばく露と補償・救済．増補新装版．森永謙二編．東京，三信図書，2008, pp 153—172.

4) Helen Clayson，長松康子，中山祐紀子：ナースのための胸膜中皮腫緩和ケアハンドブック．胸膜中皮腫看護研究会，2013.

5) 長松康子，堀内成子，名取雄司：胸膜中皮腫患者のケアにおける看護師の困難．ヒューマンケア研究　13：40—52, 2012.

6) 秋山正子：患者と家族のケアについて，医療関係者のためのアスベスト講座「石綿関連疾患—診断・ケア・予防—」．2006, pp 78—91.

7) 川井みどり，坂本清美，中山サツキ，崎山三代：終末期卵巣がん患者の看護～QOL調査票の活用による効果的な援助の試み～．大阪医科大学付属看護専門学校紀要　12：24—28, 2006.

8) 鶴若麻理，麻原きよみ：ナラティブでみる看護倫理～6つのケースで感じるちからを育む～．東京，南江堂，2013, pp 4.

別刷請求先　〒702-8055　岡山市南区築港緑町 1—10—25
岡山労災病院アスベスト研究センター
藤本　伸一

Reprint request:
Nobukazu Fujimoto
Research Center for Asbestos-related Diseases, Okayama Rosai Hospital, 1-10-25, Chikkomidorimachi, Minami-ku, Okayama, 702-8055, Japan

Appropriate Care for Patients of Malignant Pleural Mesothelioma Based on Their Needs to Maintain Quality of Life

Kanako Nomura[1], Yurie Kameya[1], Keiko Hara[1], Junko Nakagawa[1], Tomoko Ikemoto[1], Kaoru Kikuchi[1], Takumi Kishimoto[2] and Nobukazu Fujimoto[2]
[1]Department of Nursing, Okayama Rosai Hospital
[2]Asbestos Research Center, Okayama Rosai Hospital

Background: Malignant pleural mesothelioma (MPM) is a neoplasm which grows rapidly. Medical staff should give appropriate care to the patients of MPM based on their needs to maintain quality of life. However, to date, there are few studies to examine the needs of the patients and appropriate care for patients of MPM.

Methods: A semi-structured interview was given to patients who were diagnosed as MPM based on their informed consent. The interview was recorded literally according the Grounded Theory Approach and analyzed with time along the clinical course of MPM including diagnosis, treatment, and progression of the disease.

Results: 4 male patients participated in the study. Through the act of the interview, the patients talked about their suffering and expressed desires to know about the detail of the disease or to be respectfully heard by anyone else. Analysis of the content of the interview extracted 138 codes, 33 subcategories, and 14 categories. The care needs were organized in 3 processes such as 1) bewilderment by uncertainty, 2) overcome the uncertainty, and 3) get together with the uncertainty in the time left. Based on these analyses, a core category was extracted as 'get together with the uncertainty.'

Conclusions: The patients of MPM have various desires about the way of spending the time left or about self-fulfillment. It is important to draw the patient's desire and support for their accomplishment. In addition, it is essential for the care of patients of MPM to enhance the support function to provide the information that they want.

(JJOMT, 66: 164—171, 2018)

—Key words—
asbestos, pleural mesothelioma, quality of life

労災疾病等医学研究 1　R1—1

胸膜中皮腫初診時の胸部 CT 画像の検討について

岸本　卓巳，藤本　伸一
岡山労災病院アスベスト研究センター

（平成 30 年 1 月 17 日受付）

要旨：胸膜中皮腫 782 例の初診時の画像所見について胸部 CT 上以下の 7 パターンすなわち，①単発胸膜腫瘤形成，②環状胸膜肥厚，③軽度胸膜肥厚，④縦隔側胸膜肥厚，⑤胸水のみ，⑥多発性腫瘤形成，⑦特殊型に分けてその頻度を検討したところ，環状胸膜肥厚が 39.0%，多発性腫瘤形成が 14.9%，縦隔側胸膜肥厚が 14.8%，軽度胸膜肥厚 12.7%，単発胸膜腫瘤形成 9.2%，胸水のみ 8.4% であった．各組織型とも環状胸膜肥厚が最も多かったが，上皮型及び二相型では縦隔側胸膜肥厚，肉腫型では多発性腫瘤形成が 2 番目に多かった．一方，二相型では単発胸膜腫瘤形成が 6.4%，肉腫型では胸水のみが 2.7% と低率であった．

年代別では～2008 年までは環状胸膜肥厚，多発性腫瘤形成が多かったが，2009 年以降には縦隔側胸膜肥厚，胸水のみが増加傾向を示した．

岡山労災病院の 166 例について予後を検討したところ，組織型別では上皮型では生存期間中央値は 14.3 カ月と非上皮型に比較して有意（$p<0.05$）に良好であった．

Staging 別では，Stage I は 24.4 カ月，Stage II は 17.0 カ月と比較的良好であったが，Stage III は 10.4 カ月，Stage IV は 8.6 カ月と予後不良であり，早期病変と進行期の間には有意差（$p<0.05$）を認めた．画像別では単発胸膜腫瘤形成は手術により予後良好な症例が一定数いるが，生存期間中央値ではその他のパターンと差異はなかった．一方，胸水のみあるいは軽度胸膜肥厚はその他のパターンに比較して予後良好傾向を示したが，有意差はなく画像形態と予後の間には一定の関連性は認められなかった．

（日職災医誌，66：239—245，2018）

—キーワード—
胸膜中皮腫，環状胸膜肥厚，胸水のみ

はじめに

胸膜中皮腫は石綿ばく露によって発症する特異な悪性腫瘍であるが，診断後は予後が不良で，早期に診断して手術療法を施行することが唯一の治癒が望まれる治療方法である．化学療法としては 2007 月に CDDP＋pemetrexed 併用療法が有効な治療として承認されて以降，有効な治療法がないのが現状である．そこで，初診時の胸部 CT 画像に注目して，特徴を 7 パターンに分類し，そのパターン別に集計し，生存期間との関連について検討する．

対象と方法

対象は 2003～2008 年までに胸膜中皮腫で死亡した症例のうち過去の全国調査で組織型の確定できた 482 例，2000～2016 年までに岡山労災病院で診断した 166 例，2005～2016 年までに山口宇部医療センターで診断した 110 例，2006～2016 年までに札幌南三条病院で診断した 24 例の合計 782 例について，初診時の胸部 CT 画像の特徴について検討した．

方法は胸膜中皮腫の初診時の画像所見について胸部 CT 上以下の 7 パターンすなわち，①単発胸膜腫瘤形成，②環状胸膜肥厚，③軽度胸膜肥厚，④縦隔側胸膜肥厚，⑤胸水のみ，⑥多発性腫瘤形成，⑦特殊型（表 1）に分けて，その頻度を検討した．

さらに病理組織型及び年代別（2008 年までと 2009 年以降）に分けて比較検討した．

また，岡山労災病院の症例については病理組織型，Stage，画像パターン別の生存期間について検討した．Staging は IMIG1995 分類に従って分類した[1]．また，生存期間の有意差は Wilcoxon rank sum test により，$p<0.05$ を有意差ありとした．

結　果

1) 対象者は表2に示すように，782例で，男性657例，女性125例である．2005年の兵庫県尼崎市の旧クボタ神崎工場周辺の環境ばく露による中皮腫の発生が社会問題化した3年後の2008年を境界としてその前後の診断状況について検討したところ，それ以前が594例，その後が188例であった．2008年までは70歳未満が60.6%であったが，2009年以降は48.4%と高齢者が多くなる傾向にあった．782例中胸水を伴う症例が89.1%あった．また組織型別では上皮型59.6%，二相型18.3%，肉腫型21.5%，特殊型が0.6%であった．

表1　胸膜中皮腫の初診時胸部CT画像の特徴

- 1：単発胸膜腫瘤形成
- 2：環状胸膜肥厚（厚みがおおむね3mm以上）
- 3：軽度胸膜肥厚（厚みが3mm未満）
- 4：縦隔側胸膜肥厚
- 5：胸水のみ
- 6：多発性腫瘤形成（漿膜腫瘤）
- 7：特殊型（胸壁腫瘤形成，縦隔腫瘤形成等）

2) 782例の画像パターン別では，図1のごとく環状胸膜肥厚が39.0%，多発性腫瘤形成が14.9%，縦隔側胸膜肥厚が14.8%，軽度胸膜肥厚12.7%，単発胸膜腫瘤形成9.2%，胸水のみ8.4%で特殊型が1.0%であった．

組織型別の画像の特徴は図2のごとく，いずれのパターンでも環状胸膜肥厚が最も多かったが，上皮型及び二相型では縦隔側胸膜肥厚が2番目に多く，肉腫型では多発性腫瘤形成が2番目で，単発胸膜腫瘤形成が3番目であった．

一方，二相型では単発胸膜腫瘤形成が6.4%，肉腫型では胸水のみが2.7%と低率であった．

年代別では図3に示すように，環状胸膜肥厚が最も多

表2　対象症例の性別，年齢，年代別症例の一覧

		全体	～2008年まで	2009年以降
症例数		782	594	188
性別	男性	657 (84.0%)	493 (83.0%)	164 (87.2%)
	女性	125 (16.0%)	101 (17.0%)	24 (12.8%)
年齢	～60歳	159 (20.3%)	138 (23.2%)	21 (11.2%)
	61～65歳	150 (19.2%)	119 (20.0%)	31 (16.5%)
	66～70歳	142 (18.2%)	103 (17.4%)	39 (20.7%)
	71～75歳	137 (17.5%)	97 (16.3%)	40 (21.3%)
	76～80歳	111 (14.2%)	81 (13.7%)	30 (16.0%)
	81歳～	77 (9.8%)	50 (8.4%)	27 (14.4%)
	不明	6 (0.8%)	6 (1.0%)	0 (0%)

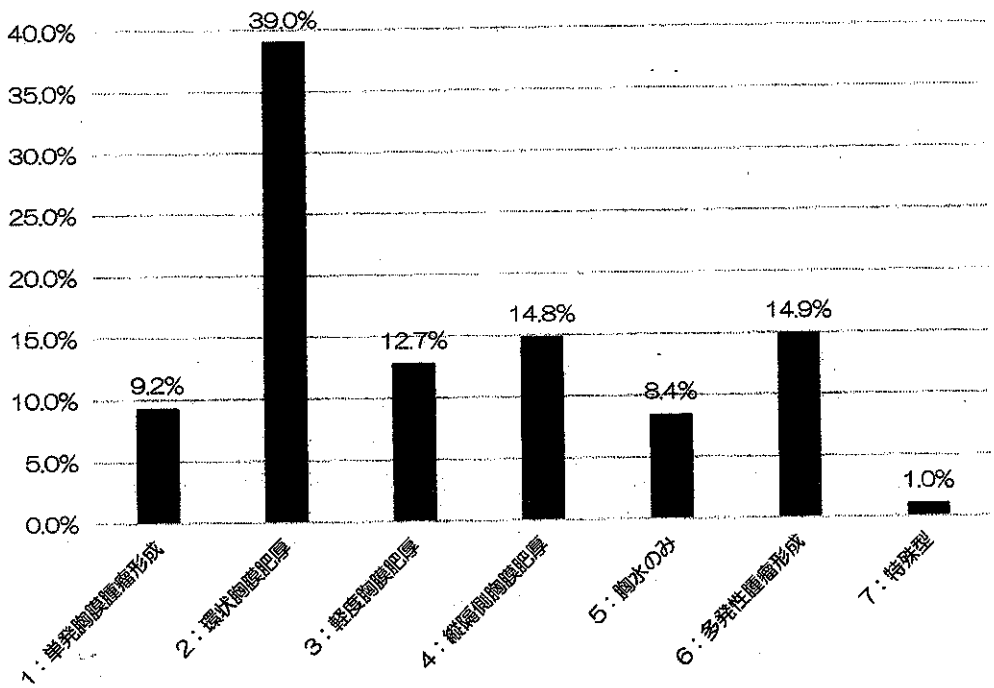

図1　全782例の胸部CT画像所見別頻度

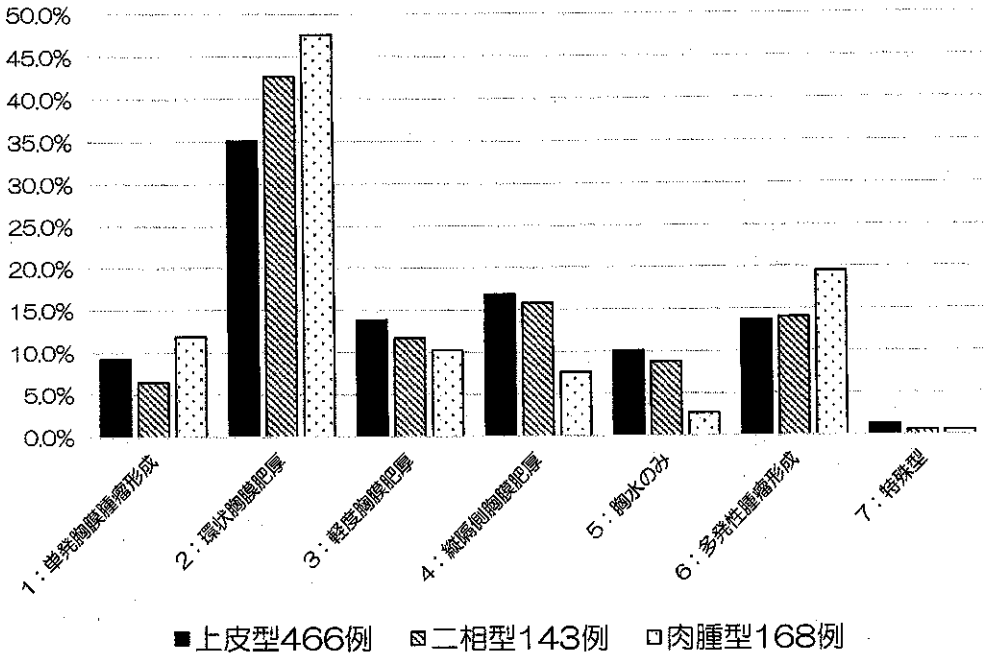

図 2　組織型別画像所見頻度

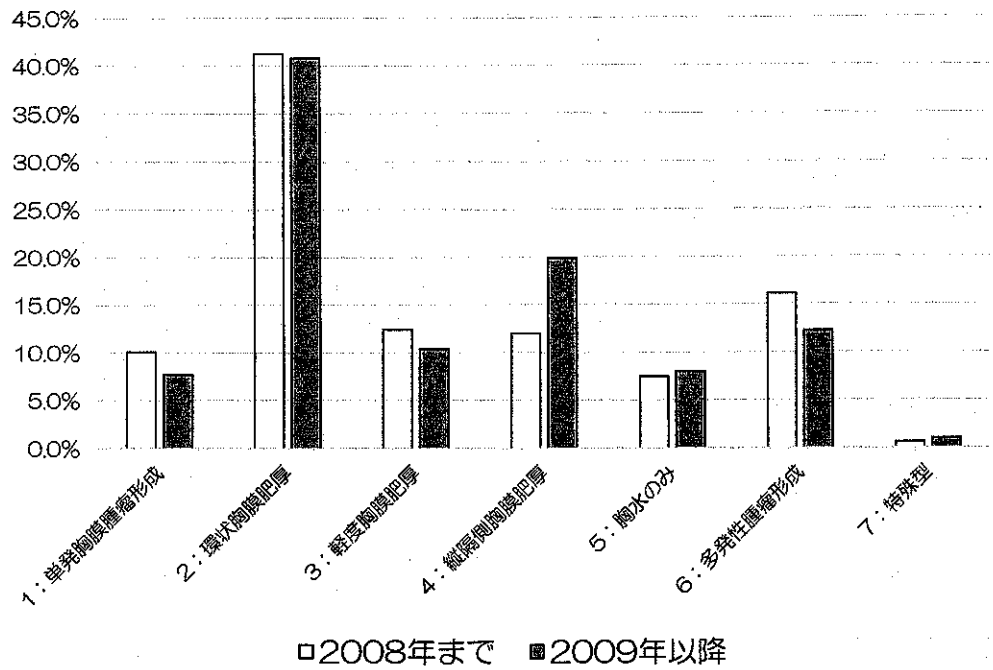

図 3　年代別画像所見頻度

かったが，～2008 年までは環状胸膜肥厚，多発性腫瘤形成が多かったが，2009 年以降には縦隔側胸膜肥厚，胸水のみが増加傾向を示した．

この傾向を組織型別に検討したところ（図 4），上皮型では縦隔側胸膜肥厚や胸水のみの方が 2009 年以降増加傾向にあった．しかし，肉腫型では環状胸膜肥厚が 56.0% と圧倒的に多く，2009 年以降も増加傾向を示した．一方，胸水のみ等早期病変を示すパターンは 10% 未満であった．

3）岡山労災病院の 166 例については組織型，Stage，画像別に生存期間について検討した．図 5 に示すように，組織型別では上皮型では生存期間中央値は 14.3 カ月と非上皮型に比較して有意（$p<0.05$）に良好であったが，二相型は 9.5 カ月，肉腫型は 6.1 カ月と同様に予後不良であり，いずれも 10 カ月には満たなかった．

IMIG1995 分類による Staging 別では，Stage I は 24.4

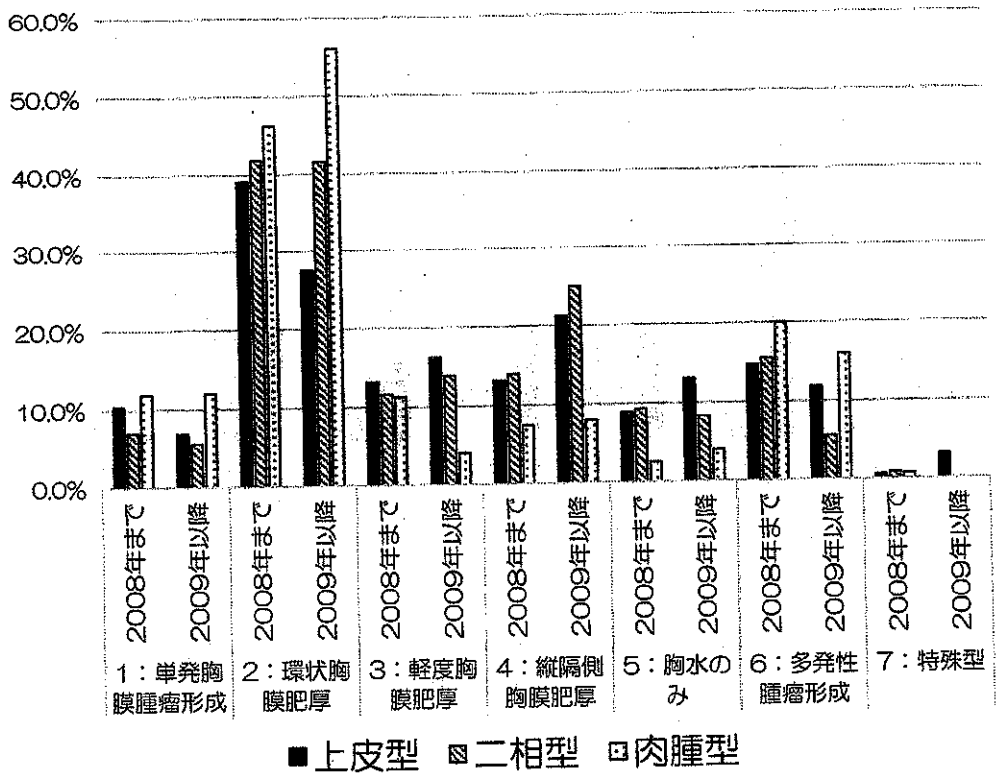

図4 年代・組織型別画像所見頻度

カ月，Stage II は 17.0 カ月と比較的良好であったが，Stage III は 10.4 カ月，Stage IV は 8.6 カ月と予後不良であり，早期病変と進行期の間には有意差（$p<0.05$）を認めた（図6）．

画像別では，図7に示すように単発胸膜腫瘤形成は手術により予後良好な症例が一定数いるが，生存期間中央値ではその他のパターンと差異はなかった．一方，胸水のみあるいは軽度胸膜肥厚はその他のパターンに比較して，予後良好傾向を示したが，有意差はなかった．以上の結果から，画像形態と予後の間には一定の関連性は認められなかった．

考　察

胸膜中皮腫 CT の典型像は壁側胸膜に発生する腫瘍が胸膜沿いに不整な肥厚像を呈して水平方向に増殖する環状胸膜肥厚（pleural rind）が最も多いと記載されている[2)~5)]．腫瘍は胸壁や肋骨浸潤を伴うこともあるが比較的まれである[4)]．今回，我々は過去の厚生労働科学研究において収集した 2003～2008 年に胸膜中皮腫で死亡した症例のご遺族及び病院の同意を得られた 651 例のうち病理組織型が確定されていた 482 例，岡山労災病院において確定診断された 166 例および山口宇部医療センターで診断された 110 例と札幌南三条病院で診断された 24 例，合計 782 例の初診時の胸部 CT 画像所見の特徴について検討した．

その結果，胸膜中皮腫の初診時の胸部 CT 画像では環状胸膜肥厚が最も多く，次いで多発性腫瘤形成，縦隔側胸膜肥厚，軽度胸膜肥厚，単発胸膜腫瘤形成で胸水のみの症例はわずか 8.4% であった．Kato[6)] も 2003～2008 年の日本の中皮腫でその 18% では，腫瘍性胸膜肥厚を示さない胸水のみあるいはわずかな胸膜肥厚のある症例であったと報告している．Kato らの報告と同様，病理組織診断において胸膜中皮腫であると組織型が確定している 782 例においてもほぼ同様のパターンを示した．一方，組織型別でも，上皮型，二相型，肉腫型のいずれにおいても環状胸膜肥厚が最も多かった．しかし，その他のパターン別では二相型では環状胸膜肥厚に次いで，縦隔側胸膜肥厚，多発性腫瘤形成が多く，単発胸膜腫瘤形成はわずか 6.4% のみであった．また，肉腫型でも環状胸膜肥厚が 47.6% と最も多く，次いで多発性腫瘤形成，3 番目に単発胸膜腫瘤形成であったが，胸水のみは 2.7% と極めて少なかった．すなわち，組織型には画像パターンの頻度が異なることが窺われた．

この画像パターンについて 2008 年（いわゆるクボタショックの 3 年後）を境界として，その前後で比較したところ，2009 年以降では胸水のみの症例が 7.5% から 8.8% へと増加しているとともに，縦隔側胸膜肥厚は 12.0% から 19.8% へと増加していた．その理由として，アスベスト問題が社会問題化したため 2009 年以降胸水を来す疾患の鑑別診断として胸膜中皮腫がクローズアップされ，胸水中のヒアルロン酸等の測定頻度が増加するとともに胸水細胞診における免疫染色の導入も加速化さ

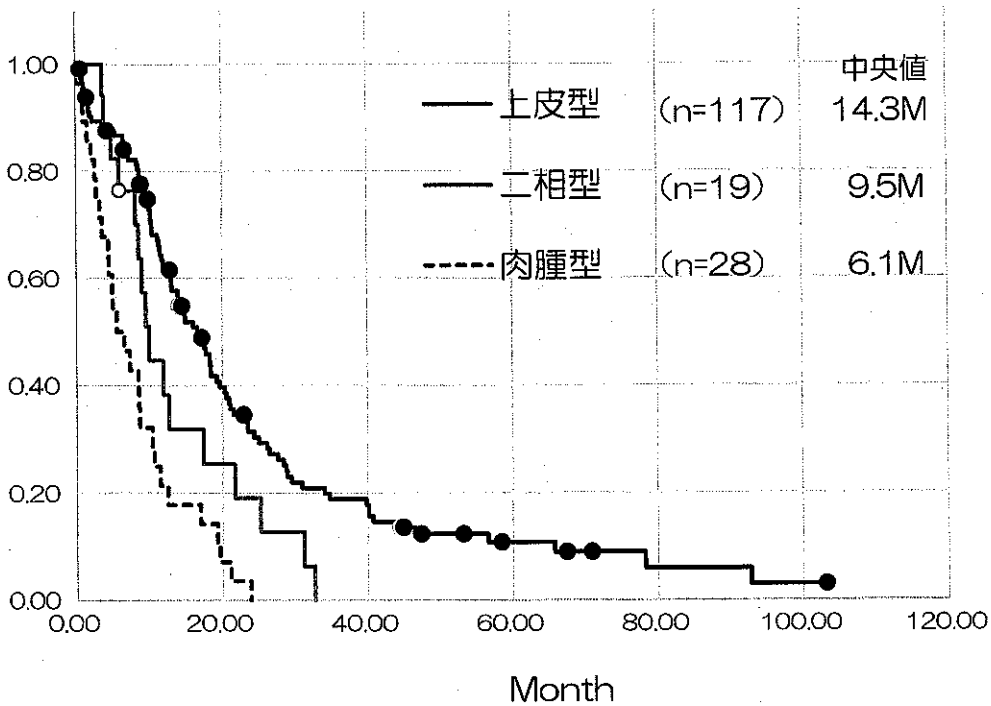

図5　岡山労災病院例の組織別生存期間

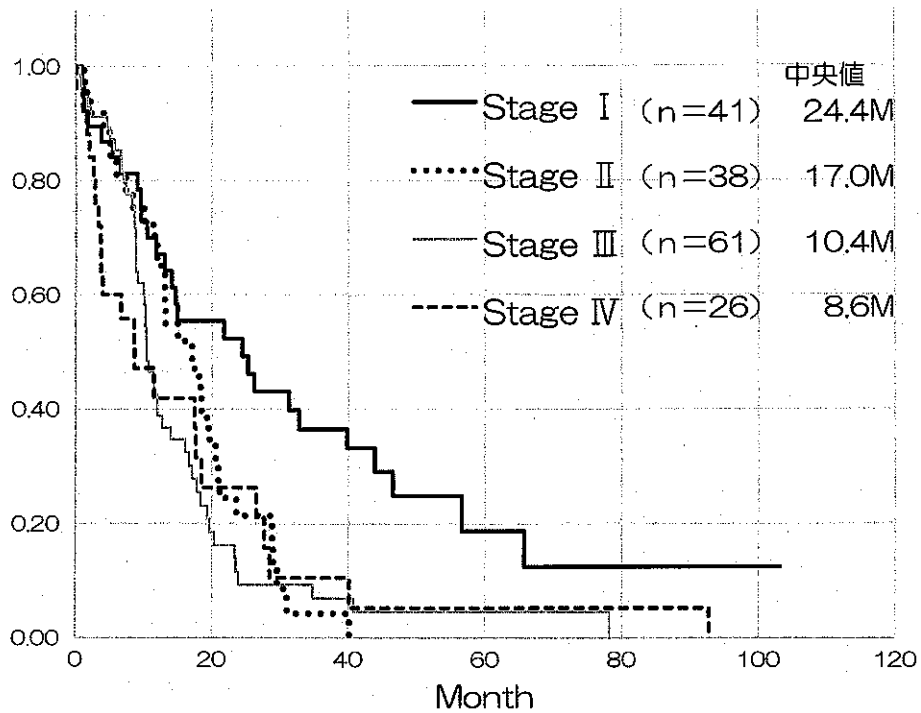

図6　岡山労災病院例 stage 別生存期間

れ，胸腔鏡下胸膜生検が積極的に行われるようになったこと，また縦隔側胸膜肥厚を比較的早期の中皮腫病変と認識するようになったことが胸膜中皮腫早期診断が行われる契機になったと思われる．

岡山労災病院では2009年以降石綿ばく露歴があって胸水を来した症例については中皮腫を除外するため，胸水ヒアルロン酸[7]，SMRP[8]を測定してその疑いがある症例では胸腔鏡検査を行って肉眼的に観察するとともに疑わしい部位を複数カ所生検することで早期診断が可能となったと考えている．

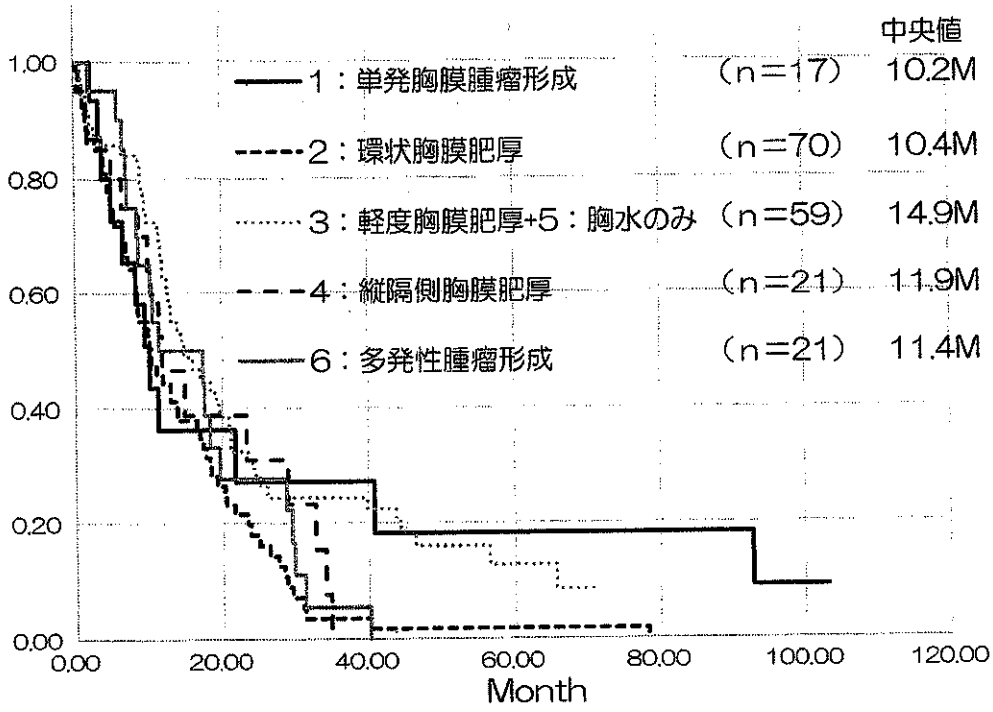

図7 岡山労災病院例の画像別生存期

画像パターン別では胸水のみや軽度胸膜肥厚が予後良好の傾向があったが，有意差は認められなかった．一方，環状胸膜肥厚や多発性腫瘤形成は肺の呼吸面積が縮小するため，呼吸不全，急性肺炎の合併等が死因として重要であった．

予後と関連する組織型及びStagingと比較して，画像パターンが予後に関連するかどうか，岡山労災病院の166例については組織型，Stage，画像別に生存期間について検討した．その結果として，上皮型の生存期間中央値は14.3カ月と比較的良好であったが，二相型は9.5カ月，肉腫型の6.1カ月と同様予後不良であり，いずれも10カ月には満たなかった．

非上皮型では上皮型よりも予後不良[9]と報告されているが，我々の今回の結果でも同様な結果となった．

一方，IMIG1995分類によるStaging別では，Stage Iは24.4カ月，Stage IIは17.0カ月と比較的良好であったが，Stage IIIは10.4カ月，Stage IVは8.6カ月であり有意（$p<0.05$）に予後不良であった．Stage別でも過去の報告と同様の結果であった．Stage I，IIでは手術療法の選択[10)~13)]も可能であり，5年生存が5例で，10年生存も2例あるため，有意に予後良好であった．

一方，画像別では，胸水のみあるいは軽度胸膜肥厚が比較的予後良好であるものの，その他のパターンとほぼ同等の生存期間であり，画像形態と予後の間には一定の関連性は認められなかった．IMIG2016分類[14]はStagingを大きく変更しているが，画像のパターンが予想外に予後因子とならなかった理由として，NあるいはM因子が大きく予後に関係する可能性が示唆された．今後とも症例を増やして検討していくつもりである．

利益相反：利益相反基準に該当無し

文 献

1) Rusch VW: A proposed new international TNM staging system fo malignant pleural mesothelioma. From International Mesothelioma Interest Group. Chest 108 (4): 1122—1128, 1995.
2) Garg K, Lynch DA: Imaging of thoracic occupational and environmental malignancies. J Thorac Imaging 17 (3): 198—210, 2002.
3) Robinson BW, Lake RA: Advances in malignant mesothelioma. N Engl J Med 353 (15): 1591—1603, 2005.
4) Truoug MT, Erasmus JJ, Marom EM, et al: Imaging evaluation in the diagnosis and staging of malignant pleural mesothelioma. Semi Roentgenol 39 (3): 386—396, 2004.
5) Ismail-Khan R, Robinson LA, Williams CC Jr, et al: Malignant pleural mesothelioma a comprehensive review. Cancer Control 13 (4): 255—263, 2006.
6) Kato K, Gemba K, Fujimoto N, et al: Fatal pleural mesothelioma in Japan (2003-2008): evaluation of computed tomography findings. Jpn J Radiol 34 (6): 432—438, 2016.
7) Fujimoto N, Gemba K, Asano M, et al: Hyaluronic acid in the pleural fluid of patients with malignant pleural mesothelioma. Respir investig 51 (2): 92—97, 2013.
8) Fujimoto N, Gemba K, Asano M, et al: Soluble mesothelin-related protein in pleural effusion from patients with malignant pleural mesothelioma. Exp Ther Med 1 (2): 313—317, 2010.
9) Borasio P, Berruti A, Billé A, et al: Malignant pleural

mesothelioma: clinicopathologic and survival characteristics in a consecutive series of 394 patients. Eur J Cardiothorac Surg 33 (2): 307—313, 2008.
10) Cao C, Tian D, Park J, et al: A systematic review and meta-analysis of surgical treatments for malignant pleural mesothelioma. Lung Cancer 83 (2): 240—245, 2014.
11) Hasegawa S: Extrapleural pneumonectomy or pleurectomy/decortication for malignant pleural mesothelioma. Gen Thorac Cardiovasc Surg 62 (9): 516—521, 2014.
12) Domen A, De Laet C, Vanderbruggen W, et al: Malignant pleural mesothelioma: single-institution experience of 101 patients over a 15-year period. Acta Chir Belg 117 (3): 157—163, 2017.
13) Nelson DB, Rice DC, Niu J, et al: Long-Term Survival Outcomes of Cancer-Directed Surgery for Malignant Pleural Mesothelioma: Propensity Score Matching Analysis. J Clin Oncol 35 (29): 3354—3362, 2017.
14) Pass H, Giroux D, Kennedy C, et al: The IASLC mesothelioma staging project: Improving staging of a rare disease through international participation. J Thorac Oncol 11 (12): 2082—2088, 2016.

別刷請求先 〒702-8055 岡山市南区築港緑町 1—10—25
岡山労災病院アスベスト研究センター長
岸本 卓巳

Reprint request:
Takumi Kishimoto
Chief of Asbestos Research Center, Okayama Rosai Hospital, 1-10-25, Minami-ku Chikko-midorimachi, Okayama, 702-8055, Japan

Evaluation for Chest CT Images at the First Visit Clinic for Pleural Mesothelioma Patients

Takumi Kishimoto and Nobukazu Fujimoto
Research Center for Asbestos-related Diseases, Okayama Rosai Hospital

The incidence for the chest CT patterns of 782 pleural mesothelioma patients was investigated for 7 patterns such as 1. Single tumor pattern, 2. Pleural rind pattern, 3. Slight thickening of pleura pattern, 4. Mediastinal thickening pattern, 5. Pleural effusion without any pleural thickening pattern, 6. Multiple mass pattern, 7. Special pattern was investigated. Pleural rind pattern occupied 39.0%, multiple mass pattern 14.9%, mediastinal thickening pattern, 14.8%, slight thickening pattern 12.7%, single mass pattern 9.2% and pleural effusion without any pleural thickening pattern 8.4%.

For 3 pathological types, pleural rind pattern is the highest percentage and 2nd is mediastinal thickening pattern for epithelioid and biphasic types but multiple mass pattern for sarcomatoid type. Single mass pattern is the lowest (6.4%) for biphasic type and pleural effusion without any pleural thickening pattern is the lowest (2.7%) for sarcomatoid type.

Before 2008, pleural rid and multiple mass patterns were the major patterns but after 2009, mediastinal thickening and pleural effusion without any pleural thickening patterns increased.

Prognosis of pleural mesothelioma in Okayama Rosai Hospital by histological classification, median survival for epithelioid type was 14.3 months which is significantly ($p<0.05$) better than non-epithelioid types. For the staging by IMIG 1995, median survival for Stage I is 24.4 months and Stage II is 17.0 months, but Stage III is 10.4 months, and Stage IV is 8.6 months. Stage I and II are significantly ($p<0.05$) better than stage III and IV. For the patterns of chest CT, single mass pattern seemed better for some patients by surgery, but no significance than other types. On the other hand, slight thickening and pleural effusion without any pleural thickening pattern showed better prognosis, but no significance than other types. We cannot detect any significance of survival for the patterns of chest CT.

(JJOMT, 66: 239—245, 2018)

—Key words—
pleural mesothelioma, pleural rind, pleural effusion without any pleural thickening pattern